Alabama Highway Drainage Conservation Design Practices - Particulate Transport in Grass Swales and Grass Filters

November 6, 2005

Yukio Nara, MSCE
Robert Pitt, Ph.D., P.E., D.E.E.

Department of Civil and Environmental Engineering
The University of Alabama
Box 870205
Tuscaloosa, Alabama 35487-0205

UNIVERSITY TRANSPORTATION CENTER FOR ALABAMA
The University of Alabama
Tuscaloosa, Alabama

Project Number 04117

Project Summary

Project Objective

The objective of this project is to show how a common AL DOT design and maintenance practice, the use of grass drainage swales, can help meet the requirements of the new Phase II Stormwater Regulations. Managing this permit can be very expensive and time-consuming. However, current drainage practices on many AL DOT transportation corridors likely meet the objectives of the conservation design strategy of the permits. This project shows the water quality and drainage benefits of grass-lined drainages. This will result in significant time and cost savings for AL DOT managers.

Project Abstract

An important element of the Phase II NPDES Stormwater Regulations is the reliance and promotion of conservation design elements. Agencies, including transportation departments, will be required to emphasize the use of stormwater drainage practices that help reduce the discharges of pollutants and excessive runoff volumes, while maintaining successful drainage objectives. The federal guidance emphasizes the use of "soft" controls over historically expensive stormwater treatment options. These include the use of grass swale drainages, minimizing the amount of paved areas, and routing runoff from paved areas to specially constructed infiltration areas. In Alabama, AL DOT already uses grass swale drainages in many suburban and rural areas. The objective of this project is to document the stormwater quality attributes of these existing drainage system elements under local conditions so that AL DOT can obtain credit for their use under this new regulatory program, reducing the need to retrofit more expensive options. We will be able to calculate the direct stormwater quality benefits of these existing cost-effective practices, reducing the need for other more expensive stormwater controls in many instances.

This project supports the UTCA main theme of the Management of Transportation Systems, and the secondary theme to support Phase II NPDES Stormwater Program components.

Project Task Descriptions:

1) laboratory-scale controlled experiments (12 months)
2) full-scale experiments (8 months)
3) data evaluation and report preparation (3 months)

Milestones and Dates

Startup – January 1, 2004
See the approximate durations for each project phase above. There will be overlap in the durations of each effort.
Conclude project – December 1, 2005

Funding Agency

Alabama Department of Transportation

Relationship to other Research Projects

This is the first UTCA funded project for this research. However, the co-PIs have received prior funding from the Water Environment Research Foundation (WERF) for some related preliminary work in this area.

Potential Benefits of the Project

The outcome of this project documents the cost-effective use of grass-limed swales to meet current storm drainage requirements.

Keywords

Stormwater management, grass swales, conservation design, sediment delivery

Contents

Abstract

The Department of Civil and Environmental Engineering at the University of Alabama has been conducting research investigating the effectiveness of grass swales for stormwater sediment transport to quantify swale hydraulic and sediment transport under relatively small flows. This research has been supported by the Water Environment Research Foundation (Johnson, *et al*. 2003) and the University Transportation Center of Alabama (this reported research). Grass swales are vegetated open channels that collect and transport stormwater runoff. They are often used as an alternative to concrete gutters for stormwater management, such as grass swales in the median of roadways, because of their advantages of infiltration and filtration of stormwater. The objectives of this research are to understand the effectiveness of grass swales in sediment transport, the associated effects of the different swale and hydraulic variables, and to develop a predictive model. To achieve these objectives, experimental grass swales were constructed and tested in an indoor greenhouse facility. The variables tested in the experiments were slope, grass type, depth of flow, sampling time, and length of swales. A water-sediment mixture with a known sediment concentration of sieved sands and fine particles of silica were used to analyze the variables. During the preliminary set of controlled experiments, 108 samples were collected and analyzed for turbidity, total solids, and particle size distributions to investigate the effects of the experimental variables. After completing the initial tests, a second set of controlled experiments was conducted. During this second set of tests, 108 samples were collected and analyzed for turbidity, total solids, total suspended solids, total dissolved solids, and particle size distribution.

To examine how the results obtained from the indoor swale experiments can be applied to full-scale swales, sediment samples were also collected at an outdoor grass swale located adjacent to the Tuscaloosa City Hall, Alabama, during actual storm events. Sixty-nine samples during 13 storm events from August to December 2004 were collected and analyzed for turbidity, total solids, total suspended solids, total dissolved solids, and particle size distributions. The total suspended solids concentrations observed during different rain events showed significant sediment reductions as a function of the length of the swale. The particle size distributions of the suspended solids at the outdoor swale site showed preferential transport of small particles for all lengths of the swale, and preferential trapping of large particles.

The first section of this report begins with a summary outlining the design of grass swales to minimize scour and channel erosion, specifically examining grass-lined swales and the use of turf-reinforced mats. This report section also describes the predictive equations developed to describe sediment trapping in the swales. Several example problems are used to illustrate how these data are used to design stable grass-lined drainage swales that maximize particulate and associated pollutant trapping. The second section of this report describes the controlled indoor experiments and the full-scale tests used to develop the predictive equations, while the third section of the report contains the detailed results in the appendices. Much of the material in this report was from the master's thesis prepared by Yukio Nara (2005).

Section 1: Design Guidance for the Use of Grass Swales for Stormwater Control

This section of the report reviews past performance information concerning grass swale use for the control of stormwater quality. This section also presents methods for the design of stable grass-lined swales and the development of the predictive equations for trapping sediment in the swales based on the controlled indoor swale experiments and the full-scale tests described in the later sections of the report.

Chapter 1: Roadside Drainage Design for Channel Stability

Allowable Velocity and Shear Stress

This chapter is a summary of selected material from Pitt, R., S. Clark, and D. Lake, *Construction Site Erosion and Sediment Controls: Planning, Design, and Performance*, to be published by DEStech Publications, Lancaster, PA, in 2006. This chapter reviews the basic approaches and techniques available for the stable design of natural and grass-lined drainage channels. There are several alternatives that can be used which are briefly described. Example problems are also presented.

An important reference on general shear stress relationships and channel bed movement is *Engineering and Design: Channel Stability Assessment for Flood Control Projects* (COE 1994; EM 1110-2-1418). Although this reference is for large channels, many of the basic concepts are similar to what occurs for smaller drainage channels, and these are specifically addressed in the following discussion. More extensive information on these topics is available in numerous textbooks and manuals on sediment transport and channel design.

Allowable Velocity Approach to Channel Design

The concept of allowable velocities for various soils and materials dates from the early days of hydraulics. An example of simple velocity criteria is given by Table 1 (COE undated, EM 1110-2-1601). Table 2 is a similar table, from U.S. Bureau of Reclamation research (Fortier and Scobey 1926) that also shows the corresponding allowable shear stresses and Manning's roughness values.

Table 1. Example of Simple Allowable Velocity Objectives (From COE undated, EM 1110-2-1601)

Channel Material	Mean Channel Velocity (ft/sec)
Fine Sand	2.0
Coarse Sand	4.0
Fine Gravel	6.0
Earth	
Sandy Silt	2.0
Silt clay	3.5
Clay	6.0
Grass-lined Earth (Slopes less than 5%)	
Bermuda Grass	
Sandy Silt	6.0
Silt Clay	8.0
Kentucky Blue Grass	
Sandy Silt	5.0
Silt Clay	7.0
Poor Rock (usually sedimentary)	10.0
Soft Sandstone	8.0
Soft Shale	3.5
Good Rock (usually igneous or hard metamorphic)	20.0

Table 2. Maximum Permissible Velocities and Corresponding Unit Tractive Force (Shear Stress) (U.S. Bureau of Reclamation research, Fortier and Scobey 1926)

Material	n	Clear Water (diversion structures)		Water Transporting Colloidal Silts (on site and down slope)	
		V (ft/sec)	τ_o (lb/ft^2)	V (ft/sec)	τ_o (lb/ft^2)
Fine sand, colloidal	0.020	1.50	0.027	2.50	0.075
Sandy loam, noncolloidal	0.020	1.75	0.037	2.50	0.075
Silt loam, noncolloidal	0.020	2.00	0.048	3.00	0.11
Alluvial silts, noncolloidal	0.020	2.00	0.048	3.50	0.15
Ordinary firm loam	0.020	2.50	0.075	3.50	0.15
Volcanic ash	0.020	2.50	0.075	3.50	0.15
Stiff clay, very colloidal	0.025	3.75	0.26	5.00	0.46
Alluvial silts, colloidal	0.025	3.75	0.26	5.00	0.46
Shales and hardpans	0.025	6.00	0.67	6.00	0.67
Fine gravel	0.020	2.50	0.075	5.00	0.32
Graded loam to cobbles when noncolloidal	0.030	3.75	0.38	5.00	0.66
Graded silts to cobbles when noncolloidal	0.030	4.00	0.43	5.50	0.80
Coarse gravel, noncolloidal	0.025	4.00	0.30	6.00	0.67
Cobbles and shingles	0.035	5.00	0.91	5.50	1.10

Note:

- an increase in velocity of 0.5 ft/sec can be added to these values when the depth of water is greater than 3 ft.
- a decrease in velocity of 0.5 ft/sec should be subtracted when the water contains very coarse suspended sediments.
- for high and infrequent discharges of short duration, up to 30% increases in velocity can be added

Figure 1 is another guidance illustration showing SCS data (USDA 1977). This figure also differentiates between "sediment-free" and "sediment-laden" flow, with clear water having more restrictive allowable velocities.

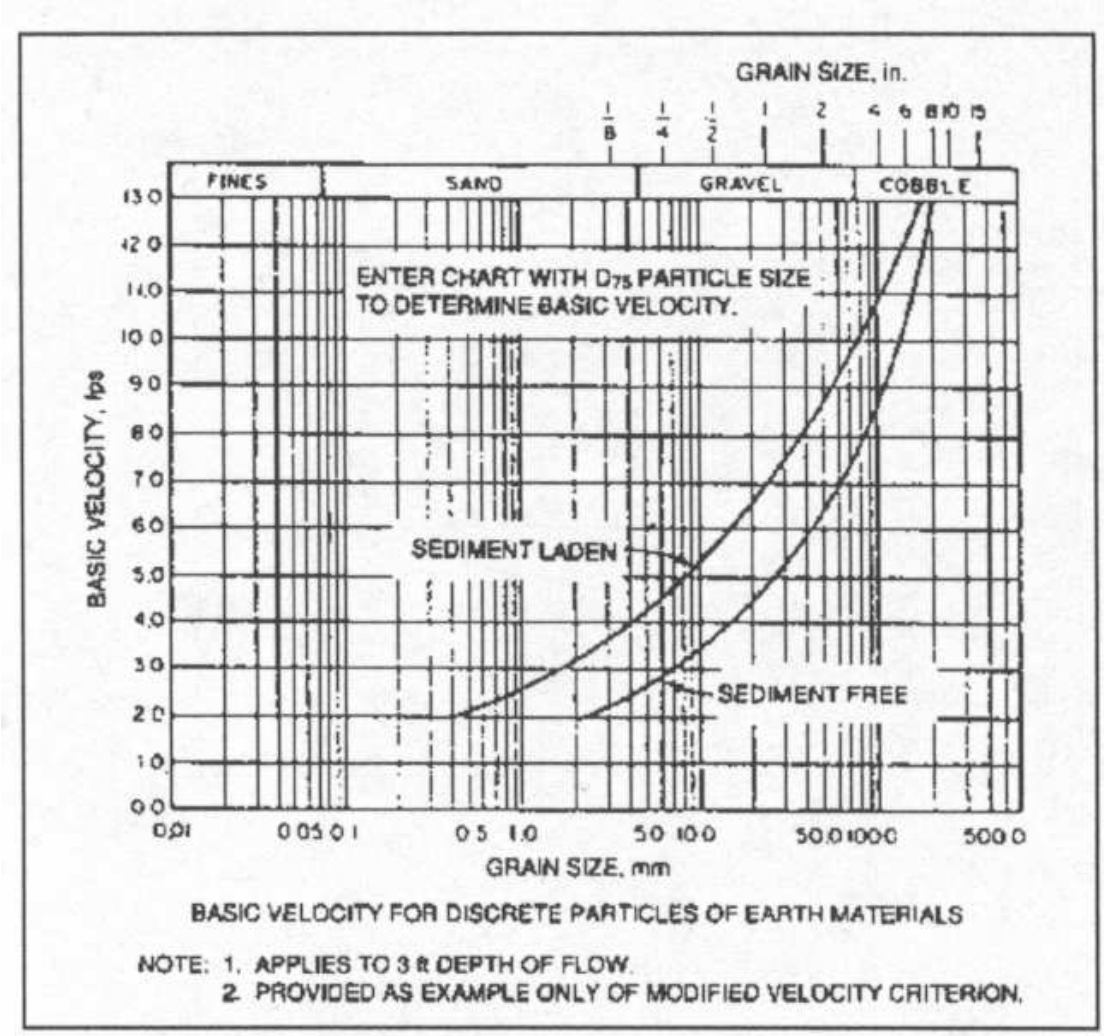

Figure 1. Example of allowable velocity data with provision for sediment transport (USDA 1977)

Allowable Shear Stress Calculations

By the 1930's, boundary shear stress (sometimes called tractive force) was generally accepted as a more appropriate erosion criterion than allowable velocity. The average boundary shear stress in uniform flow (Figure 3) is calculated by

$$\tau_o = \gamma RS \quad (\text{lb/ft}^2)$$

where:

γ = specific weight of water (62.4 lbs/ft^3)
R = hydraulic radius (ft)
S = hydraulic slope (ft/ft)

Figure 2 (Chow 1959) shows a typical distribution of the shear stresses in a channel, indicating how the maximum shear stress is applied along the center of the channel for straight channel reaches having constant depths.

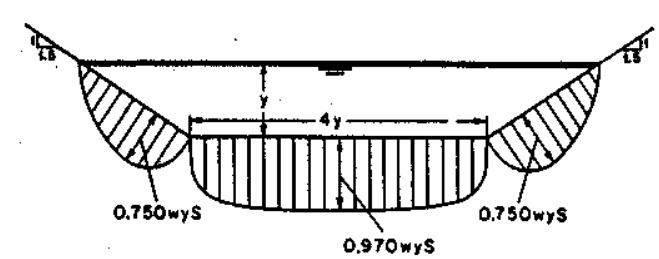

Figure 2. Typical shear stress distributions in a trapezoidal channel (Chow 1959).

If the maximum shear stress is desired (typical for design conditions), then the flow depth is used instead of the hydraulic radius. For sheetflow conditions, the hydraulic radius (R) is very close to the depth of flow, and the above equation is also modified, as shown in Figure 3, by using the depth of flow to replace the hydraulic radius.

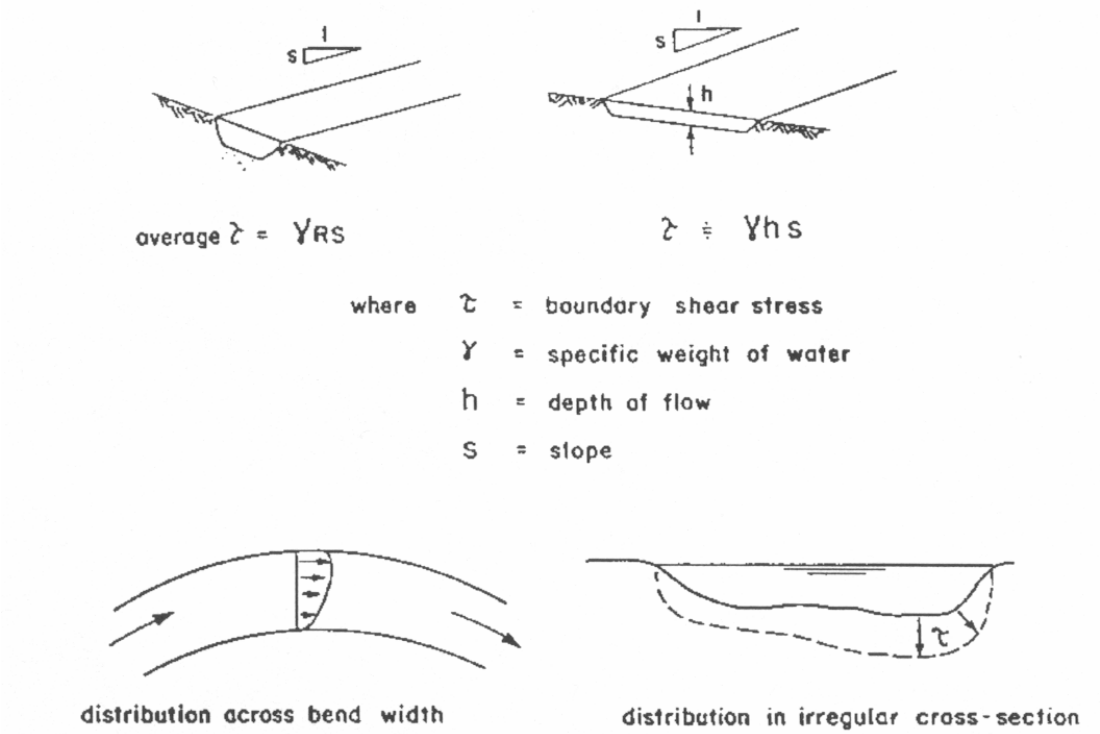

Figure 3. Boundary shear stress in uniform flow (COE 1994).

The COE (1994) shows that the use of the Shield's diagram likely greatly over-predicts the erodibility of the channel bottom material. The expected reason they give is that the Shield's diagram assumes a flat bottom channel and the total roughness is determined by the size of the granular bottom material. The actual Manning's roughness value is likely much larger because it is largely determined by bed forms, channel irregularities, and vegetation. They recommend, as a more realistic assessment, that empirical data based on field observations be used. In the absence of local data, they present Figure 4 (from Chow 1959) for applications for channels in granular materials. This figure shows the permissible unit tractive force (shear stress) as a function of the average particle diameter, and the fine sediment content of the flowing water.

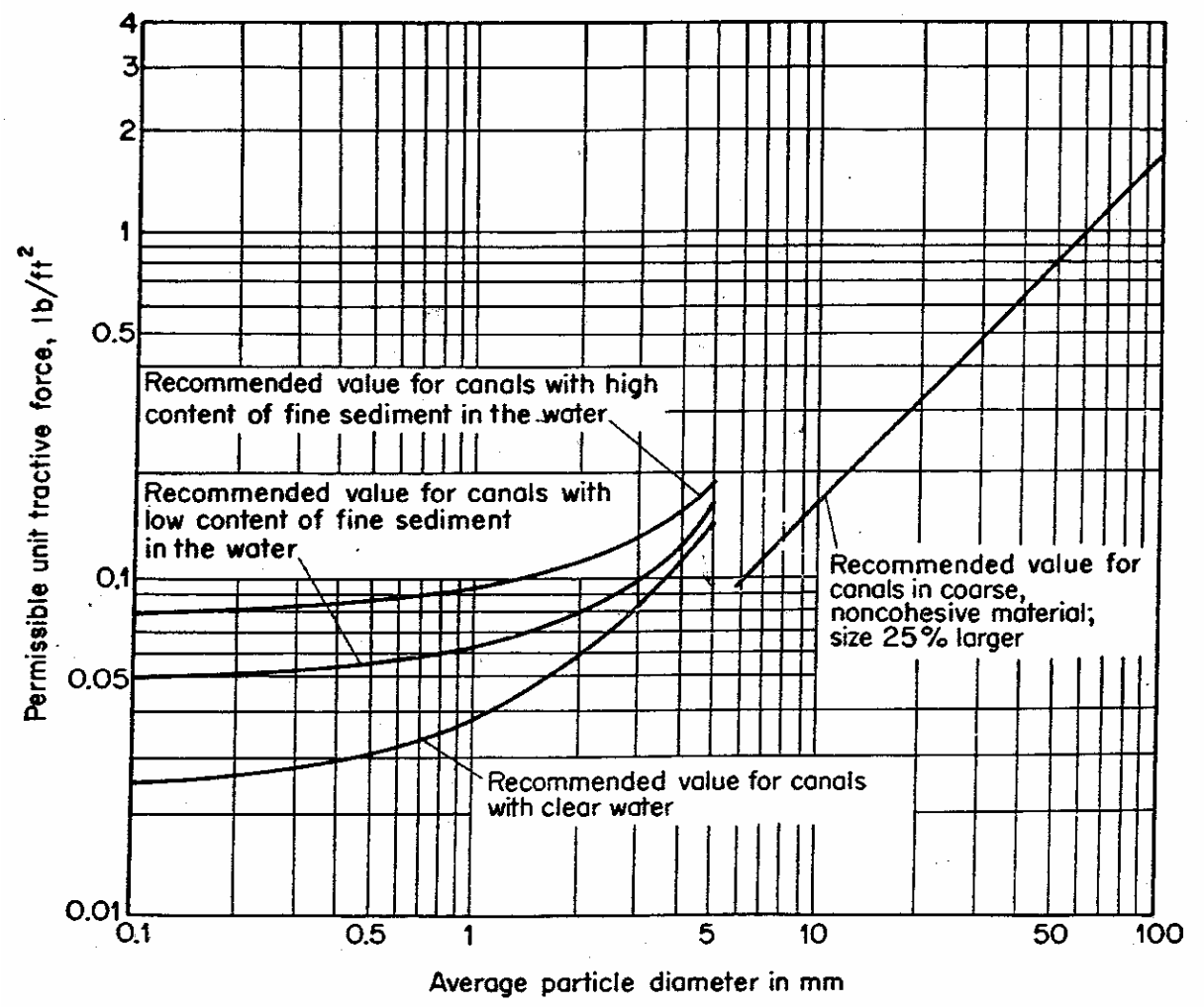

Figure 4. Allowable shear stresses (tractive forces) for canals in granular materials (U.S. Bureau of Reclamation).

The allowable shear stress concept has also been applied to semicohesive and noncohesive soils, but values do not correlate well with standard geotechnical parameters because the resistance to erosion is affected by such factors as water chemistry, history of exposure to flows, and weathering (Raudkivi and Tan 1984). Figure 5 gives an example of allowable shear stresses for a range of cohesive materials. Again, the COE recommends that local field observations or laboratory testing results be given preference.

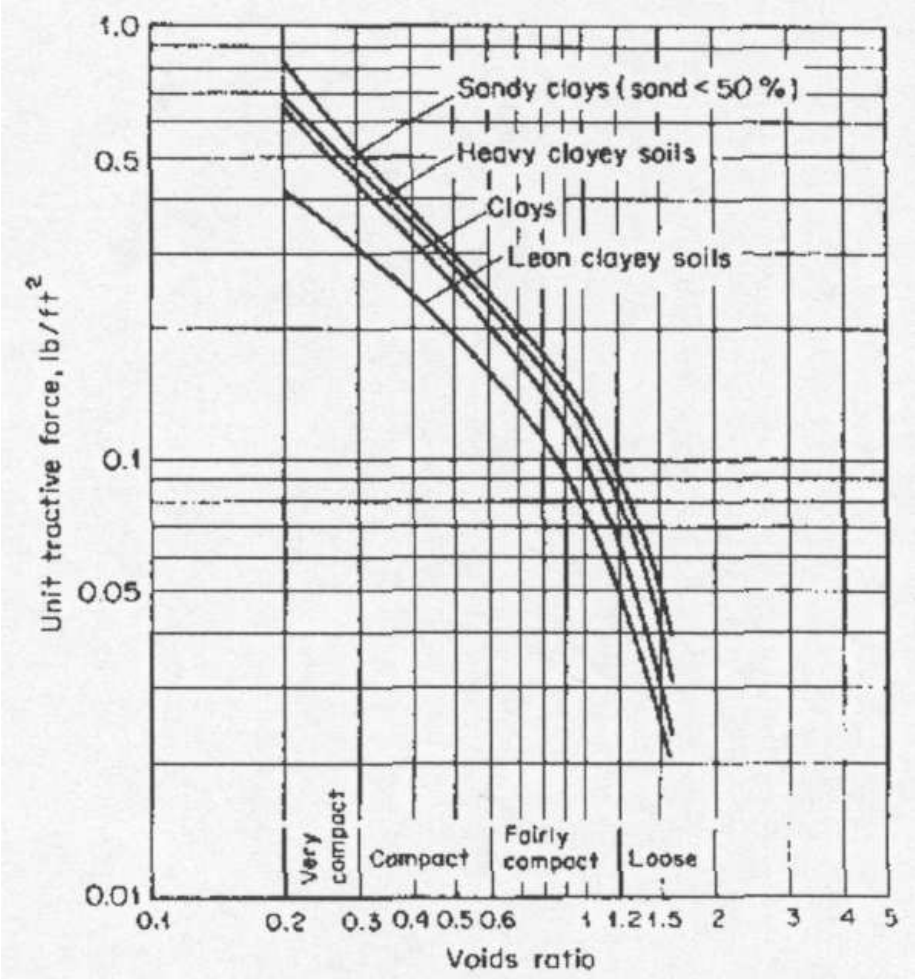

Figure 5. Example of allowable shear stresses (tractive forces) for cohesive materials (COE 1994). Note: Leon clayey soils are hardpan soils where the soil grains become cemented together with bonding agents such as iron oxide or calcium carbonate, forming a hard, impervious mass.

Shear Stress in Channels having Bends

The basic shear stress formulas can be modified to account for the increased shear stress after bends in channels. Normally, the maximum shear stress is along the center part of a channel (usually the deepest area), but a hydrodynamic force is applied to the outside bend after a change in direction. Along the outside of the bend, increased water velocity and shear stress will increase the erosion potential, while sedimentation may occur along the inside of the bend where the water velocity slows. The basic shear stress formula is modified with a bend coefficient, as follows:

$$\tau_o = \frac{\gamma RS}{K_b}$$

where:

γ = specific weight of water (62.4 lbs/ft^3)
R = hydraulic radius (ft) (can be estimated by water depth, for relatively wide channels or sheetflows)
S = hydraulic slope (ft/ft)
K_b = bend coefficient

The bend coefficient can be estimated by (Croke 2001):

$$K_b = \frac{R_c}{B}$$

where:

R_c = bend curvature (radius of the bend)
B = bottom width of the channel

As the bend curvature, R_c, increases, the effect of the bend decreases. These parameters are illustrated in Figure 6 (North American Green).

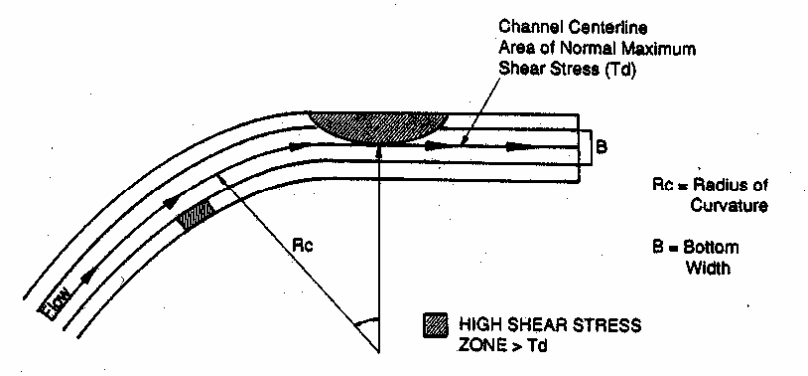

Figure 6. Location of increased shear stress due to channel bend (North American Green).

This formula obviously cannot be used for a V-shaped channel, where the bottom width is zero. The area being affected by the increased shear stress due to channel bends is usually assumed to begin immediately after the bend at the tangent to the downstream channel, as shown in Figure 6. The length of extra shear stress can be estimated by the following formula (after Croke 2001):

$$L_p = \frac{0.604R^{1.17}}{n}$$

where:

L_p = length of extra protection needed due to increased shear stress on outside of bend (same units as R)
R = hydraulic radius = ratio of cross-sectional area of flow to wetted perimeter (A/P)
n = Manning's roughness coefficient for liner in the channel bend

As an example, assume the following conditions:

R = 3.0 ft
n = 0.042

then:

$$L_p = \frac{0.604(3)^{1.17}}{0.042} = 52 \text{ ft}$$

In addition to the increased shear stress being exerted along the outside bend, water elevations will also rise due to momentum. This will require an additional channel depth needing protection at outside bends.

Design Steps for Maximum Permissible Velocity/Allowable Shear Stress Method

McCuen (1998) presents the following steps when designing a stable channel using the permissible velocity/allowable shear stress method:

1) for a given channel material, estimate the Manning's roughness coefficient (n), the channel slope (S), and the maximum permissible velocity (V) (such as from Tables 1 or 2).

2) Compute the hydraulic radius (R) using Manning's equation:

$$R = \left[\frac{Vn}{1.49 S^{0.5}} \right]^{1.5}$$

where:

R = hydraulic radius, ft.
V = permissible velocity, ft/sec
S = channel slope, ft/ft
n = roughness of channel lining material, dimensionless

Some typical values for Manning's n for open channels (Chow 1959) are as follows:

Very smooth surface (glass, plastic, machined metal)	0.010
Planed timber	0.011
Rough wood	0.012 – 0.015
Smooth concrete	0.012 – 0.013
Unfinished concrete	0.013 – 0.016
Brickwork	0.014
Rubble masonry	0.017
Earth channels, smooth no weeds	0.020
Firm gravel	0.020
Earth channel, with some stones and weeds	0.025
Earth channels in bad condition, winding natural streams	0.035
Mountain streams	0.040 – 0.050
Sand (flat bed), or gravel channels, d=median grain diameter, ft.	$0.034d^{1/6}$

Chow (1959) also provides an extensive list of n values, along with photographs. Most engineering hydrology and hydrologic texts (including McCuen 1998) will also contain extensive guidance on the selection of Manning's n values for different channel conditions. A later section in this chapter presents the usual trial-and-error method for determining Manning's n values for grass-lined channels, using measured VR-n relationships for different grass types.

3) Calculate the required cross-sectional area, using the continuity equation and the previously determined design storm peak flow rate (Q):

$$A = \frac{Q}{V}$$

where:

A = cross-sectional area of channel (wetted portion), ft^2
Q = peak discharge for design storm being considered, ft^3/sec
V = permissible velocity, ft/sec

4) Calculate the corresponding wetter perimeter (P):

$$P = \frac{A}{R}$$

where:

P = wetted perimeter, ft
A = cross-sectional area of channel (wetted portion), ft^2
R = hydraulic radius, ft.

5) Calculate an appropriate channel base width (b) and depth (y) corresponding to a specific channel geometry (usually a trapezoid channel, having a side slope of z:1 side slopes).

Figure 7 (Chow 1959) can be used to significantly shorten the calculation effort for the design of channels, by skipping step 4 above and more effectively completing step 5. This figure is used to calculate the normal depth (y) of a channel based on the channel side slopes and known flow and channel characteristics, using the Manning's equation in the following form:

$$AR^{\frac{2}{3}} = \frac{nQ}{1.49S^{0.5}}$$

Initial channel characteristics that must be know include: z (the side slope), and b (the channel bottom width, assuming a trapezoid or a rectangular cross-section). It is easy to examine several different channel options (varying z and b) by calculating the normal depth (y) for a given peak discharge rate, channel slope, and roughness. The most practical channel can then be selected from the alternatives.

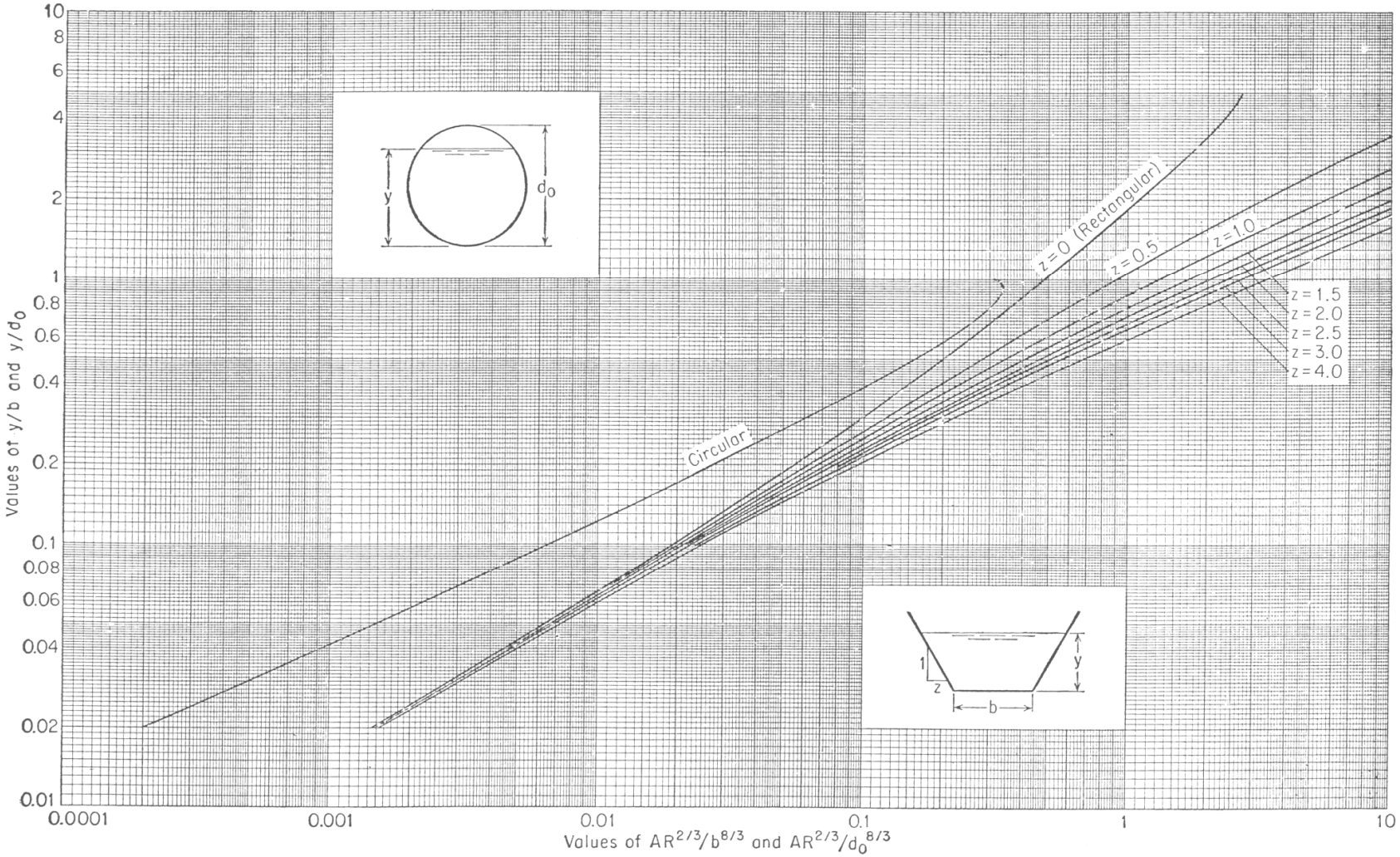

Figure 7. Chow (1959) curves for determining normal depth for various channel geometries.

As an example, assume the following conditions:

Noncolloidal alluvial silts, water transporting colloidal silts:
Manning's roughness coefficient (n) = 0.020
maximum permissible velocity (V) = 3.5 ft/sec
(the allowable shear stress is 0.15 lb/ft^2)

Peak discharge flow rate (Q) = 13 ft^3/sec

Channel slope = 1%, or 0.01 ft/ft

Therefore:

The hydraulic radius (R) using Manning's equation:

$$R = \left[\frac{Vn}{1.49S^{0.5}}\right]^{1.5} = \left[\frac{3.5(0.020)}{1.49(0.01)^{0.5}}\right]^{1.5} = 0.32\ ft.$$

The required cross-sectional area, using the continuity equation and the design storm peak flow rate (Q):

$$A = \frac{Q}{V} = \frac{13}{3.5} = 3.7\ ft^2$$

Therefore, $AR^{2/3} = (3.7)(0.32)^{2/3} = 1.7$, and the wetted perimeter is A/R = 3.7/0.32 = 12 ft. Table 3 shows the calculated normal depth (y) for different channel options that all meet the allowable velocity criteria. Also shown on this table is the calculated maximum shear stress:

$\gamma RS = (62.4\ lb/ft^3)\ (R\ ft)\ 0.01\ ft/ft) = 0.62R$

since the allowable shear stress is 0.15 lb/ft^2, the hydraulic radius must be less than 0.24 ft (only about 3 inches). This will require a relatively wide channel, as the hydraulic radius approximates the depth of flow for wide and shallow channels. Also, the depth of flow can be used instead of the hydraulic radius as a conservative approach to calculate the maximum shear stress, which is important for design purposes.

As the channel becomes wider, the side slopes have little effect on the normal depth and the calculated maximum shear stress, as expected. The safety factors are the ratios of the allowable shear stress (0.15 lb/ft^2) divided by the calculated maximum shear stress. None of these channels can satisfy the allowable shear stress with this natural material, unless the channel is wide. A minimum channel width between 15 and 25 ft would result in a stable channel. However, a channel liner can be used to reinforce the channel, resulting in a larger allowable shear stress, enabling a narrower channel.

Table 3. Alternative Channel Geometries Meeting Maximum Permissible Velocity Criterion (3.5 ft/sec)

Side slope (z)	Bottom width (b), ft	$b^{8/3}$	$AR^{2/3}/b^{8/3}$	y/b	Normal depth (y), ft	Top width (T), ft	Area (A), ft^2	Wetted perimeter (P), ft	Hydraulic radius (R), ft	b/y	R/y	Maximum shear stress using y (τ), lb/ft^2	Safety factor, using the normal depth [1]	Maximum shear stress using R (τ), lb/ft^2	Safety factor, using the hydraulic radius [2]
4	2	6.4	0.27	0.32	0.62	7.0	2.8	10.6	0.26	3.2	0.42	0.32	0.39	0.16	0.92
4	4	41	0.041	0.13	0.52	8.2	3.2	10.5	0.30	7.7	0.58	0.32	0.47	0.19	0.80
4	8	260	0.0066	0.046	0.37	11.0	3.5	11.9	0.30	21.6	0.80	0.23	0.65	0.18	0.81
4	15	1400	0.0012*	0.017	0.26	17.1	4.2	17.3	0.24	57.7	0.93	0.16	0.94	0.15	0.99
4	25	5300	0.00032*	0.008	0.2	26.6	5.2	26.5	0.19	125.0	0.97	0.12	**1.25**	0.12	**1.24**
2	2	6.4	0.27	0.38	0.76	5.0	2.7	6.9	0.39	2.6	0.51	0.47	0.32	0.24	0.62
2	4	41	0.041	0.14	0.56	6.2	2.9	7.0	0.41	7.1	0.73	0.35	0.43	0.26	0.59
2	8	260	0.0066	0.049	0.39	9.6	3.4	9.7	0.35	20.5	0.91	0.24	0.63	0.22	0.68
2	15	1400	0.0012*	0.017	0.26	16.0	4.0	15.9	0.25	57.7	0.98	0.16	0.94	0.16	0.95
2	25	5300	0.00032*	0.008	0.2	25.8	5.1	25.6	0.20	125.0	0.99	0.12	**1.25**	0.12	**1.21**
1	2	6.4	0.27	0.44	0.88	3.8	2.5	5.2	0.49	2.3	0.55	0.55	0.27	0.30	0.49
1	4	41	0.041	0.16	0.64	5.3	3.0	5.8	0.51	6.3	0.79	0.40	0.38	0.32	0.47
1	8	260	0.0066	0.049	0.39	8.8	3.3	8.8	0.37	20.5	0.95	0.24	0.63	0.23	0.65
1	15	1400	0.0012*	0.017	0.26	15.5	4.0	15.4	0.26	57.7	0.99	0.16	0.94	0.16	0.93
1	25	5300	0.00032*	0.008	0.2	25.4	5.0	25.3	0.20	125.0	1.00	0.12	**1.25**	0.12	**1.20**
0.5	2	6.4	0.27	0.5	1	3.0	2.5	4.7	0.53	2.0	0.53	0.62	0.24	0.33	0.45
0.5	4	41	0.041	0.16	0.64	4.6	2.8	5.2	0.53	6.3	0.83	0.40	0.38	0.33	0.45
0.5	8	260	0.0066	0.049	0.69	8.7	5.8	9.4	0.62	11.6	0.89	0.24	0.63	0.38	0.39
0.5	15	1400	0.0012*	0.017	0.26	15.3	3.9	15.2	0.26	57.7	0.99	0.16	0.94	0.16	0.93
0.5	25	5300	0.00032*	0.008	0.2	25.2	5.0	25.1	0.20	125.0	1.00	0.12	**1.25**	0.12	**1.20**

* estimated, as these values are under range from the plotted curves.

[1] safety factor is the ratio of the allowable shear stress/ max. shear stress using y, allowable shear stress = 0.15 lb/ft^2

[2] allowable shear stress/ max. shear stress using R, allowable shear stress = 0.15 lb/ft^2

Table 3 compares the shear stress calculated using the hydraulic radius, R, to the larger shear stress calculated using the normal depth, y. Also shown is the ratio of the hydraulic radius to the normal depth for different channel conditions. Figure 8 is a plot showing how the normal depth approaches the hydraulic depth, for this example, as the channel width to normal depth ratios increase. The maximum shear stress is therefore much larger when the normal depth is used instead of the hydraulic radius for relatively narrow channels, but the results are similar for wider channels.

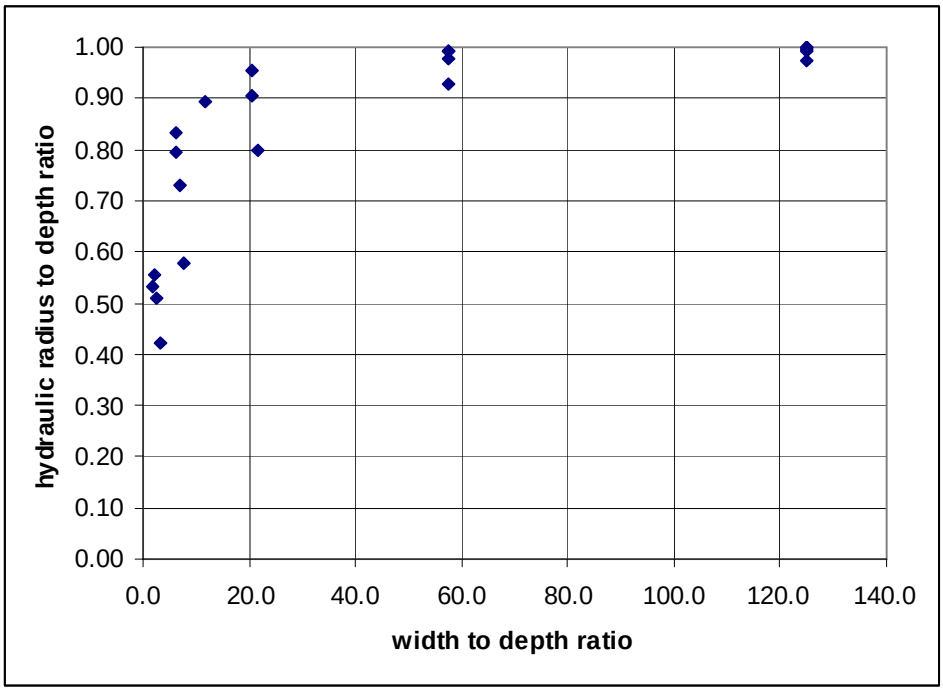

Figure 8. Relationship of hydraulic radius to normal depth for different channel width to depth conditions.

A more direct approach is to use Figure 7 in reverse order. As shown previously, the maximum depth can be calculated based on the maximum allowable shear stress and the channel slope:

$$D = \frac{\tau_c}{\gamma S} = \frac{0.15 lb/\ ft^2}{(62.4 lb/\ ft^3)(0.01 ft/\ ft)} = 0.24\, ft$$

With the known value for $AR^{2/3}$ ($3.7 \times 0.32^{2/3} = 1.7$), Table 4 shows the calculated maximum side slope for different channel bottom widths (b). All of these options will therefore meet both the allowable velocity and shear stress criteria.

Table 4. Example Calculations for Required Side Slopes for Different Bottom Widths, Meeting Allowable Velocity and Maximum Shear Stress Criteria

b (ft)	y/b (with y = 0.24ft)	$AR^{2/3}/b^{8/3}$	Required side slope (z), or longer
8	0.030	0.0066	>4
10	0.024	0.0036	>4
15	0.016	0.0012*	5 (?)
20	0.012	0.00057*	any (0.5 to 4)

* estimated, as these values are under range from the plotted curves.

For this example, side slopes of about 5:1 and with a bottom width of 15 ft may be stable, or "any" side slope may be suitable for bottom widths of 20 ft, or wider. This example has shown that it may not be possible to design a stable channel only based on allowable maximum velocity. It is a good idea to also calculate the maximum shear stress, based on the normal depth. Without a channel liner, most stable channels in soils will need to be relatively wide. Because of the increased use of land needed for wide channels (see the calculated top width "T" in Table 3), it is usually necessary to consider channel liners, either grass-lined, or re-enforced with netting mats, as described in the following sections.

Design of Grass-Lined Channels

According to Temple, *et al*. (1987) in *Stability Design of Grass-Lined Open Channels*, USDA Agricultural Handbook # 667, it is assumed that grass channel linings are used to protect an erodible soil boundary and prevent channel degradation. They found that detachment begins at levels of total stress low enough to be withstood by the vegetation without significant damage to the plants themselves: it is possible for the vegetation to be undercut and the weaker vegetation washed away. This vegetation loss decreases the density and uniformity of the vegetative cover, which in turn leads to greater stresses at the soil-water interface, resulting in an increased erosion rate. Supercritical channel flows cause a more severe problem compared to subcritical flows because small irregularities in the channel lining cause stress concentrations to develop during supercritical flow conditions. For very erosion-resistant soils, the lining vegetation may sustain damage before the effective stress at the soil-water interface becomes large enough to detach soil material. Although the limiting condition in this case is the stress on the plants, failure progresses in a similar manner: damage to the plant cover results in an increase in effective stress on the soil boundary until conditions critical to erosion are exceeded. The resulting erosion further weakens the cover, and unraveling occurs. When plant failure occurs, it is a complex process involving removing young and weak plants, shredding and tearing of leaves, and fatigue weakening of stems.

Because of the many uncertainties and different methods of failure, the use of an approximate design approach is considered appropriate for most practical applications. Temple, *et al*. (1987) state that conservative design criteria are required, as the potential for rapid unraveling of a channel lining can occur once a weak point has developed; especially considering the variability of vegetative covers. Very dense and uniform covers will likely withstand stresses substantially larger than immature or spotty covers, without significant damage. However, they recommend that poor maintenance should be assumed in conservative designs.

The design of a grass-lined open channel differs from the design of an unlined or structurally lined channel in that (1) the flow resistance is dependent on channel geometry and discharge, (2) a portion of the boundary stress is associated with drag on individual vegetation elements and is transmitted to the erodible boundary through the plant root system, and (3) the properties of the lining vary both randomly and periodically with time. Each of these differences requires special considerations in the design process. Temple, *et al*. (1987) presents detailed descriptions of the generalized step-by-step procedure for grass-lined channel design, including computer codes.

Plant Species Selection for Vegetative-Lined Channels

The following is a general discussion and does not provide site-specific guidance for different climatic regions. However, it does describe the general problems associated with establishing plants in a channel environment. Local guidance (such as from local USDA or University Extension services) needs to be sought for specific recommendations for a specific location. Obviously, channels carrying water for long periods of the year may not be

suitably lined with terrestrial vegetation. Extended wet periods will also affect plant selection. Again, local plant specialists need to be consulted for the proper selection of suitable plants for the anticipated growing conditions. The *Alabama Handbook for Erosion Control, Sediment Control, and Stormwater Management on Construction Sites and Urban Areas* (USDA 2003) contains further general guidance on plant selection for Alabama uses, for example.

Site Considerations

When a site will receive heavy use, plant species should be selected that are wear resistant and have rapid wear recovery, such as bermudagrass. Bermudagrass also has a fast establishment rate and is adapted to many geographical areas. Where a neat appearance is desired, plants that respond to frequent mowing should be used. Likely choices for quality turf in north Alabama are bermudagrass or tall fescue, while in central or south Alabama bermudagrass, centipede, or zoysia are good choices. At sites where low maintenance is desired, low fertility requirements and vegetation persistence are particularly important. Sericea lespedeza and tall fescue are good choices in north Alabama, while bahiagrass and centipede do well in central and south Alabama.

Seasonal Considerations

Growing seasons must be considered when selecting species. The most effective times for planting perennial grasses and legumes in Alabama generally extend from March through May and from late August through October. Outside these dates, the probability of failure is higher. Grasses and legumes are usually classified as warm or cool-season in reference to their season of growth. Cool-season species produce most of their growth during the spring and fall and are relatively inactive or dormant during the hot summer months. Therefore, fall is the most dependable time to plant them. Warm-season plants grow most activity during the summer, and go dormant at the first frost in the fall. Spring and early summer are the preferred planting times for warm-season species.

Plant Hardiness Zones

The US Department of Agriculture has produced plant hardiness zone maps that are normally used to help determine the suitability of different plants for an area. These maps are based on the annual average low temperatures and are therefore most appropriate for permanent vegetation. Therefore, short-term vegetation use does not necessarily have to follow the same selection guidelines needed for permanent vegetation. In all cases, it is important to contact the local NRCS office, or other erosion control specialists, for the most suitable vegetation to consider for a specific site. Figure 9 and Table 5 shows the current USDA hardiness zone map and selected cites associated with the different annual average minimum temperatures.

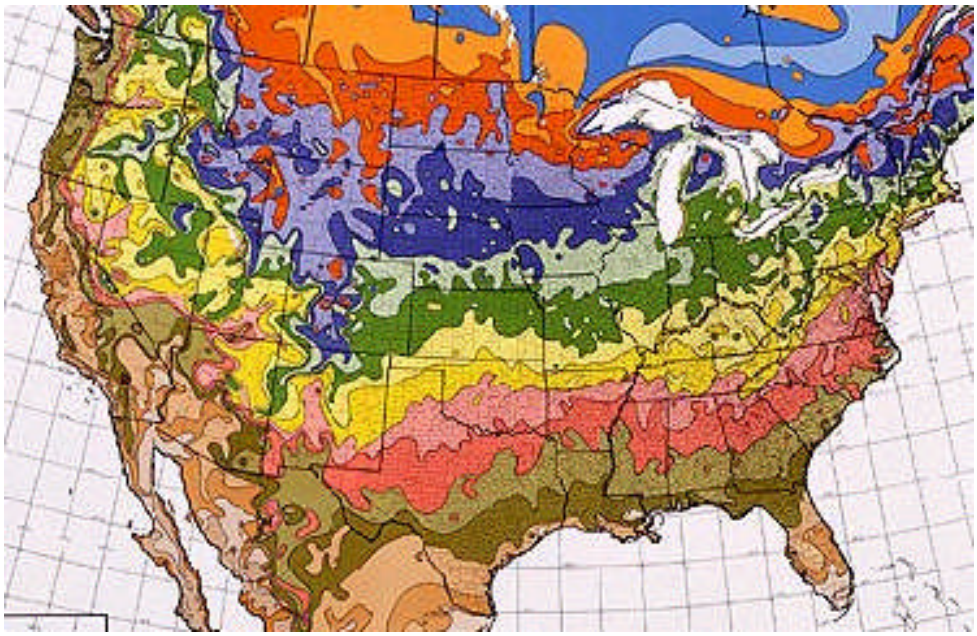

Figure 9. USDA Plant Hardiness Zone Map

Table 5. Annual Average Minimum Temperatures for Selected Cities

Fahrenheit	Celsius	Example Cities
Below -50 F	Below -45.6 C	Fairbanks, Alaska; Resolute, Northwest Territories (Canada)
-50 to -45 F	-42.8 to -45.5 C	Prudhoe Bay, Alaska; Flin Flon, Manitoba (Canada)
-45 to -40 F	-40.0 to -42.7 C	Unalakleet, Alaska; Pinecreek, Minnesota
-40 to -35 F	-37.3 to -39.9 C	International Falls, Minnesota; St. Michael, Alaska
-35 to -30 F	-34.5 to -37.2 C	Tomahawk, Wisconsin; Sidney, Montana
-30 to -25 F	-31.7 to -34.4 C	Minneapolis/St.Paul, Minnesota; Lewistown, Montana
-25 to -20 F	-28.9 to -31.6 C	Northwood, Iowa; Nebraska
-20 to -15 F	-26.2 to -28.8 C	Des Moines, Iowa; Illinois
-15 to -10 F	-23.4 to -26.1 C	Columbia, Missouri; Mansfield, Pennsylvania
-10 to -5 F	-20.6 to -23.3 C	St. Louis, Missouri; Lebanon, Pennsylvania
-5 to 0 F	-17.8 to -20.5 C	McMinnville, Tennessee; Branson, Missouri
0 to 5 F	-15.0 to -17.7 C	Oklahoma City, Oklahoma; South Boston, Virginia
5 to 10 F	-12.3 to -14.9 C	Little Rock, Arkansas; Griffin, Georgia
10 to 15 F	-9.5 to -12.2 C	Tifton, Georgia; Dallas, Texas
15 to 20 F	-6.7 to -9.4 C	Austin, Texas; Gainesville, Florida
20 to 25 F	-3.9 to -6.6 C	Houston, Texas; St. Augustine, Florida
25 to 30 F	-1.2 to -3.8 C	Brownsville, Texas; Fort Pierce, Florida
30 to 35 F	1.6 to -1.1 C	Naples, Florida; Victorville, California
35 to 40 F	4.4 to 1.7 C	Miami, Florida; Coral Gables, Florida
above 40 F	above 4.5 C	Honolulu, Hawaii; Mazatlan, Mexico

Selecting the Right Grasses for Channel Lining

According to Temple, *et al.* (1987), the selection of grass species for use in channels is based on important site-specific factors, including: (1) soil texture, (2) depth of underlying material, (3) management requirements of vegetation, (4) climate, (5) slope, and (6) type of structure or engineering design. The expected flow rates, salt tolerance in northern areas, availability of seed, ease of stand establishment, species or vegetative growth habit, plant cover, and persistence of established species, are other factors that also should be considered in selecting appropriate grasses necessary for stable channel designs for use along roads. Channel construction should be scheduled to allow establishment of the grass stand before subjecting the channel to excessive flows. The uses of modern channel lining systems, as discussed below, help alleviate this problem. The establishment of permanent covers involves liming and fertilizing, seed bed preparation, appropriate planting dates, seeding rates, and mulching.

Plants for Temporary Channel Linings

Based on flow tests on sandy clay channels, Temple, *et al.* (1987) recommends wheat (*Triticum aestivum L.*) for winter and sudangrass [*Sorghum sudanensis* (Piper) *Hitchc.*] for late-summer temporary covers. These temporary covers have been shown to rapidly increase the permissible discharge rate to five times that of an unprotected channel. Other recommended annual and short-lived perennials that can be used for temporary channel linings include:

- barley (*Hordeum vulgare L.*), noted for its early fall growth;
- oats (*Avena) sativa L.*), in areas of mild winters;
- mixtures of wheat, oats, barley, and rye (*Secale cereale L.*);
- field bromegrass (*Bromus spp.*); and
- ryegrasses (*Lolium spp.*).

Summer annuals, including German and foxtail millets (*Setaria spp.*), pearl millet [*Pennisetum americanurn (L.) Leeke*], and certain cultivated sorghums other than sudangrass, may also be used for temporary mid- to late-summer covers, according to Temple, *et al.* (1987). Since millets do not continue to grow as aggressively as sorghums after mowing, they may leave a more desirable, uniformly thin mulch for subsequent permanent seeding. Temporary seedings involve minimal cultural treatment, short-lived but quick germinating species, and little or no maintenance. The temporary covers should be close-drilled stands and not be allowed to go to seed. The protective cover provided by the temporary vegetation should provide stalks, roots, and litter into which permanent grass seeds can be drilled the following spring or fall.

Plants for Permanent Channel Linings
Many grasses can be used for permanent vegetative channel linings. Temple, *et al.* (1987) lists the following tight-sod-forming grasses as the most preferred warm- and cool-season grasses for channel linings: bermudagrass [*Cyodon dactylon var dactylon (L.) Pers*.], bahiagrass (*Paspalum notatum Fluggle*), buffalograss [*Buchloe dactyloides (Nutt.) Enge1m*.], intermediate wheatgrass [*Agropyron intermedium (Host) Beauv.*], Kentucky bluegrass (*Poa ratensis L.*), reed canarygrass (*Phalaris arundinacea L.*), smooth bromegrass, (*Bromus inermis Leyss.*), vine mesquitegrass (*Panicum obtusum H.B.K.*), and Western wheatgrass (*Agropyron Smithii Rydb.*). These grasses are among the most widely used species for channel linings and grow well on a variety of soils. A grass mixture should include species adapted to the full range of soil moisture conditions on the channel side slopes. The local NRCS and University Extension offices know the best soil-binding grass species for a particular areas, along with the associated planting and maintenance information. The most important characteristic of the selected grasses is its ability to survive and thrive in the channel environment.

Bermudagrass is probably the most widely used grass in the southern region of the U.S. It will grow on many soil types, but may require extra management. It forms a dense and persistent sod, if managed properly. Temple, *et al.* (1987) recommend that when bermudagrass is used, winter-hardy varieties should be obtained. Improved varieties, such as "Coastal," "Midland," "Greenfield," "Tifton," and "Hardie," do not produce seed, and must be established by sprigging. Where winters are mild, channels can be established quickly with seed of "Arizona Common" bermudagrass. "Seed of bermudagrass," a new seed-propagated variety with greater winter hardiness than Arizona Common, should now be available commercially. Bermudagrass is not shade tolerant and should not be used in mixtures containing tall grasses. However, the inclusion of winter annual legumes such as hairy vetch (*Vicia villosa Roth.*), narrowleaf vetch [*V. sativa L. subspecies nigra (L.) Ehrh.*], and/or a summer annual such as Korean lespedeza (*Lespedeza stipulacea Maxim.*) may be beneficial to stand maintenance.

The selection of grasses used in channels often depends on availability of seed or plant material. Chronic national seed shortages of some warm-season grasses, especially seed of native species, have often led to planting seed marginally suited to site situations. Lack of available seed of desired grass species and cultivars adapted to specific problem sites is a major constraint often delaying or frustrating seeding programs. In addition to the grass species or base mixture of grasses used for erosion control, carefully selected special-use plants may be added for a specific purpose or situation. Desirable wildlife food plants may be included in the mixture if they do not detrimentally compete with the base grasses used for erosion control. Locally adapted legumes are often added if they are compatible with the grasses and noncompetitive. Additional information on establishment and maintenance of grass-lined channels is provided in Temple, *et al*, (1987).

Determination of Channel Design Parameters
The conditions governing the stability of a grass-lined open channel are the channel geometry and slope, the erodibility of the soil boundary, and the properties of the grass lining that relate to flow retardance potential and boundary protection.

Vegetation Parameters
The design of a stable grass-lined open channel needs to consider the effective stress imposed on the soil layer (Temple, *et al*, 1987). This requires the determination of two vegetation parameters: 1) the retardance curve index (C_I) which describes the potential of the vegetal cover to develop flow resistance, and 2) the vegetation cover factor (C_f) which describes the degree to which the vegetation cover prevents high velocities and stresses at the soil-water interface. These are described below.

Retardance Potential. The parameter describing the retardance potential of a vegetal cover is the retardance curve index, C_I. This parameter determines the limiting vegetation stress. Its relation to the measurable physical properties of the vegetal cover is given by:

$$C_I = 2.5\left(h\sqrt{M}\right)^{\frac{1}{3}}$$

where:

h is the representative stem length
M is the stem density in stems per unit area.

When consistent units are used, the relation is dimensionless. This factor is commonly used in the following equation to estimate the maximum allowable stress on the vegetation (τ_{va}, in lb/ft^2):

$$\tau_{va} = 0.75 C_I$$

The stem length will usually need to be estimated directly from knowledge of the vegetation conditions at the time of anticipated maximum flow. When two or more grasses with widely differing growth characteristics are involved, the representative stem length is determined as the root mean square of the individual stem lengths.

When this equation is used to estimate the retardance potential, an estimate of the stem density is also required. The reference stem densities shown in Table 6 may be used as a guide in estimating this parameter.

Table 6. Properties of Grass Channel Linings (Temple, *et al*. 1987)

Cover Factor (C_I) (good uniform stands)	Covers Tested	Reference stem density (M), stem/ft^2
0.90	bermudagrass	500
0.90	centipedegrass	500
0.87	buffalograss	400
0.87	kentucky bluegrass	350
0.87	blue grama	350
0.75	grass mixture	200
0.50	weeping lovegrass	350
0.50	yellow bluestem	250
0.50	alfalfa	500
0.50	lespedeza sericea	300
0.50	common lespedeza	150
0.50	sudangrass	50

Since cover conditions will vary from year to year and season to season, establishing an upper and a lower bound for the curve index (C_I) is often more realistic than selecting a single value. When this approach is taken, the lower value should be used in stability computations and the upper value should be used in determining channel capacity. Such an approach will normally result in satisfactory operation for lining conditions between the specified bounds. Whatever the approach used to obtain the flow retardance potential of the lining, the values selected should represent an average for the channel reach in question, since it will be used to infer an average energy loss per unit of boundary area for any given flow.

Vegetation Cover Factor. The vegetation cover factor, C_f, is used to describe the degree to which the vegetation cover prevents high velocities and stresses at the soil-water interface. Because the protective action described by this parameter is associated with the prevention of local erosion damage which may lead to channel unraveling, the cover factor should represent the weakest area in a reach, rather than an average for the cover type.

Observations of flow behavior and available data indicate that the cover factor is dominated by the density and uniformity of density in the immediate vicinity of the soil boundary. For relatively dense and uniform covers, uniformity of density is primarily dependent on the growth characteristics of the cover, which are in turn related to grass type. This relationship was used by Temple, *et al* (1987) in the development of Table 6. This table can not obviously account for such considerations as maintenance practices, or uniformity of soil fertility or moisture conditions.

Soil Parameters

Two soil parameters are required for the application of effective stress concepts to the design of stable lined or unlined channels having an erodible soil boundary: 1) soil grain roughness (n_s), and 2) allowable effective stress (τ_a). When the effective stress approach is used, the soil parameters are the same for both lined and unlined channels, satisfying sediment transport restrictions. The relations presented here were presented by Temple, *et al* (1987) and were taken from the SCS (1977) channel stability criteria: the desired parameters, soil grain roughness and allowable stress, are determined from basic soil parameters. Ideally, the basic parameters should be determined from tests on representative soil samples from the site.

For effective stress design, soil grain roughness is defined as the roughness associated with particles or aggregates of a size that may be independently moved by the flow at incipient channel failure. Although this parameter is expressed in terms of a flow resistance coefficient (n_s), its primary importance in design of vegetated channels is its influence on effective stress, as shown below. Its contribution to the total flow resistance of a grass-lined channel is usually negligibly small.

The allowable stress is key to the effective stress design procedure. It is defined as that stress above which an unacceptable amount of particle or aggregate detachment would occur.

Noncohesive Soil. Noncohesive soils are defined as fine- or coarse-grained, based on whether d75 (the diameter for which 75 percent of the material is finer) is less than, or greater than, 0.05 in. For fine-grained soils, the soil grain roughness and allowable effective stress are constant, while for a coarse-grained soil, these parameters are a function of particle size. The allowable effective stress and roughness parameters for noncohesive soils are given in Figures 10 and 11, as a function of particle size.

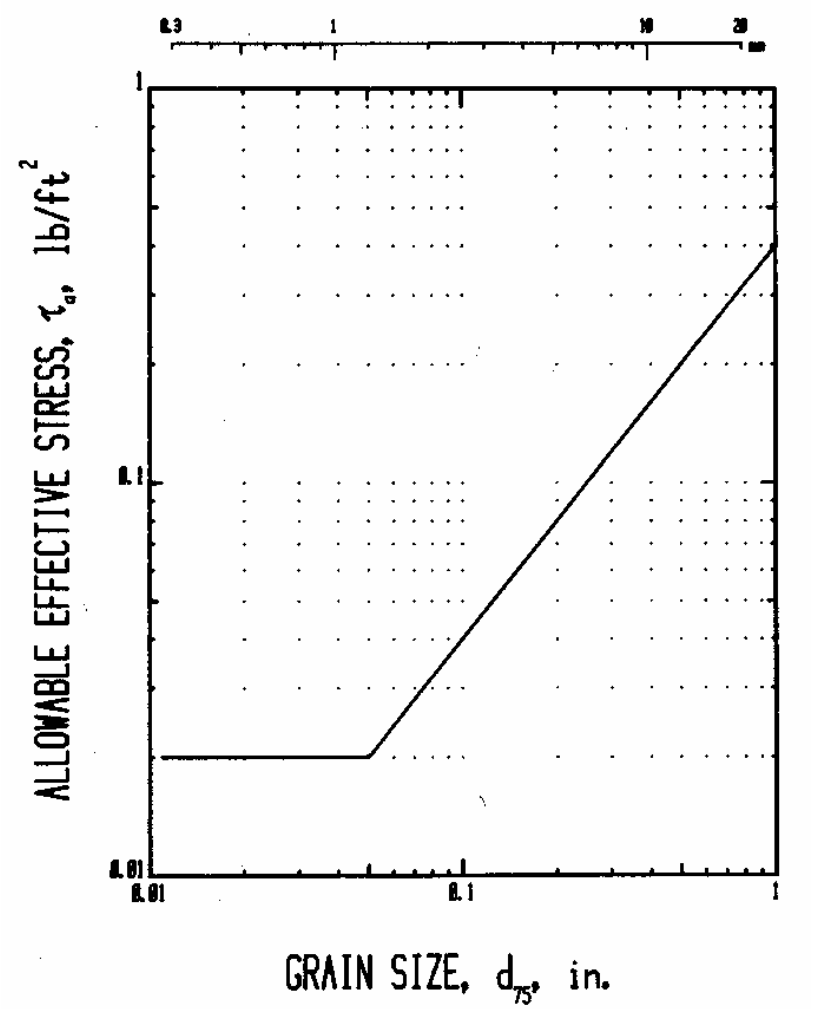

Figure 10. Allowable effective stress for noncohesive soils (Temple, *et al*. 1987).

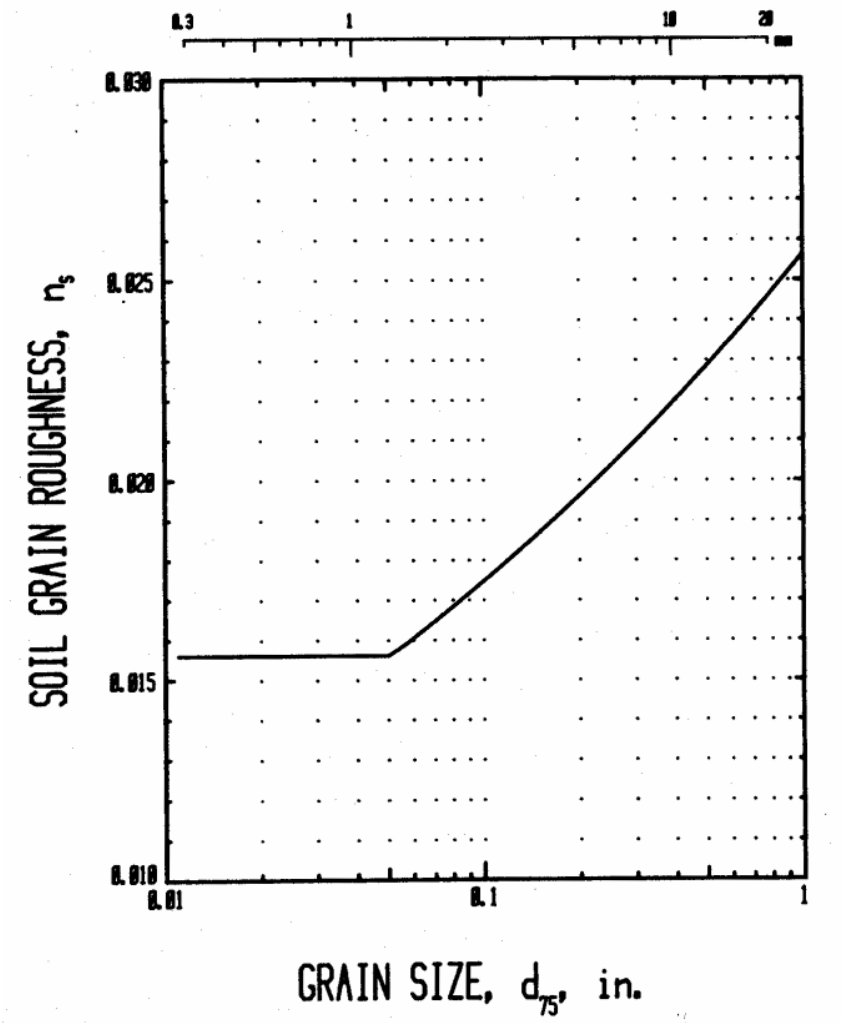

Figure 11. Soil grain roughness for noncohesive soils (Temple, *et al*. 1987).

Cohesive Soil. All cohesive soils are treated as fine-grained soils, having a constant soil grain roughness (about 0.0155, according to Figure 11). The allowable effective stresses presented here are taken directly from SCS (1977) permissible velocity design criteria. The soil properties required to determine the allowable effective stress are the soil's classification in the unified soil classification system, its plasticity index (I_w), and its void ratio (e). This calculation requires that a basic allowable effective stress (τ_{ab}) be determined from the soil classification and plasticity index. This basic value is then corrected for void ratio, according to the relation:

$$\tau_a = \tau_{ab} C_e^2$$

The basic allowable shear stress (τ_{ab}) is given in Figure 12, while the void ratio correction factor (C_e) is given in Figure 13. The soil classification information (plasticity index, I_w, and void ratio, e) are readily available for cohesive soils in standard soils references, and in Temple, *et al*. (1987).

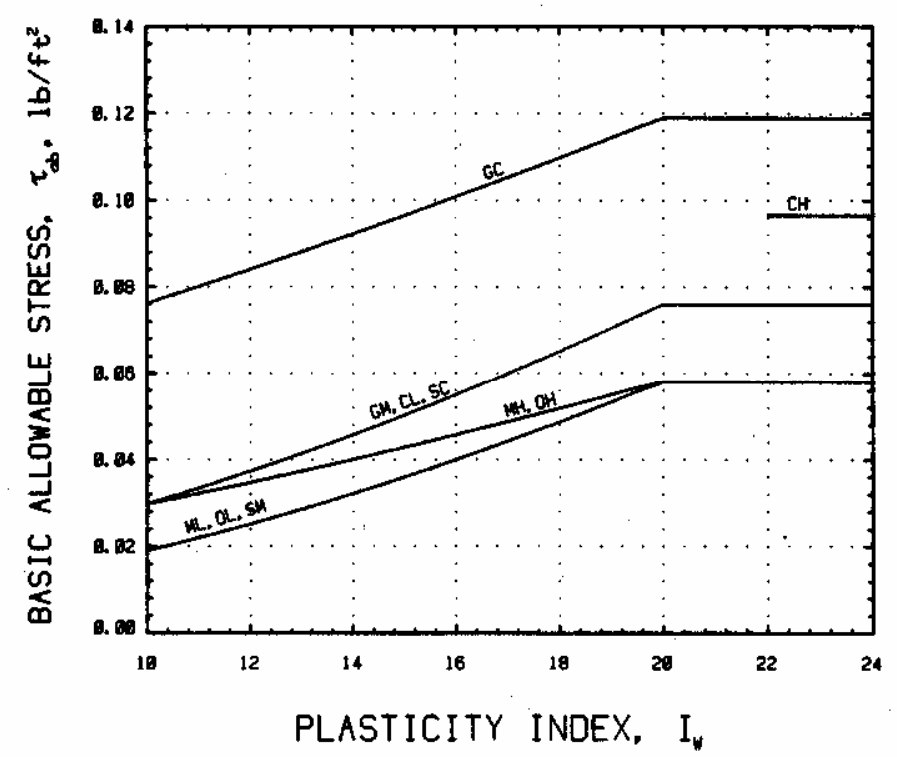

Figure 12. Basic allowable effective stress for cohesive soils (Temple, *et al*. 1987 and SCS 1977).

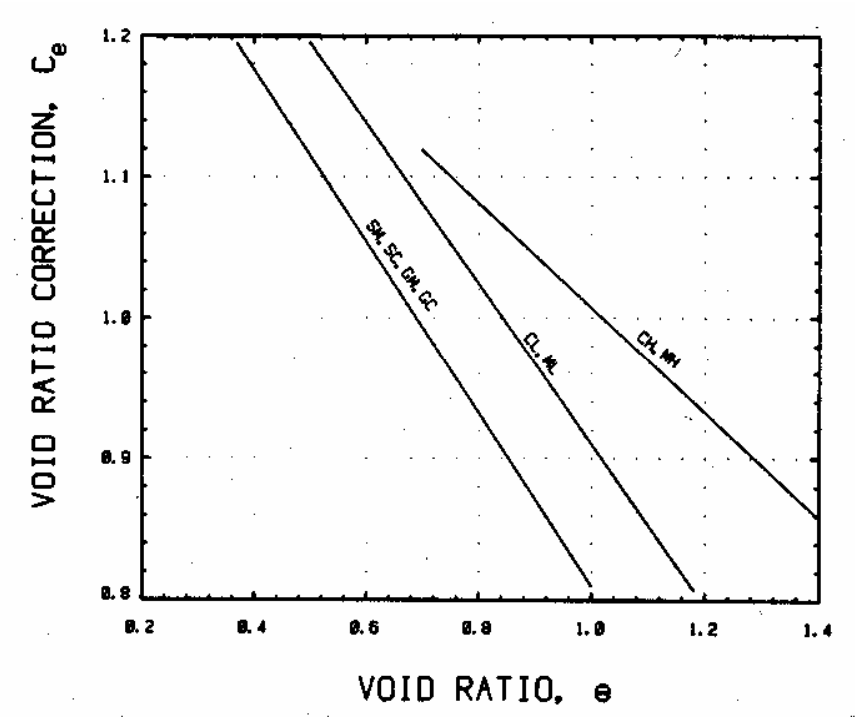

Figure 13. Void ratio correction factor for cohesive soils (Temple, *et al*. 1987 and SCS 1977).

Selection of Roughness Factor for Grass Lined Channels

The value of Manning's "n" in grasses is a function of grass type, and the product of velocity and hydraulic radius (VR). Grasses are divided into retardance classes based on their physical characteristics (height, width, density, etc.). Most sod forming grasses are classified as type C. These grasses can have "n" values ranging from 0.03 - 0.3 depending on VR, with a typical value of 0.03 in open channels. The following example shows how the correct n value is selected through a trial-and-error method, depending on the product of the velocity (V) and hydraulic radius (R).

Example Problem for the Selection of Roughness for Grass-Lined Channels

The appropriate Manning's "n" to use varies on the time frame: bare soil retention and vegetation establishment (short-term) and for fully grassed conditions (long-term) (Chow 1959). Bare soil conditions can be examined using the procedures presented earlier. Mature grass-lined channel roughness values can be determined using typical procedures as illustrated in the following example which shows how VR-n curves can be used for the proper selection of a roughness value for a grass-lined channel:

> Determine the roughness value for a 10-year design storm of 70 ft^3/sec (2 m^3/sec) in a grass-lined drainage channel having a slope of 0.05 ft/ft and a 4 foot (1.2 m) bottom width and 1:1 side slopes. The grass cover is expected to be in retardance group D.

Long-term design, based on vegetated channel stability:

- use $Q_{peak} = Q_{10year}$ = 70 ft^3/s (2 m^3/s)
- initially assume that $n_{vegetated}$ = 0.05

Determine the normal depth of flow, using Figure 7 (from Chow 1959):

$$AR^{\frac{2}{3}} = \frac{nQ}{1.49S^{0.5}} = \frac{0.05(70cfs)}{1.49(0.05)^{0.5}} = 10.51$$

and $b^{8/3} = (4\ ft)^{8/3} = 40.32$

therefore $AR^{2/3}/b^{8/3} = 10.51/40.32 = 0.26$

With a 1:1 side slope trapezoidal channel, the ratio of y/b from Figure 7 is 0.43, and the depth is therefore: 4(0.43) = 1.7 ft.

The cross-sectional area is therefore 9.7 ft^2, the velocity is (70 ft^3/sec)/(9.7 ft^2) = 7.2 ft/sec, P is 8.8 ft, and R is 9.7/8.8 = 1.1 ft. VR is therefore (7.2 ft/sec)(1.1 ft) = 7.9 ft^2/sec. From Figure 14, the estimated new value for n is therefore 0.032, using a retardance class of D. The depth must therefore be recalculated, using this new value for n:

$$AR^{\frac{2}{3}} = \frac{nQ}{1.49S^{0.5}} = \frac{0.032(70cfs)}{1.49(0.05)^{0.5}} = 6.72$$

and $b^{8/3} = (4\ ft)^{8/3} = 40.32$

therefore $AR^{2/3}/b^{8/3} = 6.72/40.32 = 0.17$

With a 1:1 side slope trapezoidal channel, the ratio of y/b from Figure 7 is 0.34, and the depth is therefore: 4(0.34) = 1.4 ft.

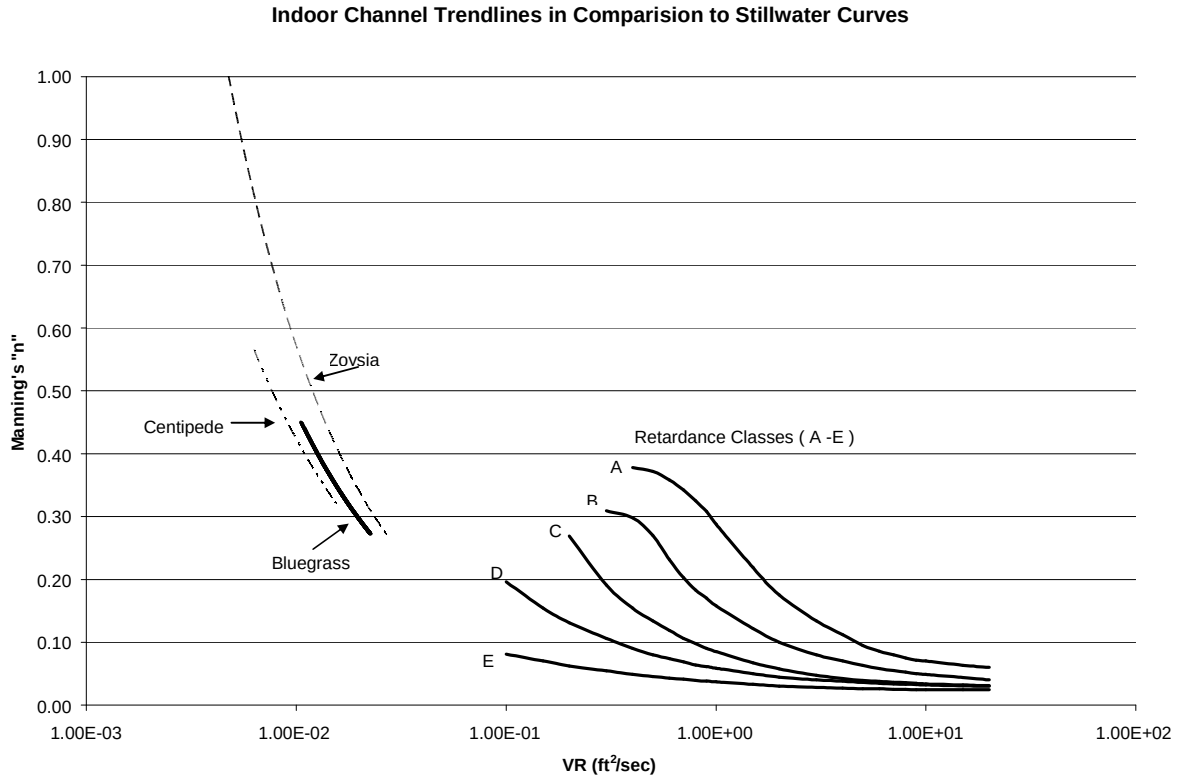

Figure 14. Hydraulic roughness of grass (Kirby 2003).

The area is therefore 7.6 ft^2, the velocity is 70/7.6 = 9.2 ft/sec, P is 8.0 ft, and R is 7.6/8.0 = 0.95 ft. The revised VR is therefore (9.2 ft/sec)(0.95 ft) = 8.7 ft^2/sec. Figure 14 shows that the revised value of n is still close to 0.032.

The maximum shear stress (using normal depth instead of hydraulic radius) is therefore:

$$\gamma DS = (62.4\ lb/ft^3)\ (1.4\ ft)\ 0.05\ ft/ft) = 4.4\ lb/ft^2$$

This channel would therefore be stable if the acceptable value is greater than this rather high value. A following discussion presents additional guidance on the selection and evaluation of a turf reinforcing mat that would likely be needed for this high shear stress condition. Currently, the use of channel lining mats protecting immature vegetation allows immediate protection of the sensitive soil boundary layer, as described in the following discussions. Also, free computer programs, such as supplied by North American Green (http://www.nagreen.com/), greatly help in the design of the most appropriate channel cross section and liner system.

Drainage Design using Turf-Reinforcing Mats

Current practice is to design channel linings based on shear stress and less on allowable velocity. Shear stress considers the weight of the water above the lining and therefore does a better job of predicting liner stability compared to only using velocity. However, allowable velocity and the flow regime (if the flow is supercritical or subcritical) still should be examined to minimize the occurrence of unusual conditions.

If a channel will have intermittent flows, it is common to use turf-reinforcing mats liners to increase the channel stability. However, if the channel will have perennial (or long-term) flows, grass will not be successful and mechanical liners must be used.

Installation of reinforced liner along thalweg of channel, with other material along sides (VA photo).

Large rocks for channel reinforcement and to reduce the velocity.

Plastic tarp, with coir logs, for a temporary liner and to slow the velocity.

Reinforced liner along channel thalweg.

Plastic tarp used as a temporary liner.

Examples of Channels Lined with Vegetation and other Materials

According to Croke (2000), drainage channel design using turf reinforcement mats must consider three phases: (1) the original channel in an unvegetated state to determine if the matting alone will provide the needed protection before the vegetation is established, (2) the channel in a partially vegetated state, usually at 50% plant density, and (3) the permanent channel condition with vegetation fully established and reinforced by the matting's permanent net structure. The basic shear stress equation can be modified to predict the shear stress applied to the soil beneath a channel mat (Temple, *et al*. 1987):

$$\tau_e = \gamma DS\left(1 - C_f\right)\left(\frac{n_s}{n}\right)^2$$

where:

τ_e = effective shear stress exerted on soil beneath vegetation
γ = specific weight of water (62.4 lbs/ft^3)
D = the maximum flow depth in the cross section (ft)
S = hydraulic slope (ft/ft)
C_f = vegetation cover factor (this factor is 0 for an unlined channel)
n_s = roughness coefficient of underlying soil
n = roughness coefficient of vegetation and/or erosion control blanket (if vegetated, or not)

The flow depth, rather than the hydraulic radius, is used in this equation because this will result in the maximum shear stress developed, rather than the average stress (Temple, *et al.* 1987), plus the depth value is very close to the hydraulic radius for most channels, especially as sheetflow conditions are approached. The cover factor is a function of the grass and stem density, as previously described, while the roughness coefficients are standard Manning's roughness values for channels. The permissible shear stress for a liner mat should also be available from manufacture's specifications, but it will vary for different growth phases, if vegetated. Obviously, the liner matting

significantly reduces the shear stress exerted on the soil. The following tables summarize some typical values for some of these equation parameters for turf-reinforcing mats, for different products supplied by North American Green (from www.nagreen.com). Included on these tables are conservation factor, C, values used in RUSLE for slope protection, along with roughness coefficients and maximum permissible shear stress values used in channel lining analyses. Only the P300 and C350 mats shown here are permanent liners and therefore have different values for different plant growth stages.

S75 straw erosion control blanket (12 month life; 314 g/m^2 mass per unit area)

RUSLE Conservation coefficients (C):		Channel Roughness Coefficients (n)	
	Slope Gradient (S)	Flow depth	Manning's n (unvegetated)
Slope length (L)	All ≤ 3:1 slope:	≤ 0.50 ft (0.15 m)	0.055
≤ 20 ft (6 m)	0.029	0.50 – 2.00 ft	0.055 - 0.021
20 to 50 ft	0.110	≥ 2.00 ft (0.60 m)	0.021
≥ 50 ft (15 m)	0.190	Max. permissible shear stress: 1.55 lbs/ft^2 (74.4 Pa)	

S150 straw erosion control blanket (12 month life; 323 g/m^2 mass per unit area)

RUSLE Conservation coefficients (C):			Channel Roughness Coefficients (n)	
	Slope Gradient (S)		Flow depth	Manning's n (unvegetated)
Slope length (L)	≤ 3:1	3:1 to 2:1	≤ 0.50 ft (0.15 m)	0.055
≤ 20 ft (6 m)	0.004	0.106	0.50 – 2.00 ft	0.055 - 0.021
20 to 50 ft	0.062	0.118	≥ 2.00 ft (0.60 m)	0.021
≥ 50 ft (15 m)	0.120	0.180	Max. permissible shear stress: 1.75 lbs/ft^2 (84.0 Pa)	

S150BN straw erosion control blanket (10 month life; 352 g/m^2 mass per unit area)

RUSLE Conservation coefficients (C):			Channel Roughness Coefficients (n)	
	Slope Gradient (S)		Flow depth	Manning's n (unvegetated)
Slope length (L)	≤ 3:1	3:1 to 2:1	≤ 0.50 ft (0.15 m)	0.055
≤ 20 ft (6 m)	0.00014	0.039	0.50 – 2.00 ft	0.055 - 0.021
20 to 50 ft	0.010	0.070	≥ 2.00 ft (0.60 m)	0.021
≥ 50 ft (15 m)	0.020	0.100	Max. permissible shear stress: 1.85 lbs/ft^2 (88.0 Pa)	

SC150 straw erosion control blanket (24 month life; 424 g/m^2 mass per unit area)

RUSLE Conservation coefficients (C):				Channel Roughness Coefficients (n)	
	Slope Gradient (S)			Flow depth	Manning's n (unvegetated)
Slope length (L)	≤ 3:1	3:1 to 2:1	≥ 2:1	≤ 0.50 ft (0.15 m)	0.050
≤ 20 ft (6 m)	0.001	0.048	0.100	0.50 – 2.00 ft	0.050 - 0.018
20 to 50 ft	0.051	0.079	0.145	≥ 2.00 ft (0.60 m)	0.018
≥ 50 ft (15 m)	0.100	0.110	0.190	Max. permissible shear stress: 2.00 lbs/ft^2 (96.0 Pa)	

SC150BN straw erosion control blanket (18 month life; 424 g/m^2 mass per unit area)

RUSLE Conservation coefficients (C):				Channel Roughness Coefficients (n)	
	Slope Gradient (S)			Flow depth	Manning's n (unvegetated)
Slope length (L)	≤ 3:1	3:1 to 2:1	≥ 2:1	≤ 0.50 ft (0.15 m)	0.050
≤ 20 ft (6 m)	0.00009	0.029	0.063	0.50 – 2.00 ft	0.050 - 0.018
20 to 50 ft	0.005	0.055	0.092	≥ 2.00 ft (0.60 m)	0.018
≥ 50 ft (15 m)	0.010	0.080	0.120	Max. permissible shear stress: 2.10 lbs/ft^2 (100 Pa)	

C125 coconut fiber erosion control blanket (36 month life; 274 g/m^2 mass per unit area)

RUSLE Conservation coefficients (C):				Channel Roughness Coefficients (n)	
	Slope Gradient (S)			Flow depth	Manning's n (unvegetated)
Slope length (L)	≤ 3:1	3:1 to 2:1	≥ 2:1	≤ 0.50 ft (0.15 m)	0.022
≤ 20 ft (6 m)	0.001	0.029	0.082	0.50 – 2.00 ft	0.022 – 0.014
20 to 50 ft	0.036	0.060	0.096	≥ 2.00 ft (0.60 m)	0.014
≥ 50 ft (15 m)	0.070	0.090	0.110	Max. permissible shear stress: 2.25 lbs/ft^2 (108 Pa)	

C125BN coconut fiber erosion control blanket (24 month life; 360 g/m^2 mass per unit area)

RUSLE Conservation coefficients (C):				Channel Roughness Coefficients (n)	
	Slope Gradient (S)			Flow depth	Manning's n (unvegetated)
Slope length (L)	≤ 3:1	3:1 to 2:1	≥ 2:1	≤ 0.50 ft (0.15 m)	0.022
≤ 20 ft (6 m)	0.00009	0.018	0.050	0.50 – 2.00 ft	0.022 – 0.014
20 to 50 ft	0.003	0.040	0.060	≥ 2.00 ft (0.60 m)	0.014
≥ 50 ft (15 m)	0.007	0.070	0.070	Max. permissible shear stress: 2.35 lbs/ft^2 (112 Pa)	

P300 polypropylene fiber erosion control blanket (permanent use; 456 g/m^2 mass per unit area)

RUSLE Conservation coefficients (C):	Slope Gradient (S)			Channel Roughness Coefficients (n)		Maximum Permissible Shear Stress	
Slope length (L)	≤ 3:1	3:1 to 2:1	≥ 2:1	Flow depth	Manning's n (unvegetated)		
≤ 20 ft (6 m)	0.001	0.029	0.082	≤ 0.50 ft (0.15 m)	0.049 – 0.034	Unvegetated	3.00 lb/ft^2 (144 Pa)
20 to 50 ft	0.036	0.060	0.096	0.50 – 2.00 ft	0.034 – 0.020	Partially vegetated	5.50 lb/ft^2 (264 Pa)
≥ 50 ft (15 m)	0.070	0.090	0.110	≥ 2.00 ft (0.60 m)	0.020	Fully vegetated	8.00 lb/ft^2 (383 Pa)

Additional permissible shear stress information for vegetated North American Green products (permanent liners):

	Manning's roughness coefficient (n) for flow depths:			Maximum Permissible Shear Stress	
Vegetated blanket type[1]:	0 to 0.5 ft	0.5 to 2 ft	>2 ft.	Short duration (<2 hours peak flow)	Long duration (>2 hours peak flow)
C350 Phase 2	0.044	0.044	0.044	6.00 lb/ft^2 (288 Pa)	4.50 lb/ft^2 (216 Pa)
P300 Phase 2	0.044	0.044	0.044	5.50 lb/ft^2 (264 Pa)	4.00 lb/ft^2 (192 Pa)
C350 Phase 3	0.049	0.049	0.049	8.00 lb/ft^2 (384 Pa)	8.00 lb/ft^2 (384 Pa)
P300 Phase 3	0.049	0.049	0.049	8.00 lb/ft^2 (384 Pa)	8.00 lb/ft^2 (384 Pa)

[1] Phase 2 is 50% stand maturity, usually at 6 months, while Phase 3 is mature growth

Values of C_f, the grass cover factor, were given in Table 6 (Temple, *et al*. 1987). They recommend multiplying the stem densities given by 1/3, 2/3, 1, 4/3, and 5/3, for poor, fair, good, very good, and excellent covers, respectively. C_f values for untested covers may be estimated by recognizing that the cover factor is dominated by density and uniformity of cover near the soil surface: the sod-forming grasses near the top of the table have higher C_f values than the bunch grasses and annuals near the bottom. For the legumes tested (alfalfa and lespedeza sericea), the effective stem count for resistance (given on the table) is approximately five times the actual stem count very close to the bed. Similar adjustment may be needed for other unusually large-stemmed, branching, and/ or woody vegetation.

As an example, consider the following conditions for a mature buffalograss on a channel liner mat:

$\tau_o = \gamma DS$ = 2.83 lb/ft^2 (previously calculated), requiring a NAG P300 permanent mat, for example

n_s for the soil is 0.016
n for the vegetated mat is 0.042
C_f for the vegetated mat is 0.87

The permissible shear stress for the underlying soil is 0.08 lb/ft^2

Therefore:

$$\tau_e = 2.83(1 - 0.87)\left(\frac{0.016}{0.042}\right)^2 = 0.053 \text{ lb/ft}^2$$

The calculated shear stress being exerted on the soil beneath the liner mat must be less than the permissible shear stress for the soil. In this example, the safety factor is 0.08/0.053 = 1.5 and the channel lining system is expected to be stable.

An example of a permanent channel design and the selection of an appropriate reinforced liner is given below. The following example is for a channel that collects runoff from 14.6 acres. This channel is 900 ft. long and has an 8% slope. The peak discharge was previously calculated to be 29 ft^3/sec.

Using the Manning's equation and the VenTe Chow (1959) shortcut on channel geometry (Figure 7):

$$AR^{\frac{2}{3}} = \frac{nQ}{1.49S^{0.5}}$$

Where n = 0.02
Q = 29 CFS
S = 8% (0.08)

$$AR^{\frac{2}{3}} = \frac{(0.02)(29)}{1.49(0.08)^{0.5}} = 1.38$$

The following drawing illustrates the channel components for this basic analysis:

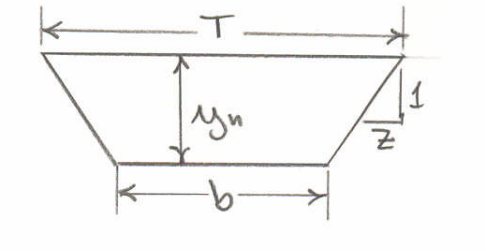

Figure 7 can be used to determine the normal depth (y_n) for many combinations of bottom with (b), and side slope (z). As an example, assume that the bottom width is 5 ft. and the side slope parameter, z, is 3. The calculated $AR^{2/3}$ value (1.38) needs to be divided by $b^{8/3}$ ($5^{8/3}$ = 73.14) for the shape factor used in Figure 7. This value is therefore: 1.38/73.14 = 0.018. For a side slope of z = 3, the figure indicates that the ratio of the depth to the bottom width (y/b) is 0.088. In this example, the bottom width was 5 ft, so the normal depth is: y_n = 0.088 (5 ft.) = 0.44 ft., which is only 5.3 inches. The following shows these dimensions on the channel cross-section:

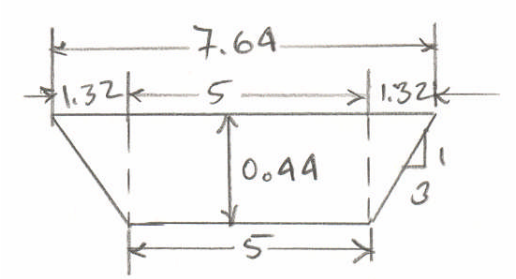

It is now possible to calculate the velocity and shear stress associated with this set of channel conditions:

$A = [(7.64+5)/2]\ (0.44) = 2.78\ ft^2$
$V = Q/A = 29\ ft^3/sec/2.78\ ft^2 = 10.4\ ft/sec$
$R = A/P$, and $P = 5 + 2(3.16)(0.44) = 7.78$ ft.; $R = A/P = 2.78\ ft^2/7.78$ ft. $= 0.36$ ft.

and $\tau = \gamma RS = (62.4 lb/ft^3)(0.36\ ft.)(0.08) = 1.8\ lb/ft^2$

With a velocity of 10.4 ft/sec and a shear stress of 1.8 lb/ft^2, it is obvious that some type of channel reinforcement will be needed (refer to Table 2), or another design option. Using Figure 7, plus liner information (such as listed previously), it is possible to create a simple spreadsheet with multiple cross section and liner alternatives, as shown in Table 7. Table 7 shows the unvegetated conditions and calculations, along with the phase 2 and phase 3 vegetation conditions, for several channel cross-sections, considering both NAG P300 and C350 permanent channel liner mats. The shear stress values are calculated using the normal depth of flow, for worst-case design conditions, and not the hydraulic radius.

Table 7. Characteristics for Alternative Designs for Drainage Channel (Q = 29 ft^3/sec and S = 8%)

		Unvegetated NAG P300, n = 0.02 (allowable shear stress = 3.0 lb/ft^2) [data not given for C350, assumed to be similar to P300 for this example]					Channel with Reinforced Liner and Vegetation						
Bottom width (b), ft	Side slope (z)	Normal depth (y_n), ft	Top width (T), ft	Hydraulic radius (R), ft	Shear stress (τ), lb/ft^2 (using depth)	Velocity (V), ft/sec	Assumed NAG material and growing conditions	Manning's roughness (n)	Normal depth (y_n), ft	Shear stress (τ), lb/ft^2 (using depth and peak Q)	Peak Velocity (V), ft/sec	Allowable shear stress for NAG product (short and long exposures), lb/ft^2	Effective soil shear stress (τ_e), n_s = 0.016; C_f = 0.50 phase 2 C_f = 0.87 phase 3
3	1	0.63	4.3	0.48	3.1	12.7	P300 phase 2	0.044	0.80	4.0	9.5	5.5/4.0	0.26
							P300 phase 3	0.049	0.89	4.4	8.4	8.0/8.0	0.06
6	4	0.31	8.5	0.26	1.5	12.9	P300 phase 2	0.044	0.57	2.8	6.1	5.5/4.0	0.19
							P300 phase 3	0.049	0.65	3.2	5.2	8.0/8.0	0.04
8	4	0.30	10.4	0.14	1.5	11.0	P300 phase 2	0.044	0.54	2.7	5.3	5.5/4.0	0.18
							P300 phase 3	0.049	0.88	4.4	3.4	8.0/8.0	0.06
5	3	0.44	7.6	0.36	2.2	10.4	C350 phase 2	0.044	0.66	3.3	6.3	6.0/4.5	0.22
							C350 phase 3	0.049	0.70*	3.5*	5.8*	8.0/8.0	0.05*
6	1.5	0.43	7.3	0.38	2.1	10.1	C350 phase 2	0.044	0.68	3.4	6.1	6.0/4.5	0.22
							C350 phase 3	0.049	0.72	3.6	5.7	8.0/8.0	0.05
10	3	0.26	11.6	0.26	1.3	10.4	C350 phase 2	0.044	0.49	2.4	5.2	6.0/4.5	0.16
							C350 phase 3	0.049	0.52	2.6	4.8	8.0/8.0	0.04

* example calculations for permanent C350 liner, 5 ft bottom width, z=3 side slope, and phase 3 vegetation plant stage (mature):

$$AR^{\frac{2}{3}} = \frac{nQ}{1.49S^{0.5}} \frac{(0.049)(29)}{1.49(0.08)^{0.5}} = 3.38$$

$b^{8/3} = 5^{8/3} = 73.1$

$AR^{2/3}/b^{8/3} = 3.38/73.1 = 0.046$

With z = 3, y/b = 0.14

Therefore $y_n = 0.14\ (5) = 0.7$ ft

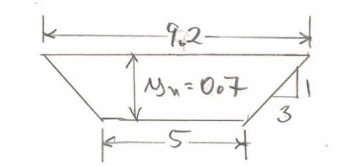

A = [(5+9.2)/2] (0.7) = 4.97 ft^2

P = 5 + 2(1.21) = 7.42 ft

R = A/P = 4.97/7.42 = 0.67

$\tau = \gamma RS = (62.4 lb/ft^3)(0.67\ ft.)(0.08) = 3.34\ lb/ft^2$ (analysis case using hydraulic radius)

$\tau = \gamma DS = (62.4 lb/ft^3)(0.70\ ft.)(0.08) = 3.49\ lb/ft^2$ (design case using normal depth)

V = Q/A = 29 ft^3/sec/4.97 ft^2 = 5.8 ft/sec

$$\tau_e = \gamma DS\left(1 - C_f\right)\left(\frac{n_s}{n}\right)^2 = 3.49 lb/ft^2 \left(1 - 0.87\right)\left(\frac{0.016}{0.049}\right)^2 = 0.048 lb/ft^2$$

$n_s = 0.016$; $C_f = 0.87$ phase 3

Based on these calculations, either the P300 or the C350 liner will be suitable for most conditions for this example. When newly placed, with no vegetation growth, the Manning's n roughness is 0.02 for these liners. The maximum calculated maximum shear stress is 3.1 lb/ft^2 for the narrowest cross section examined, slightly greater than the maximum allowable value of 3.0 lb/ft^2. The calculated shear stresses are less than this allowable maximum value for the other cross-sections. Therefore, one of the wider channels should be used. Unfortunately, the velocities are all very high, ranging from 10.1 to 12.9 ft/sec before the establishment of vegetation. The use of check dams is therefore highly recommended for this channel. These can range from coir logs, to rock check dams.

The calculations after vegetative growth show that the either liner is also acceptable. A range of conditions were examined for phase 2 (50% stand maturity) and phase 3 (mature growth), with Manning's roughness values of 0.044 and 0.049. The smallest (and steepest side sloped) channel resulted in the highest shear stress of 4.4 lb/ft^2, less than the maximum acceptable values. The short exposure critical values are for peak flows of <2 hours peak flow durations. After mature plant establishment in the channel, the maximum allowable shear stress increases to 8.0 lb/ft^2 for all conditions. The effective soil shear stress is also shown, which would be applicable for temporary channel liners. During the phase 2 plant growth stage (50% plant growth), the resulting values are larger than typical soil tolerance conditions, while they are acceptable during the phase 3 growth stage (mature plant growth). This emphasizes the need for a permanent liner in this case where the additional protection provided by the vegetation is not necessary. The steep slope (8% in this case) results in these relatively extreme solutions. If the slope for this example was about 2%, or less, temporary liners may be suitable (assuming that suitable growth conditions exist).

Summary

This chapter reviewed several techniques for designing stable channels. The shear stress method was shown to be generally necessary for channel design, compared to only using an allowable velocity approach. However, liner vegetation in erosion resistant soils may still fail due to vegetation damage, requiring careful plant selection, and possibly turf-reinforcing mats.

Chapter 2: Historical Use of Grass Swales for Stormwater Quality Control

Introduction

The treatment of stormwater is becoming more demanding as land development and urbanization increase nationwide. Urbanization changes the dynamics of stormwater conveyance systems by increasing the amounts of impervious areas. Impervious surfaces (such as a paved streets or parking lots) significantly reduce stormwater infiltration, resulting in increased stormwater runoff volumes and associated contaminant discharges. Even low density residential areas (less than 4 units/hectare) can have significant impacts on water quality by increasing phosphorus discharges 5 to 10 times over undisturbed forested areas (Dennis 1985). Moreover, urbanization radically changes the stream hydrologic balance. Research conducted by Sovern and Washington (1997) showed that the frequency of high flow rates in urbanized areas can be 10 to 100 times more than in predevelopment areas in Western Washington. They also reported decreases of low flows during dry periods, and increases in the sediment and pollutant discharges from urbanized watersheds.

Among the various stormwater management practices, grass swales are cost efficient and a proven method to treat stormwater runoff. A grass swale is a broad, shallow open channel covered by dense vegetation on the sides and bottom of a channel as an alternative to conventional stormwater conveyance such as curbs and gutters (Kirby 2003). Grass swales are often the preferred stormwater design control practice over other practices particularly because of performance and low cost, but many public works departments and developers resist their use due to perceived maintenance issues and the implication of substandard developments. Grass swales can be applied in most regions of the country where grass can be established and maintained in local climates and soils, and where sufficiently frequent rains occur for irrigation. They are not applicable in arid areas where insufficient moisture is available to keep the grass healthy. Vegetated swales cost much less to construct and maintain than curbs and gutters with underground storm sewers. As an example, a 10 ft wide, 1-1/2 ft deep grass swale was reported to have an average cost of about $12 per ft (SEWRPC 1991), while a a 36 inch diameter concrete pipe costs about $50 per ft (Heaney, *et al*. 2001). Curbs and gutter costs plus inlet costs would still have to be added to the conventional drainage system costs. SEWRPC (1991) estimated the annual maintenance costs for grass swales to be about $0.60 per ft per year. Conventional drainage pipes also have maintenance costs associated with cleaning the inlets and pipes of sediment, plus other periodic repairs. Overall, cost comparisons of swales with curb and gutter systems always show significant cost savings if swales are used (Heaney, *et al*. 2001). Besides the cost savings, existing natural features and processes can be utilized and integrated into the grass swale system to treat stormwater, rather than constructing and installing other more expensive stormwater controls, if properly planned prior to urbanization.

Many studies have shown that grass swales are an effective stormwater control practice in reducing runoff volume, sediments (total suspended solids, etc), nutrients (nitrate and phosphate), heavy metals (copper, cadmium, lead, and others), hydrocarbons, oil and grease. Particulates and other pollutants can have mass removal efficiencies ranging from 60 to 90%, as reported in numerous studies on both experimental and actual grass swales. For instance, Khan *et al.* (1992) observed average oil and grease removals of greater than 75% and an average total petroleum hydrocarbon removal of greater than 74% on a 60 m (196 ft) long grass swale. A number of researchers have concluded that grass swales are an effective method for treating stormwater based on actual measurements.

The Department of Civil and Environmental Engineering has been conducting research investigating the effectiveness of grass swales for treating stormwater pollutants, supported by the Water Environment Research Foundation (WERF) and the University Transportation Center of Alabama (UTCA). The prior WERF-supported research conducted by Johnson *et al.* (2003) focused on the removal of stormwater heavy metals (Cd, Cr, Cu, Pb, Fe, Hg, Ni, and Zn) and hydraulic characteristics of shallow open channel flow in grass swales.

The current UTCA-supported research provides information to (1) understand the effectiveness of grass swales for different sized particles, (2) understand the associated effects of different variables on these removals, and (3) to develop a predictive model in sediment transport in grass swales.

To achieve these objectives, experimental grass swales were constructed and tested in an indoor greenhouse facility (Kirby 2003). The sediment-water mixture of known sediment concentrations of sieved sands and fine particles of silica were used to simulate sediment characteristics of stormwater. For the preliminary experiments, 108 samples were collected and analyzed for turbidity, total solids, and particle size distributions to investigate the effects of swale length, grass type, flow rate, slope, and duration of the experiments. After completing the initial tests, additional experiments were conducted, with 108 samples collected and analyzed for total suspended solids, total dissolved solids, and total solids greater than and less than 106 µm, plus those listed for the first set of experiments. Using the results obtained from the second set of experiments, a predictive model of sediment transport in grass swales was developed. This model is similar to past models developed by Barfield *et al*. (1979) and Deletic (2001), but is more detailed due to the investigations of very small particle sizes and it is based on actual experimental conditions in grass swales having different height grasses. The main feature of the model is that it combines recently developed swale hydraulic information by Kirby (2003) and conventional particle settling information. The experimental tests determined the varying efficiencies of trapping different particle sizes under different hydraulic conditions. Particles from about 1 to 425 µm in diameter were included in these tests.

This report also describes stormwater monitoring at a full-size outdoor grass swale (116 ft long) located adjacent to the Tuscaloosa, Alabama, City Hall during 13 storm events. Sixty nine samples were collected during these events from August to December 2004 and analyzed for turbidity, total solids, total suspended solids, total dissolved solids, and particle size distributions. Finally, the predictive model was compared with the analytical results obtained from the outdoor swale. It was found that initial sediment concentrations were also a significant factor in sediment transport. The final predictive model is therefore dependent on initial sediment concentration (low and high concentration categories) and particle size distribution, water depth (using Kirby's 2003 swale hydraulic measurements), grass height, particle settling rate (using Stoke's law), and swale length (to determine the frequency of particle settling along the length of the swale).

Terminology

The term grass swale refers to a vegetated, open channel stormwater management practice that comprises a grass-lined drainage channel. Grass filters and buffer strips applied in agricultural management practices are similar (EPA 1999; Pope and Stoltenberg 1991). The EPA Office of Water (1999) presents the following definition for these related control practices:

Grass Channel:

> "Grass channels are the most similar to a conventional drainage ditch, with the major differences being flatter slopes and longitudinal slopes, and a slower design velocity for water quality treatment of small storm events."

Dry Swale:

> "Dry swales are similar in design to bioretention areas. The existing soil is replaced with a sand/soil mix that meets minimum permeability requirements. An underdrain system is used under the soil bed. This system is a gravel layer that encases a perforated pipe. Stormwater treated in the soil bed flows through the bottom into the underdrain, which conveys treated stormwater to the drainage system."

Wet Swale:

> "Wet swales intersect the ground water, and behave almost like a linear wetland cell. This design variation incorporates a shallow permanent pool and wetland vegetation to provide treatment. This design also has potentially high pollutant removal. It cannot be used in residential or commercial settings because the shallow standing water in the swale is viewed as a potential nuisance by homeowners."

Vegetated Buffer Strip (VBF):

> R.P. Beasley (1978) describes a vegetated buffer strip as: "Areas seeded to grasses or legumes between strips of cultivated crops, the number and location of these are selected to give desired protection from erosion."

Filter Strip:

Anderson (1983) defines a filter strip as: "A strip or area of vegetation for removing sediment, organic matter, and other pollutants from runoff and wastewater."

Reported Pollutant Removal Efficiencies for Grass Swales

Numerous studies on both experimental and actual grass swales have reported a wide range of efficiencies in reducing stormwater sediments and other pollutants. One of the main reasons for these differences is that most studies only examined concentrations in the grass swales, and did not measure volume reductions. During very low flows where shallow flow depths occur in relation to the grass height, pollutant concentration reductions can be high. However, as the flow depth increases, especially to more than 4 or 5 times the grass height, concentration reductions are greatly reduced. However, infiltration of water is usually significant in a swale-drained area. Unfortunately, not all published research reports make it clear that they only considered concentration reductions and that they did not measure flow changes, and associated pollutant mass reductions.

Most of the studies reported relatively high efficiencies in sediment removal, ranging 60% to 90%, as shown in Table 8. For example, Woodard and Rock (1995) studied phosphorus and total suspended solids retention in buffer strips (which would have shallow flows). The areas draining to the buffer strips were composed of a residential area, but in different construction phrases. Therefore, the initial total suspended solids concentrations were very high, ranging from 700 mg/L to 3,700 mg/L. The buffer strip slopes ranged from 2.3% to 12.0%, and high reductions were observed for both phosphorus and total suspended solids, ranging from 60% to 97%. Beyond 98 ft (30 m), both phosphorus and total suspended solids concentrations reached background (irreducible) concentrations. They found higher percentage reductions when the initial phosphorus and total suspended solids concentrations were higher.

Studies show that the effectiveness of grass swales in reducing soluble nutrients and metals is significant, but is highly variable, as indicated in Table 8 (Goldberg 1993; Wang *et al*. 1981). Khan *et al.* (1992) recorded average oil and grease and total petroleum hydrocarbon removals of greater than 75% for a 197 ft (60 m) long grass swale. However, studies also show that bacteria levels could increase instead of decrease in grass swales (Goldberg 1993; Wang *et al*. 1981; Seattle Metro Washington Dept. of Ecology 1981). One explanation is that bacteria thrive in the warm swale soils (EPA 1999).

Table 8. Summary of Reported Efficiencies of Grass Swales (EPA 1999: Many of the reports were summarized by EPA, but the list was expanded to include new reports)

Study	Type	Total suspended solids (%)	Total phosphorus (%)	Total nitrogen (%)	Nitrate (%)	Metals (%)	Bacteria (%)
Goldberg (1993)	Grassed channel	67.8	4.5	N/A	31.4	42 to 62	-100
Seattle Metro and Washington Dept of Ecology (1992)	Grassed channel	60 to 83	29 to 45	N/A	25	46 to 73	-25
Wang *et al.* (1981)	Dry swale	80	N/A	N/A	N/A	70 to 80	-25
Dorman *et al.* (1989)	Dry swale	98	18	N/A	45	37 to 81	N/A
Harper (1988)	Wet swale	81 to 87	17 to 83	40 to 84	52 to 80	37 to 90	N/A
Kercher *et al.* (1983)	Dry swale	99	99	99	99	99	N/A
Koon (1995)	Wet swale	67	39	N/A	9	-35 to 6	N/A
Daniels and Gilliam (1996)	Dry swale	60 to 90	50	50	N/A	N/A	N/A
Dillaha *et al.* (1989)	Dry swale	70 to 84	61 to 79	54 to 73	N/A	N/A	N/A
Barrett *et al.* (1998)	Grass swale	25 to 80	N/A	N/A	N/A	N/A	N/A
Fletcher *et al.* (2002)	Grass swale	73 to 94	58 to 72	44 to 57	N/A	N/A	N/A
Horner and Mar (1982)	N/A	80	N/A	N/A	N/A	N/A	N/A
EPA (1999)	grass swale	81	9	38	N/A	42 to 71	N/A

Note: N/A = not available

Modeling

Despite the numerous studies that have discussed grass swale performance in reducing sediments and other pollutants, few have suggested a predictive model to describe sediment retention in the grass swales. The most cited mathematical model was developed in the 1970s at the University of Kentucky (in Lexington, USA), the "Kentucky model" (Tollner *et al*. 1976, Barfield *et al*. 1979, Hayes *et al*. 1984). Metal rods were used to simulate grass, and data were obtained by measuring sedimentation of very high concentrations of beads. Deletic (2001) suggested that the Kentucky model was not accurate for urban conditions, especially for smaller particles and low concentrations, and proposed an alternative approach.

Kentucky Model

According to the Kentucky model (Tollner, *et al*. 1976, Barfield, *et al*. 1979, Hayes, *et al*. 1984), the grass strip is divided into four separate zones: A, B, C, and D as shown in Figure 15.

- Zone A: All sediments are transported.
- Zone B: sediment is deposited all along the deposition front with slope corresponding to that required to yield a transport capacity.
- Zone C: Sediment is transported as bedload.
- Zone D: All sediment reaching the bed is trapped.

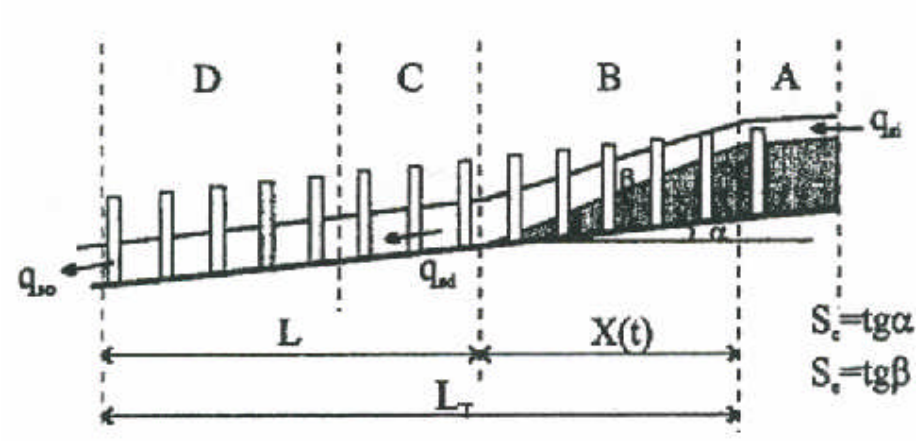

Figure 15. Schematic of sediment deposition (Tollner, *et al*. 1976; Barfield, *et al.* 1979; Hayes, *et al*. 1984).

The trapping efficiency is calculated as:

(2.1) $$Tr = \frac{q_{si} - q_{so}}{q_{si}} = 1 - \frac{q_{sd}}{q_{si}}\left[1 - \frac{q_{sd} - q_{so}}{q_{sd}}\right]$$

Where:

q_{si} = Incoming sediment load per unit channel width (g/m^2)

q_{so} = Outgoing sediment load per unit channel width (g/m^2)

q_{sd} = Total sediment load transported immediately downstream of the deposition wedge (g/m^2)

The sediment loads are calculated using the following equations:

(2.2) Zone B: $$X(t) = \frac{2(q_{si} - q_{sd})t}{\rho_{sb} g S_e}$$

Where:

$X_{(t)}$ = Length of the swale in Zone B (m)

t = Time after beginning of the flow (s)

ρ_{sd} = Blunk density of deposited sediment (g/m^3)

g = Gravity acceleration (m/s^2)

S_e = Slope of the swale in Zone B

(2.3) Zone C: $$q_{sd} = \rho_s \sqrt{(\rho_s / \rho - 1) g d_p^{\,3}} * \left[\frac{1.08 S_c R_s}{(\rho_s / \rho - 1) d_p}\right]^{3.571}$$

Where:

ρ = Density of water (g/m^3)

ρ_s = Density of particles (g/m^3)

d_p = Particle diameter (m)

S_c = Channel slope

R_s = Spacing hydraulic radius (m) calculated as:

(2.4) $$R_s = \frac{bh}{b + 2h}$$

Where:

b = Spacing between two grass blades (m)

h = Flow depth (m)

(2.5) Zone D: $$\frac{q_{sd} - q_{so}}{q_{sd}} = \exp\left[-1.05 \times 10^{-3}\left(\frac{VR_s}{\nu}\right)^{0.82}\left(\frac{hV}{LV_s}\right)^{0.91}\right]$$

Where:

V = Mean flow velocity (m/s)

V_s = Terminal settling velocity of particles (Stoke's settling velocity) (m/s)

ν = Kinetic viscosity of the water sediment mixture (m^2/s)

h = Flow depth (m)

R_s = Spacing hydraulic radius (m)

$L = L_t \sim X(t)$ effective length of grass filter strip (m)

L_t = Total length of grass filter strip.

Deletic Model

Unlike the Kentucky model, Ana Deletic (2001) used substantial amounts of very fine sediments (sediment particles less than 20 μm) as well as large particles to develop a comprehensive model. The model was developed by using an artificial medium (Astroturf) mounted on a 41 ft (12.5 m) long and 1 ft (0.3 m) wide channel, to simulate actual grass. Samples were collected at various swale locations and were analyzed for particulate concentrations and size distributions. Data obtained from the experiments were used to develop the sediment transport model by incorporating the concept of particle falling number. Three major processes of sediment behavior in grass swales were modeled: (a) particle deposition, (b) sediment transport, and (3) surface level and slope changes.

(a) Particle Deposition:

The particle fall number ($N_{f,s}$) is calculated as:

(2.6) $$N_{f,s} = \frac{lV_s}{hV}$$

Where:

l = Grass length (m)

h = Depth of the flow (m)

V_s = Stoke's settling velocity (m/s)

V = Average mean flow velocities were calculated as:

(2.7) $$V = \frac{q}{B_o h}$$

(2.8) $$V_s = \frac{g}{18\mu}(\rho_s - \rho)d_s^2$$

Where:

B_o = Open (unblocked by grass) flow width per unit width
μ = Dynamic viscosity of water (kg $s^{-1}m^{-1}$),
ρ = Water density (kg m^{-3})
d_s = Particle diameter (m)
ρ_s = Particle density (kg m^{-3}).

The trapping efficiency ($T_{r,s}$) for the sediment fraction s (particles of diameter ds) is expressed as:

(2.9) $$T_{r,s} = \frac{N_{f,s}^{0.69}}{N_{f,s}^{0.69} + 4.95}$$

(b) Sediment Transport:
Assuming that the particles transported in grass swales are very small (most of the particles are less than 20 μm (Neibling and Alberts 1979)), the model describes transport of suspended solids in grass swales. The model does not consider infiltration of water and re-suspension of deposited particles. The model is expressed as:

(2.10) $$\frac{\partial(hq_{s,s}/q)}{\partial t} + \frac{\partial q_{s,s}}{\partial x^2} = Dis\frac{\partial^2(hq_{s,s}/q)}{\partial x^2} - \lambda_s q_{s,s}$$

Where:

$q_{s,s}$ = Sediment loading rate of fraction s per unit width (g $s^{-1}m^{-1}$)
Dis = Dispersion coefficient (m^2 s)
λ_s = Trapping efficiency of fraction s per unit length (m^{-1}) calculated as:

(2.11) $$\lambda_s = \frac{T_{r,s}\left(\frac{lV_s}{Vh}\right)}{l}$$

(c) Surface Level and Slope Changes:
This model considers the channel slope changes due to deposition of sediments, especially at the upstream end of grass strips. The changes in slope (*S*) is expressed as:

(2.12) $$S(x,t) = -\frac{\partial z(x,t)}{\partial x}$$

Where:

$\partial z(x,t)$ = Rise in the surface level expressed as:

(2.13) $$\frac{\partial z(x,t)}{\partial t} = \frac{1}{1-p}\int_s \frac{1}{\rho_s}\lambda_s q_{s,s} d_s$$

Where:

P = Porosity of deposited sediment

$q_{s,s}$ = Sediment loading rate of fraction s per unit width (g $s^{-1}m^{-1}$)

d_s = Particle diameter (m)

λ_s = Trapping efficiency of fraction s per unit length (m^{-1})

Chapter 3: Sediment Trapping Model for Grass Swales and Grass Filters

Introduction

The first set of experiments using controlled flows at indoor swale facilities were designed to initially identify the significant factors affecting trapping of particulates in grass swales. From the results of these initial experiments, more carefully designed and detailed experiments were conducted in follow-up experiments. Full-scale outdoor experiments were then conducted to verify that the variables identified in the controlled indoor experiments were valid during actual rain events and in full-scale conditions. This chapter presents a sediment trapping model for grass swales (and grass "filters") using these experimental results.

Modeling Sediment Reductions in Grass Swales

The primary focus on the second set of indoor experiments was to develop a model to predict the reduction of stormwater sediments in actual grass swales. This chapter describes the model using the analytical results (total solids, total solids less than 106 µm, total suspended solids, total dissolved solids, turbidity, and particle size distribution analyses) obtained during the second series of experiments and supplemented with the outdoor observations.

Settling Frequency

The settling frequency is the number of times that sediment particles of a specific size category would fall to the bottom of the swale through the depth of water while flowing through the swale. Particles having a large settling frequency are assumed to have higher sediment removal rates than particles having a small settling frequency.

It is likely that more than 90% of all runoff particulates are in the 1 to 100 µm range, corresponding to particles that will settle with low Reynolds's numbers, and hence laminar flow conditions, and the settling rates can therefore be calculated using Stoke's law. In most cases, stormwater particulates have specific gravities in the range of 1.5 to 2.5, while construction site runoff particles would be closer to 2.5, and silica test particles have specific gravities of 2.65. This corresponds to a relatively narrow range of settling rates for a specific particle size. Settling frequency can therefore be calculated using Stoke's law to determine the settling velocity for a specific particle size class, the length of the swale, the flow rate, and the depth of flow. Larger particles have higher chances of settling for the same flow and swale conditions than smaller particles since they have larger settling velocities. Stoke's law is commonly expressed as:

(6.2)
$$Vs = \frac{2}{9}\frac{\left(R^2 g\left(\rho_p - \rho_f\right)\right)}{U}$$

Where:

Vs = Settling velocity of a particle (cm/s)
R = Equivalent radius of a particle, considering shape (cm)
g = Gravitational constant = 980 cm/s^2
ρ_p = Density of a particle = 2.65 g/cm^3 (assuming silica)
ρ_f = Density of fluid = 1.0 g/cm^3 (assuming water at standard temperature conditions)
U = Dynamic Viscosity = 0.01 g/(cm*s) (assuming water at standard temperature conditions)

The following example is a calculation of the settling frequency for one of the experimental conditions: a silica particle whose diameter is 2 µm (2 x 10^{-4} cm in diameter, or 1 x 10^{-4} cm in radius) in a 6 ft long section of a 2 ft wide synthetic turf lined swale at 1% slope and at 10 GPM (0.038 m^3/min) flow rate. The first step is to calculate the settling velocity of the particle:

(6.3) $$Vs = \frac{2}{9} * \frac{\left((1x10^{-4}cm)^2 * 980cm/s^2 * (2.65g/cm^3 - 1.0g/cm^3)\right)}{0.01g/(cm*s)}$$

Thus:

(6.4) Vs = 3.59*10^{-4} cm/s (1.41*10^{-4} inch/s)

To calculate the settling duration of the 2 µm particle for the synthetic turf at 1% slope and 10 GPM (0.038 m^3/min) of flow, the averaged flow depth of the water for these experimental conditions was divided by the settling velocity of 2 µm particles. The average flow depth of water on the synthetic turf, at 1% slope and 10 GPM (0.038 m^3/min) flow rate, was 0.87 inches (2.2 cm). Thus,

(6.5) $$Settling\_Duration(\sec ond) = \frac{flow\_depth}{Settling\_velocity} = \frac{0.87(inch)}{1.41*10^{-4}(inch/s)} = \frac{2.2(cm)}{3.6*10^{-4}(cm/s)}$$

= 6,170 (seconds)

The average velocity of the water flow on the synthetic turf, at 1% slope and 10 GPM (0.038 m^3/min) flow rate, was 1.86 inch (4.7 cm) /s. Since the length of the indoor swale was 6 ft (72 inches or 182.8 cm):

(6.6) $$Traveling\_time(\sec ond) = \frac{Swale\_length}{Flow\_velocity} = \frac{72(inch)}{1.86(inch/s)} = \frac{182.8(cm)}{4.7(cm/s)}$$

= 38.7 (seconds)

The settling frequency is the number of times which a particle settles through the flow depth on a grass swale.

(6.7) $$Settling\_frequency = \frac{Traveling\_time}{Settling\_duration} = \frac{38.7(\sec onds)}{6170(\sec onds)}$$

Settling frequency = 0.0063

Therefore, the retention of 2 µm particles in this swale under these conditions is expected to be rather poor, as the particle would barely start to settle before it reached the end of the swale. The swale would have to be about 1,000 ft long (305 m) before these small particles would strike the bottom of the swale (assuming the worst case condition of the particle starting at the top of the flow depth).

The following is an example for a larger particle (100 µm in diameter, 0.01 cm diameter, or 0.005 cm in radius) during another test condition:

(6.8) $$Vs = \frac{2}{9} * \frac{\left((0.005cm)^2 * 980cm/s^2 * (2.65g/cm^3 - 1.0g/cm^3)\right)}{0.01g/(cm*s)}$$

Vs = 0.9 cm/s (0.35 inch/s)

The flow conditions for the Zoysia-lined swale, at 3% slope and 15GPM (0.064 m^3/min) flow rate, resulted in an average flow depth of 1.91 inches.

Thus,

(6.9) $$Settling\_Duration(\text{sec}ond) = \frac{flow\_depth}{Settling\_velocity} = \frac{1.91(inch)}{0.35(inch/s)} = \frac{4.8(cm)}{0.9(cm)}$$

= 5.4 seconds

The average flow velocity for this swale and flow condition was 1.28 inch/s (3.2 cm/s). Since the length of the indoor swale was 6 ft (72 inches or 183 cm):

(6.10) $$Traveling\_time(\text{sec}ond) = \frac{Swale\_length}{Flow\_velocity} = \frac{72(inch)}{1.28(inch/s)} = \frac{182.8(cm)}{3.2(cm/s)}$$

= 56 seconds

The settling frequency is the number of times which a particle settles through the flowing water column while flowing along the grass swale:

(6.11) $$Settling\_frequency = \frac{Traveling\_time}{Settling\_duration} = \frac{56(\text{sec}onds)}{5.4(\text{sec}onds)}$$

Settling frequency = 10

This settling frequency corresponds to a very high sediment removal rate for 100 µm particles, for this flow swale condition.

Summarized Information used to Predict Grass Swale Performance

The following figures and tables summarize important information from this research, and the previous WERF work (Johnson, *et al.* 2003), to determine the hydraulic conditions in small grass swales and to predict sediment capture.

Roughness Curves

Figure 16 is the final VR-n curve developed by Kirby (2003), showing the data for the small swales (both for the controlled indoor swale tests and for outdoor tests that were conducted during the WERF research). This figure shows how the roughness relationships are extended to very high Manning's n values for small flows that occur in roadside grass swale drainages.

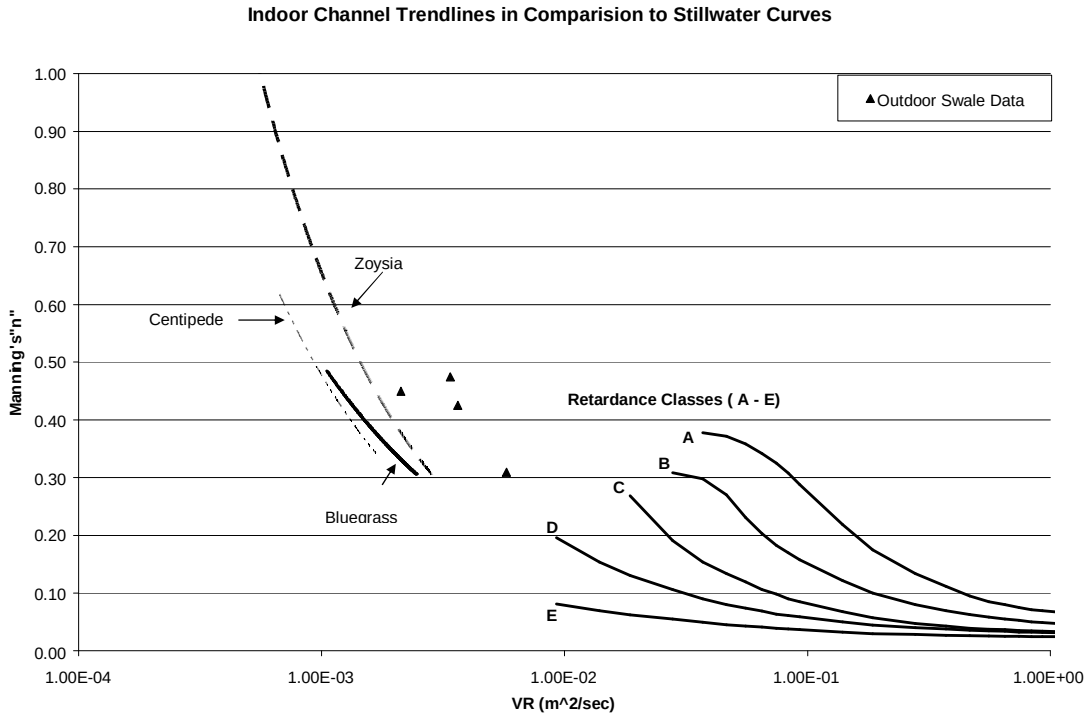

Figure 16. VR-n curve for different grasses, showing results for shallow flows (Kirby 2003) (Multiply ft^2/sec by 0.092 to obtain m^2/sec units).

Settling Frequency and Particulate Retention

Table 9 summarizes the percentage reduction values (including the confidence intervals of the means, along with the coefficient of variation (COV) values) for each set of settling frequencies for each flow depth to grass height range. These were calculated by statistically summarizing all the data observations contained in each cluster of settling frequency for all the tests combined for the indoor experiments conducted with relatively high suspended solids concentrations. Table 10 is a similar table summarizing the observations for the full-scale tests that represent shallow flows and low concentrations.

Table 9. Statistical Summaries of the Percent Reductions for High Sediment Concentrations (200 to 1,000 mg/L) and for Different (flow depth)/(grass height) Ratio Categories

Ratio: 0 to 1.0

Settling frequency	Mean reduction (%)	95% CI (lower limit)	95% CI (upper limit)	COV
TDS (< 0.45 µm)	5	1	8	0.99
0.0013 to 0.0026	75	70	80	0.19
0.01 to 0.02	72	69	75	0.23
0.045 to 0.093	72	69	75	0.18
0.33 to 0.69	75	72	78	0.11
1.6 to 3.3	80	78	82	0.15
5.4 to 11.1	85	82	88	0.14
60.6 to 124.1	97	92	100	0.05

Ratio: 1.0 to 1.5

Settling frequency	Mean reduction (%)	95% CI (lower limit)	95% CI (upper limit)	COV
TDS (< 0.45 µm)	18	7	28	0.39
0.0013 to 0.0026	56	49	63	0.37
0.01 to 0.02	64	60	68	0.28
0.045 to 0.093	70	66	74	0.25
0.33 to 0.69	77	73	81	0.13
1.6 to 3.3	84	80	88	0.09
5.4 to 11.1	88	83	93	0.12
60.6 to 124.1	97	89	100	0.08

Ratio: 1.5 to 4.0

Settling frequency	Mean reduction (%)	95% CI (lower limit)	95% CI (upper limit)	COV
TDS (< 0.45 µm)	6	2	9	0.75
0.0013 to 0.0026	43	38	48	0.5
0.01 to 0.02	46	42	50	0.24
0.045 to 0.093	52	48	56	0.19
0.33 to 0.69	63	60	66	0.14
1.6 to 3.3	74	71	77	0.11
5.4 to 11.1	84	80	88	0.05
60.6 to 124.1	99	95	100	0.03

Table 10. Statistical Summary of the Percent Reductions for Low Sediment Concentrations (40 to 160 mg/L)

Ratio: 0 to 1.0

Settling frequency	Mean reduction (%)	95% CI (Lower limit)	95% CI (Upper limit)	COV
0.02 to 0.05	41	25	58	0.32
0.09 to 0.39	58	48	68	0.28
0.7 to 5.15	71	62	81	0.14
12.99 to 24.8	78	67	87	0.11
62.6 and larger	78	67	87	0.13

Settling Rates for Different Particle Sizes

Tables 11 through 13 summarize calculated settling rates based on Stokes' Law, as presented previously. These rates can be used to predict the capture of the sediment in these particle sizes for specific grass swale flow conditions. Tables 12 and 13 show how the settling rates vary for different specific gravities. Stormwater particulates have specific gravities of about 2.5, but they can be as low as about 1.5 under some conditions.

Table 11. Particle Settling Rates (2.65 specific gravity)

Particle size range	Approx. midpoint	Settling rate of midpoint size (cm/sec)	(in/sec)
0.45 to 2 µm	1.2	1.52×10^{-4}	5.98×10^{-5}
2 to 5 µm	3.5	1.10×10^{-3}	4.34×10^{-4}
5 to 10 µm	7.5	5.05×10^{-3}	1.99×10^{-3}
10 to 30 µm	20	3.59×10^{-2}	1.42×10^{-2}
30 to 60 µm	45	0.182	0.0717
60 to 106 µm	83	0.619	0.243
106 to 425 µm	266	6.22	2.45

Table 12. Particle Settling Rates (2 µm particle) for Different Specific Gravities

Settling units	2.65 g/cm^3	2.5 g/cm^3	2.0 g/cm^3	1.5 g/cm^3
cm/sec	3.6×10^{-4}	3.27×10^{-4}	2.18×10^{-4}	1.09×10^{-4}
in/sec	1.42×10^{-4}	1.29×10^{-4}	8.58×10^{-5}	4.29×10^{-5}

Table 13. Particle Settling Rates (100 µm particle) for Different Specific Gravities

Settling units	2.65 g/cm^3	2.5 g/cm^3	2.0 g/cm^3	1.5 g/cm^3
cm/sec	0.899	0.818	0.545	0.273
in/sec	0.354	0.322	0.215	0.107

Example Problem

The channel and flow characteristics from the channel-lining example design in Chapter 1 will be used to predict the sediment retention in this grass swale:

- the discharge rate is 29 ft^3/sec (0.80 m^3/sec)
- the channel bottom width is 5 ft (1.5 m) wide, with 3 (H) to 1 (V) side slopes
- the calculated normal depth is 0.7 ft (210 mm, 21 cm) and the velocity is calculated to be 5.8 ft/sec (1.8 m/sec) after mature vegetation is established
- the swale length for this area is 1250 ft (378 m)

With water is assumed to enter the swale at the midpoint location, resulting in an effective treatment swale length of 625 ft (189 m). With a water velocity of 5.8 ft/sec (1.8 m/sec), the average travel time is 189 m/1.8 m/sec = 105 sec (1.8 m) for this length.

The mature grass is about 3 inches (75 mm) in height, so the flow depth to grass height ratio is 210 mm/75 mm = 2.8. The suspended solids concentration is determined to be 250 mg/L and the particle size distribution of the water entering the swale is typical, as shown on Figure 17 for the December 6, 2004 observations.

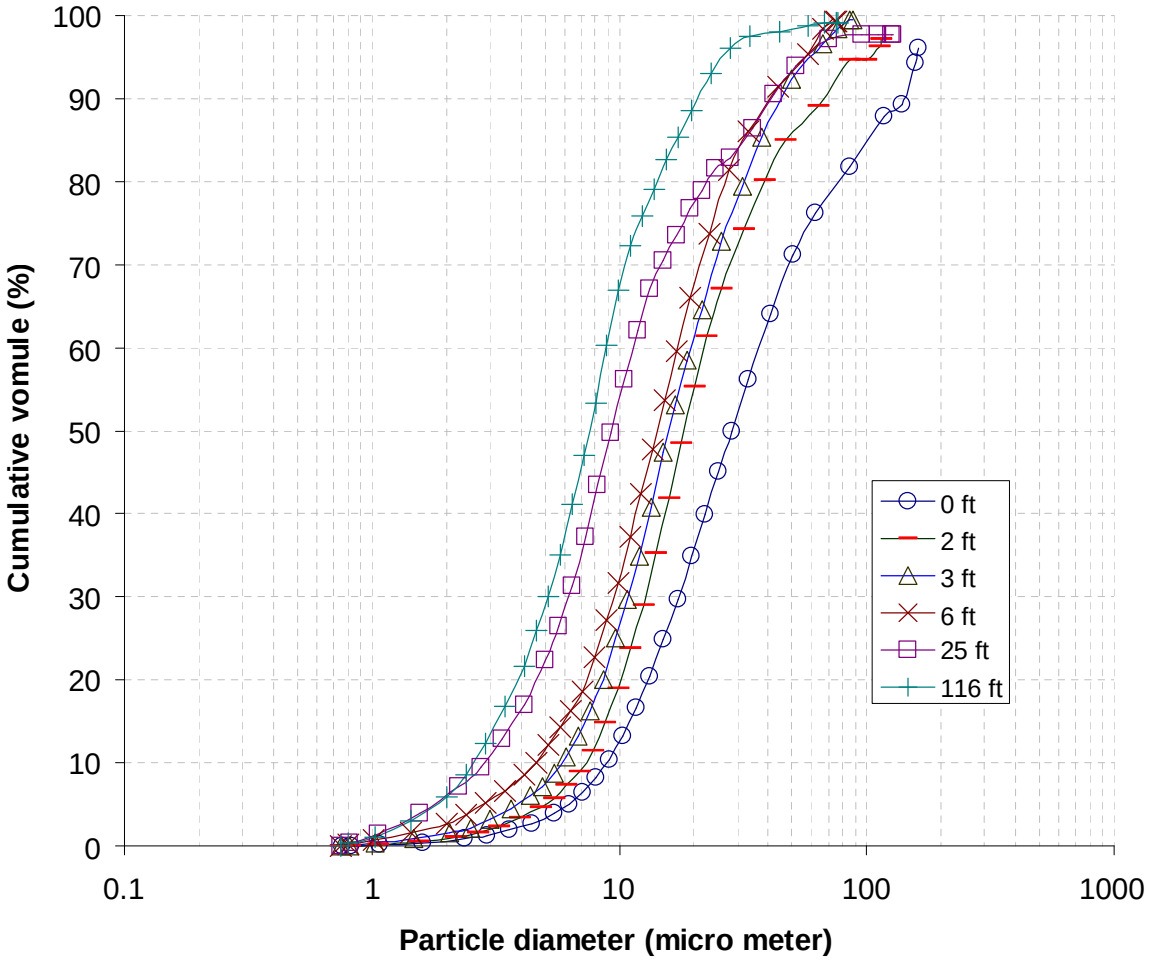

Figure 17. Example particle size distributions for different swale lengths observed on December 6, 2004.

Tables 14 and 15 show the particle size information for each size range (extracted from Figure 17) and the resulting sediment concentrations calculated using these values.

Table 14. Particle Size Distribution for Influent Water

Particle Size (µm)	% smaller than size indicated (Dec. 6, 2004 influent)
0.45	0
2	0.5
5	3.2
10	12.4
30	52.8
60	74.6
106	85.2
425	100.0

Table 15. Particulate Concentration for Each Particle Range

Particle Size Range	Approx. % of Suspended Solids in Range	Particulate Concentration in Size Range
0.45 to 2 µm	0.5	1.3
2 to 5 µm	2.7	6.8
5 to 10 µm	9.2	23.0
10 to 30 µm	40.4	101.0
30 to 60 µm	21.8	54.4
60 to 106 µm	10.6	26.5
106 to 425 µm	14.8	37.0
Total:	100.0	250 mg/L

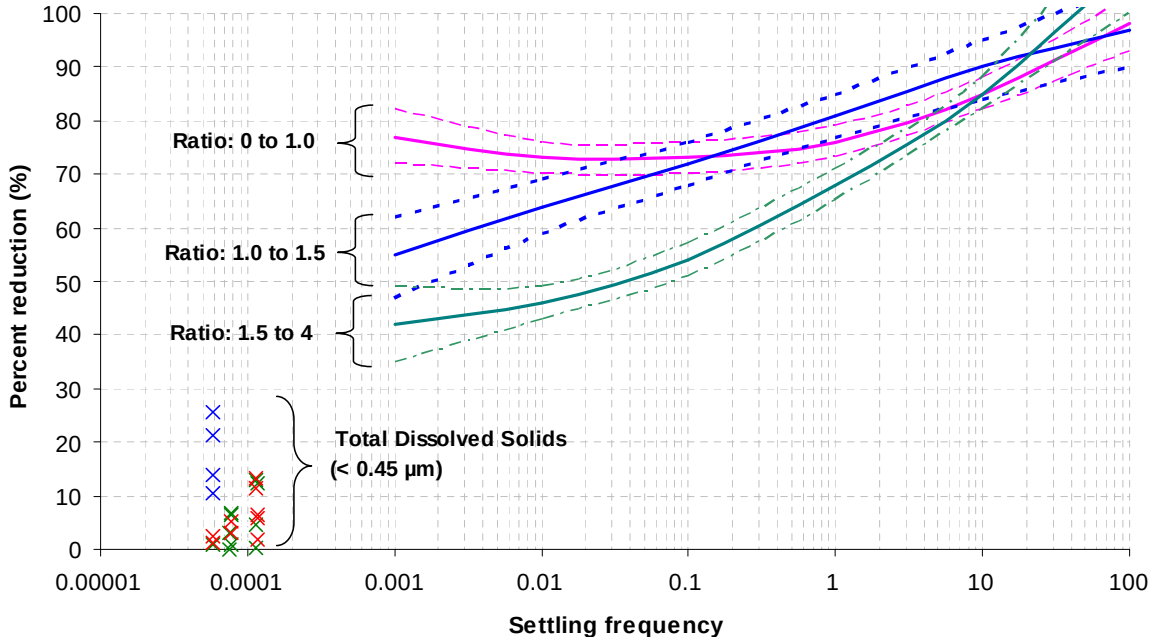

Figure 18. Comparison of regression lines with 95% confidence intervals for different (flow depth)/(grass height) ratios and for high concentrations (200 to 1,000 mg/L).

Table 16 shows the performance calculations for each particle size range.

Table 16. Particulate Trapping Calculations for Example Problem

Particle Size Range	Approx. Settling Rate (cm/sec)	Settling Time for 21 cm Flow Depth (sec)	Settling Frequency for Swale (105 sec travel time)	Percent Reduction for Particles in Size Range (from Figure 18)	Influent Particulate Concentration in Size Range (mg/L)	Irreducible Concentration for Size Range (mg/L)	Particulate Concentration for Size Range after Treatment (mg/L)	Final Resultant Concentration for Size Range (mg/L)
0.45 to 2 µm	1.52×10^{-4}	138,000	0.00076	42	1.3	7	0.8	1.3*
2 to 5 µm	1.10×10^{-3}	19,000	0.0055	44	6.8	5	3.8	5**
5 to 10 µm	5.05×10^{-3}	4,160	0.025	48	23.0	5	12.0	12.0
10 to 30 µm	3.59×10^{-2}	585	0.18	57	101.0	10	43.4	43.4
30 to 60 µm	0.182	115	0.91	68	54.4	5	17.4	17.4
60 to 106 µm	0.619	33.9	3.1	74	26.5	5	6.9	6.9
106 to 425 µm	6.22	3.38	31	96	37.0	10	1.5	10**
Total:				66% (weighted by mass), reduced by irreducible concentrations	250 mg/L	20 mg/L	86 mg/L	96 mg/L

Notes:
* the influent concentration for this particle size range is less than the irreducible concentration, so the influent concentration is not reduced by the swale treatment.
** the treated concentration for these particle size ranges are less than the irreducible concentrations, so the treated concentrations are not reduced to values smaller than the irreducible concentrations.

An overall 62% reduction in suspended solids concentration was achieved. Table 17 shows the resultant particle size distribution for the treated water, compared to the influent water.

Table 17. Particle Size Distribution for Treated Water

Particle Size (µm)	% smaller than size indicated (Dec. 6, 2004 influent)	Concentration smaller than size indicated (treated), mg/L	% smaller than size indicated, treated
0.45	0	0	0
2	0.5	1.3	1.4
5	3.2	6.3	6.6
10	12.4	18.3	19.1
30	52.8	61.7	64.3
60	74.6	79.1	82.4
106	85.2	86.0	90.0
425	100.0	96.0	100.0

Summary of Findings

This chapter presented a method to predict stormwater sediment retention in grass-lines swales or grass filters. The main factors affecting the sediment trapping in the swales was the settling frequency, which in turn is dependent on particle settling rate, flow rate, flow depth, and swale length; the ratio of the flow depth to the grass height; and the initial sediment concentration. During shallow flow conditions, relatively flat swales will provide large amounts of sediment retention, down to an irreducible concentration of about 20 mg/L of total suspended solids. Steep swales and deeper flows result in less sediment retention.

The indoor swale experiments resulted in larger sediment reductions than observed during the outdoor tests due to several reasons, including:

- The initial sediment concentrations during the second set of indoor experiments were much higher than during the outdoor swale observations. The mean of the indoor experiment total suspended solids concentrations was 480 mg/L, and ranged from 200 mg/L to 1,000 mg/L. The outdoor swale observations had mean total suspended solids concentrations of 60 mg/L, and ranged from 10 mg/L to 160 mg/L.

- There was a large fraction of larger sand particles applied to the indoor swales, while very little, if any, sand-sized particles were found at the head of the outdoor swale for most of the events. The settling frequency calculations partially accounted for this, but irreducibly low concentrations of the larger material occurred before the end of the longer outdoor swale, limiting the overall percentage removal calculations.

The regression model does not consider erosion or scour that likely occurs at the beginning of the swale. There is obviously some initial length, likely dependent on flow conditions and shear stress, where the turbulent flows are more erosive before they become more stable. This length is probably on the order of several feet for small flows, like observed during this research, but may extend longer for larger flows.

Chapter 4: Conclusions and Recommendations for Future Study

The Indoor Experiments

The indoor laboratory swale experiments demonstrated the effectiveness of grass swales in trapping sediments and reducing sediment concentrations in runoff. Significant sediment reductions in 6 ft (1.8 m) long grass-lined channels were observed for total solids, total suspended solids, turbidity, and particle size during the second experiments, but not in total dissolved solids. The experiments showed not only the effectiveness of grass swales, but also significant factors affecting sediment transport in grass swales. The affecting factors observed are grass type, channel slope, runoff flow rate, grass type*channel slope, grass type*runoff flow rate, and channel slope*runoff flow rate. Moreover, particle size distribution analysis as well as visual observations confirmed that large particles are preferentially trapped in grass swales compared to smaller particles, especially at the beginning of grass swales.

Predictive Model

A model was developed to predict the reduction of stormwater sediment in actual grass swales using data obtained from the second set of controlled experiments. The predictive model utilizes three main concepts to model sediment transport in grass swales. They are first order decay, settling frequency, and flow depth / grass height ratio. The concept of first order decay is a statistical approach used to describe the observed reductions in concentrations in the grass swales with length. Both the indoor experiments and outdoor observations showed greater sediment reductions at the beginning of the grass swales, and the sediment concentrations then tended to stabilize after some distance. Thus, first order decay was employed to describe this behavior of the stormwater sediment in grass swales. Unlike first order decay, settling frequency is a theoretical approach to describe sediment transport in grass swales. Settling frequency is defined as a number of times a particle could conceivably settle to the bottom of the flow depth until it reaches the end of the grass swales (6.0 ft, 1.8 m, during the indoor experiments and 116 ft, 35.3 m, during the outdoor observations). The settling frequency is computed as the ratio of the travel time of runoff in the swale reach to the settling duration of a particle using Stoke's law and the site hydraulic conditions (mainly depth of flow). The concept of flow depth / grass height ratio was also incorporated into the predictive model, and initial sediment concentration was also found to be important. The settling frequency concept considers the opportunities of runoff water and sediment to contact the grass cover, and recognizes the very slow rates for submerged flows. Sediment retention in grass swales is most effective when flow depth is lower than the grass height (flow depth / grass height ratio less than 1). As the flow depth increases, sediment retention is expected to be less effective because of less contact area to the grass cover and the higher flow velocities.

Outdoor Swale Observations and Model Verification

To test the predictive model, stormwater samples were collected at the full-size outdoor grass swale (116 ft or 35.3 m long) located adjacent to the Tuscaloosa, Alabama, City Hall during actual storm events from August to December 2004. Significant concentration reductions were observed in total suspended solids and turbidity. However, changes in total solids, total dissolved solids, and particle size were statistically insignificant in the grass swale. Total suspended solids analyses showed three distinct regions for sediment reduction behavior in grass swales. They are:

1) 0 ft to 3 ft (0 m to 0.9 m):	Region of instability (frequent scour, but also sedimentation observed)
2) 3 ft to 25 ft (0.9 m to 7.6 m):	High sediment reduction region
3) 25 ft to 116 ft (7.6 m to 35.3 m):	Lower sediment reduction region

The high sediment reductions observed between 3 ft (0.9 m) and 25 ft (7.6 m) were used to test the predictive model. The total sediment reductions observed in the indoor experiments were much higher than observed at the outdoor swale. The predictive model therefore overestimated the sediment reductions due to several reasons, including:

- The initial sediment concentrations during the indoor experiments were much higher than during the outdoor swale observations.

- There was a large fraction of larger sand particles applied to the indoor swales, while very little sand particles were found at the head of the outdoor swale for most of the events.

Recommended Future Research Activities

The predictive model still has high variation and overestimates sediment reductions at actual grass swales during certain conditions. Additional research efforts are needed to reduce the variability of sediment retention of the predictive model further. Future research objectives could include the following:

- Investigating the effect of initial sediment concentration on sediment trapping.

- Investigating the effects of stem density on sediment transport during low flows.

- Sensitivity analyses of the predictive model using data obtained from outdoor swale observations for different grass swales with different grass types and channel slopes.

- Modifying the predictive model using further outdoor swale observations.

Grass swales are an effective stormwater treatment practice to capture stormwater sediments and other pollutants within grass swales. However, some suggest that deposited sediments and other pollutants in grass swales are potentially hazardous to the public. It is possible that exposure to deposited contaminated sediments can be hazardous. However, most grass swales are used in low density residential areas where stormwater concentrations are low. If grass swales are used to treat high concentrations of pollutants in industrial areas, the grass cover should be routinely tested and replaced, as necessary.

Section 2: Controlled Indoor Grass Swale Experiments and Full-Scale Tests

This report section describes the two sets of controlled indoor swale experiments and the full-scale tests. These data were used to develop the predictive equations and examples presented in the first report section.

Chapter 5: Initial Indoor Controlled Experiments

Introduction

This research project extends some of the preliminary sediment transport work conducted as part of the prior work funded by the Water Environment Research Foundation (Kirby 2003; Johnson, *et al*. 2003). The previous research primarily focused on the removal of stormwater heavy metals (Cd, Cr, Cu, Pb, Fe, Hg, Ni, and Zn) in grass swales. The current research reported in this report was partially funded by the University Transportation Center of Alabama (UTCA) and is intended to develop better design guidelines to enable conservation design elements to be incorporated in transportation projects.

This current research focused on the movement of stormwater sediments in grass swales. To understand sediment transport, experiments were conducted in several phases. The first experiments, described in this chapter, used the indoor grass swales setups that were constructed by Kirby (2003) and were intended to identify the most significant factors affecting sediment transport that could be further examined in later experimental phases. The ultimate goal of these experiments was to develop a model to predict the trapping of stormwater sediments in roadside grass swales.

Objectives

The major research objectives of the first experiments was to examine the effectiveness of grass swales in sediment transport under a small variety of grass type, swale slope, stormwater flow rate, and sediment particle size conditions.

Indoor Laboratory Swales

Descriptions of the Experimental Set-up

Experimental swales were constructed in an indoor greenhouse facility located in the Bevil building on the campus of the University of Alabama, as part of a prior research project (Johnson *et al.* 2003). Artificial sunlight (ambient variations of UV and visible wavelengths) was provided, and room temperature was maintained at approximately 78 ^{o}F (25 ^{o}C) at this facility. The experimental setup consisted of three identical rectangular channels on a base which was adjustable over a range of channel slopes. A soil mixture of 70% top soil and 30% sand (by weight) was placed in the channel sections which were completely sealed by non-reactive marine-epoxy paint to prevent leakage. Each channel was 2.0 ft wide (0.6 m), 6 ft long (1.8 m), and 6.0 inches (15 cm) deep and had a specific type of lawn grass. Jason Kirby constructed these swales and tested the grasses for hydraulic resistance during his MSCE thesis (2003).

Tap water was used to fill a 150 gallon (0.57 m^3) water storage tank. Test sediments of aluminum oxide and sieved sands were mixed in the tank to reproduce the sediment characteristics of stormwater. Two 65 gallon/min (GPM) (0.25 m^3/min) sump pumps were placed at the opposite ends of the tank to ensure continuous suspension of sediments during the experiments. The sediment-water mixture was pumped using a Jacuzzi ® (Little Rock, AR) pump through a 2 inch (5.1 cm) diameter PVC piping network. A T-shaped PVC pipe with 26 quarter-inch-diameter holes (0.6 cm) was attached to the end of the piping network as shown in Figure 19 and 20. The sediment-water mixture was drained from the T-shaped pipe onto an aluminum sheet attached to the head of the swale to produce a sheet flow. The runoff was collected at the end of the swale in a second 150 gallon (0.567 m^3) tank (Kirby 2003). After each experiment during the current sediment transport tests, sediment depositions on the grass swale were washed off to avoid sediment carryover to the next experiment by re-suspension.

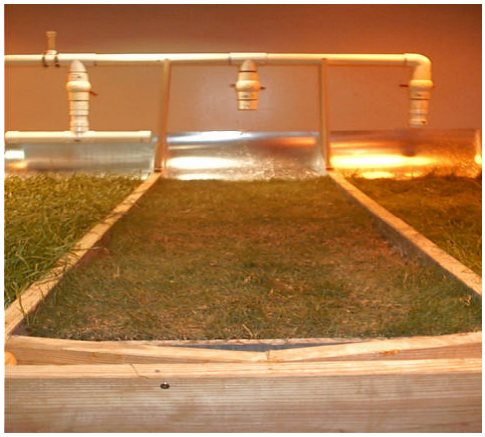

Figure 19. (*left*) Overview of the experimental setup.
Figure 20. (*Right*) Sediment-water mixture coming through the T-shaped PVC header onto the metal sheet to produce a sheet flow.

Sediment Characteristics of the Sediment-water Mixture

Aluminum oxide particles (glass grinding abrasives) ranging from 5 µm to 80 µm and sieved sands ranging from 80 µm to 240 µm were combined to produce the test sediments. The initial sediment concentration was 200 mg/L. Therefore, 0.25 lb (110 grams) of the sediment mixture was mixed with the 150 gallons (0.57 m^3) of tap water for each experiment. Table 18 shows the percentage and weight contribution of the test sediments for different particle size ranges. The resulting particle size distribution was similar to the reported sediment particle size distribution and concentration found in stormwater (Burton and Pitt 2001).

Table 18. Percentage and Weight Contributions of the Test Sediments

Sediment	Particle Size (µm)	Specific Gravity (gram/cm^3)	Percentage Contribution	Weight (gram/test)
Aluminum Oxide	0 to 5	3.7 to 4.0	45%	51
Aluminum Oxide	5 to 10	3.7 to 4.0	10%	11.3
Aluminum Oxide	10 to 25	3.7 to 4.0	20%	22.7
Aluminum Oxide	25 to 80	3.7 to 4.0	8%	9.1
Sieved Sands	80 to 240	2.65	17%	19.3
		Total	*100%*	*113.4*

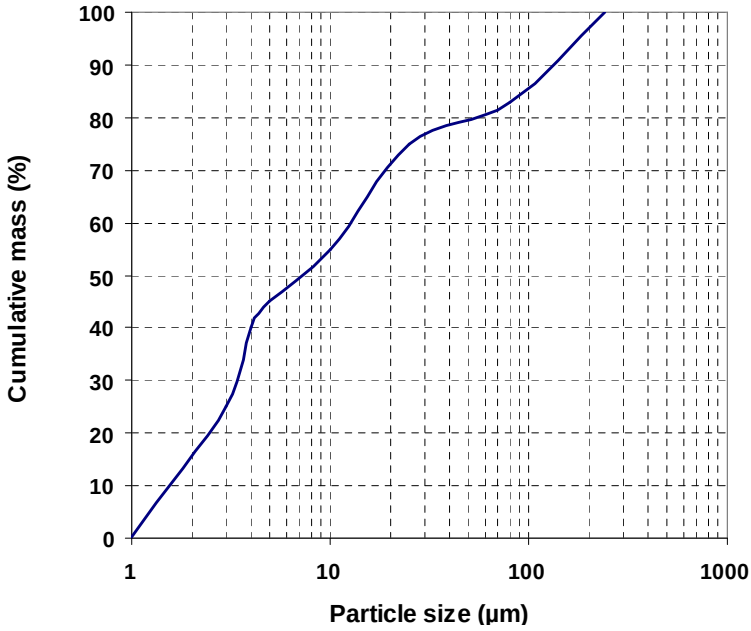

Figure 21. Resulting particle size distribution of the test sediments.

Parameters in the Initial Experiments

Five different parameters were tested in the initial experiments to identify their effects on sediment transport in grass swales. The parameters were grass type, slope, flow rate, sampling time, and swale length, as described below:

- *Grass types*: Three different types of grass were placed in the rectangular channels. These were Centipede (*Eremochloa ophiuroides*), Zoysia (*Zoysia japonica*), and Kentucky bluegrass (*Poa pratensis*). These three grasses were selected because their species are commonly found in the South and Southeast areas of the United Sates, the location of these experiments. Centipede (CENT-05-PK, Seedland®) is thick forming, uniform growing, and medium to light green in color. It has a thick and wide blade, short upright stems, and requires low maintenance. The blades of Centipede are sparser than Kentucky bluegrass or Zoysia and Centipede survives better in mild climates. Zoysia can be found from Florida to Connecticut and along the Gulf coast to Texas and in the Midwest and California (Richard n.d.). Zoysia is commonly used at golf courses. Leaf blades of Zoysia are very stiff and smooth with occasional hair near the root providing a very strong structure that has high wear-tolerance. Kentucky bluegrass is a dense grass with smooth, upright stems, very fine blades that can grow up to 18 to 24 inches (46 cm to 61 cm) tall, but is commonly mowed too much shorter heights. It is readily identified by the boat-shaped leaf tip. Kentucky bluegrass grows primary in the North and Midwest areas of the United Sates. In the Southern United Sates, Bluegrass grows in a transition zone from North Carolina, through much of Tennessee, northern Arkansas to the panhandle of Texas and Oklahoma (Richard n.d.).

  The grasses in the test swales were watered daily, and fertilizer was applied bi-weekly to keep the grass in a healthy condition. The grass was also trimmed regularly so that the heights of the grasses were maintained at about 2 inches (5 cm) in height.

Centipede Kentucky Bluegrass Zoysia

Figure 22. Different grass types tested in the first set of experiments

- *Slopes*: The effects of 1% and 5% slopes were tested. The slopes were maintained by jacking the swale test frame and placing pre-cut blocks of the correct thickness. The connecting flow distribution pipes also had alternative pre-cut sections to enable efficient slope adjustments.

- *Flow rates*: The runoff flow rates were controlled using a valve in the piping network. The flow rates were approximately 8 gallons per minute (GPM) (0.03 m^3/min) during the low flow rate tests and approximately 15GMP (0.06 m^3/min) during the high flow rate tests.

- *Time interval*: Samples were collected at three different times during each test. The duration of an experiment with 8 GPM flows (low flow rate) (0.03 m^3/min) was approximately 10 minutes (the time available until all of the sediment-water mixture was pumped from the tank to the test swale). Thus, sampling was conducted at 1, 5, and 10 minutes after the mixture was introduced to the swales. During the high flow rates, the maximum duration was 6 minutes. Therefore, samples were collected at all locations at 1, 3 minute, and 6 minute intervals.

- *Swale lengths*: To determine the sediment reduction as a function of swale length, samples are collected at the head works, 2 ft (0.6 m), and 6 ft(1.8 m) from the head works. Samples collected at the head works determined the initial sediment concentrations. Figure 23 shows the sampling locations. For each swale length, subsamples were collected at various locations across the channel and composited to represent the specific swale cross section.

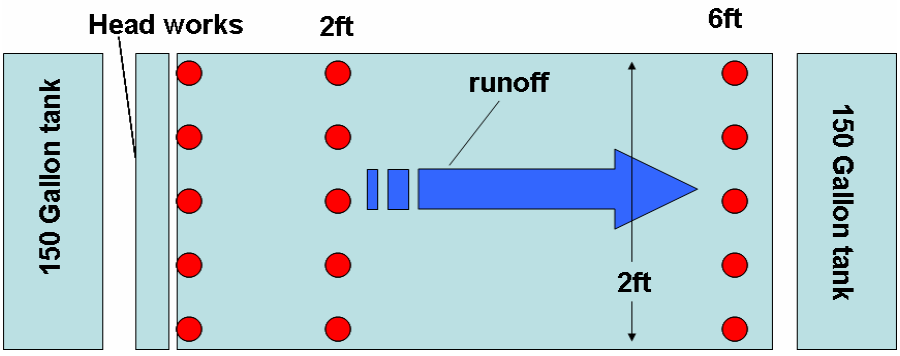

Figure 23. Sampling locations of each grass-lined channel. Red dots indicate sampling locations.

Experimental Design and Analytical Methods

The experimental design was a box design (Box, Hunter, and Hunter 1978). Since there were 3 grass types, 2 slopes, 2 flow rates, 3 time intervals, and 3 swale lengths, 108 runoff samples were collected during 12 separate tests in the initial indoor experiments. After each test, the grasses were rinsed with tap water to wash off any deposited sediment attached to the grass blades, and the setup was allowed to rest for approximately thirty minutes before the next test. The data was analyzed using a nested full-factorial design (Box, Hunter, and Hunter 1978).

The 108 runoff samples were analyzed for the following constituents:

- Total Solids (*Standard Methods* 2540B)
- Turbidity using a HACH 2100N Turbidimeter
- Particle Size Distribution using a Coulter Counter (Beckman® Multi-Sizer III™), composite of several different aperture tube measurements (30, 140, and 400 µm aperture tubes, giving a complete range of about 1.8 to 240 µm).

Much effort was spent in confirming the laboratory sediment measurement procedures. Appendix J describes the methods used to prepare the samples before analyses using a USGS Dekaport cone splitter.

Data Analysis and Results

The basic aim of the initial experiments was to examine the basic efficiency of grass swales in trapping stormwater sediments under a variety of test conditions. The complete set of analytical results from these initial experiments is presented in Appendix A. The following discussion summarizes the general findings from these experiments.

The total solids and turbidity measurements at the head works revealed that the variability of sediment concentrations between the different experiments was much higher than desired. Thus, all the measurements by the variables were normalized sediment concentrations at the head works by presenting the data as percentages of the initial values. Figure 24 and 25 are box and whisker plots of the changes in concentrations, or changes in normalized concentrations compared to initial values. Box and whisker plots of the observed actual concentrations are presented in Appendix D. Also, line plots of these data are presented in Appendix E. The boxes show the 25^{th}, 50^{th}, and 75^{th} percentiles (the lower box edge, the line in the box, and the upper box edge, respectively), and the top whisker extends to the 95^{th} percentile while the lower whisker extends to the 5^{th} percentile. The open circles show the actual data.

Total Solids Variation by Swale Length

Figures 24 and 25 show box and whisker plots of total solids concentrations for different swale lengths.

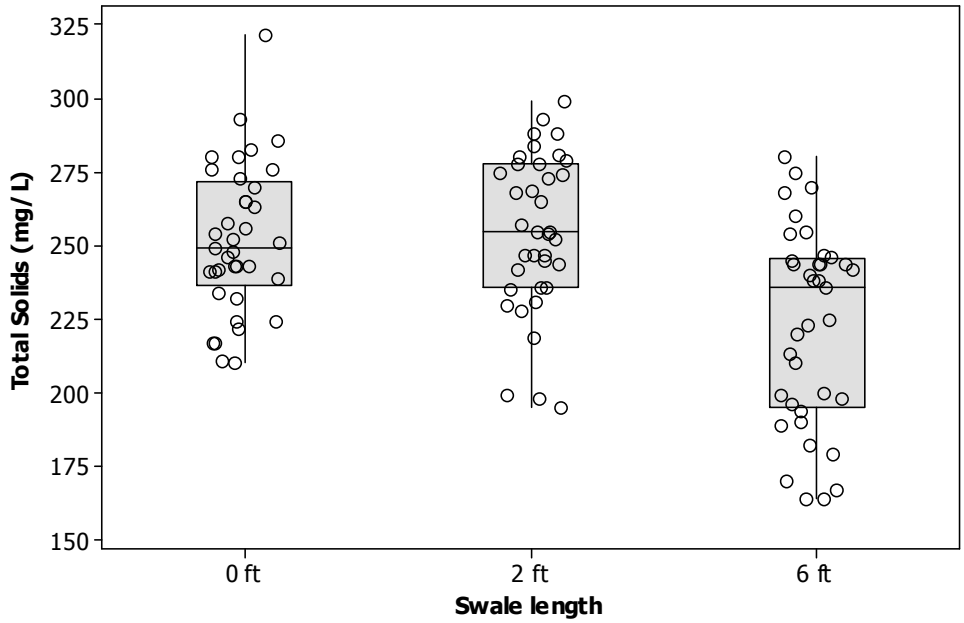

Figure 24. Box-and-whisker plots of total solids vs. swale length.

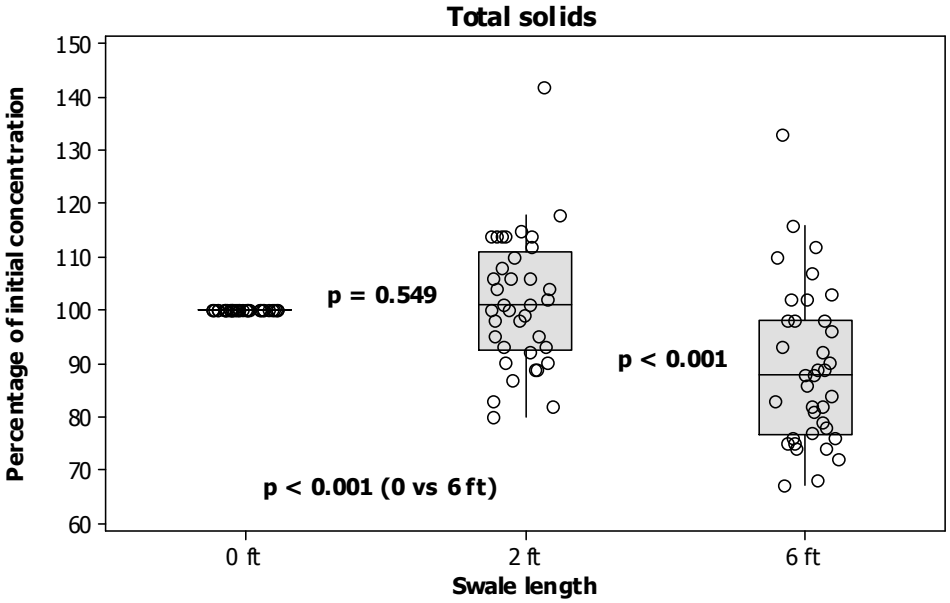

Figure 25. Box-and-whisker plots of percentages of initial concentrations of total solids and associated p-values (Kruskal-Wallis test) by swale length.

Kruskal-Wallis non-parametric statistical tests were employed to determine the equality of medians for two or more sample populations. Most of the data were not normally distributed, requiring the use of a nonparametric statistical test. The Kruskal-Wallis test hypotheses are:

- Null hypothesis (H_0): the population medians are all equal
- Alternative hypothesis (H_1): the medians are not equal

The significance level was set to be 0.05 (5%) since it is a widely accepted value for the significance level used in most research. To illustrate, when a computed probability is found to be less than 0.05, there is significant evidence suggesting that the null hypotheses is not true. Therefore, we accept the alternative hypothesis, concluding that the medians are not equal. When the computed probability is greater than 0.05, the proper conclusion is that there was not sufficient numbers of samples to verify the difference between the sample sets, at the power of the test (determined by the initial experimental design data quality objectives and number of samples collected).

Figure 25 shows a significant effect of swale length on sediment reduction, after the 2 ft (0.6 m) location (there was no significant sediment reduction between the head works and the 2 ft (0.6 m) location because the probability (p-value) was found to be 0.549). There were significant differences between the head works and 6ft (1.8 m) ($p < 0.001$) and between 2ft (0.6 m) and 6ft (1.8 m) ($p < 0.001$), although the actual reduction was quite small (an average of 11% reductions of the normalized sediment concentrations at 6ft (1.8 m) compared to the head works). These tests established that the sediment removal was only measurable between 2 ft (0.6 m) and 6 ft (1.8 m) from the head works for these tests.

Total Solids Variation by Grass Type

Figure 26 shows the variations in total solids concentrations for different grass types at the different sampling locations.

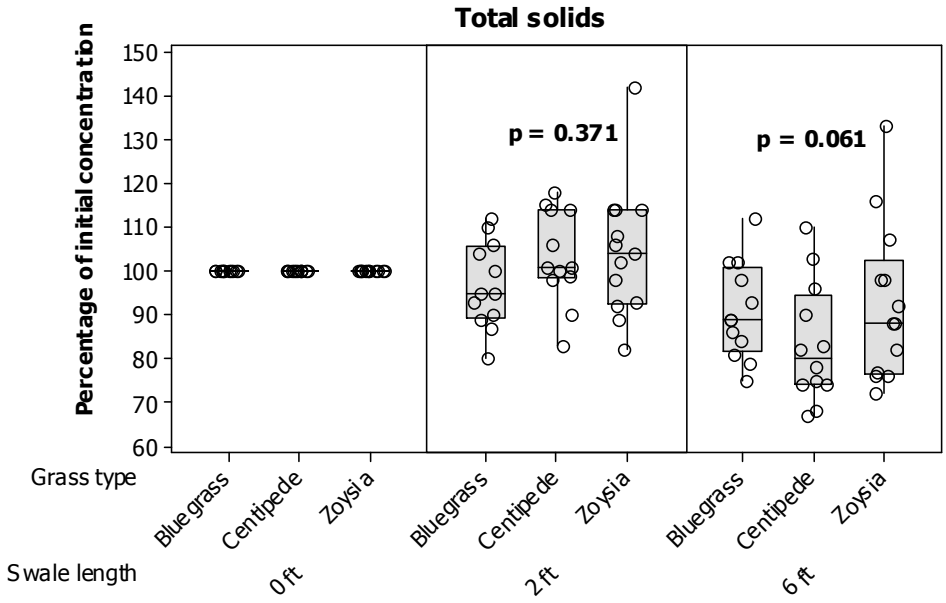

Figure 26. Box-and-whisker plots of percentages of initial concentrations of total solids and associated probabilities calculated using Kruskal-Wallis test vs. swale length and grass type (1 ft = 0.30 m).

As shown in Figure 26, there were no significant differences in the percentages of the initial total solids between Bluegrass, Centepede, and Zoysia at 2ft (0.6 m) since the probability was 0.37. At 6 ft, a marginal level of significance for grass type was observed, since the calculated probability was 0.06, close to 0.05. Centipede showed

better sediment reduction rates than bluegrass and Zoysia. There was no significant difference between bluegrass and Zoysia.

Total Solids Variation by Flow Rate

Figure 27 shows the total solids concentration changes for different flow rates at the different sampling locations.

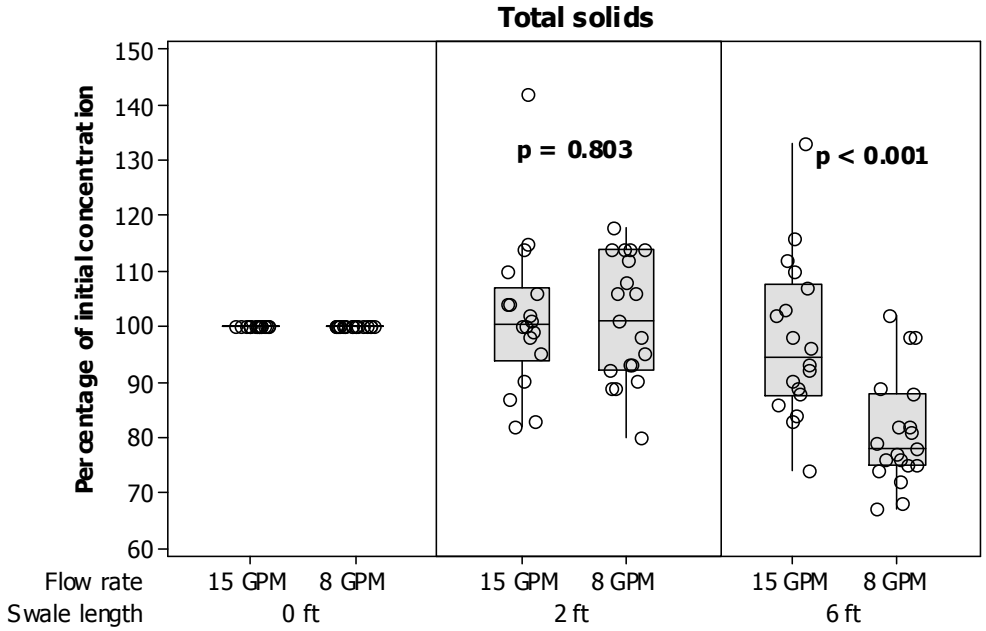

Figure 27. Box-and-whisker plots of percentages of initial concentrations of total solids and associated probabilities determined by Kruskal-Wallis test vs. swale length and flow rate (Note 1 GPM = 0.0038 m^3/min).

Reductions in normalized sediment concentrations were significantly different at 6 ft (1.8 m) ($p < 0.001$) when the 8 GPM (0.03 m^3/min) and 15 GPM (0.06 m^3/min) flow rate tests were compared. There was no significant difference at 2 ft (0.6 m) ($p = 0.803$). The median reductions at 8 GPM (0.03 m^3/min) were 16.5% lower than the mean reductions at 15 GPM (0.06 m^3/min) at 6 ft (1.8 m).

Total Solids Variation by Slope

Figure 28 shows the total solids concentration changes for different grass swale slopes for the different sampling locations.

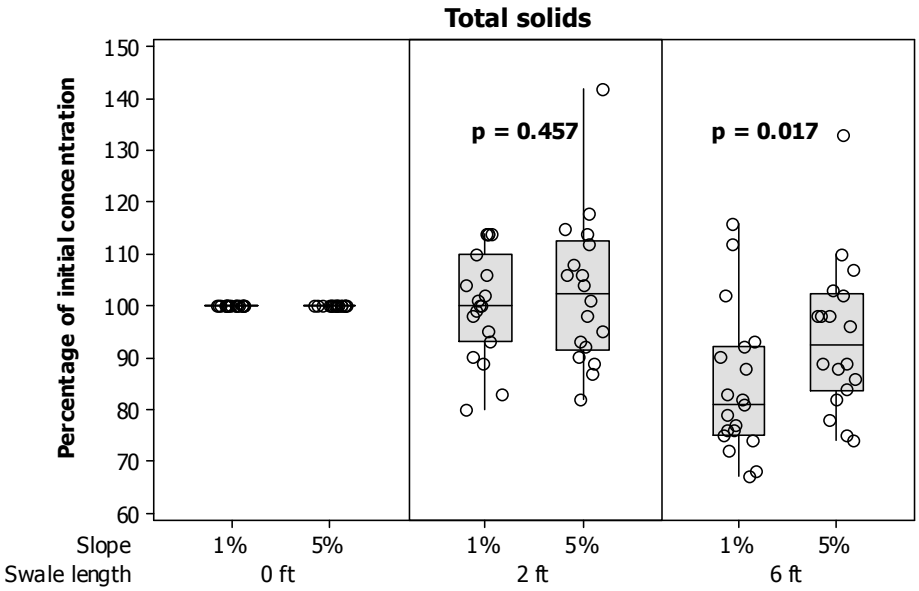

Figure 28. Box-and-whisker plots of percentages of initial concentrations of total solids and associated probabilities determined by Kruskal-Wallis test vs. swale length and slope (Note 1 ft = 0.30 m)

Sediment concentration reductions at 1% vs. 5% slope were found to be significantly different at 6 ft (1.8 m) ($p = 0.017$), but not at 2 ft (0.6 m) ($p = 0.457$). The median concentration reductions during the 1% slope tests were about 11.5% lower than during the 5% slope tests.

Total Solids Variation by Time Interval

Figure 29 shows the total solids concentration changes for different time intervals at the different sampling locations.

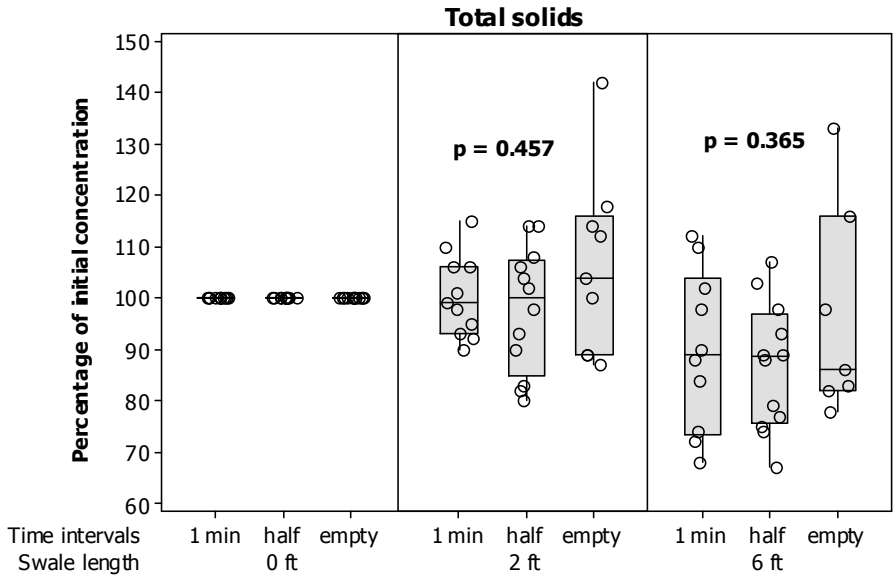

Figure 29. Box-and-whisker plots of percentages of initial concentrations of total solids and associated probabilities determined by Kruskal-Wallis test vs. swale length and time interval (Note 1 ft = 0.30 m).

There were no significant differences in sediment removal rates for the different time intervals at both the 2 ft (0.6 m) (p = 0.457) and 6 ft (1.8 m) (p = 0.365) sampling locations.

Turbidity Variation by Swale Length

Figures 30 and 31 show box and whisker plots of turbidity concentrations for different swale lengths.

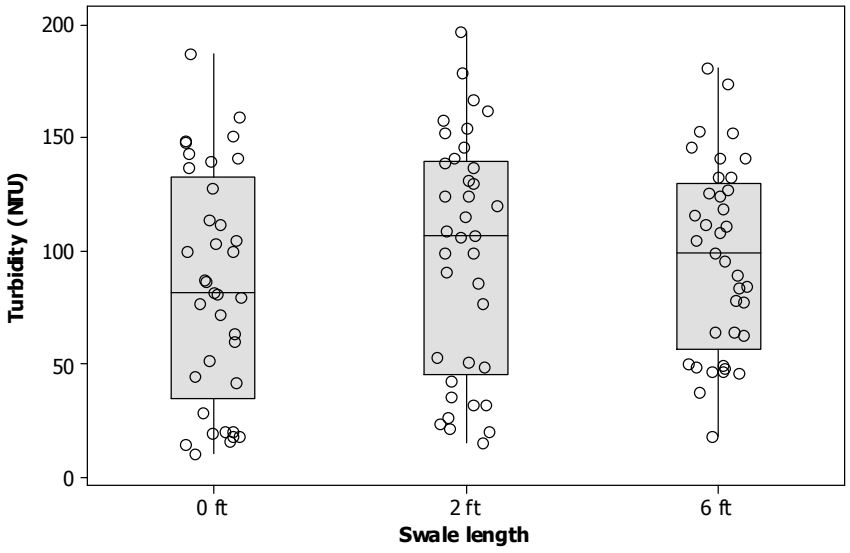

Figure 30. Box-and-whisker plots of turbidity vs. swale length (Note 1 ft = 0.30 m).

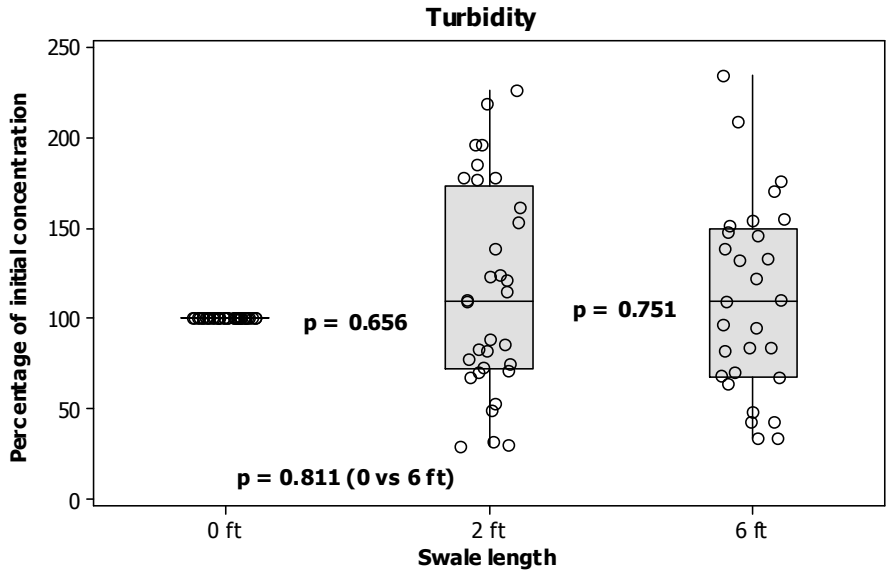

Figure 31. Box-and-whisker plots of percentages of initial concentrations of turbidity and associated probabilities determined by Kruskal-Wallis test vs. length (Note 1 ft = 0.30 m).

The probability determined by Kruskal-Wallis for overall swale length was P = 0.811, indicating no observed significant effects on turbidity reductions with sampling location.

Turbidity Variation by Grass Type

Figure 32 shows the variations in turbidity concentrations for different grass types at the different sampling locations.

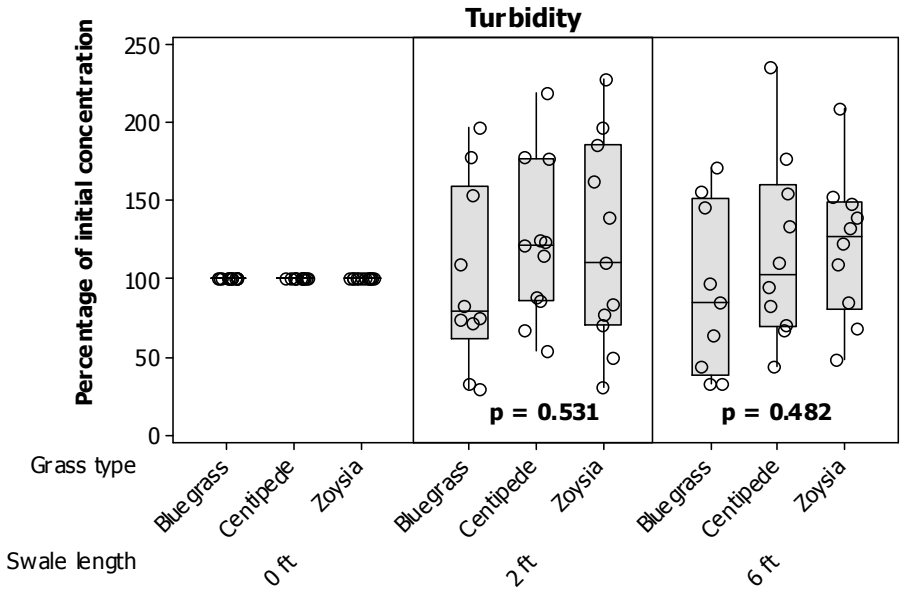

Figure 32. Box-and-whisker plots of percentages of initial concentrations of turbidity and associated probabilities determined by Kruskal-Wallis test vs. swale length and grass type (Note 1 ft = 0.30 m).

The grass type was found to be an insignificant factor affecting turbidity reductions at both 2 ft (0.6 m) ($p = 0.531$) and 6 ft (1.8 m) ($P = 0.482$).

Turbidity Variation by Flow Rate

Figure 33 shows the turbidity concentration changes for different flow rates at the different sampling locations.

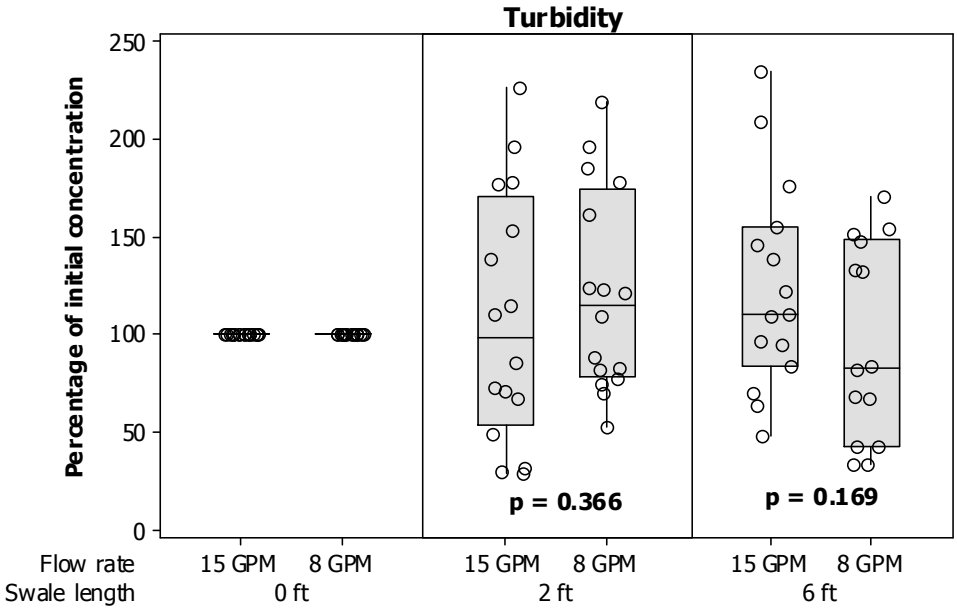

Figure 33. Box-and-whisker plots of percentages of initial concentrations of turbidity and associated probabilities determined by Kruskal-Wallis test vs. swale length and flow rate (Note 1 ft = 0.30 m, 1 GPM = 0.0038 m^3/min).

The flow rate was found to be an insignificant factor affecting turbidity reductions at both 2 ft (0.6 m) (p = 0.366) and 6 ft (1.8 m) (p = 0.169).

Turbidity Variation by Slope

Figure 34 shows the turbidity concentration changes for different grass swale slopes for the different sampling locations.

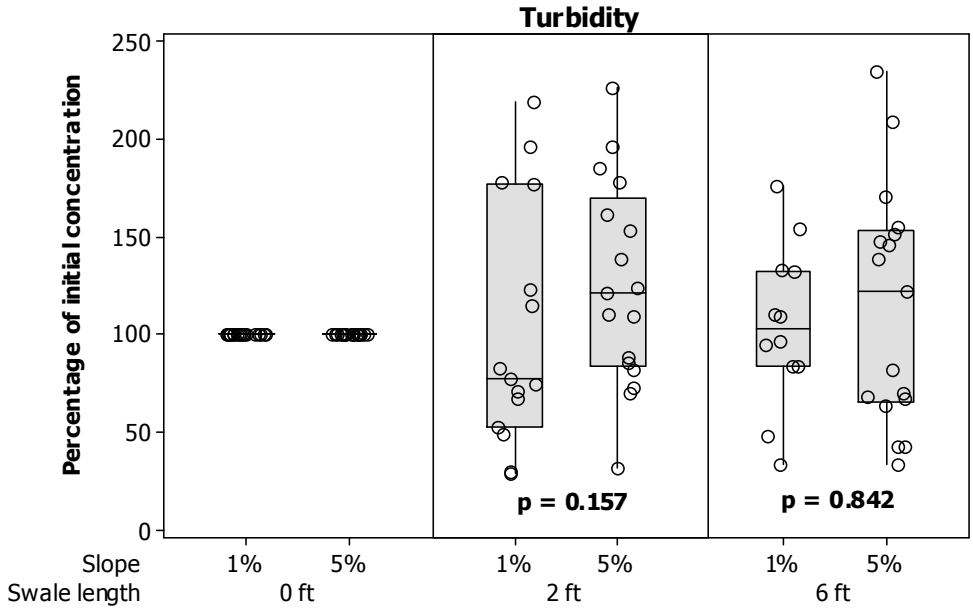

Figure 34. Box-and-whisker plots of percentages of initial concentrations of turbidity and associated probabilities determined by Kruskal-Wallis test vs. length and slope (Note 1 ft = 0.30 m).

The slope was found to be an insignificant factor affecting turbidity reductions at both 2 ft (0.6 m) ($p = 0.157$) and 6 ft (1.8 m) ($p = 0.842$).

Turbidity Variation by Time Interval

Figure 35 shows the turbidity concentration changes for different time intervals at the different sampling locations.

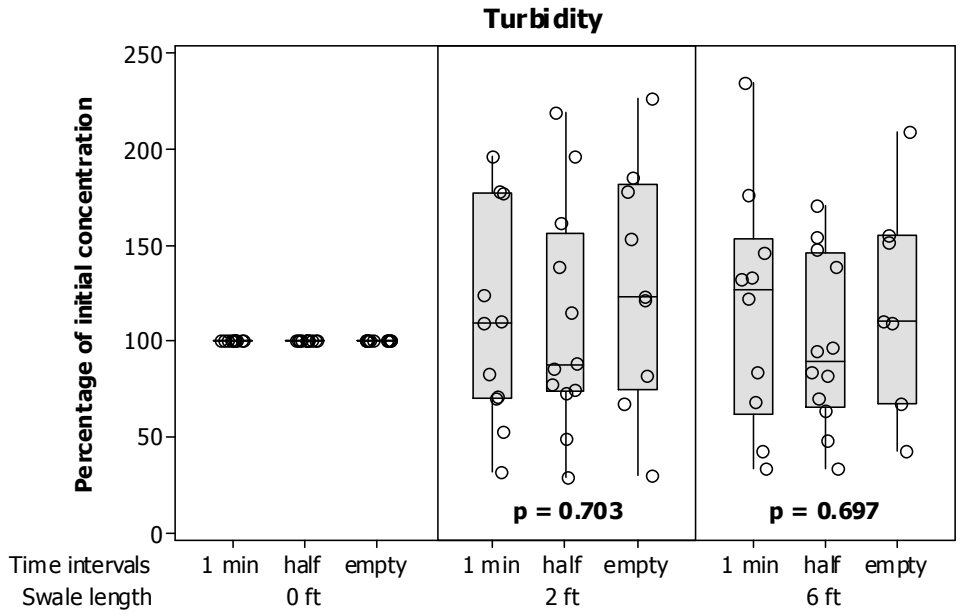

Figure 35. Box-and-whisker plots of percentages of initial concentrations of turbidity and associated probabilities determined by Kruskal-Wallis test vs. swale length and time interval (Note 1 ft = 0.30 m).

The time interval was found to be an insignificant factor affecting turbidity reductions at both 2 ft (0.6 m) ($p = 0.703$) and 6 ft (1.8 m) ($P = 0.697$).

Variables Affecting Sediment Transport

Analysis of Variance (ANOVA) tests were performed to determine the effects of the experimental variables on the normalized concentration changes. The significance level was set at 0.05 for this statistical procedure. The normalized concentration changes were normally distributed, so the more powerful ANOVA procedure was used for these comparisons.

Table 19 shows the experimental variables and associated probabilities for the normalized concentration changes at the 6 ft (1.8 m) swale location. Grass type, slope, and flow rate were all found to be significant factors affecting total solids concentration changes, but they did not affect the turbidity observations in these initial experiments. The time of sampling was not a significant factor for either total solids and turbidity changes. No interactions between variables were found to be significant, except time versus flow rate for turbidity changes.

Table 19. Experimental Variables and Associated Probabilities for the Normalized Concentration Changes at 6 ft (1.8 m)

Constituent	Variable	Probability
Total solids	Grass type	**0.048**
	Slope	**0.015**
	Flow rate	**< 0.001**
	Sampling time	0.584
	Grass type vs. Slope	0.278
	Grass type vs. Flow rate	0.162
	Slope vs. Flow rate	0.436
	Sampling time vs. Grass type	0.647
	Sampling time vs. Flow rate	0.532
	Sampling time vs. Slope	0.736
Turbidity	Grass type	0.369
	Slope	0.407
	Flow rate	0.236
	Sampling time	0.593
	Grass type vs. Slope	0.289
	Grass type vs. Flow rate	0.736
	Slope vs. Flow rate	0.181
	Sampling time vs. Grass type	0.638
	Sampling time vs. Flow rate	**0.035**
	Sampling time vs. Slope	0.263

Note: Bold probabilities represent 'significant effects' as these are less than 0.05

Particle Size Distribution Analyses

Particle size distribution (PSD) analyses were an important part of these tests. A Coulter Counter (Beckman® Multi-Sizer III™) was used to determine the particle size distributions in all of the samples collected. The results are presented in Appendix-F, and statistical summaries of PSDs are presented in Table 20.

It is important to determine how the experimental factors affected sediment transport of the different particle sizes. It is possible that some factors would affect some particle size categories more than for other size categories. The PSDs of the samples for the tests featuring the same control parameters were averaged and compared. For instance, all the PSDs of the end weir outflows (6 ft = 1.8 m) for the 5% slope tests were averaged and compared against the PSDs of the weir outflows for the 1% slope tests. Similarly, swale length, flow rate, and grass type were also compared. The affect of location was evident from the results of the 12 individual runs as described above.

Decreases in the median particle size (the 50^{th} percentile of the PSD) were used to indicate preferential trapping of larger particles in the swales during the tests. If the median size decreased at a downgradient swale location, larger particles were being preferentially trapped upgradient. For each individual test, the PSDs at the three time intervals at each location were averaged to obtain a single PSD curve. The overlay of the three curves for samples collected at the three locations also demonstrates which particles tend to move through the swale.

The original hypothesis was that grass swales would preferentially capture the larger particles and would allow the finer particles to flow through the swale with minimal trapping. Therefore, the medians of the PSDs should decrease with increasing length. Significant differences in median particle sizes were observed between 2 ft and 6 ft ($p = 0.006$), but not between 0 ft and 2 ft (0.6 m) ($p = 0.237$). In five runs, the median particle sizes at 0 ft (head works) were higher than at 2 ft (0.6 m). This could be a result of particles being scoured and eroded from the bed of the grass swale due to the force of water coming entering the swale. The metal plates used to ensure sheet flow, though effective, could not always prevent erosion.

The smallest median particle size at 6 ft (1.8 m) occurred during Test 9, for high flow with Zoysia grass at 1% slope test conditions (with a median diameter of 4.93 µm), and Test 2 which also showed a median diameter of approximately 5 µm, during a low flow with Centipede grass at 5% slope. Tests 2 and 9 are almost opposite conditions (high versus low flows and steep versus shallow slopes), indicating the need for further tests and to better control the test conditions to reduce the variability that was periodically evident during some of these initial tests. Tests 2 and 9 establish that variability in particle settling in these small swales may be too great to consistently

measure at lengths of 6 ft or less. These two tests had the lowest median sediment concentrations, but cover much of the range of experimental conditions.

The changes in median particles sizes between the head of the swale and 2 ft (0.6 m) not only reflect the high variability in settling, but also an experimental artifact. In five of twelve tests, scouring was actually indicated, probably due to incomplete dissipation of header flow momentum before the sheet flow entered the swale grass covers. Future tests should consider redesign of the metal plates to spread the flow and to prevent scour. Grass type, flow rate, and slope differences were not significant in reducing median particle sizes. Most of the probabilities presented in Figures 36 through 39 were greater than the significant level of 0.05.

Table 20. Summaries of Statistics of PSDs by Swale Length

Test-1: Centipede grass, high flow (15 GPM), 5% slope

Location	Mean (µm)	Std.dev. (µm)	10% (µm)	50% (µm)	90% (µm)
Head works	10.0	2.8	3.4	7.6	54.0
2 ft (0.6 m)	9.7	2.9	3.2	6.7	62.5
6 ft (1.8 m)	7.9	2.4	3.1	6.1	24.3

Test-2: Centipede grass, low flow (8 GPM), 5% slope

Location	Mean (µm)	Std.dev. (µm)	10% (µm)	50% (µm)	90% (µm)
Head works	8.2	2.6	3.0	5.9	30.9
2 ft (0.6 m)	13.4	3.2	3.5	11.0	79.0
6 ft (1.8 m)	5.8	2.1	2.8	5.0	16.1

Test-3: Zoysia grass, high flow (15 GPM), 5% slope

Location	Mean (µm)	Std.dev. (µm)	10% (µm)	50% (µm)	90% (µm)
Head works	23.8	4.3	3.8	19.5	169.0
2 ft (0.6 m)	9.2	2.8	3.2	6.5	55.0
6 ft (1.8 m)	7.9	2.4	3.1	6.1	24.3

Test-4: Zoysia grass, low flow (8 GPM), 5% slope

Location	Mean (µm)	Std.dev. (µm)	10% (µm)	50% (µm)	90% (µm)
Head works	7.0	2.7	2.8	5.0	34.8
2 ft (0.6 m)	13.6	3.5	3.3	10.7	96.1
6 ft (1.8 m)	10.0	3.0	3.2	7.0	62.5

Test-5: Bluegrass, high flow (15 GPM), 5% slope

Location	Mean (µm)	Std.dev. (µm)	10% (µm)	50% (µm)	90% (µm)
Head works	9.3	2.9	3.1	6.4	58.8
2 ft (0.6 m)	8.4	2.4	3.2	6.6	27.9
6 ft (1.8 m)	9.2	3.0	3.1	6.1	79.8

Test-6: Bluegrass, low flow (8 GPM), 5% slope

Location	Mean (µm)	Std.dev. (µm)	10% (µm)	50% (µm)	90% (µm)
Head works	16.9	4.7	3.2	9.5	166.0
2 ft (0.6 m)	7.6	2.4	3.1	5.8	26.0
6 ft (1.8 m)	6.3	2.2	2.9	5.2	18.0

Test-7: Bluegrass, high flow (15 GPM), 1% slope

Location	Mean (µm)	Std.dev. (µm)	10% (µm)	50% (µm)	90% (µm)
Head works	13.9	3.9	3.3	9.1	133.0
2 ft (0.6 m)	8.1	2.7	3.0	5.8	37.8
6 ft (1.8 m)	7.6	2.5	3.0	5.8	25.6

Test-8: Bluegrass, low flow (8 GPM), 1% slope

Location	Mean (µm)	Std.dev. (µm)	10% (µm)	50% (µm)	90% (µm)
Head works	10.6	3.1	3.2	7.4	70.0
2 ft (0.6 m)	8.0	2.5	3.1	6.1	28.0
6 ft (1.8 m)	6.6	2.2	3.0	5.4	19.8

Test-9: Zoysia grass, high flow (15 GPM), 1% slope

Location	Mean (µm)	Std.dev. (µm)	10% (µm)	50% (µm)	90% (µm)
Head works	15.5	3.6	3.4	13.5	113.0
2 ft (0.6 m)	6.8	2.0	3.0	5.8	19.4
6 ft (1.8 m)	5.9	2.1	2.8	4.9	17.2

Test-10: Zoysia grass, low flow (8 GPM), 1% slope

Location	Mean (µm)	Std.dev. (µm)	10% (µm)	50% (µm)	90% (µm)
Head works	11.0	3.2	3.1	7.4	73.4
2 ft (0.6 m)	9.1	2.7	3.1	6.7	42.1
6 ft (1.8 m)	7.5	2.5	3.0	5.6	26.8

Test-11: Centipede grass, high flow (15 GPM), 1% slope

Location	Mean (µm)	Std.dev. (µm)	10% (µm)	50% (µm)	90% (µm)
Head works	11.5	3.2	3.2	8.6	73.6
2 ft (0.6 m)	12.1	3.2	3.2	9.0	79.3
6 ft (1.8 m)	9.3	3.1	3.0	6.0	77.4

Test-12: Centipede grass, low flow (8 GPM), 1% slope

Location	Mean (µm)	Std.dev. (µm)	10% (µm)	50% (µm)	90% (µm)
Head works	10.2	3.2	3.1	6.6	78.3
2 ft (0.6 m)	9.7	2.9	3.2	6.9	56.4
6 ft (1.8 m)	7.9	2.9	2.9	5.5	65.4

Table 21. Summary Statistics for Particle Sizes vs. the Experimental Variables

Grass type	Mean (µm)	Std.dev. (µm)	10% (µm)	50% (µm)	90% (µm)
Bluegrass	7.3	2.5	3.0	5.6	26.1
Centipede	7.9	2.7	3.0	5.6	42.1
Zoysia	7.7	2.5	3.0	5.8	29.0

Slope	Mean (µm)	Std.dev. (µm)	10% (µm)	50% (µm)	90% (µm)
1%	7.5	2.6	3.0	5.5	33.0
5%	8.5	2.8	3.1	5.9	49.6

Flow rate	Mean (µm)	Std.dev. (µm)	10% (µm)	50% (µm)	90% (µm)
8 GPM	9.0	3.0	3.1	6.0	72.5
15 GPM	7.3	2.5	3.0	5.5	27.6

Sampling time	Mean (µm)	Std.dev. (µm)	10% (µm)	50% (µm)	90% (µm)
1 min	7.9	2.6	3.0	5.9	29.0
Half tank	7.4	2.5	2.97	5.6	26.8
Empty	9.1	3.2	3.0	5.8	85.1

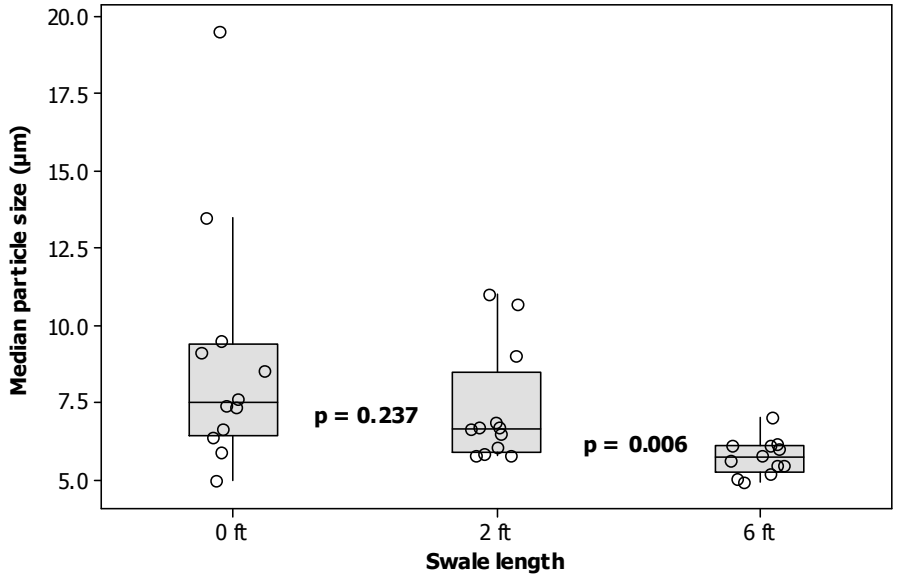

Figure 36. Box-and-whisker plots of median particle sizes and associated probabilities determined by Kruskal-Wallis test vs. swale length (Note 1 ft = 0.30 m).

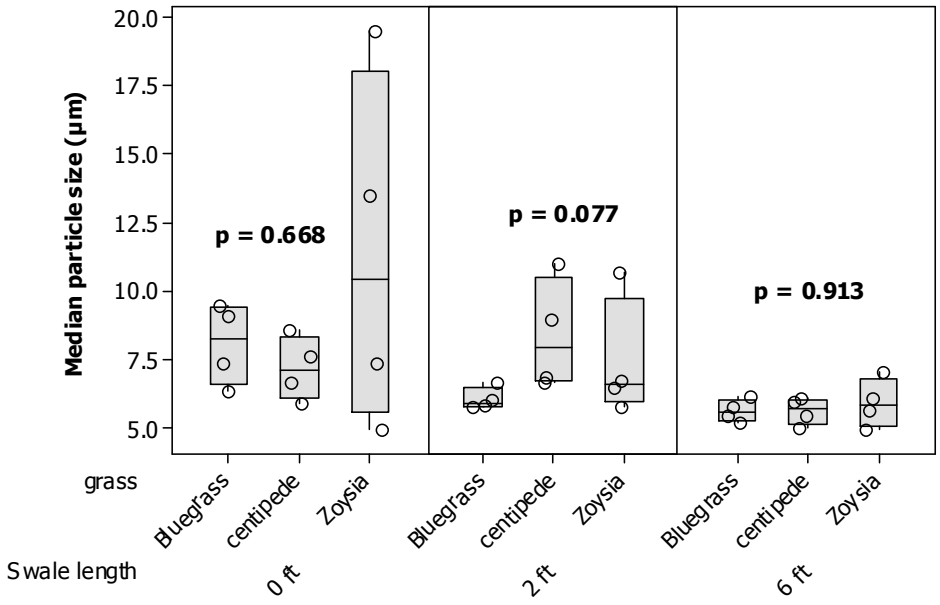

Figure 37. Box-and-whisker plots of median particle sizes and associated probabilities determined by Kruskal-Wallis test vs. swale length and grass type (Note 1 ft = 0.30 m).

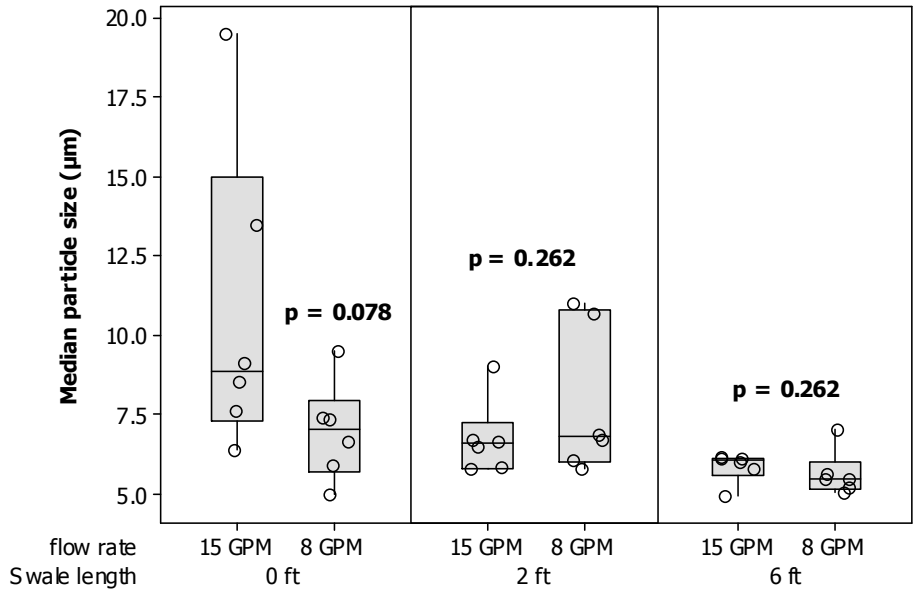

Figure 38. Box-and-whisker plots of median particle sizes and associated probabilities determined by Kruskal-Wallis test vs. swale length and flow rate (Note 1 ft = 0.30 m, 1 GPM = 0.0038 m^3/min).

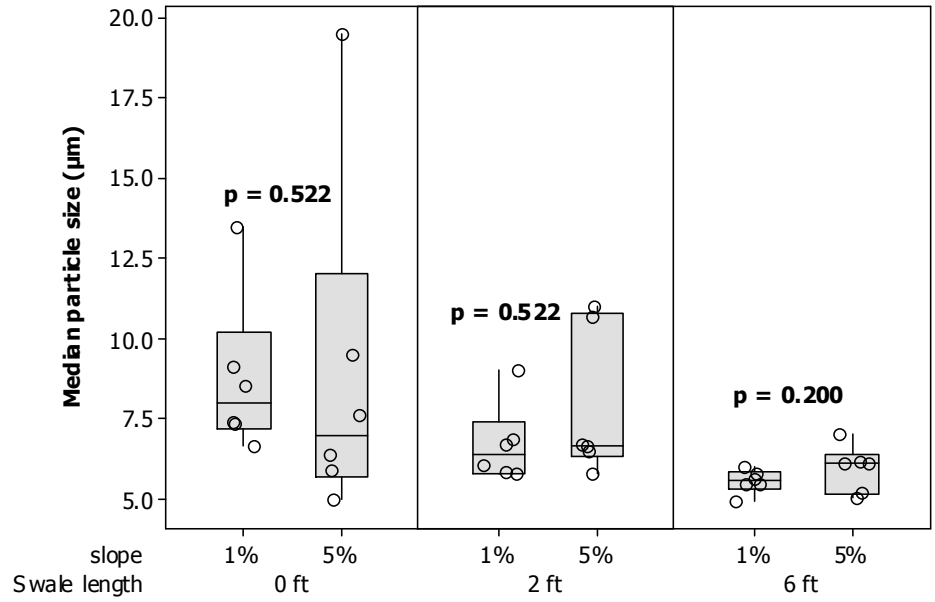

Figure 39. Box-and-whisker plots of median particle sizes and associated probabilities determined by Kruskal-Wallis test vs. swale length and slope (Note 1 ft = 0.30 m).

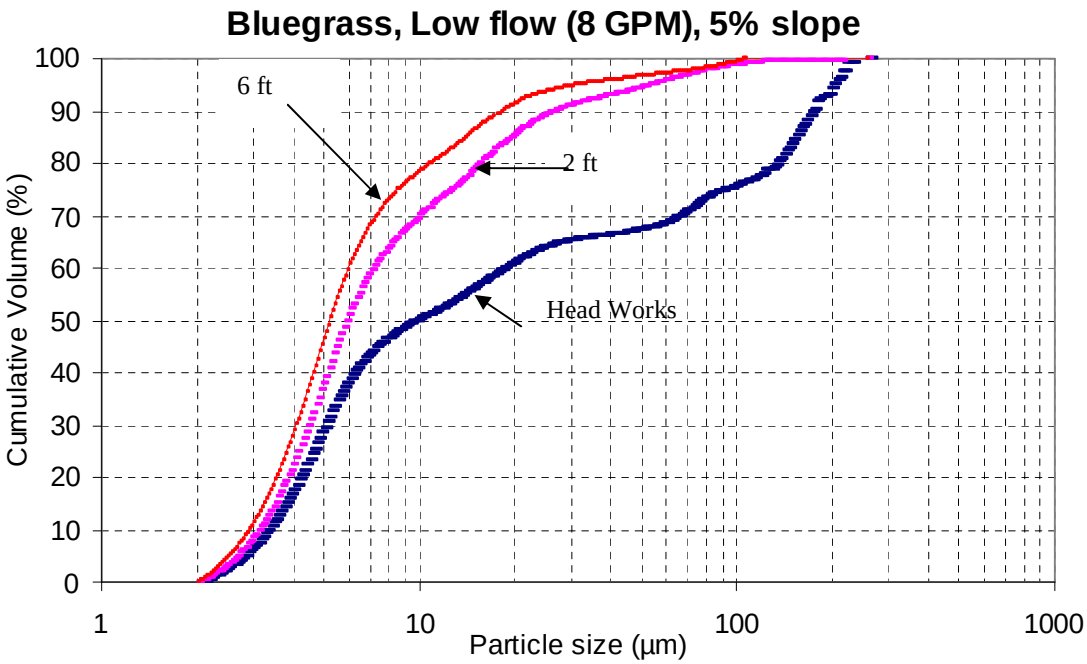

Figure 40. Example PSDs at different locations along the swale.

As shown in Figure 36, there was a significant effect of swale length in reducing median particle sizes between the head works and 6 ft (1.8 m) ($p = 0.006$), but not between the headworks and 2 ft (0.6 m) ($p = 0.237$). Figure 40 shows an example PSD at the different swale lengths (head works, 2 ft (0.6 m), and 6 ft (1.8 m)) for a Bluegrass swale during low flow (8 GPM) at 5% channel slope. In this particular test, particle sizes were significantly reduced in the grass swale especially between the head works and 2 ft (0.6m). The other three factors (flow rate, slope, and grass type) were not found to be significant in reducing median particle sizes, as shown in Figure 37, 38, and 39.

Conclusions

As expected, increased swale length, lower slopes, and lower flow rates were observed to be the most important conditions which result in increased sediment retention by grass swales.

Total Solids and Turbidity

Swale length:

- Total solids: Significant sediment reductions were observed between 2 ft (0.6 m) and 6 ft (1.8 m) ($p < 0.001$), but not between 0 ft and 2 ft (0.6 m) ($p = 0.546$). This suggests that sedimentation becomes measurable beyond 2 ft (0.6 m). An overall 12% reduction in total solids was observed.

- Turbidity: Swale length was not found to be a significant factor ($p = 0.811$ between 0 ft and 6 ft (1.8 m)) in reducing turbidity levels.

- Longer lengths provided more time for sediment to settle in the grass swales. This was more evident for the larger particles in these short swales.

Grass type:

- Total solids: A significant difference in total solids concentrations for the different grass types was observed at 6 ft (1.8 m) ($p = 0.061$), but not at 2 ft (0.6 m) ($p = 0.371$). Centipede grass was found to be the most efficient among the three grass types. At 6 ft, 20% of the sediments were retented in Centipede grass whereas Bluegrass swale was 11% and Zoysia grass swale was 12%.

- Turbidity: Grass type was not found to be a significant factor affecting turbidity levels for both 2 ft (0.6 m) ($p = 0.531$) and 6 ft (1.8 m) ($p = 0.482$).

- The stem length of Bluegrass is higher than for Zoysia. During high flows (15 GPM), the water flooded the Zoysia grass more often than Bluegrass, reducing sediment retention efficiency.

- Even though the stems of the Centipede grass are larger than for the other grasses tested, the stem density of the grass was less. The density of the grass may therefore be more important than the grass stem length in sediment capture and retention.

Flow rate:

- Total solids: A significant difference was observed in total solids reductions at 6 ft (1.8 m) ($p < 0.001$), but not at 2 ft (0.6 m) ($p = 0.803$) for the different flow rate tests. The median reductions during the 8 GPM (0.03 m^3/min) tests were 16.5% better than during the 15 GPM (0.06 m^3/min) tests at 6 ft (1.8 m).

- Turbidity: Flow rate was not found to be a significant factor affecting turbidity levels at both 2 ft (0.6 m) ($p = 0.366$) and 6 ft (1.8 m) ($p = 0.169$).

Slope:

- Total solids: A significant difference was observed in total solids reductions at 6 ft (1.8 m) ($p = 0.017$), but not at 2 ft (0.6 m) ($p = 0.457$) for the different swale slopes. The median reductions for the 1% sloped swales were 11.5% better than for the 5% sloped swales at 6 ft (1.82 m).

- Turbidity: Slope was not found to be a significant factor affecting turbidity levels for both 2 ft (0.6 m) ($p = 0.157$) and 6 ft (1.8 m) ($p = 0.842$).

• Swales at 1% slopes retained particles better than the swales at 5% slopes. The flatter slopes resulted in longer travel times for the particles to travel within the swale and allowed smaller particles to settle before the end of the swale was reached.

Sampling time:

• Total solids: The sampling time was not found to be a significant factor affecting total solids retention for both 2 ft (0.6 m) ($p = 0.457$) and 6 ft (1.8 m) ($p = 0.365$) sampling locations.

• Turbidity: The time interval of sampling was not found to be a significant factor affecting turbidity levels for 2 ft (0.6 m) ($p = 0.703$) and 6 ft (1.8 m) ($p = 0.697$) sampling locations.

Table 22. Significant Factors Affecting Total Solids and Turbidity Reductions in Grass Swales

Constituent	Variable	Probabilities
Total Solids	Grass type	0.048
	Slope	0.015
	Flow rate	< 0.001
Turbidity	Time * Flow rate	0.035

Particle Size Distribution Analyses

• There was some ambiguity in the PSD median values between the headworks and the 2 ft (0.6 m) samples; in most runs, the headworks showed a higher median particle sizes, but in 5 runs the 2 ft (1.8 m) sample showed a higher median particle size. This could be because of scouring and associated erosion of the grass bed between these locations.

• Swale length was found to be a significant factor in reducing median particle sizes. The median particle size was reduced from 7.5 µm at the head works to 5.7 µm at 6 ft. The other factors (flow rate, slope, and grass type), however, were found to be insignificant.

Findings and Suggestions

The following modifications and further studies were identified after these initial experiments in order to better understand the response of the swales to varying conditions:

• These initial analyses did not include separate total suspended solids and total dissolved solids analyses. It is expected that the retention of total dissolved solids would be minimal in a grass swale and without separating out this contribution, the total solids results from these initial experiments could be confused by "constant" total dissolved solids values.

• The length of the grass swale was too short to be able to clearly distinguish the settling of particles, especially between the head works (0 ft) and 2 ft (0.6 m). More precise control of some variables and more repetitions are needed to eliminate or confirm some of the conflicting results.

• The test setup needs a better measurement and control method for flow rate. It is critical to maintain the same flow rate for all the similar experiments. Although this was attempted, there was some unwanted flow variability.

• The density of the grass, especially for Zoysia, could have been better; the swale Zoysia grass density was sparse at certain locations.

• Overall, the control factors needed to be better controlled to get more meaningful results, although most of the results obtained during these initial tests appear reasonable. The second series of experiments described in the next chapter were set up to address many of these shortcomings.

Chapter 6: Second Set of Controlled Indoor Swale Experiments

Introduction

The initial set of experiments described in the previous chapter identified the primary factors affecting the transport of stormwater sediment in grass swales. To understand these factors further, additional experiments were conducted in the second sets of experiments described in this chapter. In addition, a number of modifications in the experimental setup were made to reduce the variability of the measured values. Centipede grass was replaced with synthetic turf to determine if the synthetic turf resulted in similar sediment transport conditions compared to actual grass. The initial experiment showed that the time of sampling since the start of the test not important, and this factor was therefore not included during these experiments. Also, additional analyses were conducted; total suspended solids, total dissolved solids, and total solids greater than and less than 106 µm. Particle size distribution and turbidity analyses were also conducted during these experiments.

Indoor Laboratory Swales

Descriptions of the Experimental Set-up

There were two experimental problems during the initial set of swale experiments that were addressed during these newer experiments. Although the two 65 GPM (0.25 m^3/min) sump pumps were employed to agitate the sediments in the 150-gallon (0.57 m^3) tank, large sediment particles, such as sands, were not well-mixed and suspended in the tank. Consequently, significant amounts of large particles were settled out on the bottom of the tank during the initial experiment and not pumped to the swale. The "headworks" sampling eliminated errors in analyzing the samples, but it was difficult to represent these larger particles in the tests. Another problem was the accuracy and repeatability of the flow rates. Flow rates were controlled by a valve attached to the piping network. However, valve movement was too sensitive and hard to control the desired flow rate.

To solve these problems, the headworks of the experimental setup was modified. The modified system for the second experiment consisted of a slurry feeding device with pump, mixing chamber, and a wood channel. Figures 41, 42, and 43 show the sediment slurry mixture feeding device, including the small pump and the mixing chamber. Known amounts of the sediment mixture and water were mixed in the feeding device and were pumped into the mixing chamber as a slurry. A regulated flow pumped from the 150 gallon (0.57 m^3) tank (filled with tap water) was mixed with the slurry in the mixing chamber. The solution was then dispersed onto the wood channel to create a 2 ft (0.6 m) wide sheet flow before entering the grass lined channel. Also, the flow rates were more accurately controlled during the second set of tests.

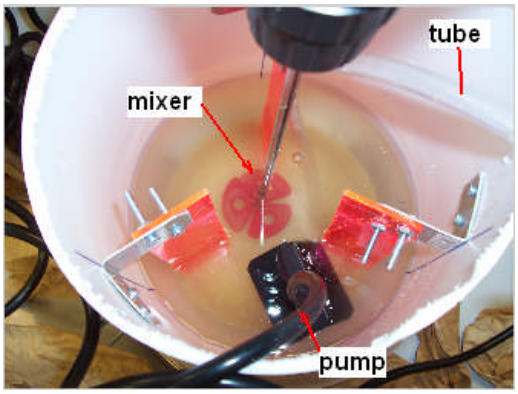

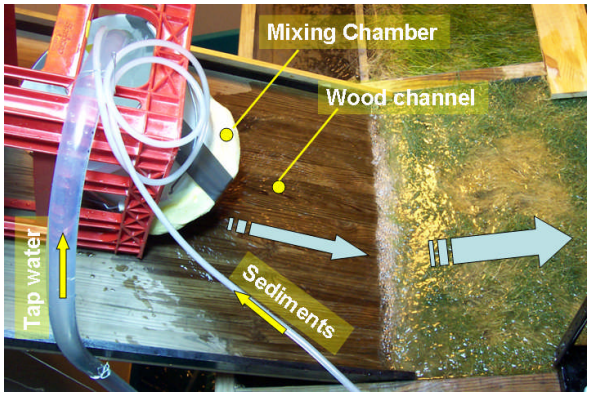

Figure 41. (*left*) Picture showing the sediment feeding device consisting of a mixer, bucket, small pump, and plastic tube.
Figure 42. (*Right*) Sediment slurry and tap water are being mixed at the mixing chamber (A sheet flow is created at the wood channel).

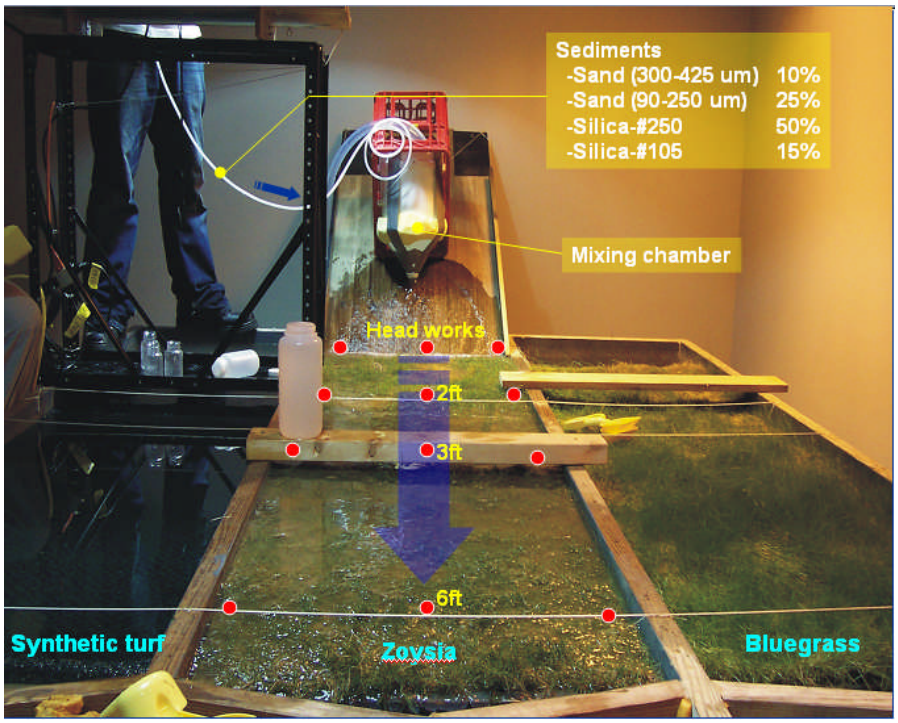

Figure 43. Picture showing the indoor experimental setup (Three different types of grass are mounted on a base which can be adjusted in slope. In this test, the sediment solution is being introduced onto the Zoysia swale).

Sediment Characteristics of the Sediment-Water Mixture

Fine-ground silica (SIL-CO-SIL® from US Silica Co.), along with sieved sands, were used in the test mixture. These fine-ground silicas are bright white, low in moisture, and chemically inert. Two different sizes of silca, SIL-CO-SIL®106 ("all" material smaller than 106 µm) and SIL-CO-SIL®250 ("all" material smaller than 250 µm) were used. Sieved sands were also used to provide larger particles, ranging from 90 to 250 µm and 300 to 425 µm. The

sediment concentration of the test flow was targeted at 500 mg/L. Table 23 shows the percentage contribution of the test sediments in different particle size ranges, while Figure 44 shows the particle size distribution of the test sediment mixture. This mixture had more of the larger particles (the median size was about 50 µm) than typical stormwater (usually median particle size of about 10 µm, although some samples have larger median sizes). This enabled us to more accurately measure the performance of the grass swales over a wide range of particles. Since each particle size range was evaluated individually, this somewhat distorted distribution did not hinder our ability in evaluating the results.

Table 23. Percentage Contribution and Specific Gravity of the Test Sediments

Sediment	Percentage contribution	Specific gravity
Silica (SIL-CO-SIL®106)	15%	2.65
Silica (SIL-CO-SIL®250)	50%	2.65
Sand (90 - 250 µm)	25%	2.65
Sand (300 - 425 µm)	10%	2.65
Total	100%	

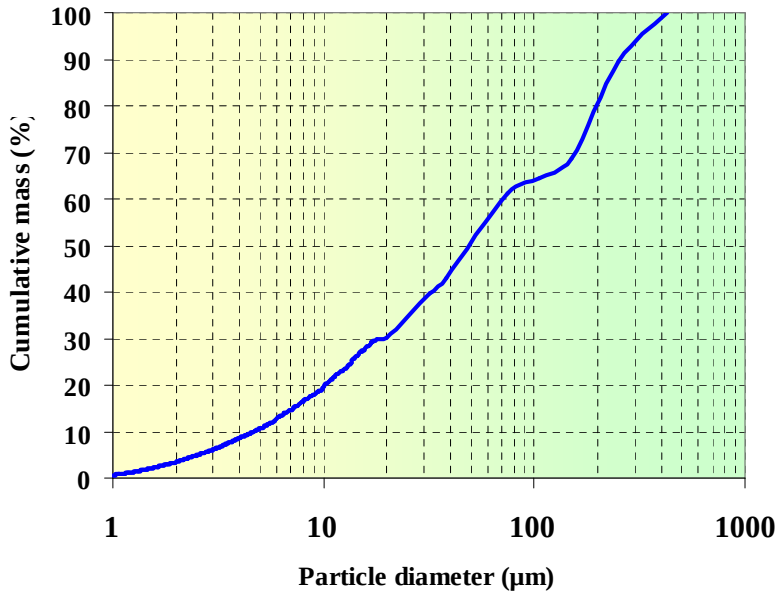

Figure 44. Particle size distribution of the test sediment mixture.

Table 24. Particle Size Distributions of SIL-CO-SIL®106 and SIL-CO-SIL®250[1]

	SIL-CO-SIL®106	SIL-CO-SIL®250
Particle size (µm)	Percentage in size range	Percentage in size range
0 to 45	73.0%	50.0%
45 to 53	7.0%	8.0%
53 to 75	12.5%	11.0%
75 to 106	5.6%	12.0%
106 to 150	1.5%	9.5%
150 to 212	0.1%	6.0%
> 212	0.0%	3.5%
Total	100%	100%

[1] particle size information from U.S. Silica Co. data sheets

Factors Tested During the Second Experiments

One result of the initial experiments indicated that the time factor since the beginning of the steady state experiment was not important in affecting the particle retention in the swales. Thus, this factor was excluded from the second experiment by taking composite samples during the experimental run. Also, Centipede grass was replaced with synthetic turf to determine whether the synthetic turf produced similar results to actual grass. Several prior swale experiments used synthetic media, so these experiments were conducted to investigate how this material compared to actual grass. The following were the variables tested during the second set of experiments:

- *Grass types*: The three different types of grass tested were synthetic turf, Zoysia, and Kentucky Bluegrass. Synthetic turf was obtained from a local household maintenance warehouse store. The height of stems of the synthetic turf was approximately 0.25 inches (0.635 cm) which was much shorter than the other grass, and the stems were quite still. The stems were made of thin and uniformly dense plastic films shown in Figure 45 and 46.

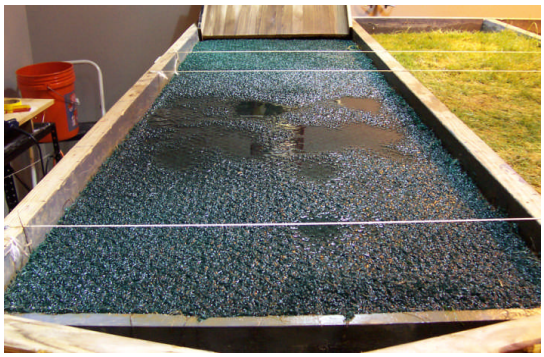

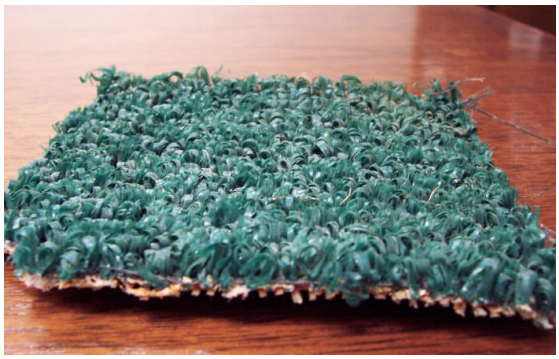

Figure 45. (*left*) Picture showing the channel with the synthetic turf.
Figure 46. (*Right*) Close-up of the synthetic turf.

- *Slopes*: 1%, 3%, and 5% channel slope were tested.
- *Flow rates*: Adequate control of flow rates was achieved by the modified headworks. Flow rates were 10 GPM (0.038 m^3/min), 15 GPM (0.064 m^3/min), and 20 GPM (0.076 m^3/min).
- *Swale lengths*: The samples were collected at the entrance (0 ft), 2 ft (0.6 m), 3 ft (0.9 m), and 6 ft (1.8 m).

Analytical Methods

During the second experiment, 108 samples were collected and analyzed for the following analytical parameters.

- Total solids (Standard Methods 2540B)
- Total solids after screening with a 106 µm sieve (total solids < 106 µm, to better match the particulates measured by the Coulter Counter)
- Total suspended solids (solids retained on a 0.45 µm filter) (Standard Methods 2540D)
- Total dissolved solids (solids passing through a 0.45 µm filter) (Standard Methods 2540C)
- Turbidity using a HACH 2100N Turbidimeter
- Particle size distribution by Coulter Counter (Beckman® Multi-Sizer III™), composite of several different aperture tube measurements (30, 100, and 400 µm apertures)

Each sample was collected in a 1 litter plastic sampling bottle and was equally divided into a subset of 10 subsamples by using the USGS/Dekaport Cone Splitter shown in Figure 47 (Rickly Hydrological Company). The cone splitter was utilized to ensure that sediment characteristics of sub-samples were identical to each other for analyzing the different analytical parameters. For each parameter, two replicates were produced and analyzed to increase the reliability of the tests. The performance of USGS/Dekaport Cone Splitter for producing identical sub-samples is presented in Appendix J.

Figure 47. UAGS/Dekaport cone sample splitter.

Head Works Study

Despite the modification of the headworks, it was still difficult to maintain consistent sediment concentrations of the sediment-water mixture entering the grass channels during the tests. Analytical results showed a larger variability of sediment concentrations than desired at the head works, especially for large particles.

Figure 48 shows that total dissolved solids (< 0.45 µm) at the head work were relatively consistent, but the concentrations of particles ranging in size from 0.45 to 106 µm and from 106 to 425 µm had greater variability during the experiments. Large particles in the 106 to 425 µm size range had the largest overall variability due to the difficulty of consistently suspending large particles in the mixture. Because of this variability, all concentration data were normalized against the initial sediment concentrations at the head works. Analysis of Variance (ANOVA) tests were performed to determine the effects of the experimental variables on these normalized concentration changes. However, residuals of the ANOVA were not normally distributed as required (normality tested using the Anderson-

Darling statistical test). Therefore, for each swale length, the normalized data were ranked. The ANOVA was then used on these ranked normalized data to determine the significance of the variables.

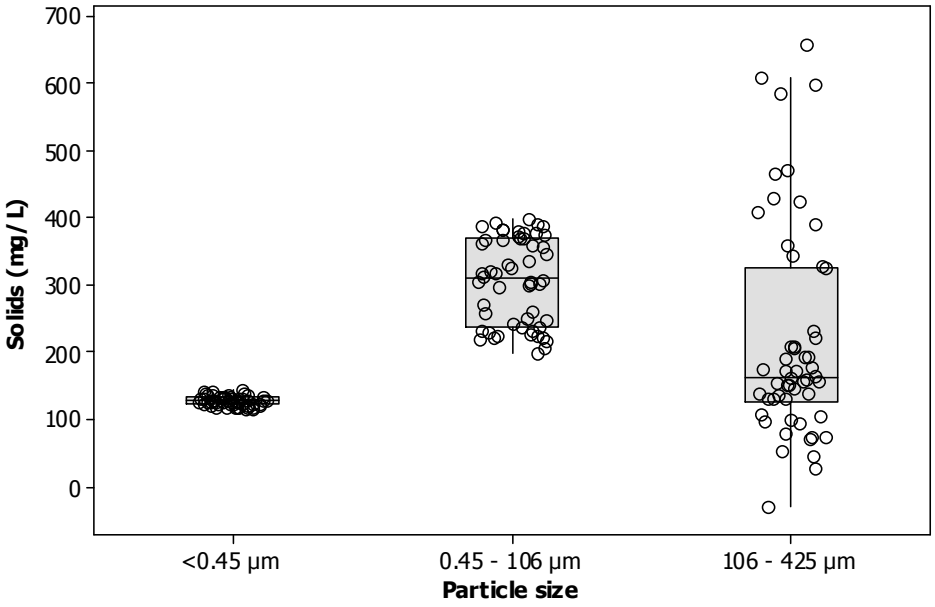

Figure 48. Box-and-whisker plots of initial sediment concentrations differentiated by the particle size ranges at the head works.

Data Analysis and Results

The complete analytical results obtained during the second set of experiments are presented in Appendix B.

Swale Length

Figures 51, 52, 53 and 55 show that significant sediment reductions were observed at 2 ft (0.6 m), 3 ft (0.9 m), and 6 ft (1.8 m) for total solids, total solids after screening with a 106 µm sieve, total suspended solids, and turbidity. Figure 54 shows that there were no significant changes in total dissolved solids as a function of swale length (the numbers of samples were too small to measure the significance of the small differences). Sediments were rapidly reduced between the head works (0 ft) and 2 ft (0.6 m) due to the settlement of large particles at the beginning of the swale. Smaller-sized sediments were gradually reduced between 2 ft (0.6 m) and 6 ft (1.8 m), as the smaller particles were more likely to be carried over longer distances than the larger particles. The median concentration of total suspended solids was reduced from 460 mg/L at 0 ft to 200 mg/L at 2 ft (0.6 m) (56% reduction), and, the median total suspended solids concentration at 6 ft (1.8 m) was 110 mg/L (76% reduction). Unlike solids, turbidity reductions shown in Figure 55 were relatively constant with swale length, since turbidity was not as affected by the larger particles which were preferentially removed. The median of turbidity was reduced from 64 NTU at 0 ft (0 m) to 38 NTU at 6 ft (1.8 m) (40% reduction).

After each experiment, sands were visually observed up to 1 ft (0.3 m) from the head works. Figure 49 and 50 show that deposition was not uniform across the swale. This visual observation confirms that large particles were predominantly captured at the beginning of the grass swales.

Figure 49. (*left*) Picture showing sand accumulation on the synthetic turf swale.
Figure 50. (*right*) Close-up of sand accumulation on the Bluegrass swale.

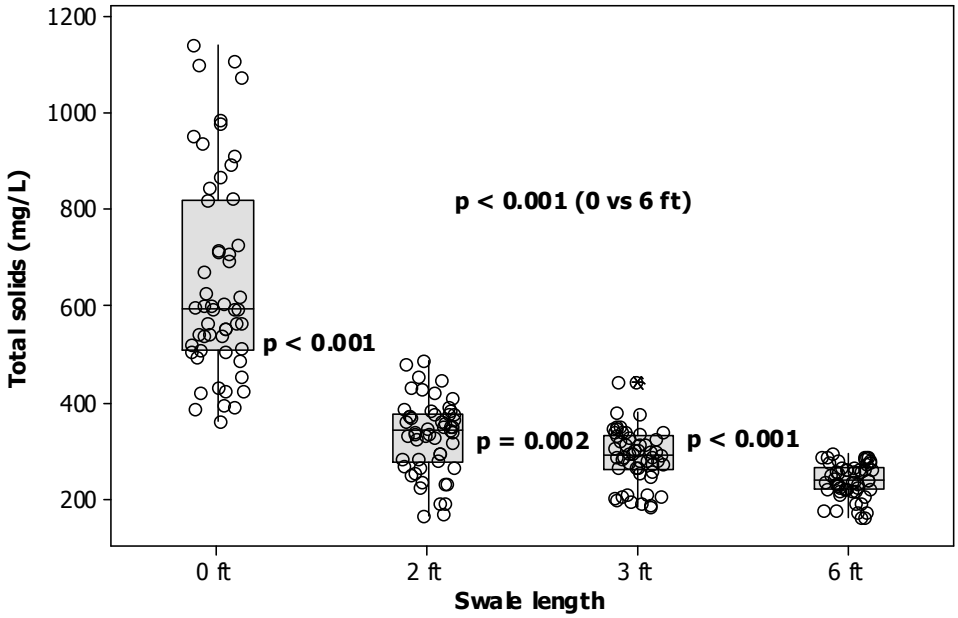

Figure 51. Box-and-whisker plots of total solids concentrations vs. swale length (Note 1 ft = 0.30 m).

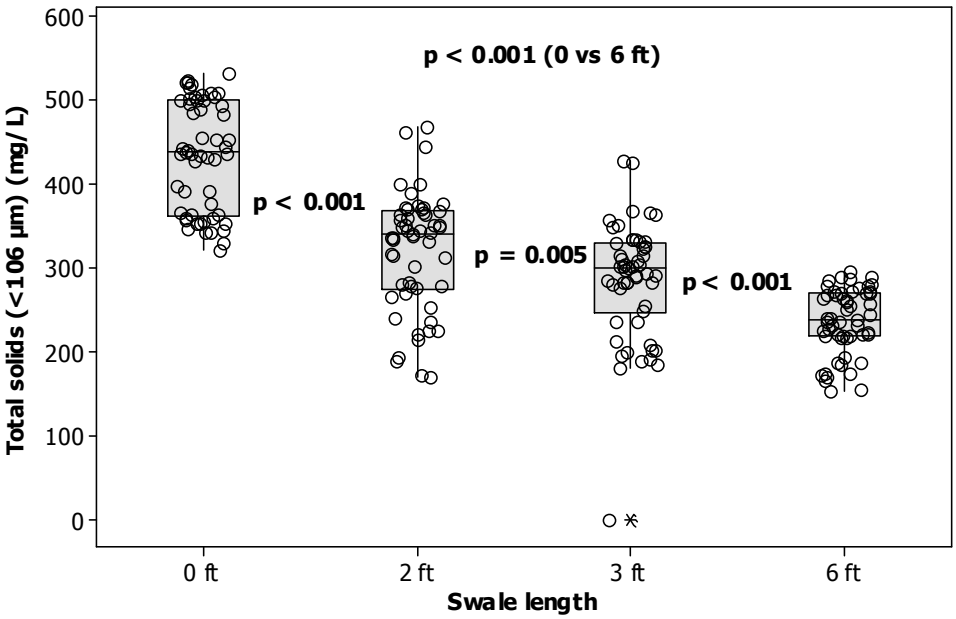

Figure 52. Box-and-whisker plots of total solids (< 106 µm) concentrations vs. swale length (Note 1 ft = 0.30 m).

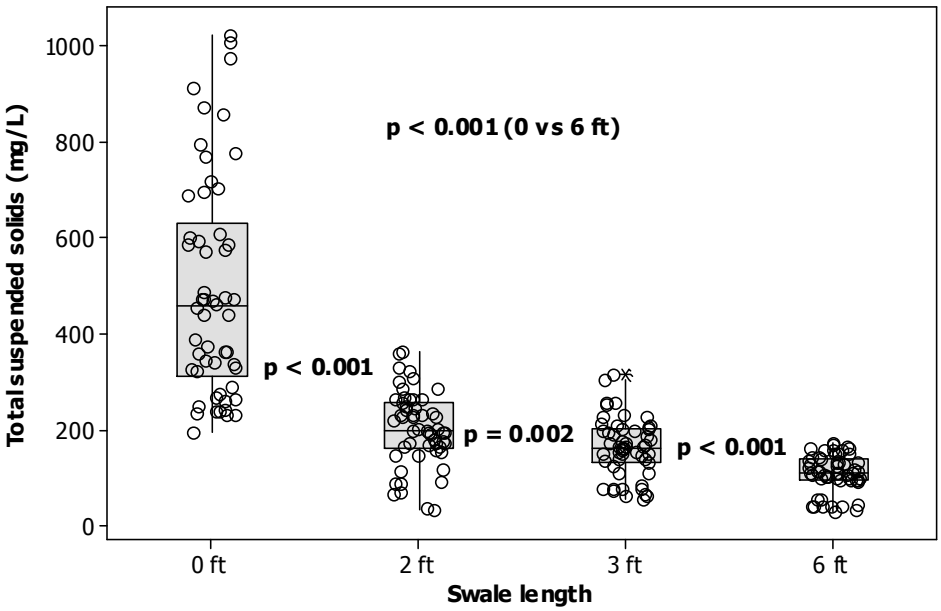

Figure 53. Box-and-whisker plots of total suspended solids concentrations vs. swale length (Note 1 ft = 0.30 m).

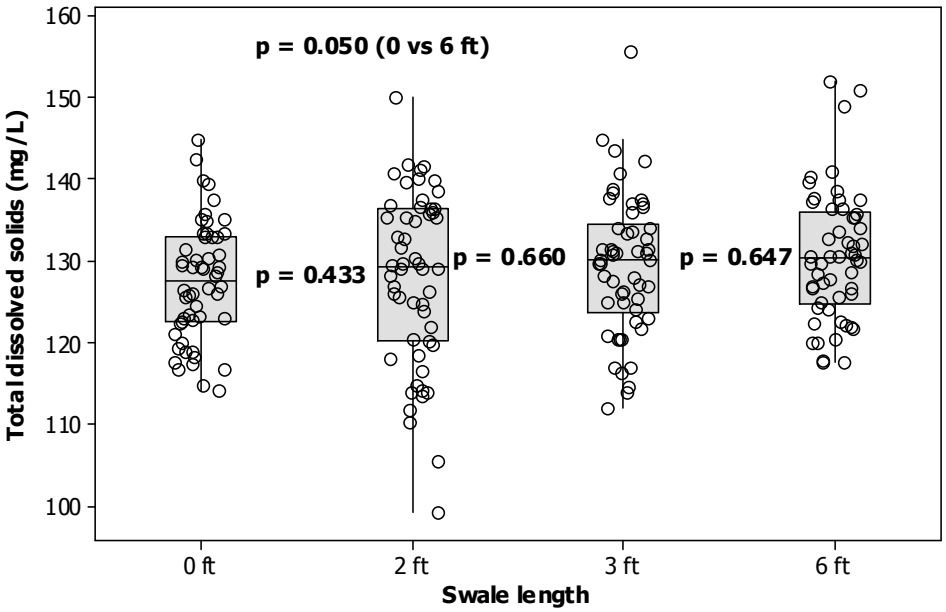

Figure 54. Box-and-whisker plots of total dissolved solids concentrations vs. swale length (Note 1 ft = 0.30 m).

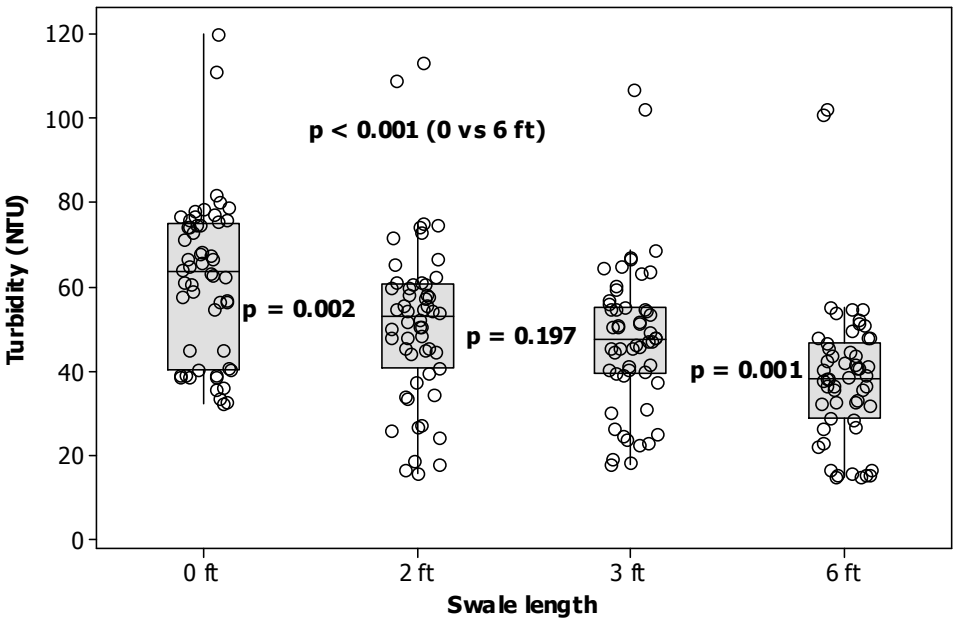

Figure 55. Box-and-whisker plots of turbidity concentrations vs. swale length (Note 1 ft = 0.30 m).

Variables Affecting Sediment Transport

ANOVA was performed to determine the effects of the experimental variables on the ranked normalized concentration changes. The significance level was set at 0.05 for this statistical procedure. Swale length, grass type, slope, and flow rate were significant factors for most of the particulate constituents. In contrast, all variables were insignificant for total dissolved solids. Among the three grass types, synthetic turf was found to be the least effective, and Zoysia and Kentucky Bluegrass had similar sediment reduction rates. The effects of channel slope and flow rate were marginal for total solids and total suspended solids. However, these effects were clearly significant for turbidity. A 1% slope was found to be much more efficient in trapping the particulates than the 3% and 5% slopes, and the low flow rate of 10 GPM (0.038 m3/min) was more effective in reducing turbidity than the higher flow rates of 15 GPM (0.064 m3/min) and 20 GPM (0.076 m3/min). Some of the interactions between the factors were also important and need to be considered when explaining sediment transport in grass swales. Table 25 shows the variables and interaction terms and associated probabilities for each constituent. The followings are Box and whisker plots of the changes in concentrations compared to initial values. Also, Box and whisker plots of the actual observed concentrations are presented in Appendix G.

Table 25. Variables and Associated Probabilities at 6 ft (1.8 m)

Constituent	Variable	Probabilities
Total solids	**Grass type**	**< 0.001**
	Slope	**0.006**
	Flow rate	**< 0.001**
	Grass type*Slope	0.333
	Grass type*Flow rate	**0.023**
	Slope*Flow rate	0.429
Total solids (< 106 µm)	**Grass type**	**< 0.001**
	Slope	0.746
	Flow rate	0.879
	Grass type*Slope	0.641
	Grass type*Flow rate	**< 0.001**
	Slope*Flow rate	**< 0.001**
Total suspended solids	**Grass type**	**< 0.001**
	Slope	**0.047**
	Flow rate	0.247
	Grass type*Slope	0.194
	Grass type*Flow rate	**0.005**
	Slope*Flow rate	**0.013**
Total dissolved solids	Grass type	0.701
	Slope	**0.049**
	Flow rate	0.498
	Grass type*Slope	0.842
	Grass type*Flow rate	**0.044**
	Slope*Flow rate	0.244
Turbidity	**Grass type**	**< 0.001**
	Slope	**0.02**
	Flow rate	0.144
	Grass type*Slope	**0.001**
	Grass type*Flow rate	**< 0.001**
	Slope*Flow rate	0.387

* Bolded probabilities represent 'significant effects' because these are less than 0.05

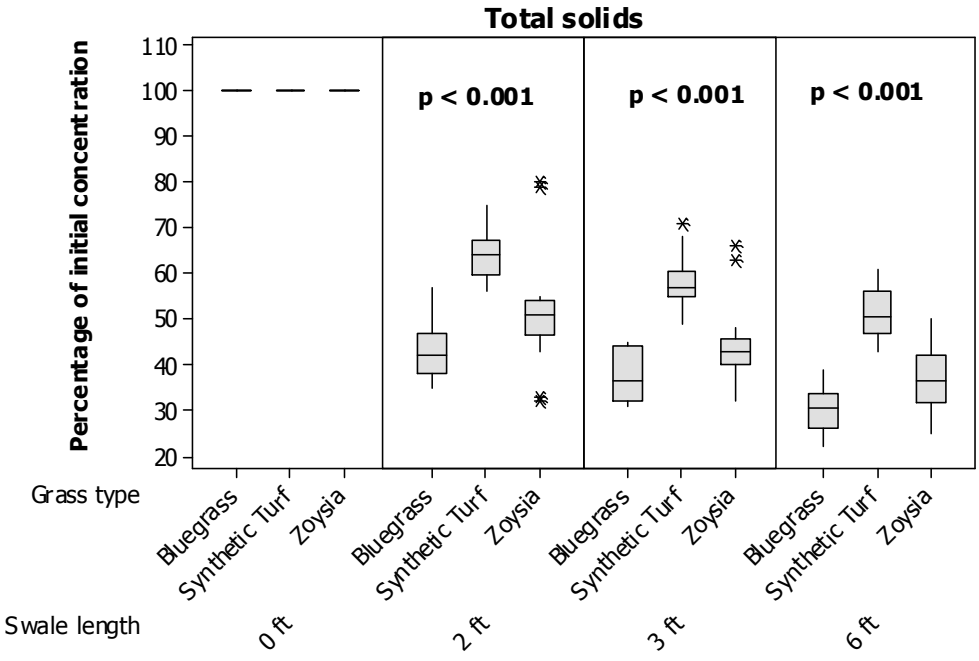

Figure 56. Box-and-whisker plots of total solids vs. swale length and grass type (Note 1 ft = 0.3048 m).

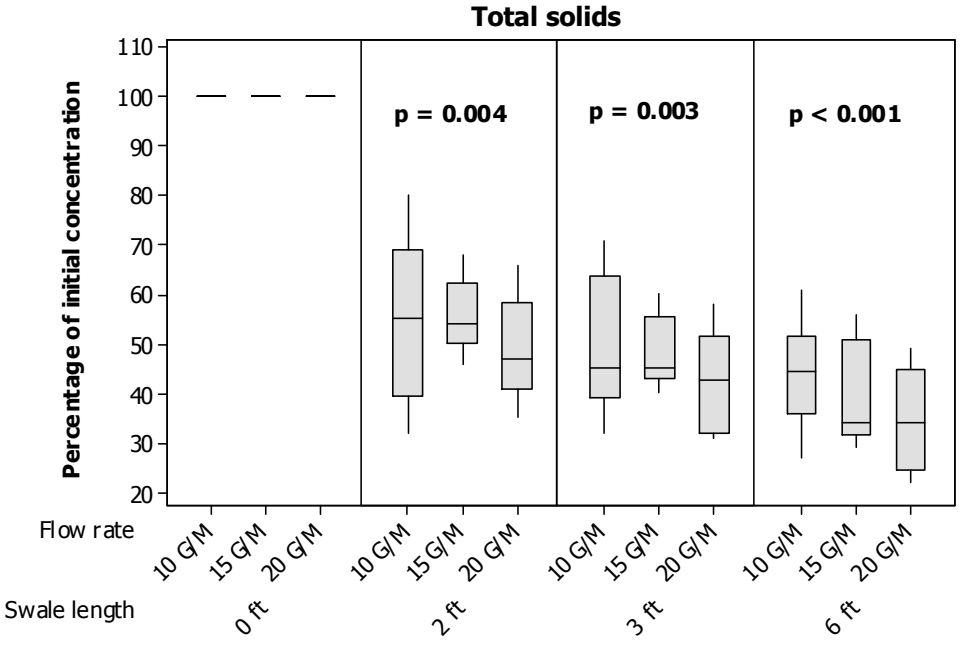

Figure 57. Box-and-whisker plots of total solids vs. swale length and flow rate (Note 1 ft = 0.30 m, 1 GPM = 0.0038 m^3/min).

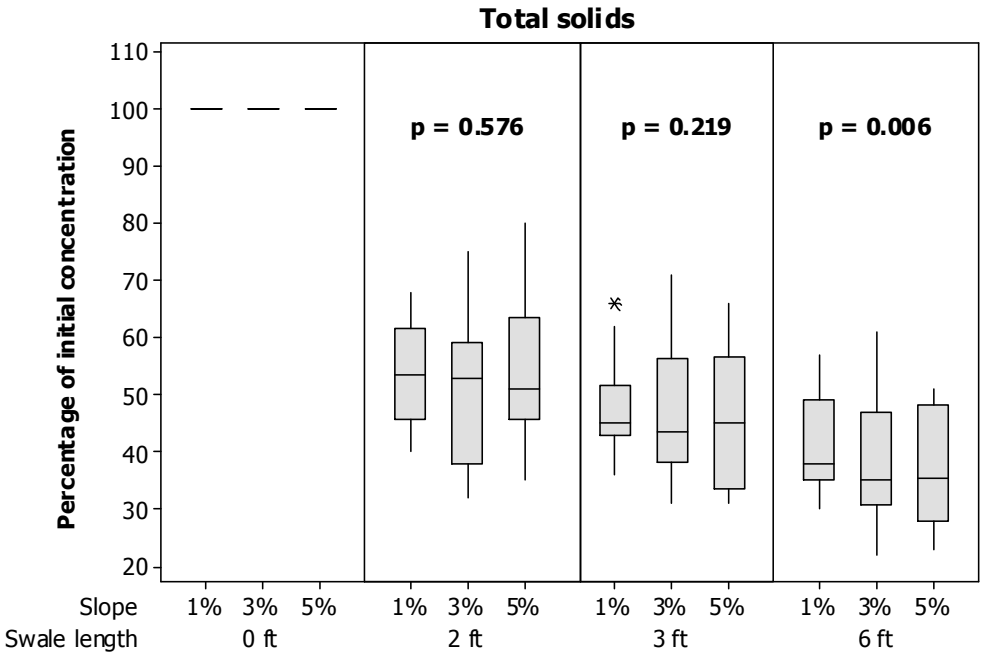

Figure 58. Box-and-whisker plots of total solids vs. swale length and slope (Note 1 ft = 0.30 m).

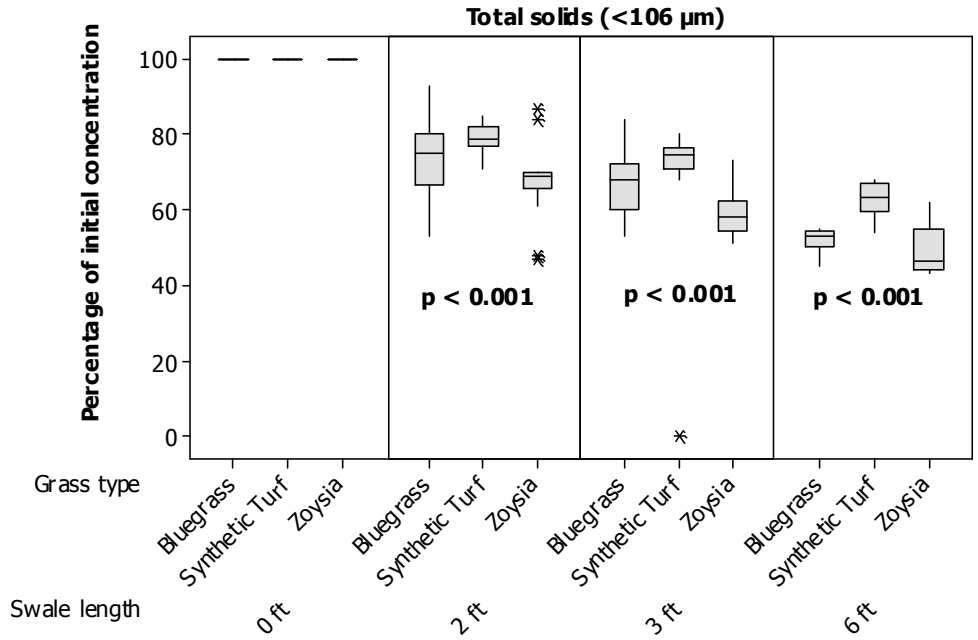

Figure 59. Box-and-whisker plots of total solids (< 106 µm) vs. swale length and grass type (Note 1 ft = 0.30 m).

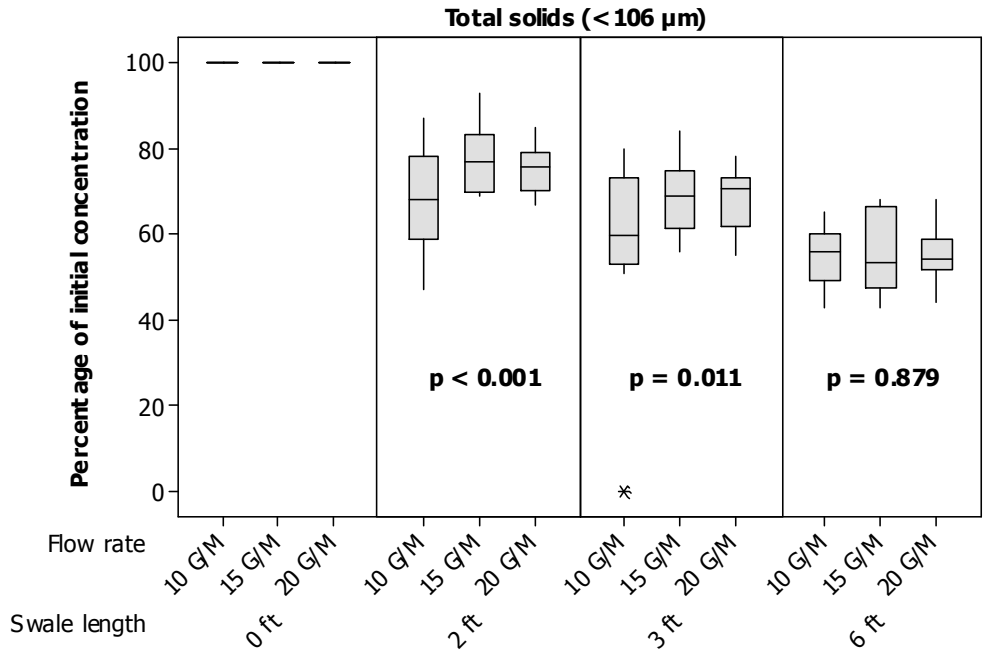

Figure 60. Box-and-whisker plots of total solids (< 106 µm) vs. swale length and flow rate (Note 1 ft = 0.3048 m, 1 GPM = 0.003785 m^3/min).

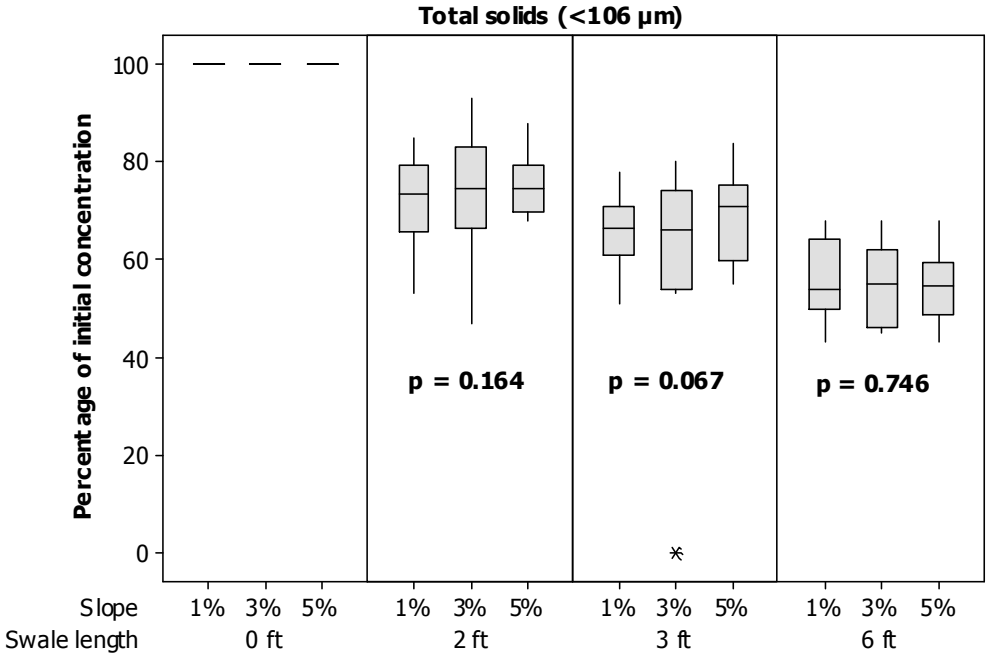

Figure 61. Box-and-whisker plots of total solids (< 106 µm) vs. swale length and slope (Note 1 ft = 0.30 m).

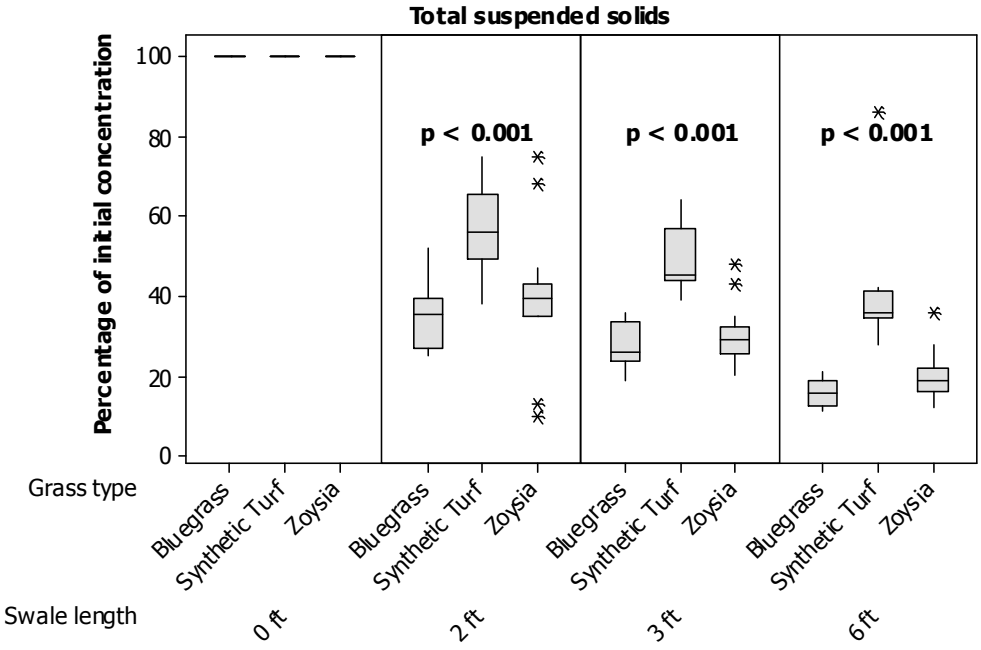

Figure 62. Box-and-whisker plots of total suspended solids vs. swale length and grass type (Note 1 ft = 0.30 m).

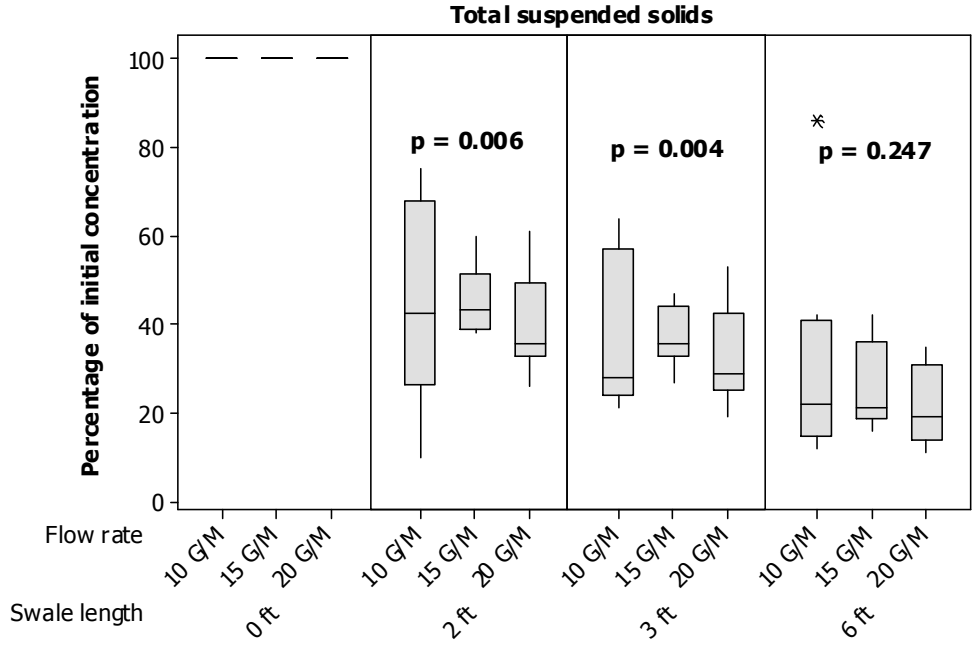

Figure 63. Box-and-whisker plots of total suspended solids vs. swale length and flow rate (Note 1 ft = 0.30 m, 1 GPM = 0.0038 m^3/min).

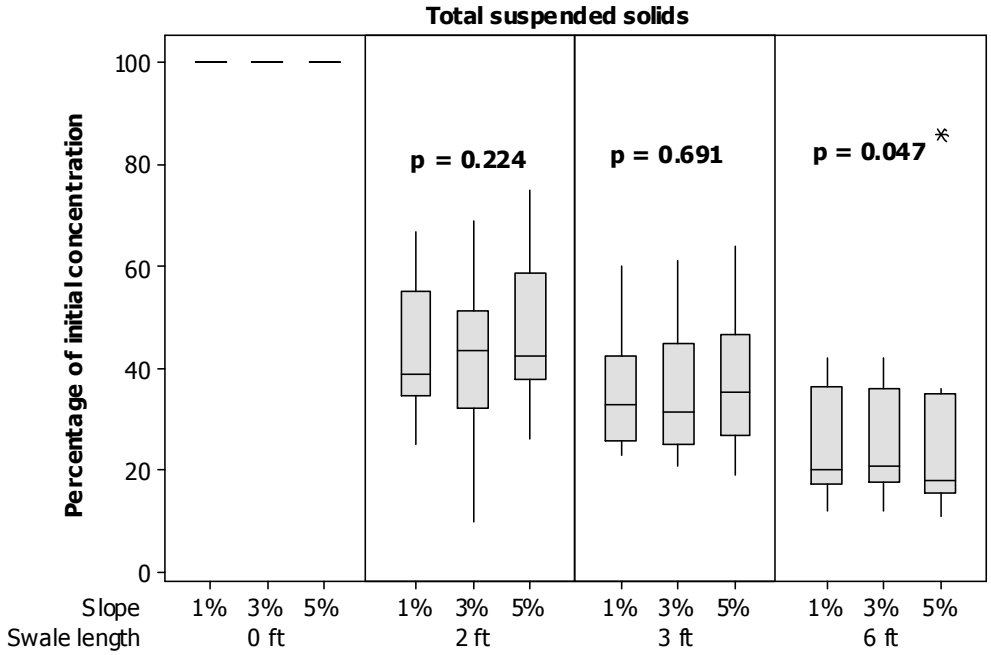

Figure 64. Box-and-whisker plots of total suspended solids vs. swale length and slope (Note 1 ft = 0.30 m).

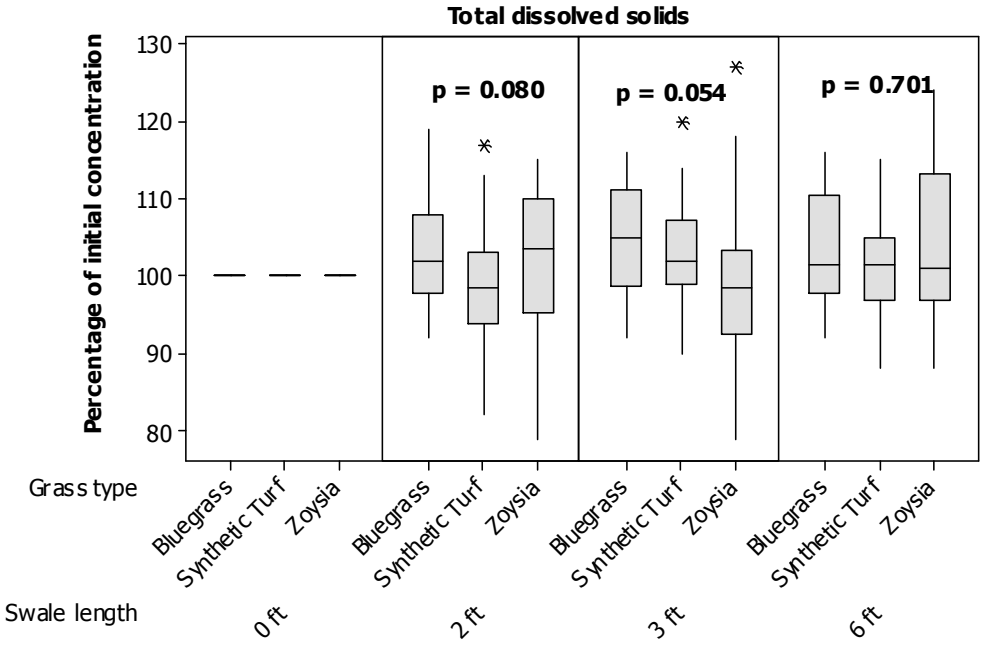

Figure 65. Box-and-whisker plots of total dissolved solids vs. swale length and grass type (Note 1 ft = 0.30 m).

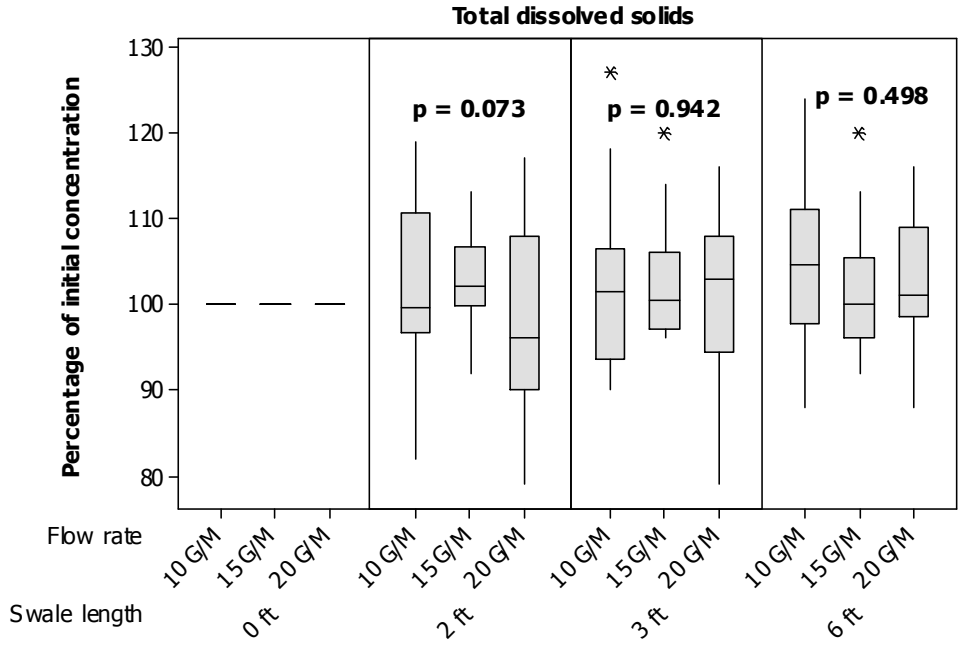

Figure 66. Box-and-whisker plots of total dissolved solids vs. swale length and flow rate (Note 1 ft = 0.30 m, 1 GPM = 0.0038 m^3/min).

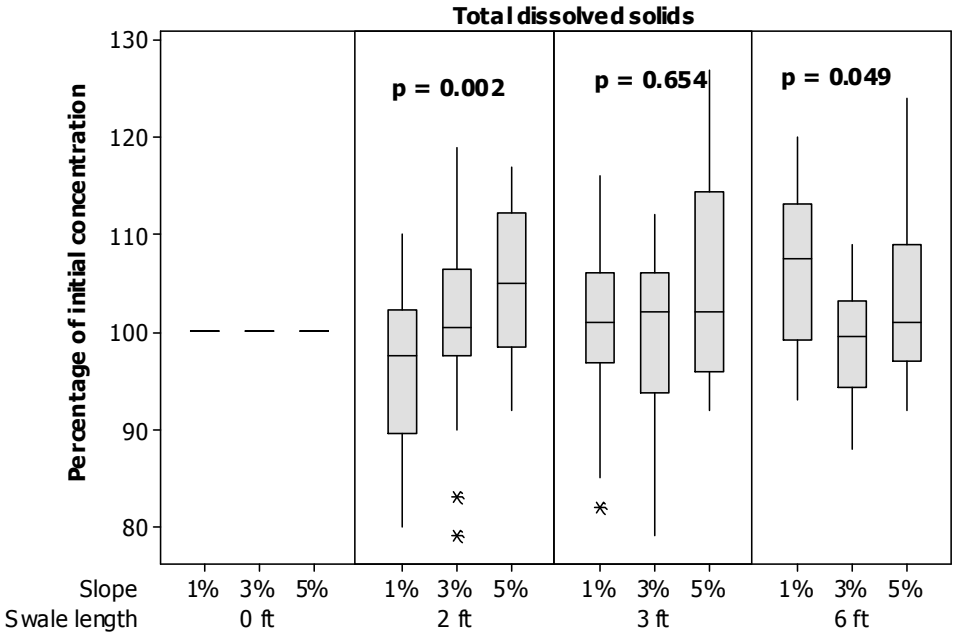

Figure 67. Box-and-whisker plots of total dissolved solids vs. swale length and slope (Note 1 ft = 0.30 m).

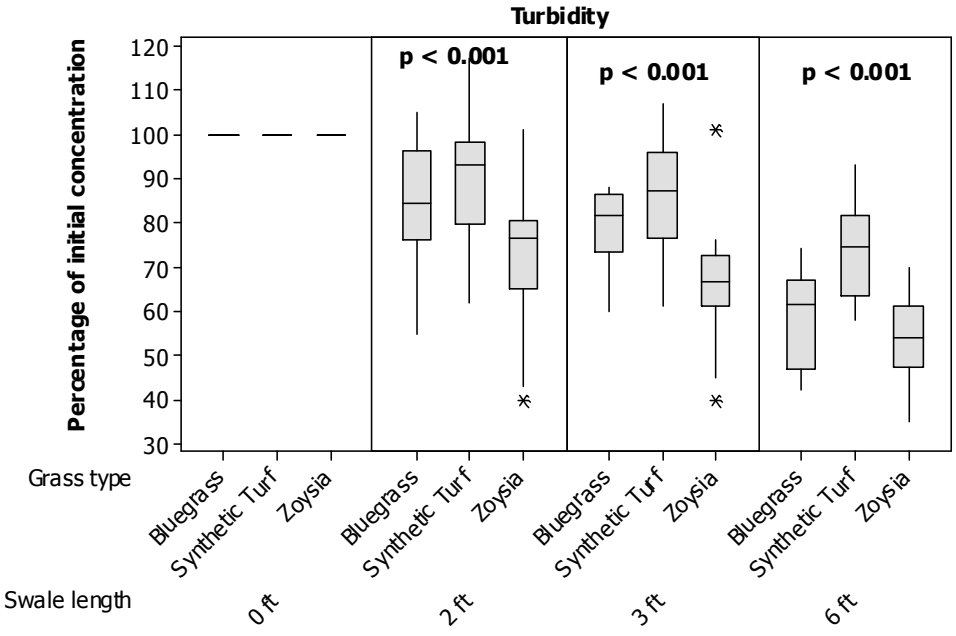

Figure 68. Box-and-whisker plots of turbidity vs. swale length and grass type (Note 1 ft = 0.30 m).

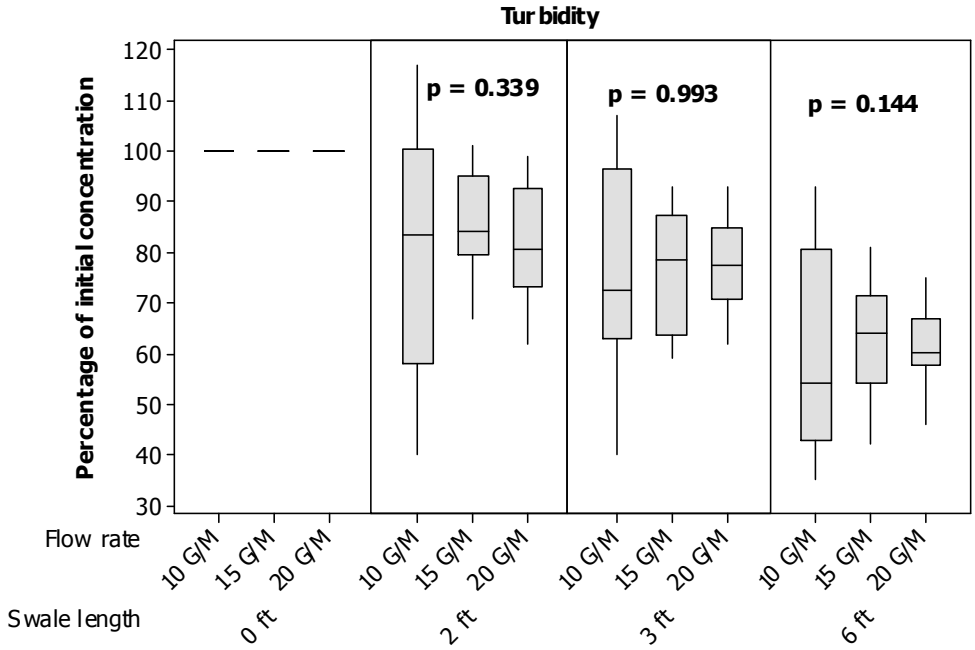

Figure 69. Box-and-whisker plots of turbidity vs. swale length and flow rate (Note 1 ft = 0.30 m, 1 GPM = 0.00385 m^3/min).

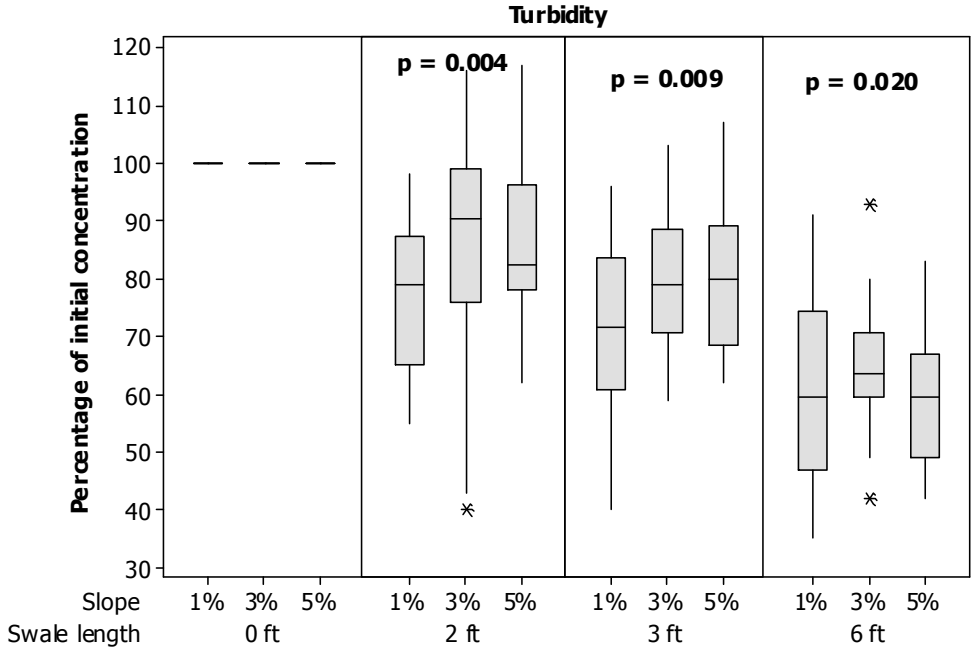

Figure 70. Box-and-whisker plots of turbidity vs. swale length and slope (Note 1 ft = 0.30 m).

Particle Size Distribution Analyses

Swale length was the only significant factor affecting particle size distributions ($P \leq 0.001$), while the three other factors (flow rate, slope, and grass type) as well as the interactions between the variables were insignificant. Figure 71 shows the median particle sizes of runoff particulates for each swale length. The median particle sizes consistently decreased by swale length, as expected, indicating a preferential trapping of larger particles near the upper end of the swale. Overall, the median particle sizes decreased from 15 µm at 0 ft (0 m) to 11 µm at 6 ft (1.8 m) (30% reduction). Figures 72 and 73 show that grass type and flow rate were insignificant factors affecting particle size distributions. Figure 73 shows that slope was also an insignificant factor affecting particle size distributions at 6 ft (1.8 m), however, there were significant changes in median particle sizes by the different slopes at 2 ft (0.6 m) and 3 ft (0.9 m). At 2 ft (0.6 m) and 3 ft (0.9 m), median particle sizes were smaller for 1% slope than at 3% and 5% slopes. Statistical summaries of particle size distributions observed in the second experiments are presented in Appendix H. Also, particle size distributions of each experiment are presented in Appendix I.

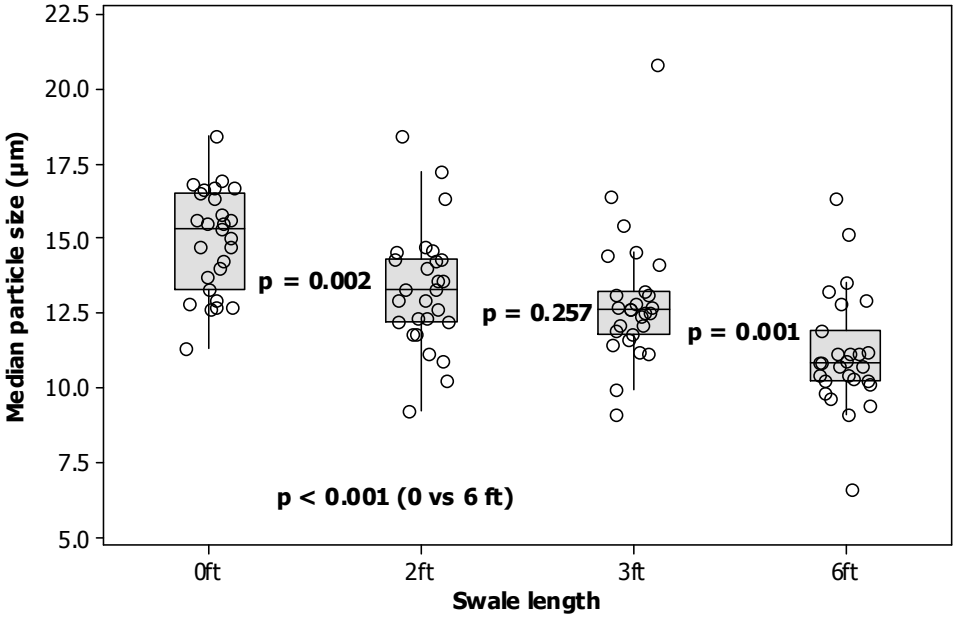

Figure 71. Box-and-whisker plots of median particle sizes vs. swale length (Note 1 ft = 0.30 m).

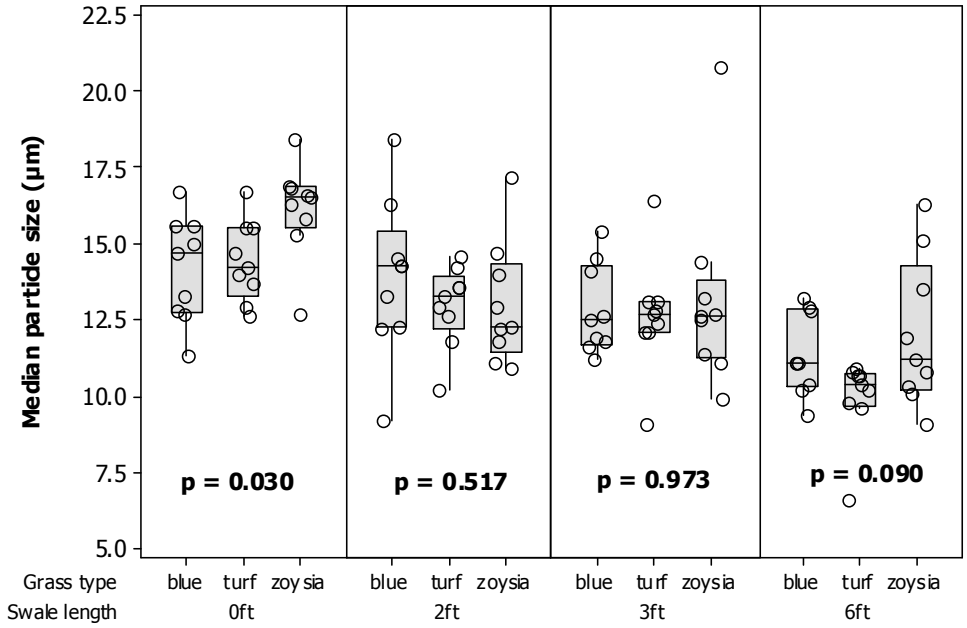

Figure 72. Box-and-whisker plots of median particle sizes by swale length and grass type (Note 1 ft = 0.30 m).

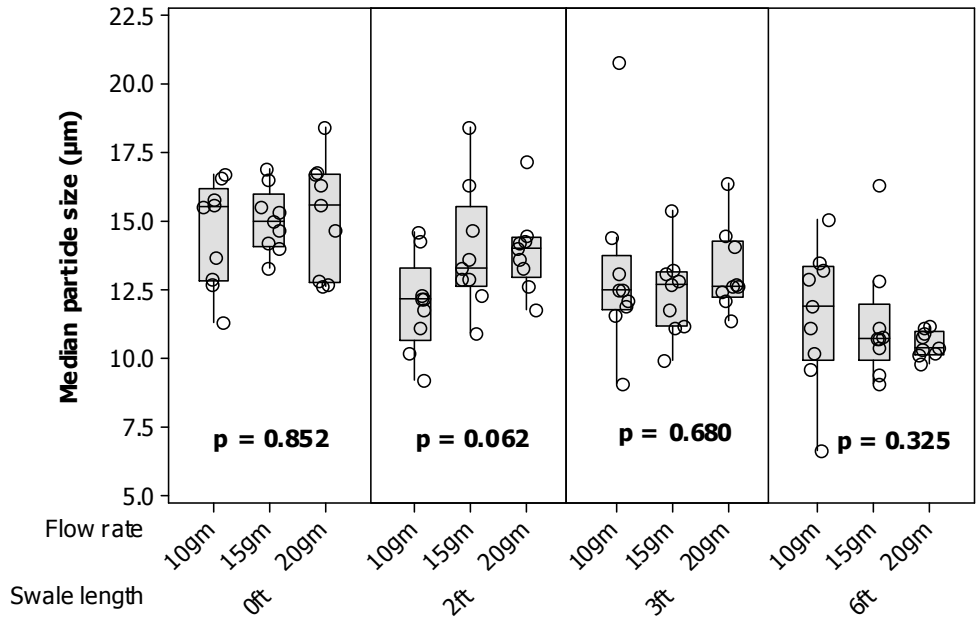

Figure 73. Box-and-whisker plots of median particle sizes by swale length and flow rate (Note 1 ft = 0.30 m, 1 GPM = 0.0038 m^3/min).

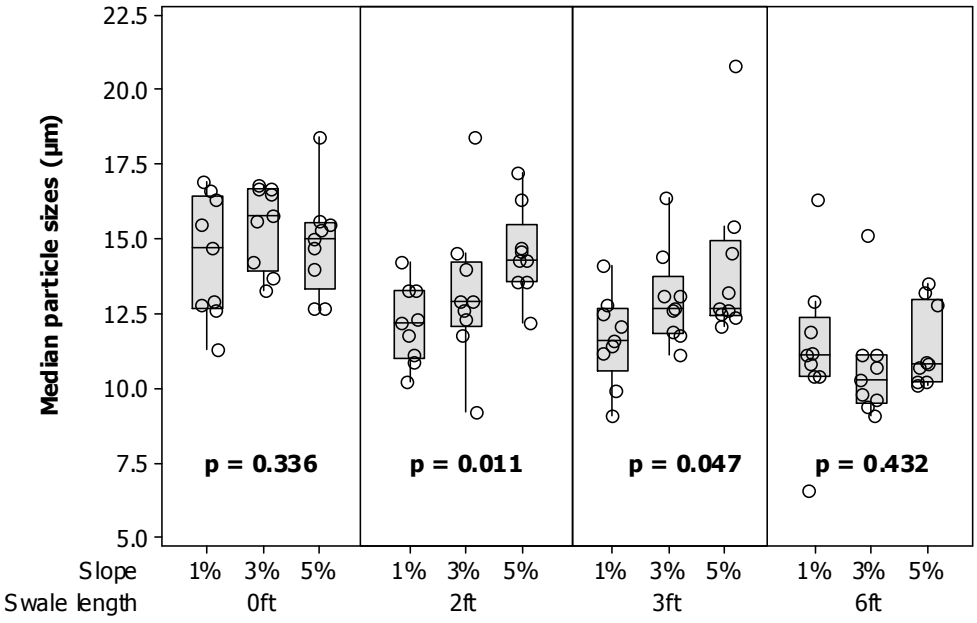

Figure 74. Box-and-whisker plots of median particle sizes by swale length and slope (Note 1 ft = 0.30 m).

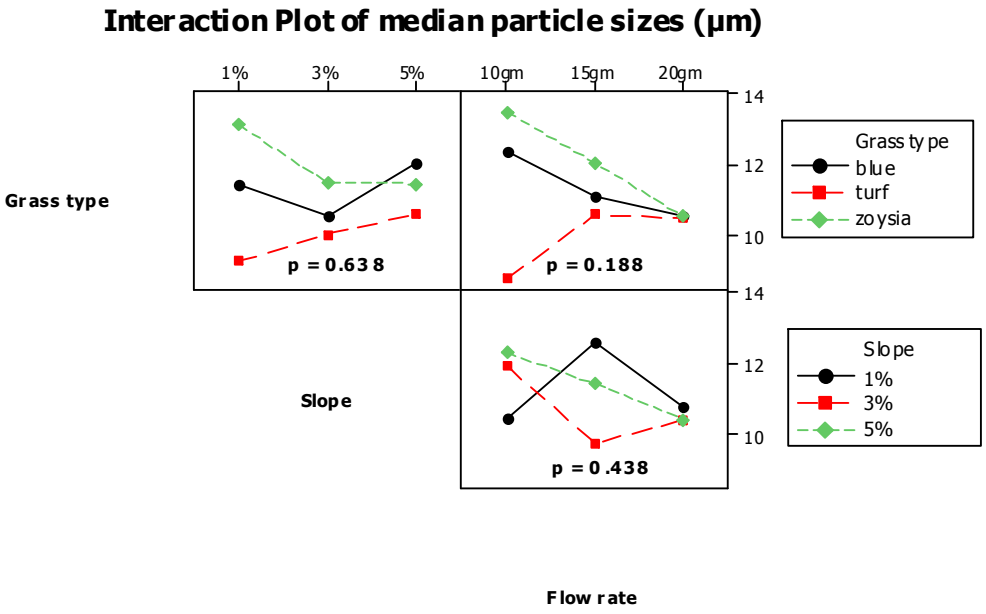

Figure 75. Interaction plots of median particle sizes.

Summary of Findings

• Significant reductions were observed at 2 ft (0.6 m), 3 ft (0.9 m), and 6 ft (1.8 m) from the head works for total solids, total solids after screening with a 106 µm sieve, total suspended solids, and turbidity, but not for total dissolved solids.

• Sediment concentrations rapidly declined between the head works (0 ft) and 2 ft (0.6 m) due to the settlement of large particles at the beginning of the swale. Sand accumulation was visually observed at the beginning of the swales.

• Turbidity was gradually reduced in the swales.

• Swale length, grass type, slope, and flow rate were all found to be significant factors for most of the particulate constituents. However, all variables were insignificant for total dissolved solids, except for the interaction of flow rate and grass type.

Table 26. Significant Factors and Associated Probabilities

Constituent	Variable	Probabilities
Total solids	Grass type	< 0.001
	Slope	0.006
	Flow rate	< 0.001
	Grass type*Flow rate	0.023
Total solids (< 106 µm)	Grass type	< 0.001
	Grass type*Flow rate	< 0.001
	Slope*Flow rate	0.006
Total suspended solids	Grass type	< 0.001
	Slope	0.047
	Grass type*Flow rate	0.005
	Slope*Flow rate	0.013
Total dissolved solids	Grass type*Flow rate	0.044
Turbidity	Grass type	< 0.001
	Slope	0.02
	Grass type*Slope	0.001
	Grass type*Flow rate	< 0.001

Swale Length

- Total solids: Significant sediment reductions were observed between all the swale lengths ($p < 0.001$ from 0 ft (0 m) to 2 ft (0.6 m), $p = 0.002$ from 2 ft (0.6 m) to 3 ft (0.9 m), $p < 0.001$ from 3 ft (0.9 m) to 6 ft (1.8 m)). The highest sediment reduction was observed between 0 ft (0m) and 2 ft (0.6 m) (42% reduction in median total solids). Overall 60% of sediment reduction was observed.

- Total solids < 106 µm: Significant sediment reductions were observed between all the swale lengths ($p < 0.001$ from 0 ft (0 m) to 2 ft (0.6 m), $p = 0.005$ from 2 ft (0.6 m) to 3 ft (0.9 m), $p < 0.001$ from 3 ft (0.9 m) to 6 ft (1.8 m)). Sediment reductions in total solids < 106 µm were not as rapid as for total solids, especially between 0 ft (0 m) and 2 ft (0.6 m). This suggests that the larger particles greater than 106 µm contributed to the high sediment removals between 0 ft (0 m) and 2 ft (0.6 m). Overall, a 54% reduction in total solids < 106 µm was observed between 0 and 6 ft.

- Total suspended solids: Significant sediment reductions were observed between all the swale lengths ($p < 0.001$ from 0 ft (0 m) to 2 ft (0.6 m), $p = 0.002$ from 2 ft (0.6 m) to 3 ft (0.9 m), $p < 0.001$ from 3 ft (0.9 m) to 6 ft (1.8 m)). Like total solids, the highest sediment reduction was observed between 0 ft (0 m) and 2 ft (0.6 m) (56% reduction in median TSS). Overall, a 76% reduction of total suspended solids was observed between 0 and 6 ft.

- Total dissolved solids: Slight increase (2%) in TDS concentrations were observed, possibly due to soil mineralization contributions. Significant increases in total dissolved solids were observed between 0 ft (0 m) and 6 ft (1.8 m) ($p = 0.050$). Initial total dissolved solids concentrations did not change or slightly increased in the grass swales.

- Turbidity: Significant sediment reductions were observed between 0 ft (0 m) and 2 ft (0.6 m) ($p = 0.002$) and between 3 ft (0.9 m) and 6 ft (1.8 m) ($p = 0.001$). Overall, turbidity was consistently decreased by swale length (70% reductions in the median turbidity levels).

Grass Type

- Total solids: Grass type was found to be a significant factor at 2 ft (0.6 m) ($p < 0.001$), 3 ft (0.9 m) ($p < 0.001$), and 6 ft (1.8 m) ($p < 0.001$). Blue grass was most efficient in reducing total solids, whereas synthetic turf was the least effective.

- Total solids < 106 µm: Grass type was found to be a significant factor at 2 ft (0.6 m) ($p < 0.001$), 3 ft (0.9 m) ($p < 0.001$), and 6 ft (1.8 m) ($p < 0.001$). Unlike total solids, Zoysia grass was found to be the most efficient in reducing total solids < 106 µm. Synthetic turf was the least effective among the three grass types.

- Total suspended solids: Grass type was found to be a significant factor at 2 ft (0.6 m) ($p < 0.001$), 3 ft (0.9 m) ($p < 0.001$), and 6 ft (1.8 m) ($p < 0.001$). Blue grass was the most efficient in reducing total suspended solids, while synthetic turf was the least effective.

- Total dissolved solids: There was no significant evidence showing the significance of grass type in reducing total dissolved solids.

- Turbidity: Grass type was found to be a significant factor at 2 ft (0.6 m) ($p < 0.001$), 3 ft (0.9 m) ($p < 0.001$), and 6 ft (1.8 m) ($p < 0.001$). Zoysia grass was the most efficient in reducing turbidity, whereas synthetic turf was the least effective.

Flow Rate

- Total solids: Flow rate was found to be a significant factor at 2 ft (0.6 m) ($p = 0.004$), 3 ft (0.9 m) ($p = 0.003$), and 6 ft (1.8 m) ($p < 0.001$). At 6 ft (1.8 m), 15 GPM (0.064 m^3/min) and 20 GPM (0.0767 m^3/min) were more efficient in reducing total solids than 10 GPM (0.038 m^3/min) flows.

- Total Solids < 106 µm: Flow rate was found to be a significant factor at 2 ft (0.6 m) ($p < 0.001$), 3 ft (0.9 m) ($p = 0.011$), but not at 6 ft (1.8 m) ($p = 0.879$). 10 GPM (0.038 m^3/min) was the most efficient in reducing total solids < 106 µm among the three flow rates. These suggest that the effect of flow rate is significant at the beginning of the grass swales, but diminishes beyond 6 ft.

- Total suspended solids: Like total solids < 106 µm, flow rate was a significant factor at 2 ft (0.6 m) ($p = 0.006$), 3 ft (0.9 m) ($p = 0.004$), but not at 6 ft (1.8 m) ($p = 0.247$).

- Total dissolved solids: There was no evidence showing the significance of flow rates in reducing total dissolved solids.

- Turbidity: There was no evidence showing the significance of flow rates in reducing turbidity.

Slope

- Total solids: Slope was found to be a significant factor only at 6 ft (1.8 m) ($p = 0.006$). 3% slope and 5% slope were slightly better in reducing total solids than 1% slope.

- Total solids < 106 µm: Slope was not found to be significant factor at any of the swale lengths.

- Total suspended solids: Slope was found to be a significant factor in reducing TSS concentrations; however, 5% slope was only slightly better than 1% and 3% slopes.

- Total dissolved solids: Although slope was found to be a significant factor at 2 ft and 6 ft, the effect of slope was hard to determine.

- Turbidity: Slope was found to be a significant factor at 2 ft (0.6 m) ($p = 0.004$), 3 ft (0.9 m) ($p = 0.009$), and 6 ft (1.8 m) ($p = 0.020$). 1% slope was found to be the most effective in reducing turbidity, however, the differences among the three slopes in reducing turbidity decreased as swale length increased.

Particle Size Distributions

- Overall, the median particle sizes consistently decreased from 15 µm at 0 ft (0 m) to 11 µm at 6 ft (1.8 m) (30% reduction), indicating a preferential trapping of larger particles near the upper end of the swale.

- Swale length was found to be the only significant factor ($p < 0.001$) while the three other factors (flow rate, slope, and grass type) as well as the interactions between them, were not found to be significant.

Chapter 7: Outdoor Swale Observations

Introduction

Both the initial and second sets of indoor experiments were conducted to identify the significant factors affecting, the transport of sediment in grass swales, and to develop an associated model. Sampling of stormwater at a full-size outdoor grass swale located adjacent to the Tuscaloosa, Alabama, City Hall during actual storm events was used to test the model obtained from the indoor experiments. Sixty-seven samples were collected at various locations along the swale during 13 storm events from August to December 2004. These samples were analyzed for the same constituents as analyzed during the second indoor tests (total solids, total solids < 106 µm, suspended solids, total dissolved solids, turbidity, and particle size distributions).

Descriptions of the Site

The outdoor grass swale test site is located adjacent to the Tuscaloosa City Hall, Tuscaloosa, Alabama. This full-size swale has a length of 116 ft (35.3 m) and is planted with Zoysia grass. Although this is a full-scale swale, the drainage area is very small, only comprising about 0.1 acres (4,200 ft^2 or 390 m^2) of paved roads and side walks, shown on Figure 80. Table 27 and Figure 77 show the channel slopes at various swale lengths. The slopes are steeper at the beginning of the swale and are flatter at the end. Figure 78 shows an example of cross-sectional elevations surveyed, illustrating the typical parabolic shape of the swale. This cross-sectional shape forces runoff to flow along a concentrated area on the bottom of the channel. Grass stems were collected at 11 different locations to determine the stem density of Zoysia grass cover as shown in Table 28. The mean stem density was 524 (stems/ft^2) (5640 stems/m^2) with coefficient of variation of 0.28.

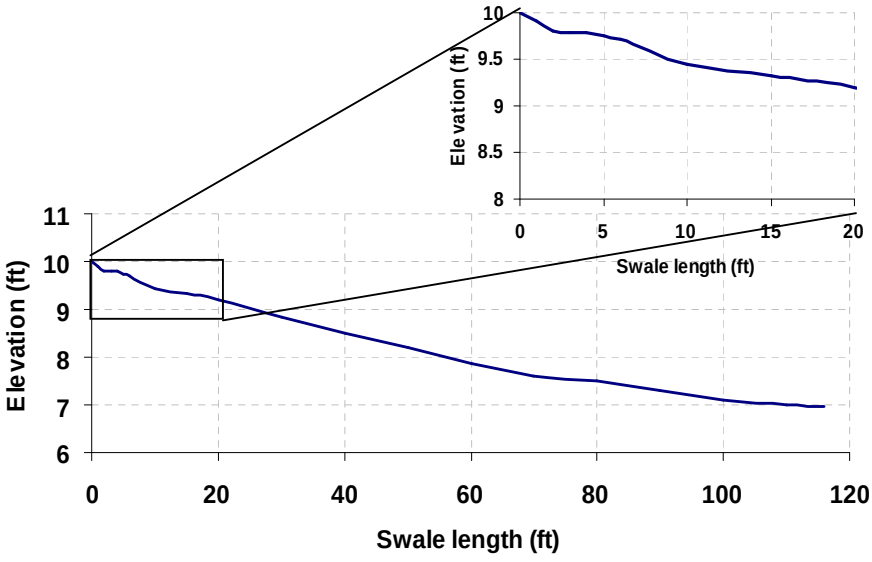

Figure 76. Longitudinal elevation profile of the outdoor swale.

Table 27. Channel Slopes over Various Swale Regions

Swale region	Mean channel slope
0 to 5 ft (0 to 1.5 m)	5.20%
5 to 10 ft (1.5 to 3.0 m)	4.80%
10 to 70 ft (3 to 21.3 m)	3.00%
70 to 116 ft (21.3 to 35.3 m)	1.40%

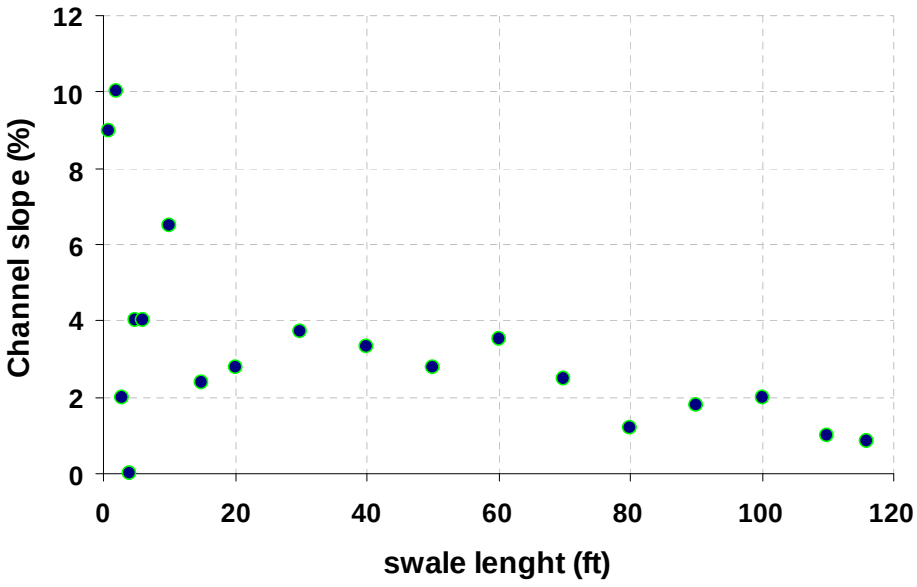

Figure 77. Longitudinal slopes surveyed on the outdoor swale.

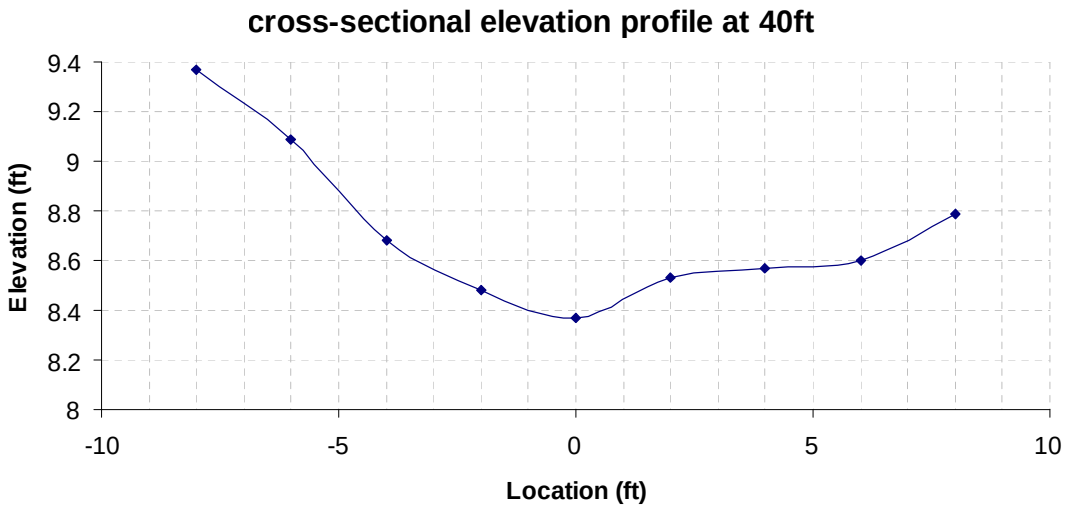

Figure 78. Example of cross-sectional elevations surveyed (40 ft (12 m) from the entrance) (All cross-sectional elevation profiles are presented in Appendix M).

Table 28. Stem Densities Observed at the Outdoor Grass Swale

Stem density	
Sample ID	Count (stems per inch^2)
1	4
2	5
3	3
4	2
5	4
6	4
7	4
8	4
9	3
10	2
11	5
Mean	*3.64*
Std. dev	*1.03*
COV	*0.28*

A soil survey conducted in accordance with U.S. Department of Agriculture (USDA) classification methods at the outdoor swale determined the soil was compacted loamy sand. In addition to surveying the slope and topsoil of the grass swale, infiltration rates of the swale soils were also measured using small double-ring infiltrometers (Turf-Tec, Inc.). The infiltration tests were conducted during both dry and wet conditions. Most of the infiltration rates were less than 1 inch/hour (2.54 cm/hour), as shown in Figure 82 and in Appendix L. The detailed soil survey also found sediment accumulation at the head of the swale, with grass growing through the top of the accumulated sediments. During storm events, the accumulated sediment created a small puddle at the head of the swale, preventing large particles from entering the swale due to sedimentation on the sidewalk.

Figure 79. Picture showing the outdoor test swale (116 ft (35.3 m) in length draining 0.1 acres (390 m^2) of paved road).

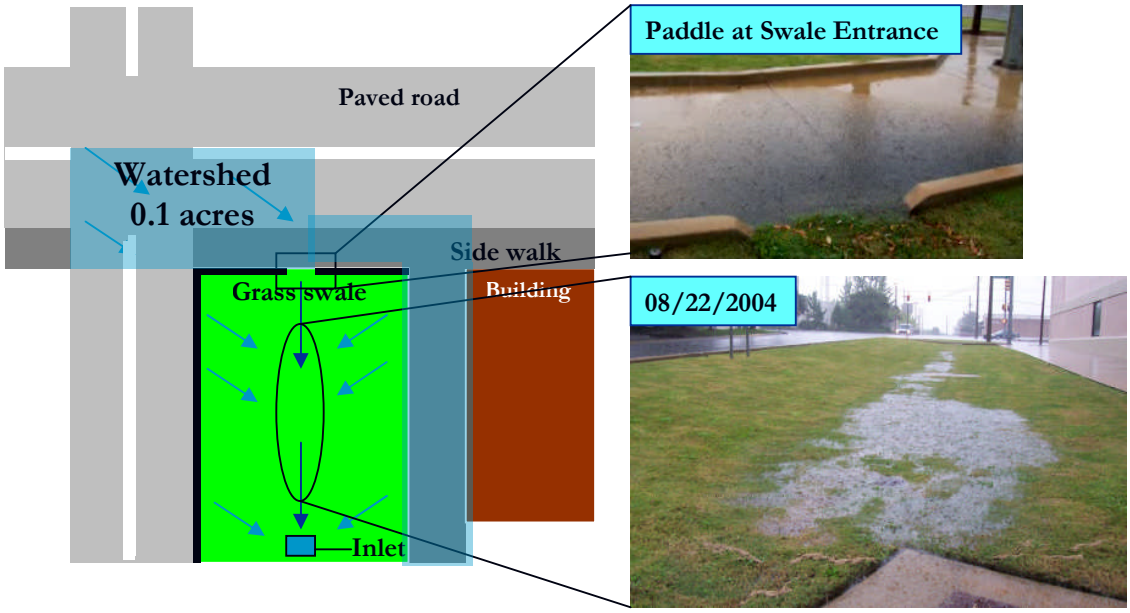

Figure 80. Outdoor grass swale monitoring site and surrounding land uses (Pictures of the entrance and overview of the swale during 08/22/2004 storm event).

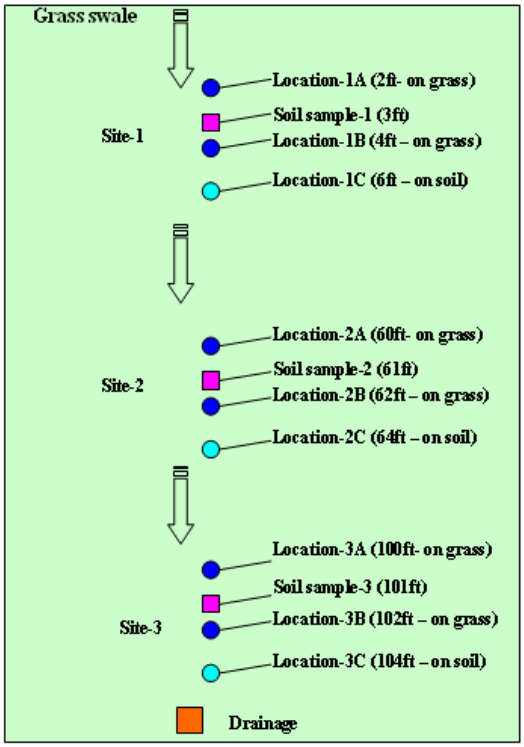

Figure 81. Locations of the infiltration testing and soil sampling (Note 1 ft = 0.30 m).

Table 29. Soil Densities of the Soil Samples

	Soil density (g/cm^2)	
	Dry condition	Wet condition
Site-1 (2 ft to 6 ft) (0.6 to 0.9 m)	1.76	1.94
Site-2 (60 ft to 64 ft) (18.2 to 19.5 m)	1.93	1.51
Site-3 (100 ft to 104 ft) (30.5 to 31.7 m)	1.95	1.87

Table 30. Moisture Content of the Soil Samples

	Moisture content (%)	
	Dry condition	Wet condition
Site-1 (2 ft to 6 ft) (0.6 to 0.9 m)	15.8	30.1
Site-2 (60 ft to 64 ft) (18.2 to 19.5 m)	15.6	24.7
Site-3 (100 ft to 104 ft) (30.5 to 31.7 m)	10.4	25.1

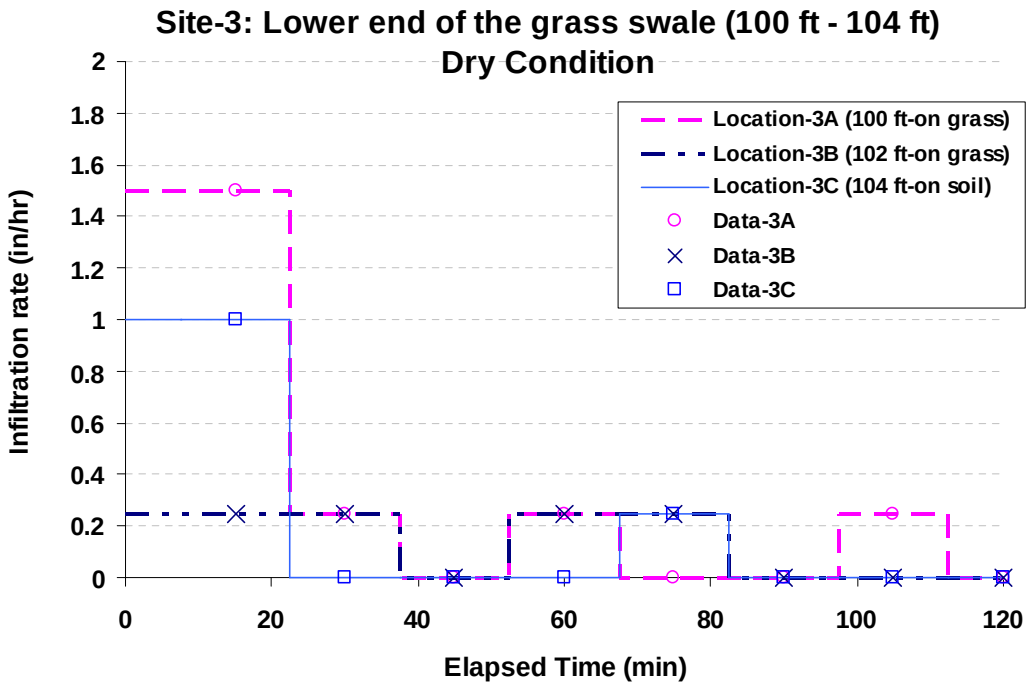

Figure 82. Example of infiltration rates of the grass swale (lower end of the swale) (All the results of the infiltration tests are presented in Appendix L).

Table 31. Summary of Averaged Infiltration Rates of the Grass Swale in Different Test Durations

	Dry Condition		
Location	First 30 min (inch/hour)	First 1 hour (inch/hour)	2 hours (inch/hour)
2 ft (grass)	0.25	0.19	0.16
4 ft (grass)	0.25	0.19	0.09
60 ft (grass)	0.63	0.38	0.25
62 ft (grass)	1	0.56	0.31
100 ft (grass)	0.88	0.5	0.28
102 ft (grass)	0.25	0.19	0.13
Mean	*0.54*	*0.34*	*0.20*
Std.dev	*0.34*	*0.17*	*0.09*
COV	*0.63*	*0.50*	*0.44*

	Dry Condition		
Location	First 30 min (inch/hour)	First 1 hour (inch/hour)	2 hours (inch/hour)
6 ft (soil)	0.38	0.25	0.16
64 ft (soil)	0.75	0.44	0.25
104 ft (soil)	0.5	0.25	0.16
Mean	*0.54*	*0.31*	*0.19*
Std.dev	*0.19*	*0.11*	*0.05*
COV	*0.35*	*0.35*	*0.27*

Wet Condition			
Location	First 30 min (inch/hour)	First 1 hour (inch/hour)	2 hours (inch/hour)
2 ft (grass)	0	0.06	0.03
4 ft (grass)	0.5	0.5	0.31
60 ft (grass)	0.25	0.19	0.16
62 ft (grass)	0.38	0.31	0.16
100 ft (grass)	0.88	0.5	0.28
102 ft (grass)	0.63	0.31	0.16
Mean	*0.44*	*0.31*	*0.18*
Std.dev	*0.31*	*0.17*	*0.10*
COV	*0.69*	*0.55*	*0.55*

Wet Condition			
Location	First 30 min (inch/hour)	First 1 hour (inch/hour)	2 hours (inch/hour)
6 ft (soil)	< 0.01	< 0.01	< 0.01
64 ft (soil)	0.13	0.06	0.03
104 ft (soil)	0.25	0.19	0.13
Mean	*0.19*	*0.13*	*0.08*
Std.dev	*0.08*	*0.09*	*0.07*
COV	*0.45*	*0.74*	*0.88*

Sample Collection and Preparation

A total of 67 samples were collected at the swale entrance (0 ft), 2 ft (0.6 m), 3 ft (0.9 m), 6 ft (1.8 m), 25 ft (7.6 m), 75 ft (22.8 m), and 116 ft (35.3 m) locations during 13 storm events from August 22, 2004 to December 8, 2004. However, not all events were completely sampled. During some events, runoff was insufficient for collecting a runoff sample at the time of sampling at some locations due to the rain and flow ceasing before all samples could be collected. All the samples were collected in 1 litter polyethylene bottles and stored in a refrigerator before analysis.

Descriptions of Storm Events

Weather information during monitoring at the outdoor swale was obtained from a weather station on a University of Alabama building (H.M. Comer) located 1.5 miles (2.4 km) from the site. Table 32 describes weather information for the storm events sampled. Most of the events were small rains, but some had very high rainfall intensities typical of the area. The highest rainfall intensities (3.24 inch/hour (8.2 cm/hour) during 5 min.) were observed on 10/23/2004 and 12/08/2004. During sampling on 12/08/2004, the rainfall intensity increased dramatically, and the flow on the grass swale significantly increased during the sampling period.

Table 32. Summary of Weather Information for the Sampled Storm Events

	Event-1	Event-2	Event-3	Event-4	Event-5	Event-6	Event-7
Date	8/22/2004	10/09/2004	10/10/2004	10/10/2004	10/11/2004	10/19/2004	10/23/2004
Sampling time	**N/P	10:30 AM	1:00 PM	9:00 PM	4:00 PM	4:00 PM	9:10 PM
Air temperature (Fahrenheit)	73	64	68	68	72	73	67
Preceding dry period (hour)	44.4	0.8	26.0	1.5	19.4	190.5	64.8
Total rain (inch)	0.58	0.05	0.15	0.16	0.11	0.17	0.84
Duration (minute)	80	25	200	110	45	20	115
Average intensity (inch/hour)	0.44	0.12	0.05	0.09	0.15	0.51	0.44
Max. rain fall intensity (inch/hour) in 5 minutes	1.92	0.12	0.12	0.24	0.24	1.08	3.24

	*Event-8	Event-9	Event-10	Event-11	Event-12	Event-13
Date	11/01/2004	11/11/2004	11/21/2004	11/22/2004	12/6/2004	12/8/2004
Sampling time	11:00 AM	12:40 AM	11:00 AM	1:50 PM	12:50 AM	12:50 AM
Air temperature (Fahrenheit)	67	64	60	64	57	59
Preceding dry period (hour)	91.3	168.9	13.5	24.8	5.7	39.4
Total rain (inch)	**N/A	0.23	1.12	2.84	0.32	0.7
Duration (minute)	**N/A	135	495	230	80	85
Average intensity (inch/hour)	**N/A	0.10	0.14	0.74	0.24	0.49
Max. rain fall intensity (inch/hour) in 5minutes	**N/A	0.36	1.08	2.28	1.08	3.24

Rain graphs of the storm events are presented in Appendix K.

* There was no rain detected by the weather station on 11/01/2004. This was likely due to the location difference between the weather station and the swale monitoring site. However, rain was obviously observed during sampling on this date, along with sufficient runoff for sampling.
** N/A = not available

Analytical Methods

The 67 samples collected from 13 storm events were analyzed for the following constituents:

- Total Solids (Standard Methods 2540B)
- Total Solids after screening with a 106 µm sieve
- Total Suspended Solids (solids retained on a 0.45 µm filter) (Standard Methods 2540D)
- Total Dissolved Solids (solids passing through a 0.45 µm filter) (Standard Methods 2540C)
- Turbidity using a HACH 2100N Turbidimeter
- Particle Size Distribution by Coulter Counter (Beckman® Multi-Sizer III™), composite of several different aperture tube measurements

Results and Discussions

While collecting samples, sediment concentrations obviously decreased visually with increasing swale length during most of the events. Figure 87 shows the runoff samples and sediment captured on glass fiber filters at various swale lengths, collected on October 11, 2004. It was clear that runoff sediments were captured as the stormwater passed through the grass swale. All results are presented in Appendix C. Removal efficiencies for each constituent are presented in Appendix N.

Total Solids and Total Solids (< 106 µm) Variation by Swale Length

Figures 83 and 85 show that total solids and total solids less than 106 µm were very similar to each other for most of the events. This suggests that particle sizes of runoff sediments from the roads and in the grass swales were primary less than 106 µm. However, particles greater than 106 µm may have been present in the road runoff, but were captured at the small pool adjacent to the swale entrance. High sediment reduction rates in total solids and total solids less than 106 µm were observed between the swale entrance and 6 ft (1.8 m). Beyond 6 ft (1.8 m), there was no significant change in sediment concentrations. Total solids and total solids less than 106 µm were not reduced as much as total suspended solids. This suggests that total dissolved solids were the predominant portion of the total solids and total solids less than 106 µm for the samples collected in the grass swale.

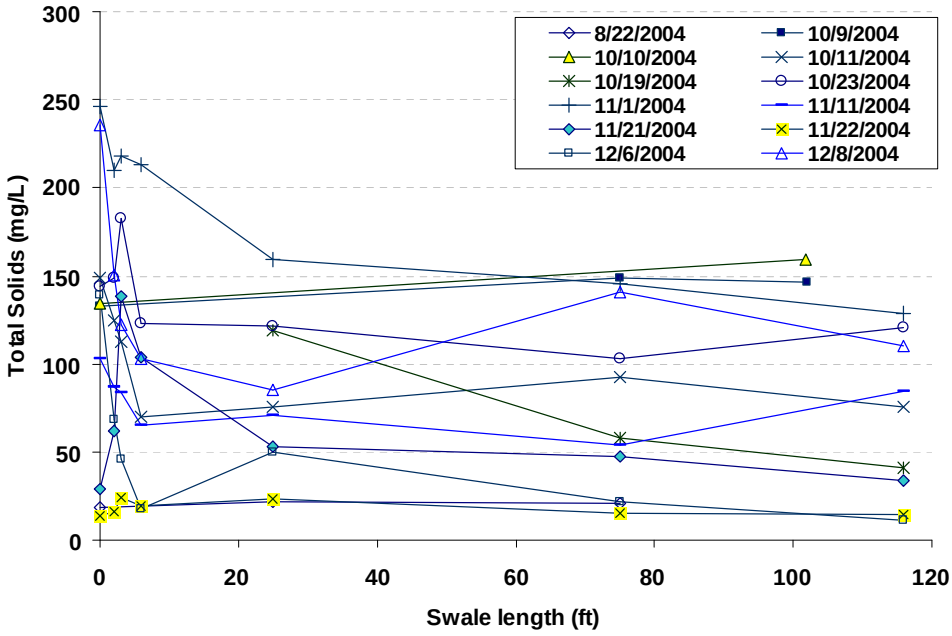

Figure 83. Total solids concentrations vs. swale length observed at the outdoor grass swale (Note 1 ft = 0.30 m).

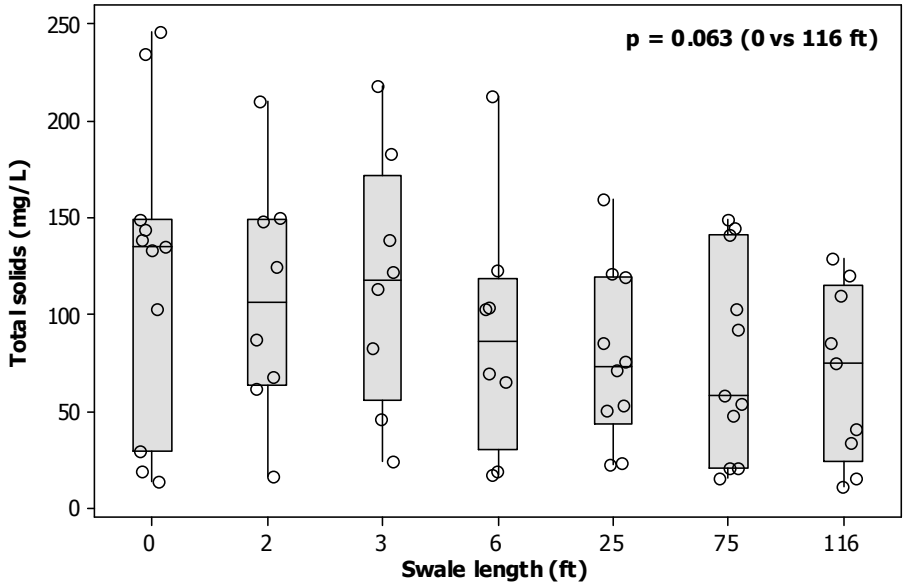

Figure 84. Box-and-whisker plots of total solids concentrations vs. swale length observed at the outdoor grass swale (Note 1 ft = 0.30 m).

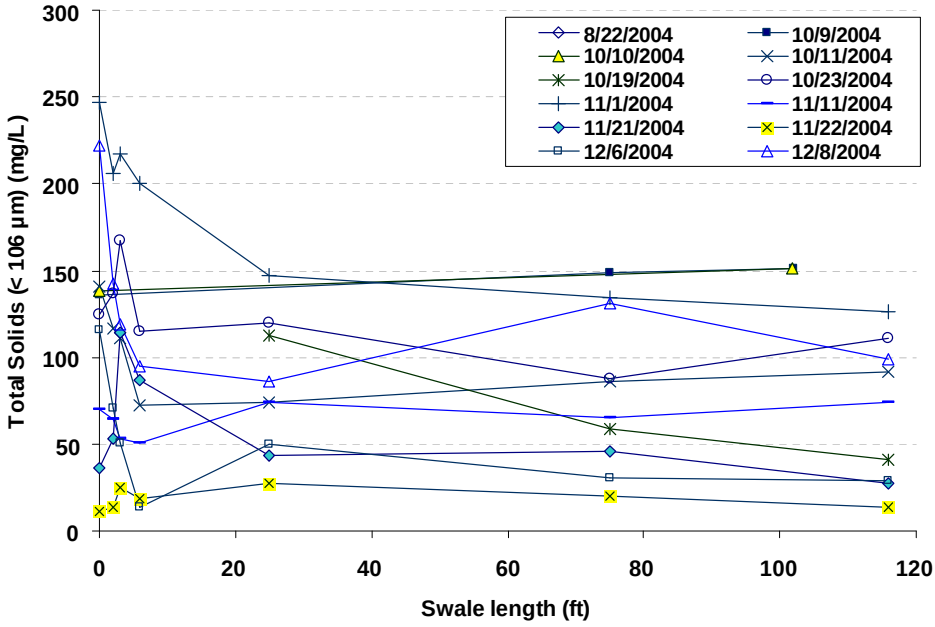

Figure 85. Total solids (< 106 µm) concentrations vs. swale length observed at the outdoor grass swale (Note 1 ft = 0.30 m).

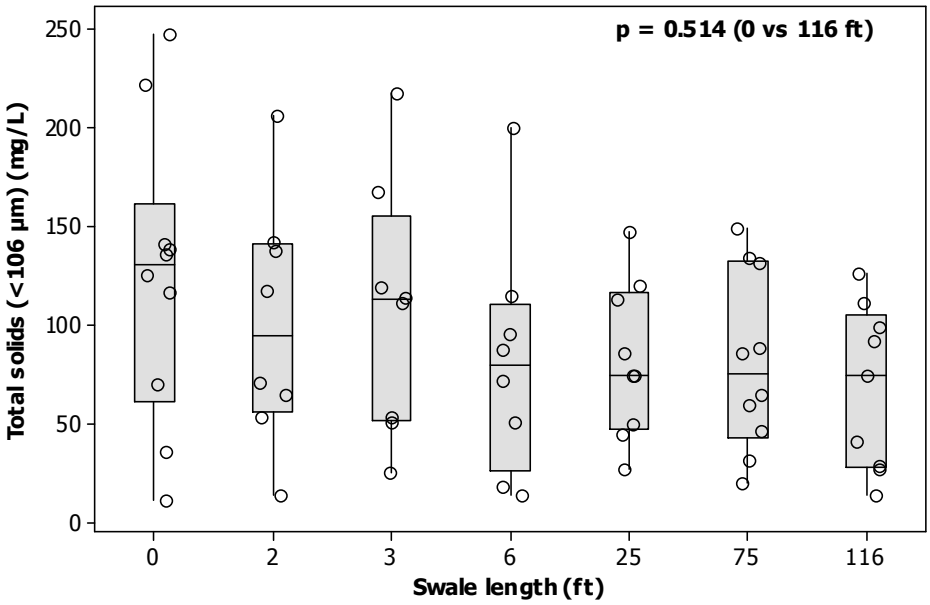

Figure 86. Box-and-whisker plots of total solids (< 106 µm) concentrations vs. swale length observed at the outdoor grass swale (Note 1 ft = 0.30 m).

Total Suspended Solids Concentration Variation by Swale Length

Initial total suspended solids concentrations at the entrance of the swale varied greatly for different rain events, ranging from 4 mg/L to 157 mg/L. Large sediment reductions were normally observed between the swale entrance (0 ft) and 25 ft (7.6 m). Beyond 25 ft (7.6 m), the total suspended solids concentrations were more consistent, with much less sediment reductions in the grass swale. During two events (10/23/2004 and 11/11/2004), total suspended solids concentrations increased between the entrance (0 ft) and 6 ft (1.8 m) instead of decreasing, likely due to scouring of previously deposited sediments at the entrance of the swale. An unusual sediment increase of 51 mg/L between 25 ft (7.6 m) and 75 ft (22.8 m) was observed on 12/08/2004. During this sampling period, the rain intensity and runoff flow rate significantly increased after collecting the upgradient samples. The higher flow rate likely scoured the soil from the swale, resulting in much higher total suspended solids concentrations at 75 ft (23 m) than at 25 ft (7.6 m) during that event, or sediment was more effectively being transported down the swale during the short period of higher flows.

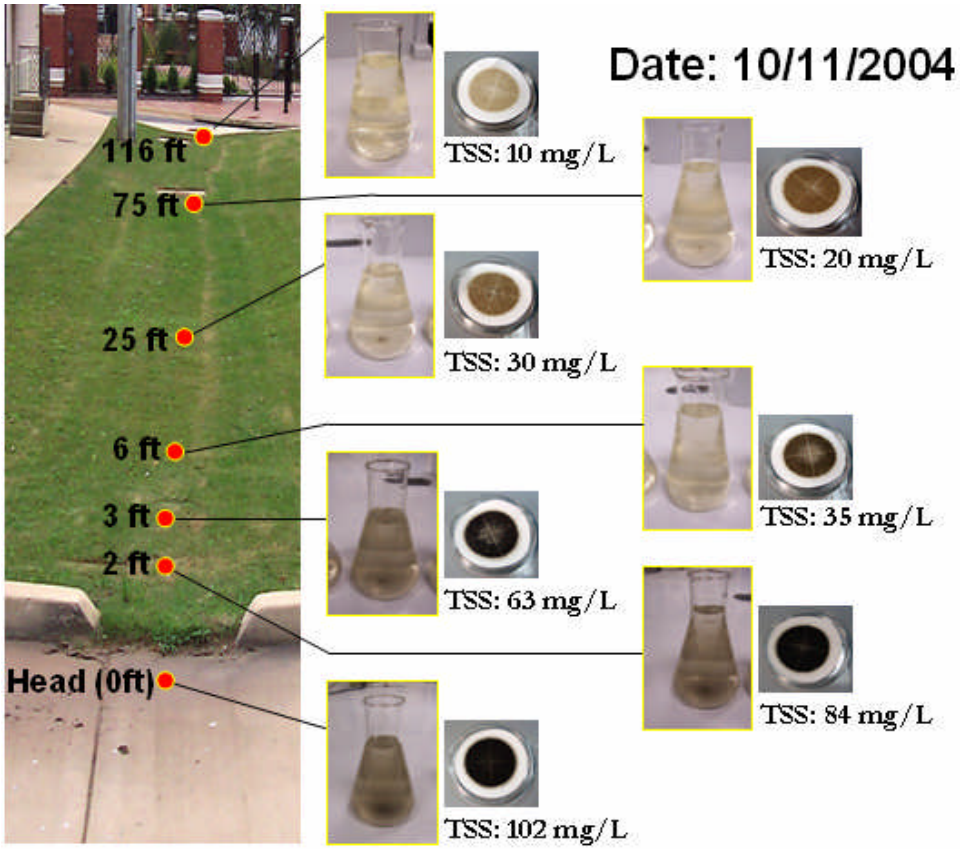

Figure 87. Sampling locations at the outdoor swale monitoring site (Example sediment samples from 10/11/2004).

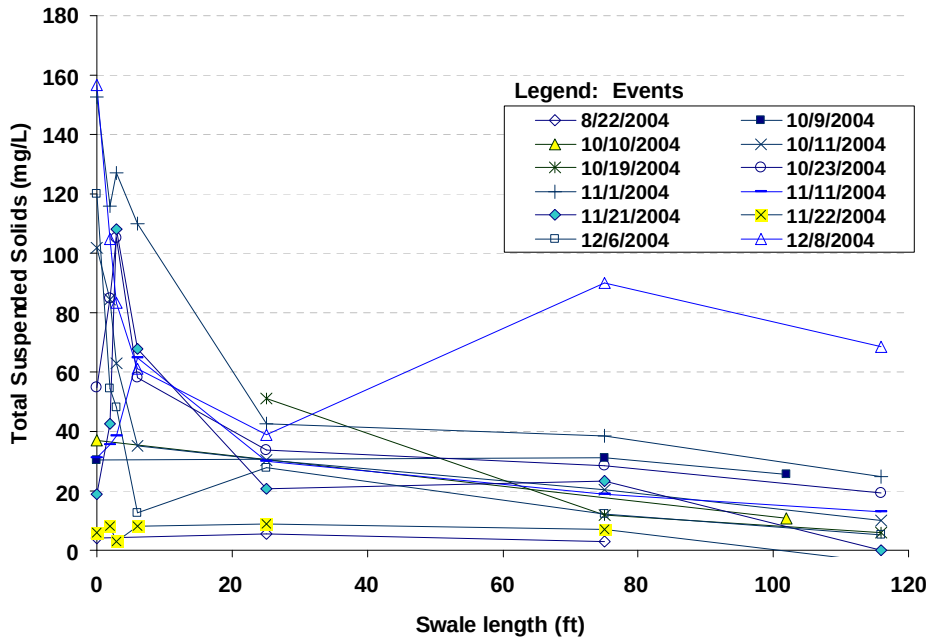

Figure 88. Total suspended solids concentrations vs. swale length, observed at the outdoor grass swale (Note 1 ft = 0.30 m).

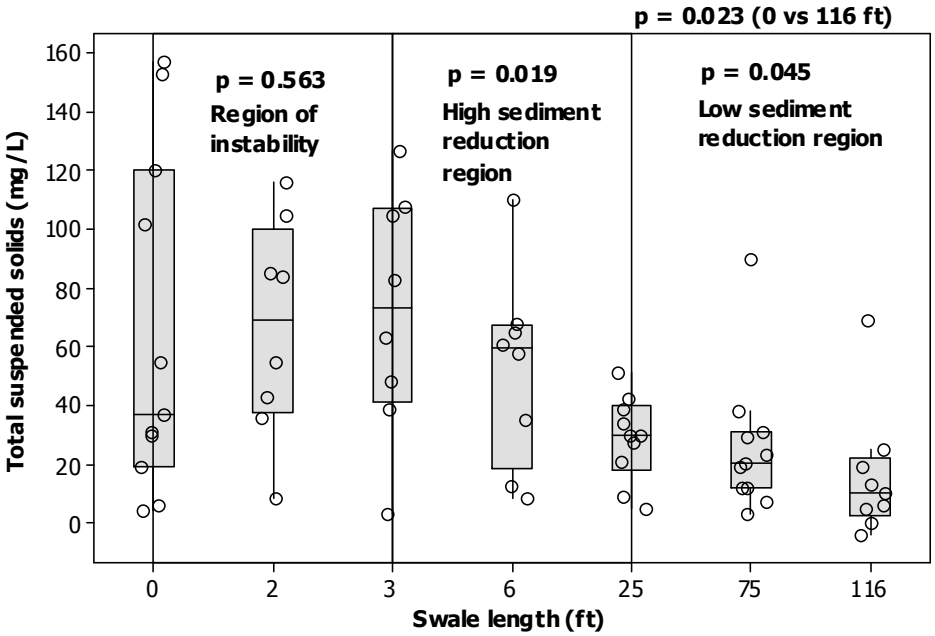

Figure 89. Box-and-whisker plots of total suspended solids concentrations vs. swale length observed at the outdoor grass swale (Note 1 ft = 0.30 m).

Figure 89 indicates that the concentrations were highly variable during the first three feet (0.9 m) of the swale (p = 0.563), then significantly decreased between 3 ft (0.9 m) and 25 ft (7.6 m) (p = 0.019), and decreased only slightly more to the end of the swale (at 116 ft or 35.3 m) (p = 0.045). Thus, the results of total suspended solids show three regions of the swale pertaining to sediment reductions. These regions are:

0 ft to 3 ft (0 m to 0.9 m):	Region of instability
3 ft to 25 ft (0.9 m to 7.6 m):	High sediment reduction region
25 ft to 116 ft (7.6 m to 35.3 m):	Lower sediment reduction region

Total Dissolved Solids Variation by Swale Length

There were no significant changes in total dissolved solids concentrations (particulates < 0.45 µm); total dissolved solids concentrations were neither reduced or increased along the grass swale, except during the rain event occurring on 12/08/2004. On 12/08/2004 an initial total dissolved solids of 69 mg/L at the swale entrance rapidly reduced to 26 mg/L at 6 ft (1.8 m). Then, total dissolved solids concentrations became stable from 6 ft (1.8 m) to 116 ft (35.3 m) with total dissolved solids concentrations of 34 mg/L.

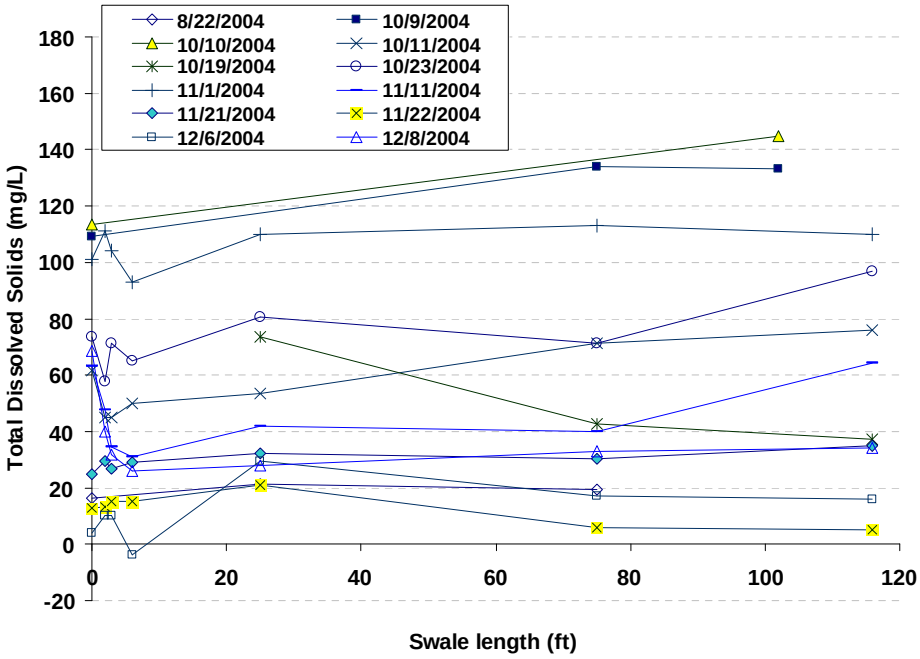

Figure 90. Total dissolved solids concentrations vs. swale length, observed at the outdoor grass swale (Note 1 ft = 0.30 m).

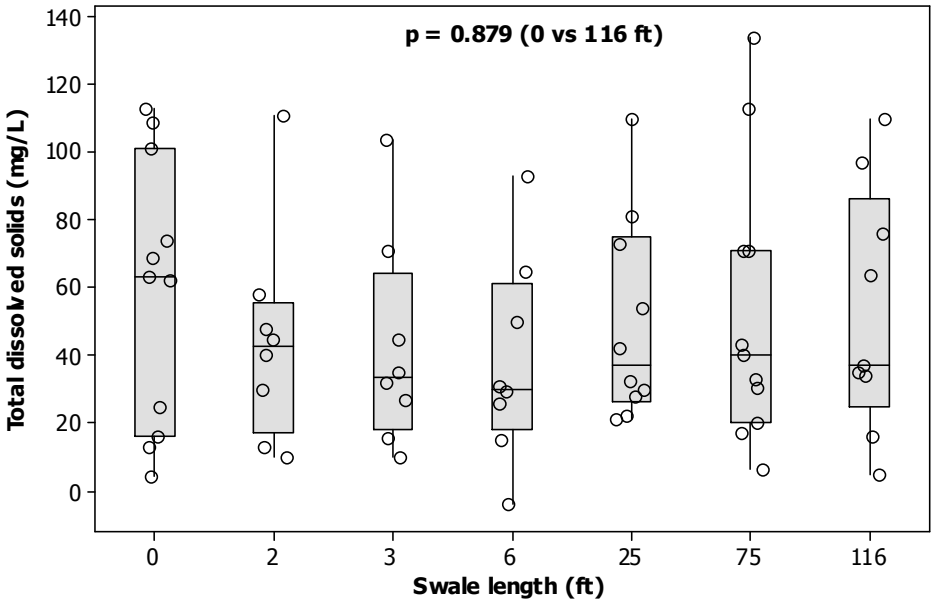

Figure 91. Box-and-whisker plots of total dissolved solids concentrations vs. swale length observed at the outdoor grass swale (Note 1 ft = 0.30 m).

Turbidity Variation by Swale Length

Significant reductions in turbidity were observed at the outdoor swale. Although initial turbidity values at the entrance ranged from 2 NTU to 137 NTU, all turbidity values (except on 12/08/2004) were reduced to levels below 20 NTU at 116 ft (35.3 m). Increased turbidity at 75 ft (22.8 m) on 12/08/2004 was possibly due to scouring of the soil during a short period of high flows, or due to more efficient transport during a short period of higher flows, as mentioned previously.

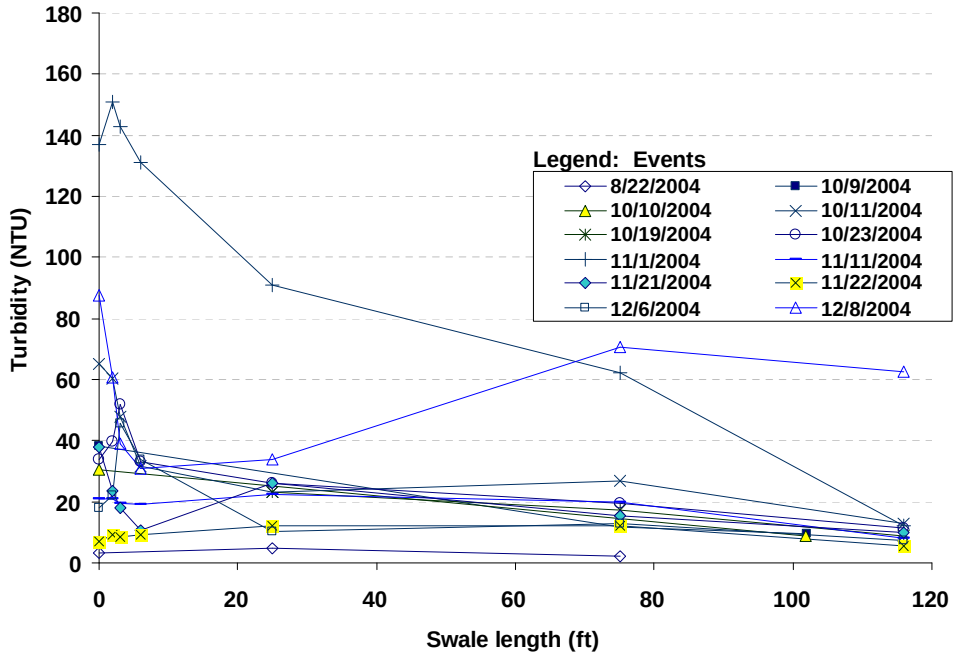

Figure 92. Turbidity vs. swale length, observed at the outdoor grass swale (Note 1 ft = 0.30 m).

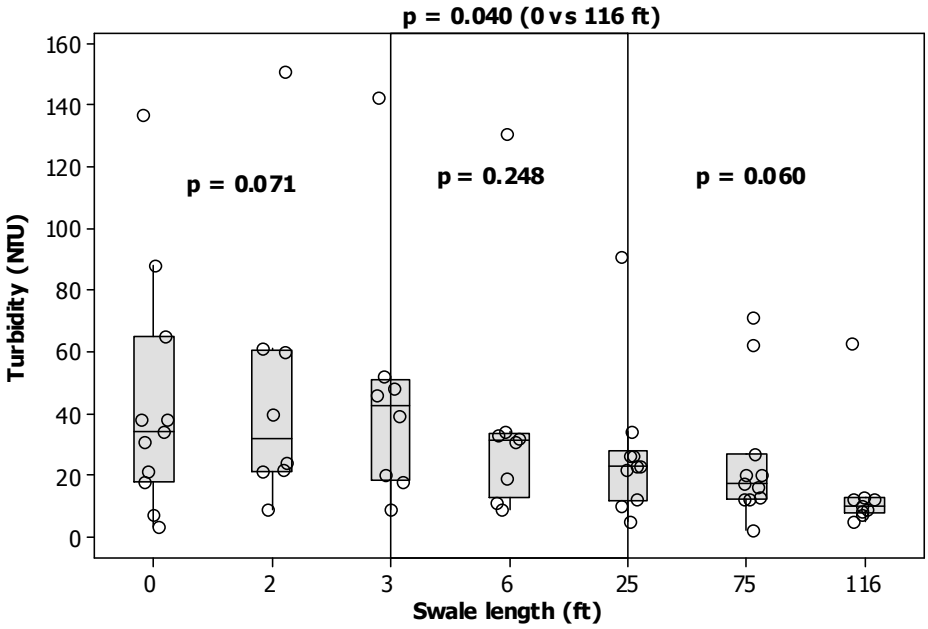

Figure 93. Box-and-whisker plots of turbidity vs. swale length observed at the outdoor grass swale (Note 1 ft = 0.30 m).

Particle Size Distribution Analyses

Figures 94 and 95 show the median particle sizes of runoff particulates for each swale length location. There was no significant change in median particle sizes between the swale entrance (0 ft) and 6 ft (1.8 m) ($p = 0.248$), between 6 ft (1.8 m) and 25 ft (7.6 m) ($p = 0.149$), and between 25 ft (7.6 m) and 116 ft (35.3 m) ($p = 0.935$).

Although the collective samples show no significant change in median particle sizes, reductions in particle sizes were observed during particular storm events. For example, particle sizes were consistently reduced in the grass swale on 12/06/2004 as shown in Figure 96. Median particle size was reduced from 18.4 µm at the entrance (0 ft or 0 m) to 7.5 µm at 116 ft (35.3 m). Similarly, median particle size was reduced from 10.6 µm at the entrance (0 ft or 0 m) to 2.8 µm at 116 ft (35.3 m) on 11/11/2004 as shown in Figure 97. These observations suggests that grass swales preferentially remove the larger particles, as expected. In addition, particle size distributions were consistently shifted to the left as swale length increased, indicating that smaller particles were also being captured in the grass swales.

Table 33. Summaries of Particle Size Distributions for 12 Storm Events

Date: 10/09/2004					
swale location	10% (µm)	25% (µm)	50% (µm)	75% (µm)	90% (µm)
0 ft (0 m)	1.6	2.5	4.8	9.5	20.6
75 ft (22.8 m)	5.9	19.7	39.2	70.1	105.8
102 ft (31.1 m)	3.6	10.1	26.2	86.1	147.4

Date: 10/10/2004 - 100 PM					
swale location	10% (µm)	25% (µm)	50% (µm)	75% (µm)	90% (µm)
0 ft (0 m)	2.2	4.1	9.6	19.6	34.0
102 ft (31.1 m)	2.2	5.4	12.5	25.3	47.7

Date: 10/10/2004 - 900 PM

swale location	10% (µm)	25% (µm)	50% (µm)	75% (µm)	90% (µm)
75 ft (22.8 m)	9.4	18.0	36.6	64.7	92.7
116 ft (35.3 m)	10.5	20.0	38.2	66.2	100.2

Date: 10/11/2004

swale location	10% (µm)	25% (µm)	50% (µm)	75% (µm)	90% (µm)
0 ft (0 m)	3.4	6.6	11.4	18.1	26.2
2 ft (0.6 m)	3.9	6.9	11.8	19.6	30.4
3 ft (0.9 m)	3.6	7.1	13.4	24.6	47.3
6 ft (1.8 m)	2.8	5.6	11.4	20.5	38.2
25 ft (7.6 m)	2.2	4.6	14.4	47.8	82.9
75 ft (22.8 m)	1.8	3.0	5.8	17.9	38.3
116 ft (35.3 m)	1.7	2.8	8.5	28.2	60.3

Table 33. Summaries of Particle Size Distributions for 12 Storm Events – *Continued*

Date: 10/19/2004

swale location	10% (µm)	25% (µm)	50% (µm)	75% (µm)	90% (µm)
25 ft (7.6 m)	6.1	19.9	45.9	75.5	97.7
75 ft (22.8 m)	1.9	6.9	26.5	58.1	84.3
116 ft (35.3 m)	1.4	3.3	33.2	50.0	67.6

Date: 10/23/2004

swale location	10% (µm)	25% (µm)	50% (µm)	75% (µm)	90% (µm)
0 ft (0 m)	1.8	3.9	9.1	21.6	46.2
2 ft (0.6 m)	3.4	8.9	20.3	39.1	59.5
3 ft (0.9 m)	3.3	7.4	14.7	25.5	44.3
6 ft (1.8 m)	3.0	7.4	17.6	35.3	64.4
25 ft (7.6 m)	1.7	4.5	13.6	38.9	81.3
75 ft (22.8 m)	1.5	4.1	15.4	44.2	75.5
116 ft (35.3 m)	1.1	2.0	5.5	27.9	44.2

Date: 11/01/2004

swale location	10% (µm)	25% (µm)	50% (µm)	75% (µm)	90% (µm)
0 ft (0 m)	1.7	4.1	10.7	21.0	33.9
2 ft (0.6 m)	1.2	2.3	5.9	14.7	29.0
3 ft (0.9 m)	1.3	2.8	8.6	21.9	38.1
6 ft (1.8 m)	1.2	2.6	8.6	19.8	38.1
25 ft (7.6 m)	1.0	1.6	3.9	24.2	50.5
75 ft (22.8 m)	1.2	2.8	32.5	52.6	74.7
116 ft (35.3 m)	1.2	2.7	18.6	37.6	59.5

Date: 11/11/2004

swale location	10% (µm)	25% (µm)	50% (µm)	75% (µm)	90% (µm)
0 ft (0 m)	1.8	3.9	10.6	23.6	49.3
2 ft (0.6 m)	2.9	7.5	14.1	26.4	53.8
3 ft (0.9 m)	3.1	8.1	17.5	32.9	70.0
6 ft (1.8 m)	2.7	6.3	17.4	35.9	67.2
25 ft (7.6 m)	1.3	2.9	7.0	14.6	42.3
75 ft (22.8 m)	1.0	1.8	3.8	7.8	17.3
116 ft (35.3 m)	1.0	1.4	2.8	5.8	22.0

Table 33. Summaries of Particle Size Distributions for 12 Storm Events – *Continued*

Date: 11/21/2004

swale location	10% (µm)	25% (µm)	50% (µm)	75% (µm)	90% (µm)
0 ft (0 m)	3.2	5.5	9.2	14.9	23.9
2 ft (0.6 m)	3.8	6.9	13.5	29.2	53.4
3 ft (0.9 m)	5.4	9.5	16.6	28.5	46.0
6 ft (1.8 m)	6.2	11.4	20.8	40.6	73.6
25 ft (7.6 m)	2.3	5.6	11.9	23.3	43.0
75 ft (22.8 m)	3.5	7.9	20.7	51.7	82.5
116 ft (35.3 m)	1.9	5.1	10.6	23.0	44.4

Date: 11/22/2004

swale location	10% (µm)	25% (µm)	50% (µm)	75% (µm)	90% (µm)
0 ft (0 m)	1.7	6.9	13.0	21.5	35.8
2 ft (0.6 m)	4.5	10.9	19.8	38.2	62.9
3 ft (0.9 m)	4.4	9.1	15.9	26.6	46.3
6 ft (1.8 m)	4.1	10.0	20.0	41.3	89.4
25 ft (7.6 m)	2.3	5.6	11.9	23.3	43.0
75 ft (22.8 m)	3.4	7.0	12.8	33.0	54.0
116 ft (35.3 m)	2.2	5.8	12.5	33.6	53.0

Date: 12/06/2004

swale location	10% (µm)	25% (µm)	50% (µm)	75% (µm)	90% (µm)
0 ft (0 m)	8.9	15.1	28.4	58.9	148.6
2 ft (0.6 m)	7.3	11.3	18.2	32.3	64.4
3 ft (0.9 m)	5.9	9.5	15.7	27.4	44.7
6 ft (1.8 m)	4.6	8.4	14.3	23.8	40.5
25 ft (7.6 m)	2.8	5.4	9.2	17.7	41.3
75 ft (22.8 m)	2.8	5.4	9.2	17.7	41.3
116 ft (35.3 m)	2.6	4.5	7.5	12.0	20.8

Date: 12/08/2004

swale location	10% (µm)	25% (µm)	50% (µm)	75% (µm)	90% (µm)
0 ft (0 m)	8.6	13.4	21.3	34.6	54.1
2 ft (0.6 m)	8.2	12.9	19.1	29.6	55.1
3 ft (0.9 m)	9.9	15.3	22.3	33.3	53.6
6 ft (1.8 m)	7.8	13.0	19.1	28.7	42.1
25 ft (7.6 m)	7.3	11.8	17.3	24.9	38.7
75 ft (22.8 m)	7.0	10.7	15.5	23.9	39.4
116 ft (35.3 m)	6.5	9.8	14.4	24.3	41.9

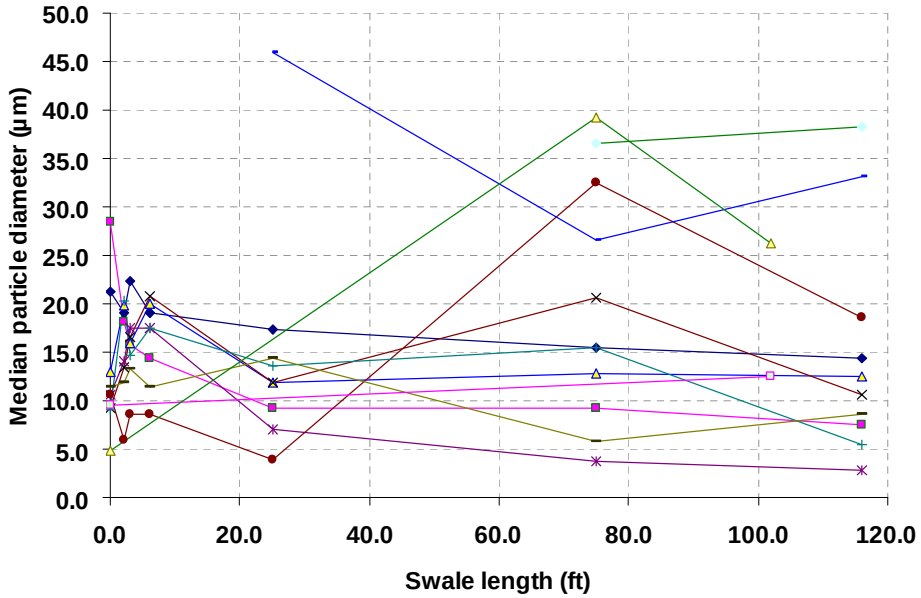

Figure 94. Median particle sizes vs. swale length observed at the outdoor grass swale (Note 1 ft = 0.30 m).

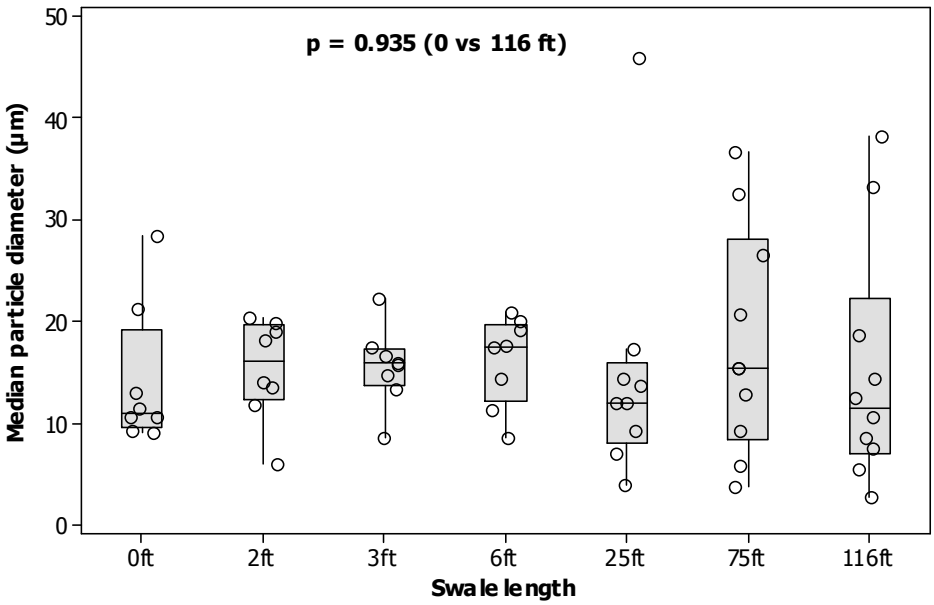

Figure 95. Box-and-whisker plots of median particle diameters vs. swale length observed at the outdoor grass swale (Note 1 ft = 0.30 m).

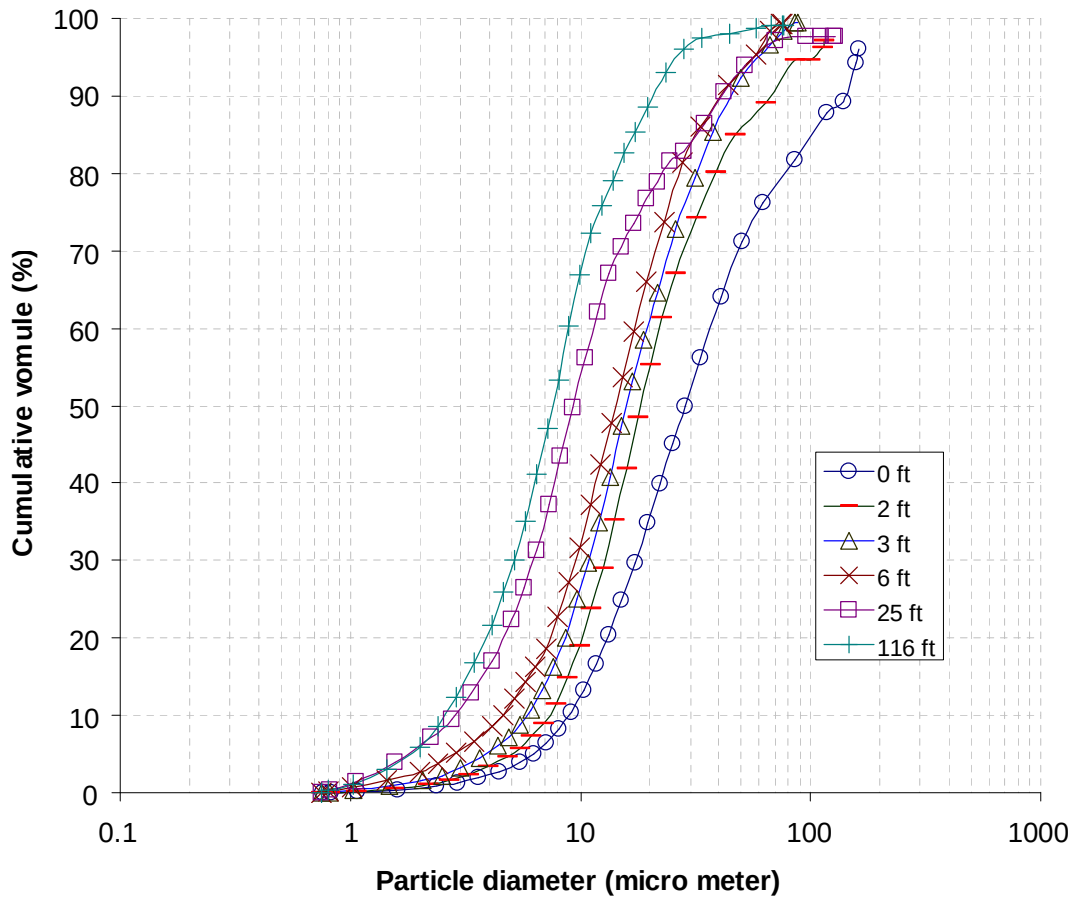

Figure 96. Example particle size distributions for different swale lengths observed on December 6, 2004.

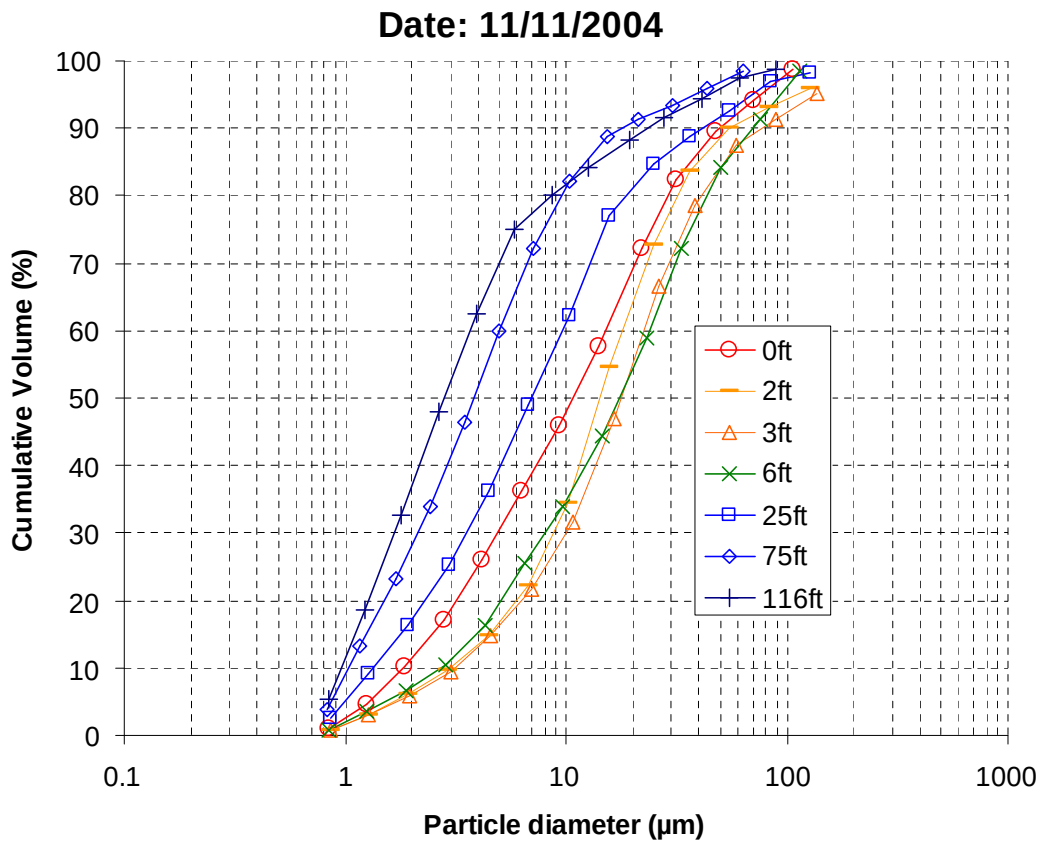

Figure 97. Example particle size distributions for different swale lengths observed on November 11, 2004 (Particle size distributions of all the storm events are presented in Appendix O).

Summary of Findings

Total Solids and Total Solids (< 106 µm)

• Although some storm events (10/11/04, 11/11/04, and 12/08/04) showed sediment reductions, there was no significant changes in total solids concentrations between 0 ft (0 m) and 6 ft (1.8 m) ($p = 0.328$ for total solids and $p = 0.248$ for total solids < 106 µm). There was weak evidence suggesting reductions in total solids and total solids < 106 µm ($p = 0.063$ for total solids and $p = 0.060$ for total solids < 106 µm).

• Total solids and total solids < 106 µm were very similar to each other for most of the events. This suggests that particle sizes of runoff sediments from the roads and in the grass swale were primary less than 106 µm.

• Total dissolved solids were the predominant portion of the total solids and total solids < 106 µm especially beyond 6 ft (1.8 m).

Total Suspended Solids

• Although initial total suspended solids concentrations at the entrance of the swale varied greatly for different rain events, large sediment reductions were normally observed between 3 ft (0.9 m) and 25 ft (7.6 m) ($p = 0.019$). Beyond 25 ft (7.6 m), the total suspended solids concentrations were more consistent, with much less, but significant, sediment reductions in the grass swale ($p = 0.045$).

• In some storm events (10/23/04, 11/11/04, and 11/21/04), total suspended solids concentrations increased between 0 ft (0 m) and 3 ft (0.9 m) instead of decreasing, likely due to scouring of previously deposited sediments at the entrance of the swale. However, there was no overall significant total suspended solids concentration changes between 0 ft (0 m) and 6 ft (1.8 m) ($p = 0.934$).

• Total suspended solids removals ranging from 56% to 100% were observed, with a mean removal of 80% between 0 ft (0 m) and 116 ft (35.3 m). As an example, a reduction of 90% in total suspended solids was observed (102 mg/L to 10 mg/L) during the rain event occurring on 10/11/2004.

Total Dissolved Solids

• There were no significant changes ($p = 0.879$) in total dissolved solids concentrations (particulates < 0.45 µm), except during the rain event occurring on 12/08/2004.

Turbidity

• Although initial turbidity varied from 2 NTU to 137 NTU, significant reductions in turbidity were observed at the outdoor swale ($p = 0.040$). Overall, median turbidity reduction of 70.5% was observed between the entrance of the swale and 116 ft.

• Turbidity increased between 25 ft (7.6 m) and 75 ft (22.8 m) on 12/08/2004 due to scouring of the top soil during an intermittent period of high flows

Particle Size Distributions

• There was no noticeable change in particle size in the three distinct swale regions; between the swale entrance (0 ft or 0 m) and 6 ft (1.8 m) ($p = 0.248$) due to possible scouring, between 6 ft (1.8 m) and 25 ft (7.6m) ($p = 0.149$), and beyond 25 ft (7.6 m) ($p = 0.935$).

• Particle sizes were consistently reduced on the grass swale during some events. On 12/06/2004, the median particle size was reduced from 18.4 µm at the entrance (0 ft or 0 m) to 7.5 µm at 116 ft (35.3 m), for example.

• Some event showed evidence of scouring of sediment from the swale. The median particle sizes increased from 10.6 µm at 0 ft to 17.4 µm at 6 ft (1.8 m) and then were consistently reduced from 17.4 µm at 6 ft (1.8 m) to 2.8 µm at 116 ft (35.3 m) during the storm event of 11/11/2004. Total suspended solids also increased between 0 ft (0 m) and 6 ft (1.8 m) and decreased consistently from 6 ft (1.8 m) to 116 ft (35.3 m). These suggest that scouring of the sediments between 0 ft (0 m) and 6 ft (1.8 m), which increased total suspended solids, may change particle size because of re-suspension of the deposited particles.

Chapter 8: Predictive Model

First-Order Decay

During both the indoor experiments and outdoor observations, greater sediment reductions were observed at the beginning of the grass swales, and the concentrations then tended to stabilize after some distance. During the outdoor swale observations, high sediment reductions occurred between 0 ft (0 m) and 25 ft (7.6 m), and lower sediment reductions occurred between 25 ft (7.6 m) to 116 ft (35.3 m) (the location of the drainage inlet). Thus, the concept of first order decay was applied to describe the behavior of the stormwater sediment in grass swales and to statistically identify the significant experimental factors. The following is the equation of first order decay that was used to describe the concentration reductions observed:

(6.1) $$Ln\left(\frac{C_{out}}{C_{in}}\right) = -kt$$

Where:

C_{out} = Sediment concentration at downgradient sampling locations
C_{in} = Initial sediment concentration at the head works
k = First order constant
t = Swale length in feet from the head works

The first order constant (k-constant) is a function of swale length and determines the sediment reduction rate for each experimental condition. Since we are also interested in the effects of the experimental conditions on particles of different size, k-constants for various particle size ranges (listed below) were also computed:

- < 0.45 µm (total dissolved solids)
- 0.45 to 2 µm
- 2 to 5 µm
- 5 to 10 µm
- 10 to 30 µm
- 30 to 60 µm
- 60 to 106 µm
- 106 to 425 µm (total solids minus total solids less than 106 µm)

Also, settling frequency (how many times the particle could conceivably settle to the bottom of the flow depth during the swale length) for each particle size range and for the test length of the grass swales (6 ft (1.8 m) during the second indoor swale tests) was determined using Stoke's law, considering the depths of flow and the flow velocities.

Box and whisker plots of the calculated k-constants for the various particle ranges are shown in Figure 98. This plot shows that no reductions in particles smaller than 0.45 µm in diameter (total dissolved solids) occurred, while the largest particles would be trapped in relatively short swales, depending on flow and depth. Particles larger than 0.45 µm show significant sediment trapping, especially when larger than 30 µm. The largest sediment reductions were observed for the largest particles, in the range between 106 and 425 µm in diameter. The frequencies of settling (the number of times the particle could fall through the flow depth during the length of the swale, considering the flow

velocity) for these larger particles are much greater than the for the smaller particle sizes. There also were large variations in the k-constant for these larger particles, likely because of the fewer particles found in this large size. Particles from 0.45 to 30 µm showed similar k-constant values (and therefore sediment reduction rates), while the particles from 30 to 106 µm had intermediate values.

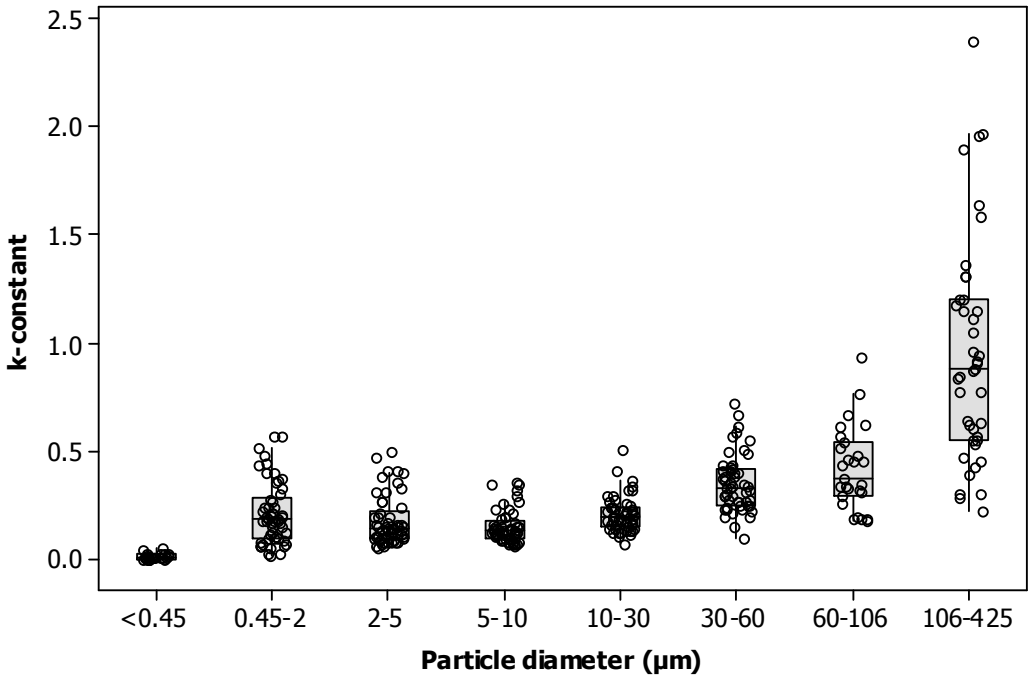

Figure 98. Box-and-whisker plots showing k-constants vs. various particle size ranges (0 to 6 ft).

Settling Frequency

Figure 99 shows percent reductions from the initial sediment concentrations at the head works over the 6 ft (1.8 m) length of the indoor experimental swales. The three grass types are represented by different symbols. The statistical analyses using the data from the second set of indoor tests showed that the percent reductions of sediment in the synthetic turf lined swales for various particle size ranges were significantly less than for the Zoysia and Bluegrass lined swales. This is also illustrated in Figure 99, where the synthetic turf data points are generally all much lower than for the other grasses for the same settling frequencies. However, the differences in sediment reductions between the Zoysia and Bluegrass planted swales were found to be insignificant. Since the synthetic turf lined swale was not representative of grass-lined swales, the data collected during the synthetic turf lined swale tests were not used to develop the final sediment trapping model described below. The sediment transport observations obtained with the Zoysia and Bluegrass swales were combined.

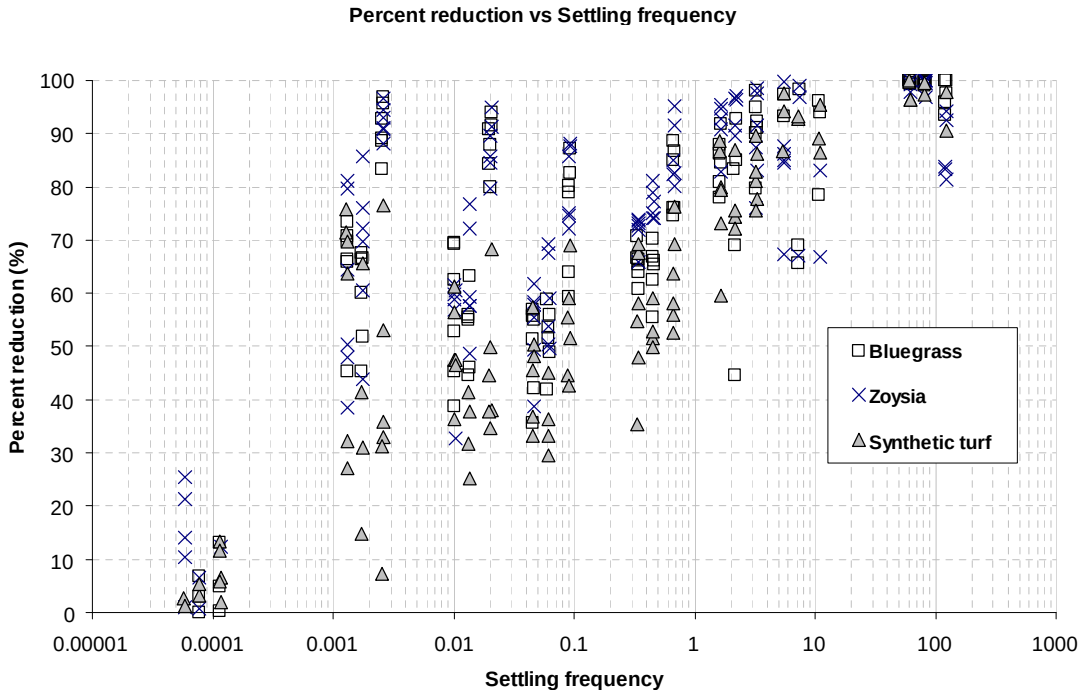

Figure 99. Percent sediment reductions vs. settling frequencies for the different grass types (results of the second indoor experiments).

Figure 99 also contains vertical clusters of observations. Each of these clusters of data represents a narrow particle size range. Particle less than 0.45 µm (total dissolved solids) shows very low sediment reductions (0 to 25% reductions) for all flow conditions. Large particles ranging from 106 to 425 µm had the highest reductions (80 to 100% reductions) for all flow conditions.

The effects of flow rate were found to be significant. This is illustrated on Figure 100. The sediment reductions during the 10 GPM (0.038 m^3/min) tests were much higher than during the 15 GPM (0.064 m^3/min) and 20 GPM (0.076 m^3/min) tests for the particles ranging from 0.45 to 30 µm. However, there were no significant differences found in sediment reductions between the 15 GPM (0.064 m^3/min) and 20 GPM tests (0.076 m^3/min).

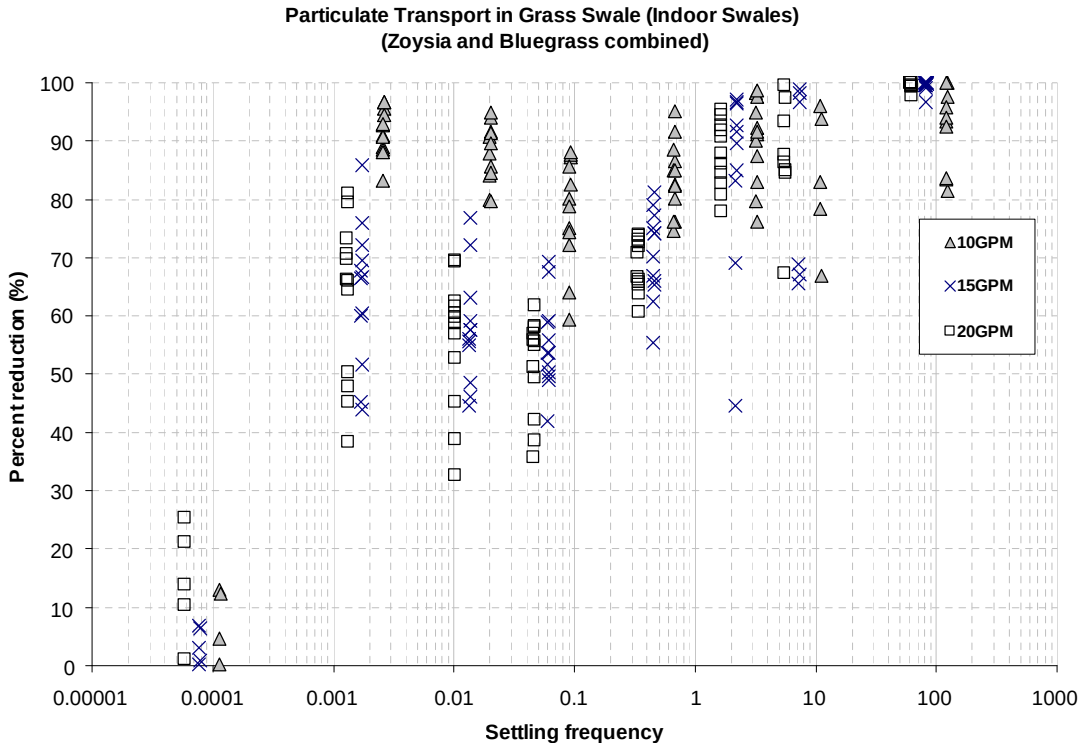

Figure 100. Percent sediment reductions vs. settling frequencies for the different flow rates (Zoysia and Bluegrass data combined).

The relationship between flow depth and grass height is shown to be very promising when explaining the variation in settling frequency and sediment retention, as shown on Figure 101. This factor considers the opportunities of the runoff water and entrained sediment to contact the grass plant. When the water is flowing within the height of the grass, the settled sediment is much better protected from scour, as the water velocity is quite low, and associated Manning's n, is very large (Kirby 2003). In addition, the grass may act like inclined tube or plate settlers, effectively increasing the settling area. To determine the effect of the flow depth to grass height ratio, this ratio was computed for each experimental condition. The percent reduction-settling frequency plots were then separated into three distinct flow depth to grass height ratio categories: 0 to 1.0, 1.0 to 1.5, and 1.5 to 4. A ratio less than 1.0 means that the grass height is higher than the flow depth. These separate categories are seen to have much reduced variabilities in reductions of sediment for each settling frequency category.

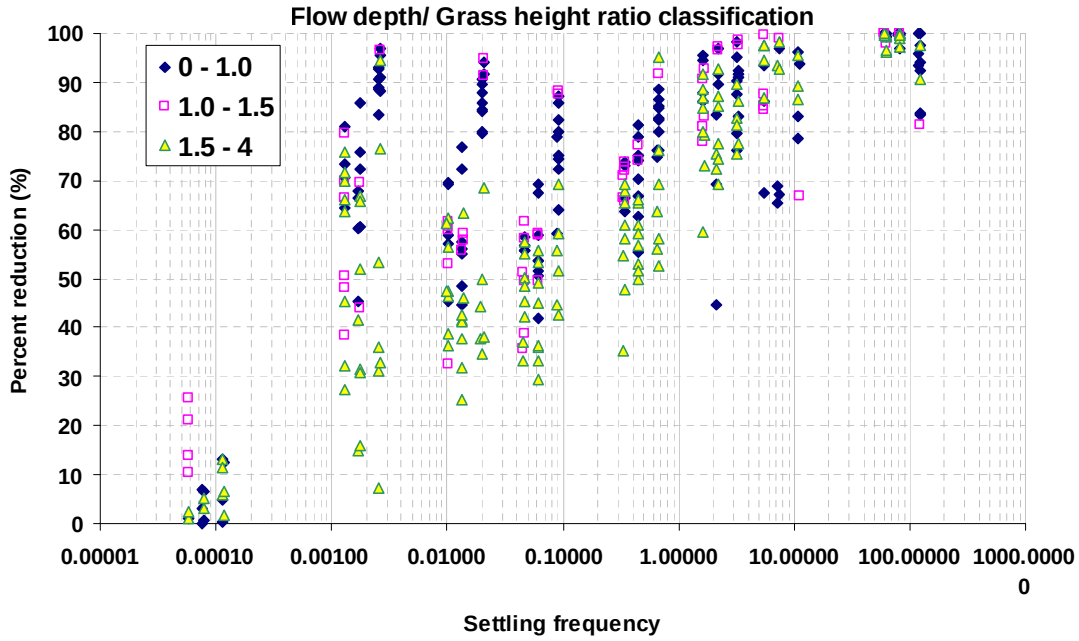

Figure 101. Percent sediment reductions vs. settling frequencies for the different flow depth to grass height ratios (Zoysia and Bluegrass data combined).

A sensitivity analysis of shear stress and slope was also conducted to determine their relative significance on sediment retention. When plotted, these factors did not provide any further resolution of the observed variance, such as indicated in Figure 102. Related plots are presented in Appendix Q. It was therefore concluded that shear stress and slope were not as important as the flow depth and grass height when describing sediment retention in grass swales.

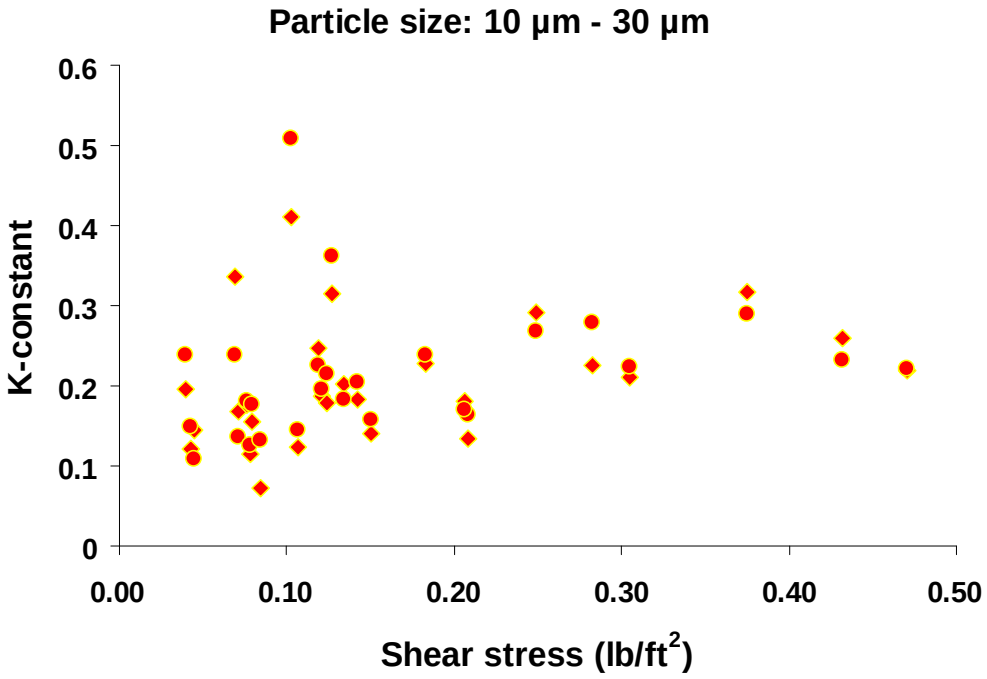

Figure 102. Example of k-constants vs. shear stress.

Predictive Model

Data obtained from the Zoysia and Bluegrass tests were used to create a sediment reduction predictive model. Third-order polynomial regression equations were fitted to the percent reduction-settling frequency graphs for the three different flow depth to grass ratio categories. Obviously, assuming that if the settling frequency is ≥ 1 would result in complete capture and settling frequencies < 1 would result in complete transport of the associated particle is overly simplified. The polynomial regression model was therefore used to fit the data since there seemed to be three distinct performance regions across the range of settling frequencies: very small (dissolved) particles, very large (> 250 µm) particles, and intermediate-sized particles.

The following figures show the percent reductions against settling frequencies, the regression lines, and the 95% confidence intervals for the means. Also shown are the residual analyses indicating that the equations were properly determined, although the residuals are smaller for the larger particles as they approach the 100% retention upper limit, a physical barrier to performance.

As indicated previously, the percent reductions of dissolved solids (indicated by the clusters of data points at the lowest settling frequency) are very low compared to the larger particles. These data were therefore not included in the regressions as they would have distorted the results for the sediment retention predictions. Large particles of 250 and 425 µm in diameter (associated with 100 settling frequencies) had the largest percent reductions for all three flow to grass height ratio categories. When the flow depth to grass height ratios are less than 1, indicating shallow flow, the percent reductions are high and fairly consistent for the different settling frequencies, except for the dissolved solids which are poorly controlled and the large particles that are much better controlled. As the ratio of flow depth and grass height increases to greater than 1, the percent retention of the small particles in the swales decrease, especially for particles whose settling frequencies are between 0.001 and 1.

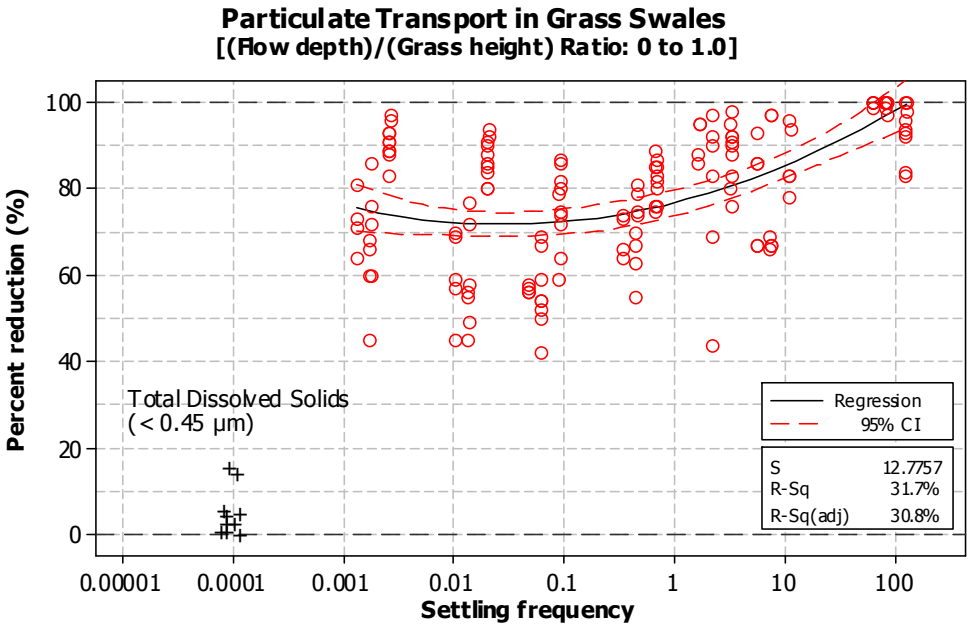

Figure 103. Polynomial regression line and observed percent reductions vs. settling frequency for the (flow depth)/(grass height) ratio between 0 to 1.0.

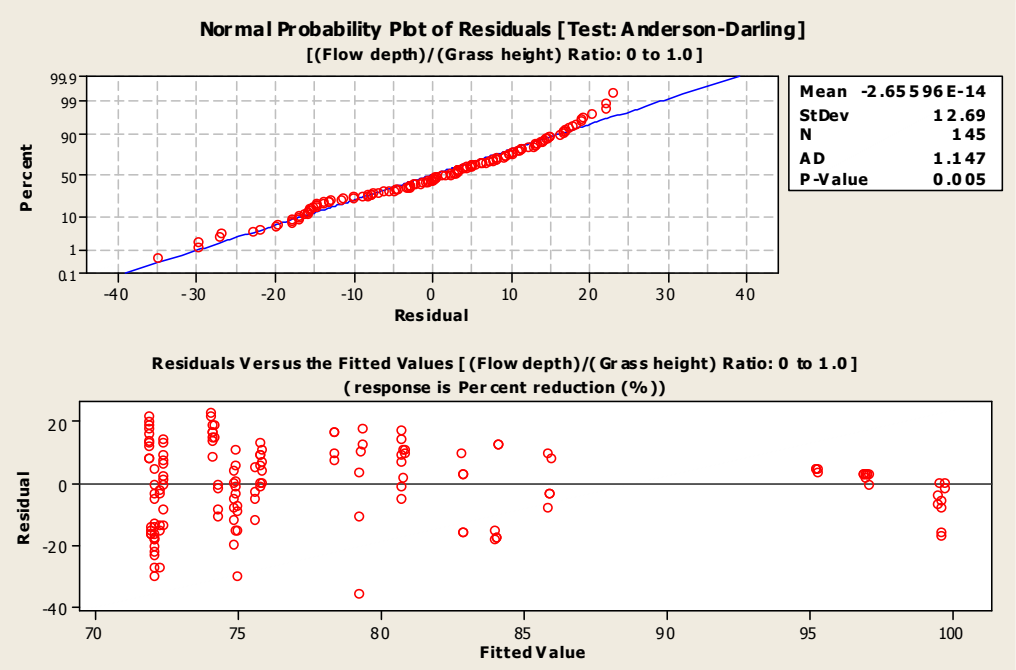

Figure 104. Normal probability plot and residual plot of the residuals vs. fitted values for the (flow depth)/(grass height) ratio between 0 to 1.0.

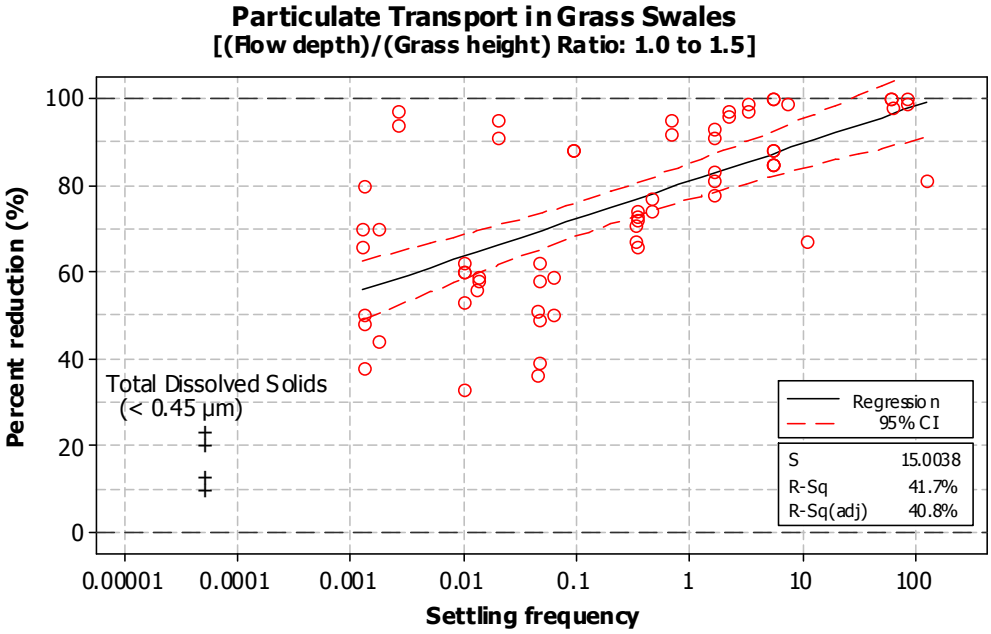

Figure 105. Polynomial regression line and observed percent reductions vs. settling frequency for the (flow depth)/(grass height) ratio between 1.0 to 1.5.

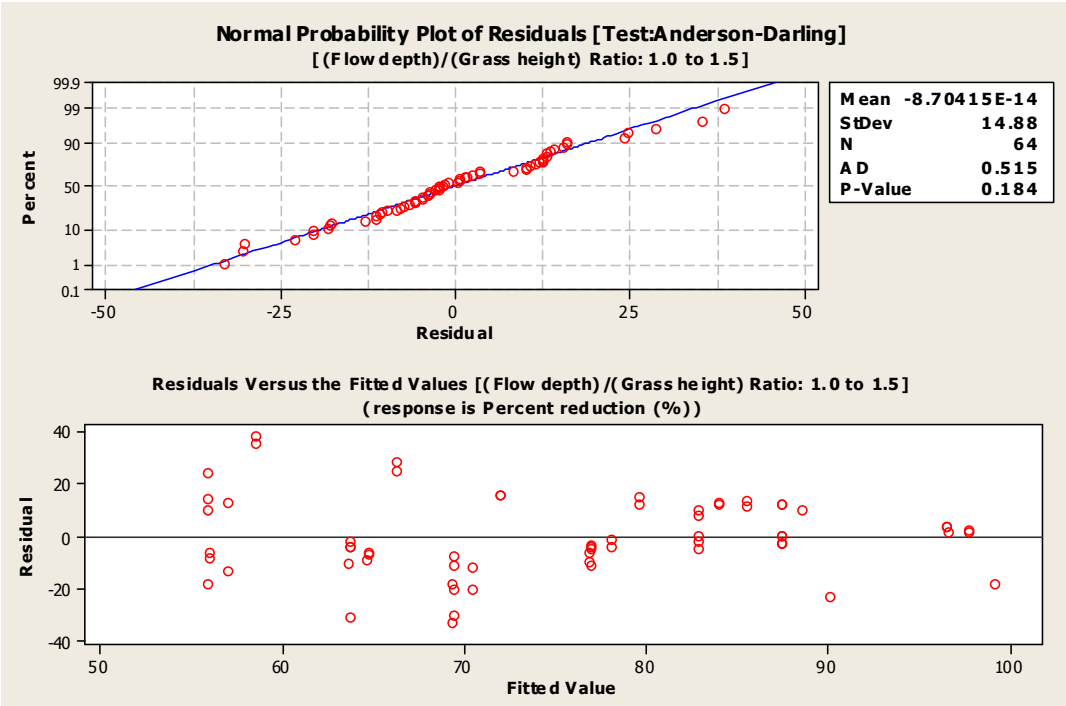

Figure 106. Normal probability plot and residual plot of the residuals vs. fitted values for the (flow depth)/(grass height) ratio between 1.0 to 1.5.

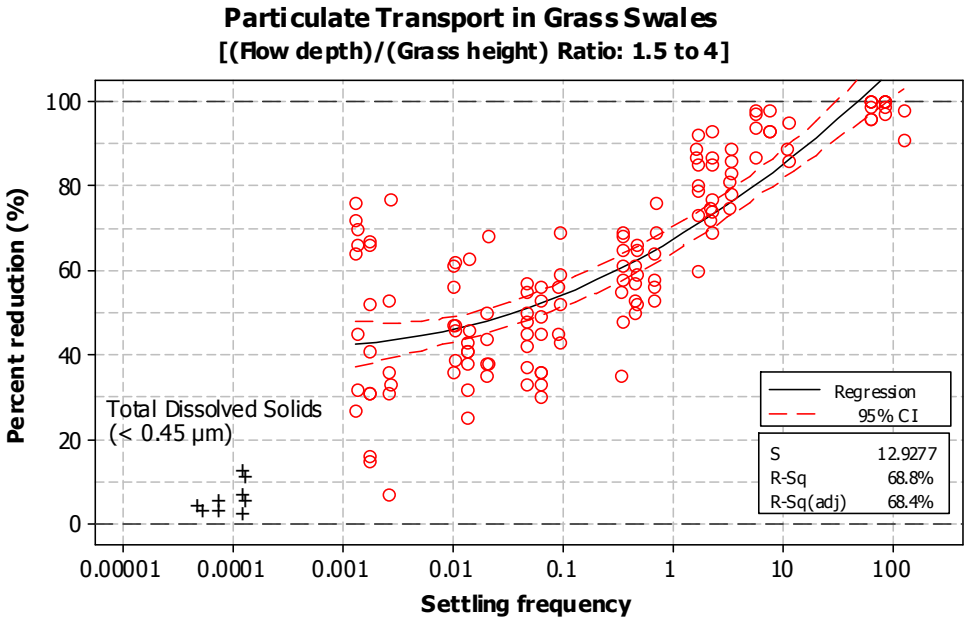

Figure 107. Polynomial regression line and observed percent reductions vs. settling frequency for the (flow depth)/(grass height) ratio between 1.5 to 4.0.

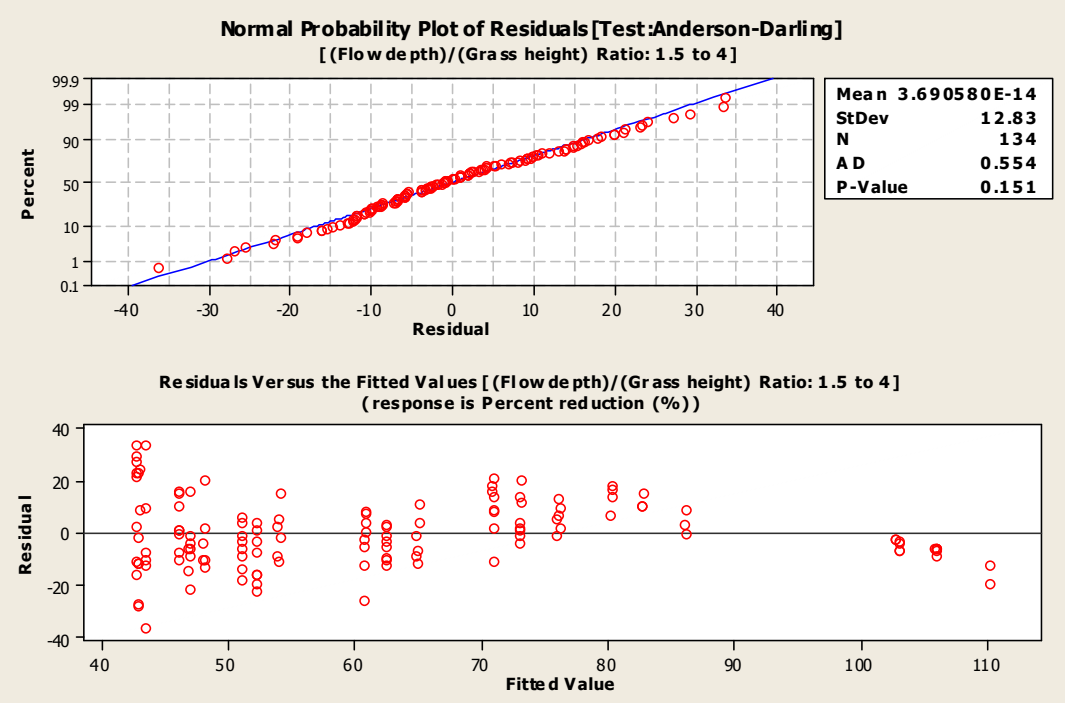

Figure 108. Normal probability plot and residual plot of the residuals vs. fitted values for the (flow depth)/(grass height) ratio between 1.5 to 4.0.

The following lists the equations and the ANOVA analyses for the polynomial regression lines for each flow depth to grass height ratio category:

Flow to Grass Height Ratio: 0 to 1.0

(6.12) $$Y = 2.101 * \log(X)^2 + 6.498 * \log(X) + 76.82$$

Where:

Y = Percent reduction

X = Settling frequency

Analysis of Variance

Source	DF	SS	MS	F	P
Regression	2	10765.9	5382.93	32.98	< 0.001
Error	142	23177.0	163.22		
Total	144	33942.8			

Sequential Analysis of Variance

Source	DF	SS	F	P
Linear	1	7728.35	42.16	< 0.001
Quadratic	1	3037.51	18.61	< 0.001

Flow to Grass Height Ratio: 1.0 to 1.5

(6.13) $$Y = 8.692 * \log(X) + 80.94$$

Where:

Y = Percent reduction

X = Settling frequency

Analysis of Variance

Source	DF	SS	MS	F	P
Regression	1	9986.4	9986.44	44.36	< 0.001
Error	62	13957.0	225.11		
Total	63	23943.5			

Flow to Grass Height Ratio: 1.5 to 4.0

(6.14) $$Y = 2.382 * \log(X)^2 + 15.47 * \log(X) + 67.46$$

Where:

Y = Percent reduction

X = Settling frequency

Analysis of Variance

Source	DF	SS	MS	F	P
Regression	2	48358.8	24179.4	144.68	< 0.001
Error	131	21893.5	167.1		
Total	133	70252.3			

Sequential Analysis of Variance

Source	DF	SS	F	P
Linear	1	45055.2	236.03	< 0.001
Quadratic	1	3303.5	19.77	< 0.001

As indicated in the above ANOVA tests, the regression equations are all highly significant ($p < 0.001$). Sequential analysis of variance tests were also performed to determine the significance of the terms of the regression equations. All the linear, quadratic, and cubic terms of all the ratios were found to be significant since all probabilities were less than 0.001.

Model Application to Outdoor Swale Performance Observations

The data obtained during the outdoor swale observations were examined to verify the suitability of the regression equations obtained from the second indoor controlled experiments to larger swales during actual rains. Initially, the k-constants were computed using data collected at 0 ft (0 m) and 116 ft (35.3 m). However, the regression lines from these computed k-constants had very poor correlations with the data points. The data were further examined to distinguish separate performance zones along the swale. When examining the total suspended solids data obtained for the outdoor swale, there seemed to be three distinct regions for sediment reduction behavior. These were found to be located at 0 to 3 ft (0 to 0.9 m), 3 to 25 ft (0.9 to 7.6 m), and 25 to 116 ft (7.6 to 35.3 m). Although there were some high sediment reductions observed between 0 ft (0 m) and 3 ft (0.9 m) for some events, large increases in sediment concentrations were also observed. This was likely due to scouring occurring at the upper end of the swale, causing some re-suspension of previously deposited sediments, and possibly eroding of the swale lining soil. As noted before, there was a noticeable mound of large sediment close to the upper end of the swale. This material was likely scoured during some events. Further analyses are needed to confirm sediment transport at the upper end of the swale. Thus, it is the region of unknown behavior, or a buffer zone/transition. The region between 3 ft (0.9 m) and 25 ft (7.6 m) showed the highest and most consistent sediment reductions. Data from this range were therefore evaluated and are presented in Figure 109. Sediment reductions for other swale regions were presented in Appendix R.

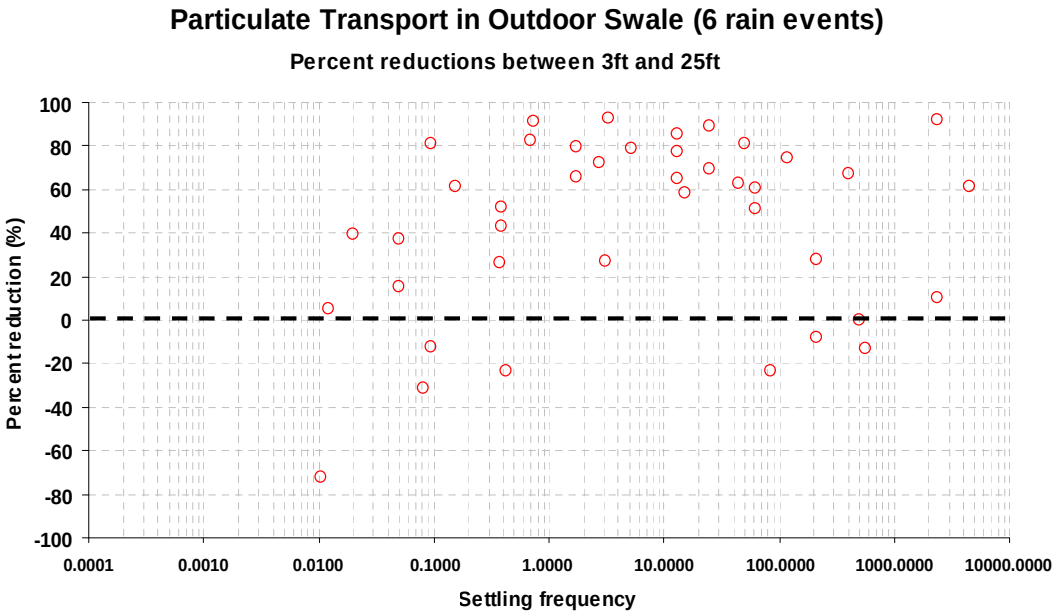

Figure 109. Percent reductions vs. settling frequencies observed at the outdoor swale between 3 ft (0.9 m) and 25 ft (7.6 m) (data from twelve storm events).

Figure 109 indicates a wide variation in sediment reductions for the different settling frequencies. There are many low reduction rates noted. It was determined that these negative and low percent reductions occurred during events that had very low initial sediment concentrations. Appendix P shows sediment concentrations between 3 ft (0.9 m) and 25 ft (7.6 m) for each particle size range. These figures clearly show that higher initial sediment concentrations correspond to higher sediment reduction rates than lower initial sediment concentrations (except for dissolved solids). Also, looking at each particle range, there are "irreducible" concentrations due to very low initial concentrations. "Irreducible" concentrations for each particle size range are shown on Table 34.

Table 34. Approximate "Irreducible" Concentrations Determined for the Different Particle Size Ranges (using data obtained from the outdoor swale observations)

Particle size range	Irreducible concentration
< 0.45 µm (TDS)	N/A
0.45 to 2 µm	7 mg/L
2 to 5 µm	5 mg/L
5 to 10 µm	5 mg/L
10 to 30 µm	10 mg/L
30 to 60 µm	5 mg/L
60 to 106 µm	5 mg/L
106 to 425 µm	10 mg/L
> 0.45 µm (TSS)	20 mg/L

Note: N/A = not available

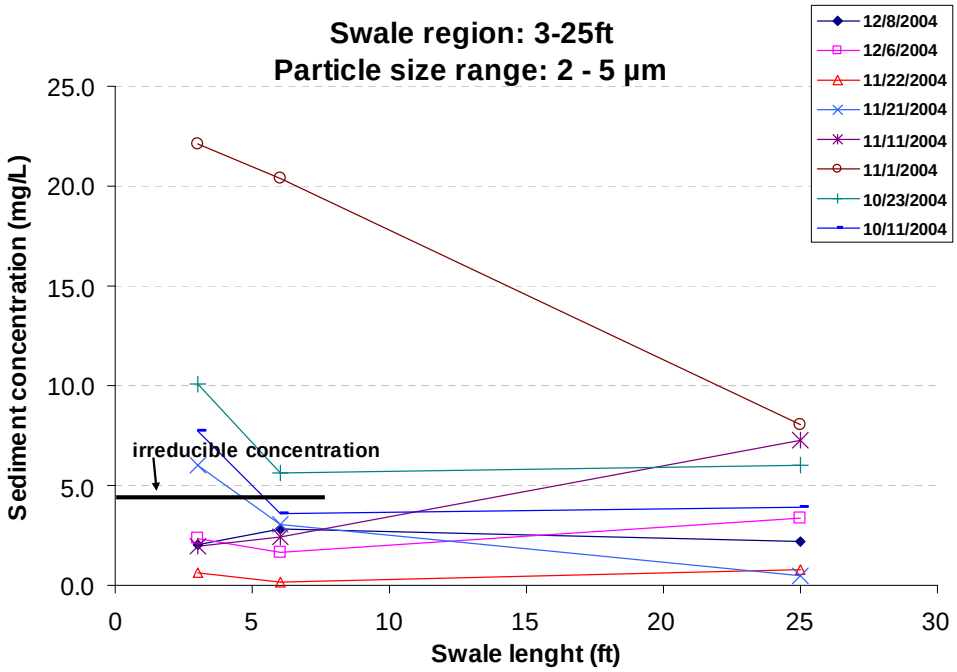

Figure 110. Example of the 'irreducible' sediment concentrations.

Negative and very low percent reductions were generated during events having initial concentrations close to, or less, than the irreducible concentrations. Therefore, these data were eliminated from the sediment reduction calculations for the outdoor swale tests. Figure 111 shows the sediment reductions and settling frequencies for the outdoor swale observations after eliminating the observations that had initial concentrations below the "irreducible" concentrations.

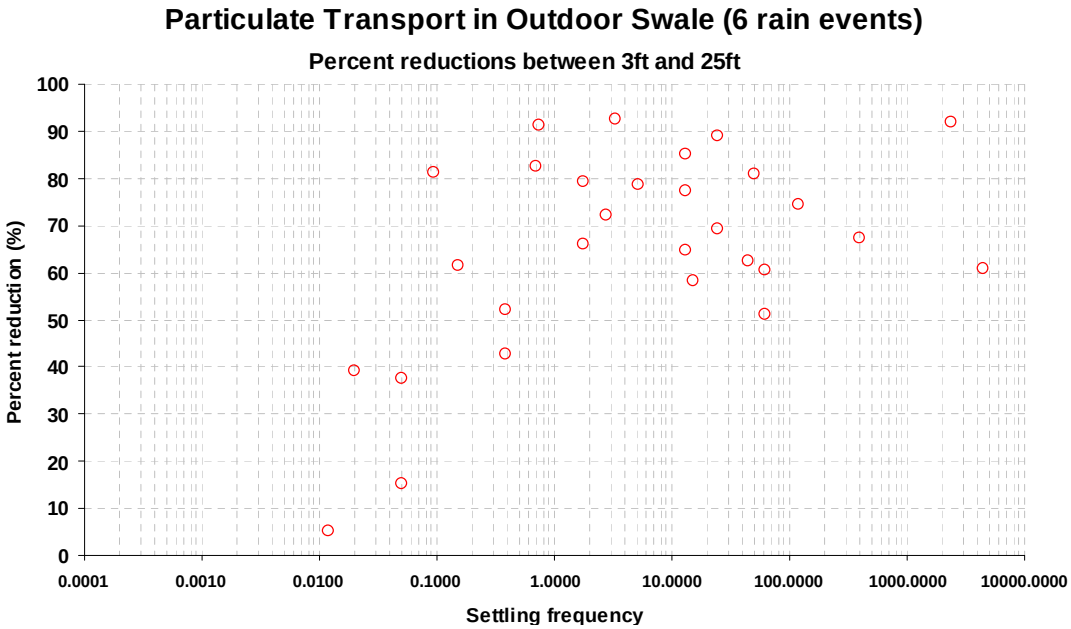

Figure 111. Percent reductions vs. settling frequency observed at the outdoor swale between 3 ft (0.9 m) and 25 ft (7.6 m) (data from six storm events), after eliminating the observations that had initial concentrations below the "irreducible" concentrations.

Settling frequencies above 1.0 are surprisingly consistent, with about 75% removals, while the percentage removals drop dramatically for smaller settling frequencies (down to about 0% for 0.01 settling frequencies).

Descriptions of Events Having Outdoor Swale Observations

Tables 35 through 37 summarize information for the eight rain events that had suitable data for determining sediment reductions using the outdoor swales.

Table 35. Storm Events Which Had Suitable Data for the Different Particle Size Ranges

Particle size	Event							
< 0.45 µm	12/8/04	12/6/04	11/22/04	11/21/04	11/11/04	11/1/04	10/23/04	10/11/04
0.45 to 2 µm	11/1/04							
2 to 5 µm	11/21/04	11/1/04	10/23/04	10/11/04				
5 to 10 µm	12/8/04	12/6/04	11/21/04	11/1/04	10/23/04	10/11/04		
10 to 30 µm	12/8/04	12/6/04	11/21/04	11/1/04	10/23/04	10/11/04		
30 to 60 µm	12/8/04	12/6/04	11/21/04	11/1/04	10/23/04	10/11/04		
60 to 106 µm	12/8/04	11/21/04	10/23/04	10/11/04				
106 to 425 µm	11/21/04	11/11/04	10/23/04					

Table 36. Weather Information of the Storm Events Which Had Suitable Data for Producing the Percent Reductions between 3 ft (0.9 m) and 25 ft (7.6 m)

	10/11/2004	10/23/2004	*11/1/2004	11/11/2004
Air temperature (Fahrenheit)	72	67	67	64
Preceding dry period (hour)	19.4	64.8	91.3	168.9
Total rain (inch)	0.11	0.84	N/A	0.23
Duration (minute)	45	115	N/A	135
Average intensity (inch/hour)	0.15	0.44	N/A	0.1
Max. rain fall intensity (inch/hour) in 5 minutes	0.24	3.24	N/A	0.36

	11/21/2004	11/22/2004	12/6/2004	12/8/2004
Air temperature (Fahrenheit)	60	64	57	59
Preceding dry period (hour)	13.5	24.8	5.7	39.4
Total rain (inch)	1.12	2.84	0.32	0.7
Duration (minute)	495	230	80	85
Average intensity (inch/hour)	0.14	0.74	0.24	0.49
Max. rain fall intensity (inch/hour) in 5 minutes	1.08	2.28	1.08	3.24

* Rain observed at the site, but not recorded at the rain gage on the campus
Note: N/A = not available

Table 37. Initial Sediment and Turbidity Concentrations for Storm Events Having Suitable Data of Sediment Trapping between 3 ft (0.9 m) and 25 ft (7.6 m)

Date	Total solids (mg/L)	Total solids < 106 µm (mg/L)	Total suspended solids (mg/L)	Total dissolved solids (mg/L)	Turbidity (NTU)
10/11/2004	149	141	102	62	65
10/23/2004	144	125	55	74	34
11/1/2004	246	247	153	101	137
11/11/2004	103	70	31	63	21
11/21/2004	29	36	18	24	38
11/22/2004	14	11	6	13	7
12/6/2004	139	116	120	4	18
12/8/2004	235	222	157	69	88

During sampling, flow depth and velocity were determined for most storm events. However, only the flow depths of the six storm events from 11/01/2004 to 12/08/2004 were determined. Despite the effort, it was almost impossible to observe flow velocities during the storm events because there was no equipment that could observe flow velocities of a very shallow flow disturbed by a thick vegetation. Thus, velocities were estimated by Manning's equation using the observed flow depths and channel slopes. Table 38 summarizes the observed flow depths and computed flow velocities for the six storm events.

Manning's equation:

$$V = 1.49 \frac{R^{2/3}}{n} * S^{1/2} \quad (6.15)$$

Where:

V = flow velocity (ft/s)
R = Hydraulic radius ~ Flow depth (ft)
S = Channel slope (fraction)
n = Manning's n (Kirby 2003 VR-n curves)

Table 38. Observed Flow Depths and Computed Flow Velocities during the Six Storm Events from 11/01/2004 to 12/08/2004 (Note 1 inch = 2.54 cm)

		11/1/2004		11/11/2004		11/21/2004	
Swale length	Slope	Flow depth (inch)	Flow velocity (inch/s)	Flow depth (inch)	Flow velocity (inch/s)	Flow depth (inch)	Flow velocity (inch/s)
0 ft to 6 ft (0 m to 1.8 m)	7%	0.50	0.27	0.53	0.28	0.34	0.21
6 ft to 75 ft (1.8 m to 22.8 m)	3%	1.17	0.32	0.50	0.18	0.50	0.18
75 ft to 116 ft (22.8 m to 35.3 m)	1%	1.25	0.23	1.00	0.20	1.25	0.23

		11/22/2004		12/6/2004		12/8/2004	
Swale length	Slope	Flow depth (inch)	Flow velocity (inch/s)	Flow depth (inch)	Flow velocity (inch/s)	Flow depth (inch)	Flow velocity (inch/s)
0 ft to 6 ft (0 m to 1.8 m)	7%	1.13	0.47	1.39	0.54	0.75	0.36
6 ft to 75 ft (1.8 m to 22.8 m)	3%	1.25	0.33	1.35	0.35	1.80	0.42
75 ft to 116 ft (22.8 m to 35.3 m)	1%	1.83	0.30	1.73	0.28	2.88	0.40

The calculated flow velocities are all very small.

Comparing Second Indoor Swale and Outdoor Swale Observations

Figure 112 is a comparison of the sediment reductions obtained from the second set of indoor swale experiments and the sediment reductions obtained from the outdoor swale observations. Only data for the experiments having flow depths to grass height ratios of less than 1 are used, as most of the events at the outdoor swale had very shallow flows.

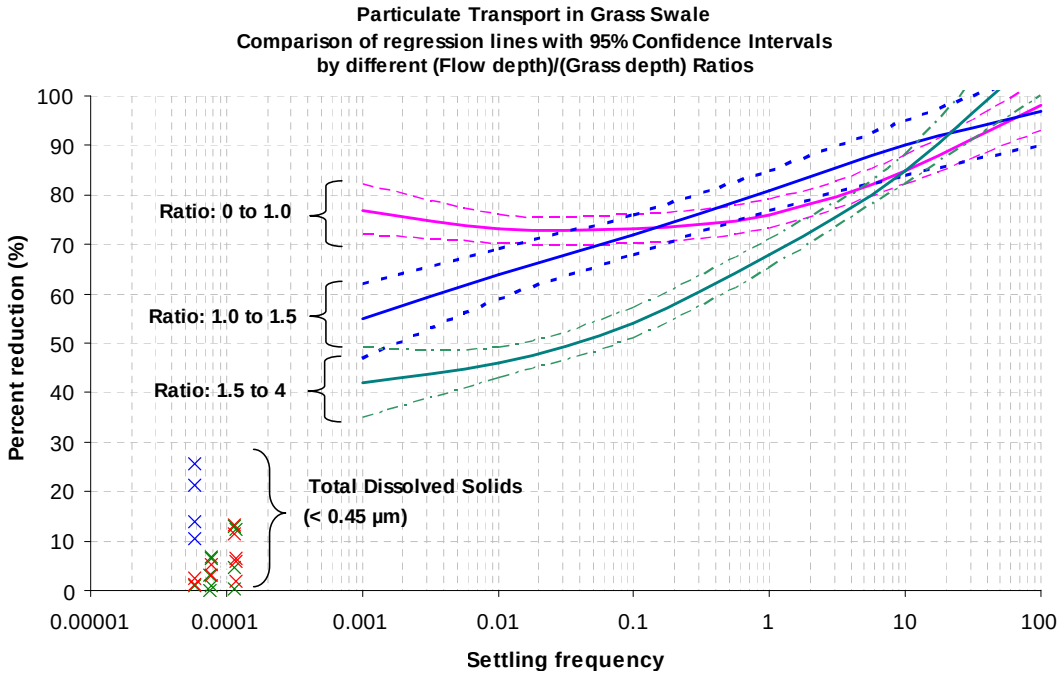

Figure 112. Comparison of regression lines with 95% confidence intervals for different (flow depth)/(grass height) ratios.

The sediment reduction confidence intervals associated with settling frequencies between 0.2 and 40 overlap. The sediment reductions at the outdoor swale for other settling frequencies were significantly lower than for the indoor swale experiments, as shown on Figure 113. It is assumed that the high total suspended solids concentrations during the indoor swale experiments (average of 500 mg/L range of 200 to 1,000 mg/L) resulted in higher percentage removals, compared to the lower concentrations (average of 60 mg/L, range of 10 to 160 mg/L) observed at the outdoor swales. This is commonly observed for all stormwater control practices: high influent concentrations result in larger percentage removals than lower influent concentrations. This is especially evident when the influent concentrations are close to the irreducible concentrations. Therefore, the important factors for these predictive equations are the settling frequency, flow height to grass height ratio, and the influent concentration.

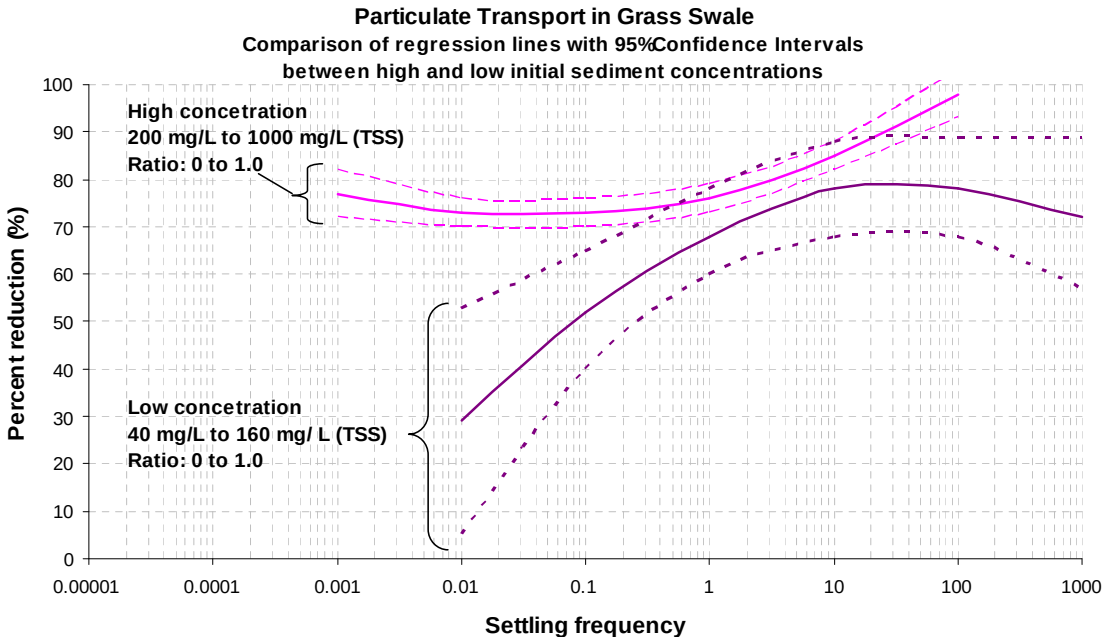

Figure 113. Regression lines with 95% confidence intervals for the low and high initial sediment concentrations (high concentrations from the second indoor experiment, average of 500 mg/L, range of 200 to 1,000 mg/L; low concentrations from the outdoor swale observations, average of 60 mg/L, range of 10 to 160 mg/L).

References

Anderson, C. Water Quality Field Guide. U.S.D.A. Soil Conservation Service. Pub. No. SCS-TP-160. 1983.

ASCE. *Sedimentation Engineering*. Edited by Vito A. Vanoni. Manuals and Reports on Engineering Practice, No. 54. 1975.

Barfield, B.J., Tollner, E.W., and Hayes, J.C., *Filtration of Sediment by Simulated Vegetation I. Steady-State Flow with Homogeneous Sediment.* Transaction of the ASAE 22(3), 540 – 548. 1979.

Barret, M.E., Walsh, P.M., Malina, J.F., and Charbeneau, R.J., *Performance of Vegetative Control for Treating Highway Runoff*. J. Environ. Engng 124 (11), 1121 – 1128. 1998.

Beasley, R.P. *Erosion and Sediment Pollution Control*. Ch. 11. Iowa State University Press. 1978.

Box G.E.P., W.G. Hunter, and J.S. Hunter. *Statistics for Experiments*. John Wiley and Sons. New York. 1978.

Burton, Allen, and Robert Pitt. *Stormwater Effects Handbook. A Toolbox for Watershed Managers, Scientists, and Engineers*. Boca Raton, Florida : Lewis Publishers. 2002.

Center for Watershed Protection and R. Pitt. *Illicit Discharge Detection and Elimination; A Guidance Manual for Program Development and Technical Assessments*. U.S. Environmental Protection Agency, Office of Water and Wastewater. EPA Cooperative Agreement X-82907801-0. Washington, D.C., 357 pgs. Oct. 2004.

Chang, H.H. *Fluvial Processes in River Engineering*. John Wiley & Sons. 1988.

Chow, Ven Te. *Open Channel Hydraulics*. McGraw-Hill. 1959.

Croke, T. "Accounting for bends in channel design." *Erosion Discussion*. Vol. 6, No. 1. North American Green (availabe from their web page: www.nagreen.com). Summer 2001.

Croke, T. "Reliable channel design using turf reinforcement mats." *Erosion Discussion.* Vol. 5, No. 1. North American Green (availabe from their web page: www.nagreen.com). June 2000.

Daniels R.B., and Gilliam J.W. *Sediment and Chemical Load Reduction by Grass and Riparian Filters.* Soil Sci. Soc. Am. J. 60: 246 – 251. 1996.

Deletic, Ana. *Modeling of Water and Sediment Transport over Grassed Areas*. Journal of Hydrology 248 (2001) 168 – 182. 2001.

Dennis, Jeffrey. *Phosphorus Export from a Low-Density Residential Watershed and an Adjacent Forested Watershed*. P.410 – 407. Lake and Reservoir Management, Vol II, Proc. North Amer. Lake Manage. Soc. Annual Conf., Washington, D.C. 1985.

Dillaha, T.A., Reneau, R.B., and Mostaghimi, S., Lee, D., *Vegetative Filter Strips for Agricultural Non Point Source Pollution Control.* Trans. ASAE 32 (2), 513 – 519. 1989.

Dorman, M., J. Hartigan, J. Steg and T. Quaserbarth. *Retention/Detention and Overland Flow for Pollutant Removal From Highway Stormwater Runoff.* Vol I. Research Report. Federal Highway Administration. FHWA/RD-89/202. 202pp. 1989.

EPA. *Post-construction Storm Water Management in New Development and Redevelopment: Grassed Swale*. Washington D.C.: EPA Office of Water. 1999.

Fletcher, T.D., Peljo, L., Fielding, J., and Wong, T.H.F. *The Performance of Vegetated Swales*. 9th International Conference on Urban Drainage, Portland, Oregon. 2002.

Fortier, S. and F.C. Scobey. "Permissible canal velocities." *Trans. ASCE*, Vol. 89, paper No. 1588, pp. 940-984. 1926.

Goldberg. *Dayton Avenue Swale Biofiltration Study*. *Seattle Engineering Department*. Seattle, WA. p36. 1993.

Harper, H. *Effects of Stormwater Management Systems on Groundwater Quality*. Final Report. Environmental Research and Design, Inc. Prepared for Florida Department of Environmental Regulation. p460. 1988.

Hayes, J.C., Barfield, B.J., and Barnhisel, R.I. *Performance of Grass Filters Under Laboratory and Field Conditions*. Transaction of the ASAE 27(5), 1321 – 1331. 1984.

Heaney, James P., Sample, David, and Field R. *Cost of Best Management Practices and Associated Land for Urban Stormwater Control*. Journal of Water Resources Planning and Management, Vol. 129, No.1. pp.55 – 68. 2003.

Horner, R.R. and Mar, B.W. *Guide for Water Quality in Assessment of Highway Operations and Maintenance.* Washington State Department of Transportation, Seattle, WA., Report UW-WA-RD-39-14. 1982.

Johnson, P.D., R. Pitt., S.D. Durrans., M. Urrutia., and S. Clark. *Innovative Metal Removal Technologies for Urban Stormwater*. Alexandria, VA: Water Environmental Research Foundation, WERF-97-IRM-2. 2003.

Kercher, W.C., J.C. Landon, and R. Massarelli. "Grassy swales prove cost-effective for water pollution control". *Public Works*. Vol. 16: 53 – 55. 1983.

Khan Z., Thrush C. Cohen P., Kulzer L., Franklin R., Field D., Koon J., and Horner R. Biofiltration Swale Performance: Recommendations and Design Considerations. Seattle Metro and Washington Ecology. Publication No. 657. Washington Dept. of Ecology p220. 1992.

Kirby, Jason. *Determination of Vegetal Retardance in Grass Swale.* M.S. thesis. University of Alabama. 2003.

Koon, J. *Evaluation of Water Quality Ponds and Swales in the Issaquah/East Lake Sammamish Basin*. King County Surface Water Management and Washington Department of Ecology. Seattle, WA. 75p. 1995.

McCuen, R.H. *Hydrologic Analysis and Design*, 2nd Edition. Prentice Hall. 1998.

Nara, Y. *Sediment Transport in Grass Swales*. Master of Science, Environmental Engineering thesis, Department of Civil and Environmental Engineering, The University of Alabama, Tuscaloosa, Alabama. 2005.

Neibling, W.H. and E.E. Alberts. *Composition and yield of soil particles transported through sod trips*. ASAE paper no. 79-2065. St.Joseph, MI: ASAE. 1979.

Pitt, R., S. Clark, and D. Lake, *Construction Site Erosion and Sediment Controls: Planning, Design, and Performance*, to be published by DEStech Publications, Lancaster, PA, in 2006.

Pope, Richard O., and Stoltenberg, David E. *A Review of Literature Related to Vegetative Filter Strip*. Water Quality TD441. P66. Iowa State University. 1991.

Pratap, Mukesh. *Designing and Operation of Upflow Filters for the Rapid and Effective Treatment of Stormwater at Critical Source Areas*. M.S. thesis. University of Alabama at Birmingham. 2003.

Raudkivi, A. J., and Tan, S. K. "Erosion of cohesive soils," *Journal of Hydraulic Research*, Vol 22, No. 4, pp 21X-233. 1984.

Ree, W.O. "Hydraulic Characteristics of Vegetation for Vegetated Waterways." *Agricultural Engineering*, April: 184-189. 1949.

Ree, W.O. and Palmer, V.J. *Flow in Channels Protected by Vegetative Linings*. Technical Bulletin No. 967, USDA: 1-22, 44-48. 1949.

Ree, W.O. *Friction Factors for Vegetation Covered, Light Slope Waterways*. Research Report No. 335, USDA: 1-34. 1960.

Richard L. Duble. n.d. "Turfgrass Management and Use," Texas Cooperative Extension. Texas A&M University; Available from http://aggie-horticulture.tamu.edu/plantanswers/turf/publications.html; internet; accessed 26 August 2005.

SCS (Soil Conservation Service). *Design of Open Channels*. TR-25. 1977.

SCS (Soil Conservation Service). *Handbook for Channel Design for Soil and Water Conservation*. SCS-TP-61, rev. 1954.

Seattle Metro and Washington Department of Ecology. *Biofiltration Swale Performance: Recommendations and Design Considerations*. Publication No. 657. Water pollution Control Department, Seattle Washington. 220p. 1992.

Southeastern Wisconsin Regional Planning Commission. *Cost of Urban Nonpoint Source Water Pollution Control Measure*. Waukesha, WI 1991.

Sprague, C.J. "Green Engineering; Design principles and applications using rolled erosion control products." *CE News On-Line*, March 1999, at: http://www.cenews.com/edenviroeng0399.html

Temple, D.M. "Flow Retardance of Submerged Grass Channel Linings." *Transactions of the ASAE*: 1300-1303. 1982.

Temple, D.M. *Erosionally Effective Soil Stress in Grass Lined Open Channels*. ASAE Paper No SWR84-102. 1984.

Tollner, J.C., Barfield, B.J., and Barnhisel, R.I. *Suspended Sediment Filtration Capacity of Simulated Vegetation.* Transaction of the ASAE 19(4), 678 – 682. 1976.

U.S. Army Corps of Engineers (COE). *Engineering and Design: Channel Stability Assessment for Flood Control Projects*. EM 1110-2-1418. U.S. Army Engineer Waterways Experiment Station, Vicksburg, MS. 1994.

U.S. Army Corps of Engineers (COE). *Hydraulic Design of Flood Control Channels*. EM 1110-2-1601. U.S. Army Engineer Waterways Experiment Station, Vicksburg, MS. undated.

U.S. Department of Agriculture (USDA). *Design of Open Channels*. Technical Release No. 25, Soil Conservation Service, Washington, DC. 1977.

USDA. *Alabama Handbook for Erosion Control, Sediment Control, and Stormwater Management on Construction Sites and Urban Areas*, prepared by the Alabama Soil and Water Conservation Committee, Montgomery, AL. 2003.

USDA. *Handbook of Channel Design for Soil and Water Conservation*. Technical Paper TP-61, USDA: 1-34. 1954.

USDA. *Stability Design of Grass-Lined Open Channels.* Agricultural Handbook 667. 1987:

Wang, T. *Transport Deposition and Control of Heavy Metals in Highway Runoff.* Seattle: U.S. Dept. of Transportation and Washington State Dept. of Transportation, WA-RD-39.10. 1980.

Wang, T.D., Spyridakis B., and Horner R. *Transport, Deposition, and Control of Heavy Metals in Highway Runoff*. FHWA-WA-RD-39-10. Dept. of Civil Engineering. University of Washington. Seattle, WA. 1981.
Williams, D. T., and Julien, P. Y. "Examination of stage-discharge relationships of compound/composite channels," *Proceedings of the International Conference on Channel Flow and Catchment Runoff.* B.C. Yen, ed., University of Virginia, Charlottesville, 22-26 May 1989, pp 478-488. 1989.
Woodward, S., and C.A. Rock. *Control of Residential Stormwater by Natural Buffer Strip*. Lake and Reservoir Management (Vol. 11, No. 1): 37 – 45. 1995.

Section 3: Appendices

This report section contains the detailed data obtained during the controlled indoor swale tests and the full-scale outdoor swale tests.

Appendix A: Raw Data – Initial Indoor Experiments

Table A1

Flow rate	Grass type	Slope	Sampling time	Swale length	Turbidity (NTU)	Total solids (mg/L)
15 GPM (High flow)	Centipede	5%	1 min	0 ft	60	251
15 GPM (High flow)	Centipede	5%	3 min	0 ft	159	252
15 GPM (High flow)	Centipede	5%	6 min	0 ft	28	280
15 GPM (High flow)	Centipede	5%	1 min	2 ft	107	288
15 GPM (High flow)	Centipede	5%	3 min	2 ft	137	288
15 GPM (High flow)	Centipede	5%	6 min	2 ft	162	284
15 GPM (High flow)	Centipede	5%	1 min	6 ft	141	275
15 GPM (High flow)	Centipede	5%	3 min	6 ft	111	260
15 GPM (High flow)	Centipede	5%	6 min	6 ft	124	268

Table A2

Flow rate	Grass type	Slope	Sampling time	Swale length	Turbidity (NTU)	Total solids (mg/L)
8 GPM (Low flow)	Centipede	5%	1 min	0 ft	112	270
8 GPM (Low flow)	Centipede	5%	5 min	0 ft	137	265
8 GPM (Low flow)	Centipede	5%	10 min	0 ft	148	232
8 GPM (Low flow)	Centipede	5%	1 min	2 ft	139	244
8 GPM (Low flow)	Centipede	5%	5 min	2 ft	120	281
8 GPM (Low flow)	Centipede	5%	10 min	2 ft	179	274
8 GPM (Low flow)	Centipede	5%	1 min	6 ft	48	200
8 GPM (Low flow)	Centipede	5%	5 min	6 ft	112	198
8 GPM (Low flow)	Centipede	5%	10 min	6 ft	99	182

Table A3

Flow rate	Grass type	Slope	Sampling time	Swale length	Turbidity (NTU)	Total solids (mg/L)
15 GPM (High flow)	Zoysia	5%	1 min	0 ft	143	258
15 GPM (High flow)	Zoysia	5%	3 min	0 ft	105	239
15 GPM (High flow)	Zoysia	5%	6 min	0 ft	86	211
15 GPM (High flow)	Zoysia	5%	1 min	2 ft	158	254
15 GPM (High flow)	Zoysia	5%	3 min	2 ft	146	195
15 GPM (High flow)	Zoysia	5%	6 min	2 ft	197	299
15 GPM (High flow)	Zoysia	5%	1 min	6 ft	174	254
15 GPM (High flow)	Zoysia	5%	3 min	6 ft	146	255
15 GPM (High flow)	Zoysia	5%	6 min	6 ft	181	280

Table A4

Flow rate	Grass type	Slope	Sampling time	Swale length	Turbidity (NTU)	Total solids (mg/L)
8 GPM (Low flow)	Zoysia	5%	1 min	0 ft	187	276
8 GPM (Low flow)	Zoysia	5%	5 min	0 ft	103	224
8 GPM (Low flow)	Zoysia	5%	10 min	0 ft	76	256
8 GPM (Low flow)	Zoysia	5%	1 min	2 ft	130	255
8 GPM (Low flow)	Zoysia	5%	5 min	2 ft	167	242
8 GPM (Low flow)	Zoysia	5%	10 min	2 ft	141	228
8 GPM (Low flow)	Zoysia	5%	1 min	6 ft	127	244
8 GPM (Low flow)	Zoysia	5%	5 min	6 ft	152	220
8 GPM (Low flow)	Zoysia	5%	10 min	6 ft	116	210

Table A5

Flow rate	Grass type	Slope	Sampling time	Swale length	Turbidity (NTU)	Total solids (mg/L)
15 GPM (High flow)	Bluegrass	5%	1 min	0 ft	81	286
15 GPM (High flow)	Bluegrass	5%	3 min	0 ft	149	265
15 GPM (High flow)	Bluegrass	5%	6 min	0 ft	81	280
15 GPM (High flow)	Bluegrass	5%	1 min	2 ft	26	273
15 GPM (High flow)	Bluegrass	5%	3 min	2 ft	109	275
15 GPM (High flow)	Bluegrass	5%	6 min	2 ft	124	245
15 GPM (High flow)	Bluegrass	5%	1 min	6 ft	119	240
15 GPM (High flow)	Bluegrass	5%	3 min	6 ft	95	236
15 GPM (High flow)	Bluegrass	5%	6 min	6 ft	126	242

Table A6

Flow rate	Grass type	Slope	Sampling time	Swale length	Turbidity (NTU)	Total solids (mg/L)
8 GPM (Low flow)	Bluegrass	5%	1 min	0 ft	140	241
8 GPM (Low flow)	Bluegrass	5%	5 min	0 ft	10	254
8 GPM (Low flow)	Bluegrass	5%	10 min	0 ft	151	249
8 GPM (Low flow)	Bluegrass	5%	1 min	2 ft	152	255
8 GPM (Low flow)	Bluegrass	5%	5 min	2 ft	20	236
8 GPM (Low flow)	Bluegrass	5%	10 min	2 ft	124	280
8 GPM (Low flow)	Bluegrass	5%	1 min	6 ft	46	247
8 GPM (Low flow)	Bluegrass	5%	5 min	6 ft	17	225
8 GPM (Low flow)	Bluegrass	5%	10 min	6 ft	64	244

Table A7

Flow rate	Grass type	Slope	Sampling time	Swale length	Turbidity (NTU)	Total solids (mg/L)
15 GPM (High flow)	Bluegrass	1%	1 min	0 ft	44	241
15 GPM (High flow)	Bluegrass	1%	3 min	0 ft	51	263
15 GPM (High flow)	Bluegrass	1%	6 min	0 ft	14	234
15 GPM (High flow)	Bluegrass	1%	1 min	2 ft	32	265
15 GPM (High flow)	Bluegrass	1%	3 min	2 ft	14	236
15 GPM (High flow)	Bluegrass	1%	6 min	2 ft	115	235
15 GPM (High flow)	Bluegrass	1%	1 min	6 ft	37	270
15 GPM (High flow)	Bluegrass	1%	3 min	6 ft	50	245
15 GPM (High flow)	Bluegrass	1%	6 min	6 ft	46	238

Table A8

Flow rate	Grass type	Slope	Sampling time	Swale length	Turbidity (NTU)	Total solids (mg/L)
8 GPM (Low flow)	Bluegrass	1%	1 min	0 ft	15	242
8 GPM (Low flow)	Bluegrass	1%	5 min	0 ft	141	246
8 GPM (Low flow)	Bluegrass	1%	10 min	0 ft	18	224
8 GPM (Low flow)	Bluegrass	1%	1 min	2 ft	51	231
8 GPM (Low flow)	Bluegrass	1%	5 min	2 ft	106	198
8 GPM (Low flow)	Bluegrass	1%	10 min	2 ft	32	199
8 GPM (Low flow)	Bluegrass	1%	1 min	6 ft	49	196
8 GPM (Low flow)	Bluegrass	1%	5 min	6 ft	46	194
8 GPM (Low flow)	Bluegrass	1%	10 min	6 ft	62	167

Table A9

Flow rate	Grass type	Slope	Sampling time	Swale length	Turbidity (NTU)	Total solids (mg/L)
15 GPM (High flow)	Zoysia	1%	1 min	0 ft	18	243
15 GPM (High flow)	Zoysia	1%	3 min	0 ft	99	243
15 GPM (High flow)	Zoysia	1%	6 min	0 ft	71	210
15 GPM (High flow)	Zoysia	1%	1 min	2 ft	35	257
15 GPM (High flow)	Zoysia	1%	3 min	2 ft	48	247
15 GPM (High flow)	Zoysia	1%	6 min	2 ft	21	219
15 GPM (High flow)	Zoysia	1%	1 min	6 ft	77	223
15 GPM (High flow)	Zoysia	1%	3 min	6 ft	47	213
15 GPM (High flow)	Zoysia	1%	6 min	6 ft	78	244

Table A10

Flow rate	Grass type	Slope	Sampling time	Swale length	Turbidity (NTU)	Total solids (mg/L)
8 GPM (Low flow)	Zoysia	1%	1 min	0 ft	63	248
8 GPM (Low flow)	Zoysia	1%	5 min	0 ft	100	222
8 GPM (Low flow)	Zoysia	1%	10 min	0 ft	20	217
8 GPM (Low flow)	Zoysia	1%	1 min	2 ft	52	230
8 GPM (Low flow)	Zoysia	1%	5 min	2 ft	76	252
8 GPM (Low flow)	Zoysia	1%	10 min	2 ft	98	247
8 GPM (Low flow)	Zoysia	1%	1 min	6 ft	84	179
8 GPM (Low flow)	Zoysia	1%	5 min	6 ft	84	170
8 GPM (Low flow)	Zoysia	1%	10 min	6 ft	133	164

Table A11

Flow rate	Grass type	Slope	Sampling time	Swale length	Turbidity (NTU)	Total solids (mg/L)
15 GPM (High flow)	Centipede	1%	1 min	0 ft	87	273
15 GPM (High flow)	Centipede	1%	3 min	0 ft	114	322
15 GPM (High flow)	Centipede	1%	6 min	0 ft	128	293
15 GPM (High flow)	Centipede	1%	1 min	2 ft	154	269
15 GPM (High flow)	Centipede	1%	3 min	2 ft	131	268
15 GPM (High flow)	Centipede	1%	6 min	2 ft	85	293
15 GPM (High flow)	Centipede	1%	1 min	6 ft	153	246
15 GPM (High flow)	Centipede	1%	3 min	6 ft	108	238
15 GPM (High flow)	Centipede	1%	6 min	6 ft	141	244

Table A12

Flow rate	Grass type	Slope	Sampling time	Swale length	Turbidity (NTU)	Total solids (mg/L)
8 GPM (Low flow)	Centipede	1%	1 min	0 ft	79	276
8 GPM (Low flow)	Centipede	1%	5 min	0 ft	41	283
8 GPM (Low flow)	Centipede	1%	10 min	0 ft	19	243
8 GPM (Low flow)	Centipede	1%	1 min	2 ft	42	279
8 GPM (Low flow)	Centipede	1%	5 min	2 ft	90	278
8 GPM (Low flow)	Centipede	1%	10 min	2 ft	23	278
8 GPM (Low flow)	Centipede	1%	1 min	6 ft	105	189
8 GPM (Low flow)	Centipede	1%	5 min	6 ft	63	190
8 GPM (Low flow)	Centipede	1%	10 min	6 ft	89	199

Appendix B: Raw Data – Second Indoor Experiments

Table B1

Grass type	Slope	Flow rate	Swale length	Duplicate	Total solids (mg/L)	Total solids (<106 µm) (mg/L)	TSS (mg/L)	TDS (mg/L)	Turbidity (NTU)
Synthetic turf	1%	10 GPM	0 ft	A	387.2	341.8	236.7	121.1	111.0
Synthetic turf	1%	10 GPM	0 ft	B	394.0	342.4	236.0	120.0	120.0
Synthetic turf	1%	10 GPM	2 ft	A	264.9	278.7	153.1	99.1	109.0
Synthetic turf	1%	10 GPM	2 ft	B	265.9	270.3	158.7	105.4	113.0
Synthetic turf	1%	10 GPM	3 ft	A	254.0	254.3	134.8	116.9	107.0
Synthetic turf	1%	10 GPM	3 ft	B	244.8	250.0	140.9	120.4	102.0
Synthetic turf	1%	10 GPM	6 ft	A	221.5	222.0	99.0	126.7	101.0
Synthetic turf	1%	10 GPM	6 ft	B	220.6	186.5	95.8	121.9	102.0

Table B2

Grass type	Slope	Flow rate	Swale length	Duplicate	Total solids (mg/L)	Total solids (<106 µm) (mg/L)	TSS (mg/L)	TDS (mg/L)	Turbidity (NTU)
Synthetic turf	1%	15 GPM	0 ft	A	504.1	430.0	389.6	130.2	75.6
Synthetic turf	1%	15 GPM	0 ft	B	509.4	435.2	374.5	126.5	62.6
Synthetic turf	1%	15 GPM	2 ft	A	340.2	342.9	227.5	129.4	58.0
Synthetic turf	1%	15 GPM	2 ft	B	345.6	333.7	225.8	124.7	61.0
Synthetic turf	1%	15 GPM	3 ft	A	300.9	301.8	171.0	125.0	46.4
Synthetic turf	1%	15 GPM	3 ft	B	292.8	298.1	168.6	127.6	39.9
Synthetic turf	1%	15 GPM	6 ft	A	284.7	286.0	157.4	125.7	53.9
Synthetic turf	1%	15 GPM	6 ft	B	281.0	278.1	155.9	117.6	50.7

Table B3

Grass type	Slope	Flow rate	Swale length	Duplicate	Total solids (mg/L)	Total solids (<106 µm) (mg/L)	TSS (mg/L)	TDS (mg/L)	Turbidity (NTU)
Synthetic turf	1%	20 GPM	0 ft	A	554.6	397.2	362.5	126.9	54.7
Synthetic turf	1%	20 GPM	0 ft	B	552.9	391.8	358.0	130.0	56.6
Synthetic turf	1%	20 GPM	2 ft	A	334.3	337.1	193.9	114.1	52.2
Synthetic turf	1%	20 GPM	2 ft	B	330.2	331.0	189.1	123.8	47.8
Synthetic turf	1%	20 GPM	3 ft	A	272.2	302.0	149.0	131.4	45.5
Synthetic turf	1%	20 GPM	3 ft	B	279.2	305.1	150.5	129.7	40.2
Synthetic turf	1%	20 GPM	6 ft	A	259.4	269.7	124.5	137.7	41.0
Synthetic turf	1%	20 GPM	6 ft	B	257.7	255.7	127.1	149.0	32.6

Table B4

Grass type	Slope	Flow rate	Swale length	Duplicate	Total solids (mg/L)	Total solids (<106 µm) (mg/L)	TSS (mg/L)	TDS (mg/L)	Turbidity (NTU)
Synthetic turf	3%	10 GPM	0 ft	A	360.6	391.5	239.4	133.3	40.5
Synthetic turf	3%	10 GPM	0 ft	B	389.8	363.3	242.9	134.9	39.0
Synthetic turf	3%	10 GPM	2 ft	A	268.9	278.8	163.3	110.2	45.2
Synthetic turf	3%	10 GPM	2 ft	B	282.0	282.2	166.4	135.4	45.3
Synthetic turf	3%	10 GPM	3 ft	A	256.8	0.0	137.5	125.0	41.6
Synthetic turf	3%	10 GPM	3 ft	B	263.4	290.5	148.1	120.8	37.3
Synthetic turf	3%	10 GPM	6 ft	A	218.5	227.1	100.0	117.8	32.4
Synthetic turf	3%	10 GPM	6 ft	B	224.7	225.6	98.8	120.5	36.4

Table B5

Grass type	Slope	Flow rate	Swale length	Duplicate	Total solids (mg/L)	Total solids (<106 µm) (mg/L)	TSS (mg/L)	TDS (mg/L)	Turbidity (NTU)
Synthetic turf	3%	15 GPM	0 ft	A	595.0	435.0	441.0	128.6	66.6
Synthetic turf	3%	15 GPM	0 ft	B	564.0	432.6	463.0	135.2	75.7
Synthetic turf	3%	15 GPM	2 ft	A	370.8	364.4	231.7	136.6	59.6
Synthetic turf	3%	15 GPM	2 ft	B	368.0	360.6	231.1	135.0	62.5
Synthetic turf	3%	15 GPM	3 ft	A	322.9	329.1	208.9	136.6	60.2
Synthetic turf	3%	15 GPM	3 ft	B	340.0	323.0	207.8	140.8	54.7
Synthetic turf	3%	15 GPM	6 ft	A	296.0	295.4	172.4	126.7	51.3
Synthetic turf	3%	15 GPM	6 ft	B	288.1	288.5	168.3	138.6	54.9

Table B6

Grass type	Slope	Flow rate	Swale length	Duplicate	Total solids (mg/L)	Total solids (<106 µm) (mg/L)	TSS (mg/L)	TDS (mg/L)	Turbidity (NTU)
Synthetic turf	3%	20 GPM	0 ft	A	594.3	441.5	472.3	116.8	59.1
Synthetic turf	3%	20 GPM	0 ft	B	601.0	435.7	469.7	118.2	61.2
Synthetic turf	3%	20 GPM	2 ft	A	344.3	348.9	228.6	114.8	54.6
Synthetic turf	3%	20 GPM	2 ft	B	349.0	345.5	180.0	114.0	57.9
Synthetic turf	3%	20 GPM	3 ft	A	334.3	325.7	211.1	131.3	54.8
Synthetic turf	3%	20 GPM	3 ft	B	340.4	333.0	206.1	131.2	50.4
Synthetic turf	3%	20 GPM	6 ft	A	263.9	269.1	132.4	122.2	35.6
Synthetic turf	3%	20 GPM	6 ft	B	257.6	273.2	138.9	117.6	37.7

Table B7

Grass type	Slope	Flow rate	Swale length	Duplicate	Total solids (mg/L)	Total solids (<106 µm) (mg/L)	TSS (mg/L)	TDS (mg/L)	Turbidity (NTU)
Synthetic turf	5%	10 GPM	0 ft	A	506.3	360.2	193.0	123.0	38.6
Synthetic turf	5%	10 GPM	0 ft	B	494.0	357.4	345.5	114.1	40.1
Synthetic turf	5%	10 GPM	2 ft	A	282.0	265.3	144.9	118.4	45.1
Synthetic turf	5%	10 GPM	2 ft	B	280.6	253.8	145.9	116.5	39.6
Synthetic turf	5%	10 GPM	3 ft	A	266.3	276.6	124.2	125.3	41.2
Synthetic turf	5%	10 GPM	3 ft	B	271.1	282.2	133.3	113.8	39.1
Synthetic turf	5%	10 GPM	6 ft	A	221.5	217.0	166.0	121.7	28.5
Synthetic turf	5%	10 GPM	6 ft	B	237.0	219.8	108.2	122.4	33.1

Table B8

Grass type	Slope	Flow rate	Swale length	Duplicate	Total solids (mg/L)	Total solids (<106 µm) (mg/L)	TSS (mg/L)	TDS (mg/L)	Turbidity (NTU)
Synthetic turf	5%	15 GPM	0 ft	A	566.0	428.6	440.6	125.5	68.2
Synthetic turf	5%	15 GPM	0 ft	B	566.3	436.5	452.9	114.7	67.6
Synthetic turf	5%	15 GPM	2 ft	A	359.0	340.4	229.1	136.9	50.2
Synthetic turf	5%	15 GPM	2 ft	B	351.8	351.0	218.3	129.8	54.1
Synthetic turf	5%	15 GPM	3 ft	A	332.3	314.0	202.8	143.5	63.1
Synthetic turf	5%	15 GPM	3 ft	B	312.6	326.5	196.2	137.1	59.5
Synthetic turf	5%	15 GPM	6 ft	A	288.5	290.0	157.7	120.0	52.3
Synthetic turf	5%	15 GPM	6 ft	B	287.6	287.0	161.9	120.0	43.6

Table B9

Grass type	Slope	Flow rate	Swale length	Duplicate	Total solids (mg/L)	Total solids (<106 µm) (mg/L)	TSS (mg/L)	TDS (mg/L)	Turbidity (NTU)
Synthetic turf	5%	20 GPM	0 ft	A	543.5	438.4	325.8	133.0	60.7
Synthetic turf	5%	20 GPM	0 ft	B	537.8	440.0	341.4	128.3	65.6
Synthetic turf	5%	20 GPM	2 ft	A	359.4	336.4	197.9	126.8	47.8
Synthetic turf	5%	20 GPM	2 ft	B	350.5	343.8	198.0	150.0	40.8
Synthetic turf	5%	20 GPM	3 ft	A	313.1	308.4	172.3	137.6	51.9
Synthetic turf	5%	20 GPM	3 ft	B	303.0	314.0	177.2	130.7	51.1
Synthetic turf	5%	20 GPM	6 ft	A	260.0	250.5	112.6	135.8	40.5
Synthetic turf	5%	20 GPM	6 ft	B	262.5	256.6	118.6	129.9	39.2

Table B10

Grass type	Slope	Flow rate	Swale length	Duplicate	Total solids (mg/L)	Total solids (<106 µm) (mg/L)	TSS (mg/L)	TDS (mg/L)	Turbidity (NTU)
Zoysia	1%	10 GPM	0 ft	A	432.1	353.9	251.0	126.0	40.1
Zoysia	1%	10 GPM	0 ft	B	424.5	354.1	229.7	122.8	45.0
Zoysia	1%	10 GPM	2 ft	A	236.1	215.6	89.5	135.8	24.0
Zoysia	1%	10 GPM	2 ft	B	231.8	220.6	91.9	135.4	26.0
Zoysia	1%	10 GPM	3 ft	A	192.7	180.6	63.0	126.9	18.0
Zoysia	1%	10 GPM	3 ft	B	183.7	184.2	54.4	127.2	18.1
Zoysia	1%	10 GPM	6 ft	A	175.5	155.6	30.2	135.4	14.8
Zoysia	1%	10 GPM	6 ft	B	173.7	153.6	34.3	140.4	15.9

Table B11

Grass type	Slope	Flow rate	Swale length	Duplicate	Total solids (mg/L)	Total solids (<106 µm) (mg/L)	TSS (mg/L)	TDS (mg/L)	Turbidity (NTU)
Zoysia	1%	15 GPM	0 ft	A	604.8	453.5	471.4	117.3	80.1
Zoysia	1%	15 GPM	0 ft	B	594.3	455.4	475.5	123.5	68.0
Zoysia	1%	15 GPM	2 ft	A	323.5	316.8	194.2	120.2	53.9
Zoysia	1%	15 GPM	2 ft	B	318.3	314.7	195.8	119.8	54.1
Zoysia	1%	15 GPM	3 ft	A	290.7	283.8	164.0	117.0	47.0
Zoysia	1%	15 GPM	3 ft	B	287.6	283.7	158.2	120.4	50.6
Zoysia	1%	15 GPM	6 ft	A	222.2	222.1	105.0	141.0	38.4
Zoysia	1%	15 GPM	6 ft	B	221.5	219.2	105.0	139.6	36.6

Table B12

Grass type	Slope	Flow rate	Swale length	Duplicate	Total solids (mg/L)	Total solids (<106 µm) (mg/L)	TSS (mg/L)	TDS (mg/L)	Turbidity (NTU)
Zoysia	1%	20 GPM	0 ft	A	619.6	444.9	486.9	142.4	64.7
Zoysia	1%	20 GPM	0 ft	B	627.1	453.7	474.3	135.8	63.0
Zoysia	1%	20 GPM	2 ft	A	296.0	311.9	172.2	113.4	44.4
Zoysia	1%	20 GPM	2 ft	B	293.9	302.9	169.1	111.7	50.3
Zoysia	1%	20 GPM	3 ft	A	280.9	288.8	153.1	120.4	40.2
Zoysia	1%	20 GPM	3 ft	B	278.4	281.4	152.0	112.0	45.4
Zoysia	1%	20 GPM	6 ft	A	228.2	238.1	94.8	135.4	32.6
Zoysia	1%	20 GPM	6 ft	B	224.5	244.2	94.9	137.4	28.8

Table B13

Grass type	Slope	Flow rate	Swale length	Duplicate	Total solids (mg/L)	Total solids (<106 µm) (mg/L)	TSS (mg/L)	TDS (mg/L)	Turbidity (NTU)
Zoysia	3%	10 GPM	0 ft	A	513.9	358.8	288.5	126.0	38.6
Zoysia	3%	10 GPM	0 ft	B	518.8	363.3	361.5	139.4	38.8
Zoysia	3%	10 GPM	2 ft	A	164.4	170.7	38.1	141.2	16.7
Zoysia	3%	10 GPM	2 ft	B	168.7	171.9	34.7	138.6	15.6
Zoysia	3%	10 GPM	3 ft	A	211.2	189.8	73.7	128.3	22.9
Zoysia	3%	10 GPM	3 ft	B	206.9	191.6	76.8	126.3	25.0
Zoysia	3%	10 GPM	6 ft	A	233.3	221.2	105.3	130.5	26.9
Zoysia	3%	10 GPM	6 ft	B	238.3	218.8	100.0	122.6	26.1

Table B14

Grass type	Slope	Flow rate	Swale length	Duplicate	Total solids (mg/L)	Total solids (<106 µm) (mg/L)	TSS (mg/L)	TDS (mg/L)	Turbidity (NTU)
Zoysia	3%	15 GPM	0 ft	A	695.0	518.8	587.5	129.2	74.6
Zoysia	3%	15 GPM	0 ft	B	727.3	520.6	586.0	129.0	74.3
Zoysia	3%	15 GPM	2 ft	A	373.2	357.0	256.1	140.8	59.6
Zoysia	3%	15 GPM	2 ft	B	376.9	366.7	251.0	130.4	74.8
Zoysia	3%	15 GPM	3 ft	A	297.9	311.0	179.4	137.1	56.7
Zoysia	3%	15 GPM	3 ft	B	312.5	303.1	185.4	131.1	54.9
Zoysia	3%	15 GPM	6 ft	A	243.6	240.6	119.2	130.8	40.1
Zoysia	3%	15 GPM	6 ft	B	235.0	235.2	113.5	126.0	47.8

Table B15

Grass type	Slope	Flow rate	Swale length	Duplicate	Total solids (mg/L)	Total solids (<106 µm) (mg/L)	TSS (mg/L)	TDS (mg/L)	Turbidity (NTU)
Zoysia	3%	20 GPM	0 ft	A	708.4	514.1	570.1	130.9	78.3
Zoysia	3%	20 GPM	0 ft	B	673.7	501.0	575.0	144.8	66.5
Zoysia	3%	20 GPM	2 ft	A	335.0	351.0	201.1	118.1	54.5
Zoysia	3%	20 GPM	2 ft	B	328.0	338.4	200.0	113.9	51.6
Zoysia	3%	20 GPM	3 ft	A	287.5	300.0	163.7	121.6	55.1
Zoysia	3%	20 GPM	3 ft	B	296.0	304.1	164.6	114.6	47.1
Zoysia	3%	20 GPM	6 ft	A	235.8	231.7	110.9	131.8	45.2
Zoysia	3%	20 GPM	6 ft	B	232.7	235.6	109.4	127.4	44.4

Table B16

Grass type	Slope	Flow rate	Swale length	Duplicate	Total solids (mg/L)	Total solids (<106 µm) (mg/L)	TSS (mg/L)	TDS (mg/L)	Turbidity (NTU)
Zoysia	5%	10 GPM	0 ft	A	421.4	321.4	231.8	122.4	39.0
Zoysia	5%	10 GPM	0 ft	B	423.5	330.2	261.0	123.0	44.8
Zoysia	5%	10 GPM	2 ft	A	333.3	281.0	174.0	137.5	34.1
Zoysia	5%	10 GPM	2 ft	B	337.7	276.2	176.5	141.8	33.4
Zoysia	5%	10 GPM	3 ft	A	276.0	236.2	110.4	155.7	39.5
Zoysia	5%	10 GPM	3 ft	B	266.7	235.8	111.2	144.9	29.9
Zoysia	5%	10 GPM	6 ft	A	204.0	186.9	54.2	151.0	22.9
Zoysia	5%	10 GPM	6 ft	B	210.3	194.6	54.1	152.0	22.0

Table B17

Grass type	Slope	Flow rate	Swale length	Duplicate	Total solids (mg/L)	Total solids (<106 µm) (mg/L)	TSS (mg/L)	TDS (mg/L)	Turbidity (NTU)
Zoysia	5%	15 GPM	0 ft	A	712.7	503.9	594.3	135.2	74.3
Zoysia	5%	15 GPM	0 ft	B	716.3	508.4	600.0	129.5	75.9
Zoysia	5%	15 GPM	2 ft	A	360.0	350.0	234.3	136.4	60.6
Zoysia	5%	15 GPM	2 ft	B	363.0	350.5	240.7	136.1	65.2
Zoysia	5%	15 GPM	3 ft	A	283.7	282.4	160.0	131.4	46.0
Zoysia	5%	15 GPM	3 ft	B	286.1	286.1	160.0	124.0	47.8
Zoysia	5%	15 GPM	6 ft	A	217.3	223.7	92.2	130.1	36.5
Zoysia	5%	15 GPM	6 ft	B	218.4	216.3	95.2	130.5	31.9

Table B18

Grass type	Slope	Flow rate	Swale length	Duplicate	Total solids (mg/L)	Total solids (<106 µm) (mg/L)	TSS (mg/L)	TDS (mg/L)	Turbidity (NTU)
Zoysia	5%	20 GPM	0 ft	A	953.5	524.0	608.1	129.3	77.1
Zoysia	5%	20 GPM	0 ft	B	940.0	531.1	793.8	133.0	64.0
Zoysia	5%	20 GPM	2 ft	A	409.9	368.1	287.0	141.7	57.1
Zoysia	5%	20 GPM	2 ft	B	419.2	371.8	286.3	140.0	50.3
Zoysia	5%	20 GPM	3 ft	A	306.1	293.7	162.2	133.7	51.0
Zoysia	5%	20 GPM	3 ft	B	298.0	292.0	155.2	126.0	44.4
Zoysia	5%	20 GPM	6 ft	A	238.0	232.3	101.0	125.0	43.7
Zoysia	5%	20 GPM	6 ft	B	233.0	240.0	103.0	132.3	38.1

Table B19

Grass type	Slope	Flow rate	Swale length	Duplicate	Total solids (mg/L)	Total solids (<106 µm) (mg/L)	TSS (mg/L)	TDS (mg/L)	Turbidity (NTU)
Bluegrass	1%	10 GPM	0 ft	A	455.3	347.7	267.3	124.5	32.5
Bluegrass	1%	10 GPM	0 ft	B	486.0	355.3	273.7	116.8	32.1
Bluegrass	1%	10 GPM	2 ft	A	191.7	192.9	68.0	122.0	18.0
Bluegrass	1%	10 GPM	2 ft	B	192.7	188.4	67.6	120.4	18.5
Bluegrass	1%	10 GPM	3 ft	A	207.1	202.9	64.3	137.8	22.6
Bluegrass	1%	10 GPM	3 ft	B	207.9	199.1	63.9	136.1	19.3
Bluegrass	1%	10 GPM	6 ft	A	177.3	172.3	39.4	136.5	15.4
Bluegrass	1%	10 GPM	6 ft	B	172.9	186.1	40.6	132.7	15.1

Table B20

Grass type	Slope	Flow rate	Swale length	Duplicate	Total solids (mg/L)	Total solids (<106 µm) (mg/L)	TSS (mg/L)	TDS (mg/L)	Turbidity (NTU)
Bluegrass	1%	15 GPM	0 ft	A	819.4	493.9	690.5	118.9	78.2
Bluegrass	1%	15 GPM	0 ft	B	823.2	495.0	696.1	123.3	78.7
Bluegrass	1%	15 GPM	2 ft	A	384.6	375.2	263.5	129.8	61.1
Bluegrass	1%	15 GPM	2 ft	B	390.0	371.8	265.3	126.3	66.6
Bluegrass	1%	15 GPM	3 ft	A	350.0	334.7	225.5	132.7	68.8
Bluegrass	1%	15 GPM	3 ft	B	346.2	333.7	227.2	130.1	63.5
Bluegrass	1%	15 GPM	6 ft	A	263.9	263.4	136.7	133.7	54.8
Bluegrass	1%	15 GPM	6 ft	B	261.8	262.1	133.0	132.1	48.1

Table B21

Grass type	Slope	Flow rate	Swale length	Duplicate	Total solids (mg/L)	Total solids (<106 µm) (mg/L)	TSS (mg/L)	TDS (mg/L)	Turbidity (NTU)
Bluegrass	1%	20 GPM	0 ft	A	910.8	485.0	776.2	137.6	62.4
Bluegrass	1%	20 GPM	0 ft	B	894.3	502.1	771.4	131.4	57.6
Bluegrass	1%	20 GPM	2 ft	A	376.4	370.6	266.0	129.1	44.2
Bluegrass	1%	20 GPM	2 ft	B	374.3	362.9	245.2	126.0	48.5
Bluegrass	1%	20 GPM	3 ft	A	329.5	331.3	200.0	142.2	53.3
Bluegrass	1%	20 GPM	3 ft	B	318.6	331.0	198.9	138.9	45.4
Bluegrass	1%	20 GPM	6 ft	A	275.3	268.9	142.3	129.8	41.9
Bluegrass	1%	20 GPM	6 ft	B	272.9	270.0	144.7	131.1	42.4

Table B22

Grass type	Slope	Flow rate	Swale length	Duplicate	Total solids (mg/L)	Total solids (<106 µm) (mg/L)	TSS (mg/L)	TDS (mg/L)	Turbidity (NTU)
Bluegrass	3%	10 GPM	0 ft	A	598.0	376.0	330.9	125.8	38.7
Bluegrass	3%	10 GPM	0 ft	B	600.0	366.7	336.3	117.6	33.6
Bluegrass	3%	10 GPM	2 ft	A	225.7	226.3	172.9	125.0	27.0
Bluegrass	3%	10 GPM	2 ft	B	230.8	225.8	89.7	140.2	26.9
Bluegrass	3%	10 GPM	3 ft	A	194.1	202.0	77.8	131.5	24.6
Bluegrass	3%	10 GPM	3 ft	B	199.1	195.9	76.0	123.0	23.7
Bluegrass	3%	10 GPM	6 ft	A	162.0	173.7	38.5	124.0	16.4
Bluegrass	3%	10 GPM	6 ft	B	161.0	165.7	38.9	126.9	16.4

Table B23

Grass type	Slope	Flow rate	Swale length	Duplicate	Total solids (mg/L)	Total solids (<106 µm) (mg/L)	TSS (mg/L)	TDS (mg/L)	Turbidity (NTU)
Bluegrass	3%	15 GPM	0 ft	A	867.7	509.0	718.6	130.4	76.8
Bluegrass	3%	15 GPM	0 ft	B	847.6	503.2	704.6	133.0	74.8
Bluegrass	3%	15 GPM	2 ft	A	488.6	462.2	362.4	131.7	72.9
Bluegrass	3%	15 GPM	2 ft	B	479.6	467.3	358.8	135.3	71.5
Bluegrass	3%	15 GPM	3 ft	A	378.1	364.0	255.8	129.8	66.8
Bluegrass	3%	15 GPM	3 ft	B	374.5	368.7	252.4	130.1	64.3
Bluegrass	3%	15 GPM	6 ft	A	275.8	279.4	151.0	128.4	47.9
Bluegrass	3%	15 GPM	6 ft	B	278.4	272.4	149.5	127.8	46.5

Table B24

Grass type	Slope	Flow rate	Swale length	Duplicate	Total solids (mg/L)	Total solids (<106 µm) (mg/L)	TSS (mg/L)	TDS (mg/L)	Turbidity (NTU)
Bluegrass	3%	20 GPM	0 ft	A	1142.7	483.3	1021.6	122.5	56.2
Bluegrass	3%	20 GPM	0 ft	B	1076.6	490.3	911.5	129.2	56.5
Bluegrass	3%	20 GPM	2 ft	A	432.1	399.1	307.9	132.7	55.5
Bluegrass	3%	20 GPM	2 ft	B	427.7	389.6	301.0	133.0	55.7
Bluegrass	3%	20 GPM	3 ft	A	351.0	350.0	257.0	131.0	49.2
Bluegrass	3%	20 GPM	3 ft	B	345.4	350.5	230.8	128.0	48.1
Bluegrass	3%	20 GPM	6 ft	A	253.0	263.5	129.0	134.0	35.6
Bluegrass	3%	20 GPM	6 ft	B	251.6	260.2	131.5	130.6	38.3

Table B25

Grass type	Slope	Flow rate	Swale length	Duplicate	Total solids (mg/L)	Total solids (<106 µm) (mg/L)	TSS (mg/L)	TDS (mg/L)	Turbidity (NTU)
Bluegrass	5%	10 GPM	0 ft	A	544.0	352.3	263.6	133.3	35.9
Bluegrass	5%	10 GPM	0 ft	B	538.6	344.2	320.8	126.7	35.6
Bluegrass	5%	10 GPM	2 ft	A	250.5	239.8	114.0	129.0	34.3
Bluegrass	5%	10 GPM	2 ft	B	252.9	235.2	117.1	125.7	37.5
Bluegrass	5%	10 GPM	3 ft	A	185.9	213.7	78.3	122.6	31.1
Bluegrass	5%	10 GPM	3 ft	B	201.0	209.0	83.8	116.2	26.3
Bluegrass	5%	10 GPM	6 ft	A	189.7	175.3	41.6	129.7	15.4
Bluegrass	5%	10 GPM	6 ft	B	191.9	171.0	45.5	124.2	14.8

Table B26

Grass type	Slope	Flow rate	Swale length	Duplicate	Total solids (mg/L)	Total solids (<106 µm) (mg/L)	TSS (mg/L)	TDS (mg/L)	Turbidity (NTU)
Bluegrass	5%	15 GPM	0 ft	A	978.4	507.1	872.6	140.0	76.8
Bluegrass	5%	15 GPM	0 ft	B	988.0	521.2	857.4	133.3	81.8
Bluegrass	5%	15 GPM	2 ft	A	447.1	444.4	329.2	128.1	74.3
Bluegrass	5%	15 GPM	2 ft	B	455.4	400.0	324.0	139.6	75.1
Bluegrass	5%	15 GPM	3 ft	A	441.2	426.7	314.4	134.0	64.9
Bluegrass	5%	15 GPM	3 ft	B	444.0	425.7	303.9	134.0	66.7
Bluegrass	5%	15 GPM	6 ft	A	288.1	281.3	160.4	128.7	49.5
Bluegrass	5%	15 GPM	6 ft	B	285.7	277.2	152.1	136.5	55.0

Table B27

Grass type	Slope	Flow rate	Swale length	Duplicate	Total solids (mg/L)	Total solids (<106 µm) (mg/L)	TSS (mg/L)	TDS (mg/L)	Turbidity (NTU)
Bluegrass	5%	20 GPM	0 ft	A	1100.0	501.0	974.7	118.9	72.9
Bluegrass	5%	20 GPM	0 ft	B	1109.4	500.9	1009.3	119.4	71.2
Bluegrass	5%	20 GPM	2 ft	A	388.0	376.3	265.4	136.5	60.7
Bluegrass	5%	20 GPM	2 ft	B	384.8	371.1	263.0	129.0	57.5
Bluegrass	5%	20 GPM	3 ft	A	337.9	356.9	193.6	138.3	55.8
Bluegrass	5%	20 GPM	3 ft	B	340.7	365.7	191.9	133.3	54.1
Bluegrass	5%	20 GPM	6 ft	A	256.1	271.1	114.6	137.5	40.7
Bluegrass	5%	20 GPM	6 ft	B	259.6	272.0	109.4	137.5	41.5

Appendix C: Raw Data – Outdoor Swale Observations

Table C1

Sampling date	Swale length (ft)	Total solids (mg/L)	Total solids (< 106 µm) (mg/L)	TSS (mg/L)	TDS (mg/L)	Turbidity (NTU)
8/22/2004	0	19	N/A	4	16	3
8/22/2004	25	22	N/A	5	22	5
8/22/2004	75	21	N/A	3	20	2

Note: N/A = not available

Table C2

Sampling date	Swale length (ft)	Total solids (mg/L)	Total solids (< 106 µm) (mg/L)	TSS (mg/L)	TDS (mg/L)	Turbidity (NTU)
10/9/2004	0	133	136	30	109	38
10/9/2004	75	149	149	31	134	12
10/9/2004	102	147	151	25	133	9

Table C3

Sampling date	Swale length (ft)	Total solids (mg/L)	Total solids (< 106 µm) (mg/L)	TSS (mg/L)	TDS (mg/L)	Turbidity (NTU)
10/10/2004	0	135	138	37	113	31
10/10/2004	101.9	159	151	11	145	9

Table C4

Sampling date	Swale length (ft)	Total solids (mg/L)	Total solids (< 106 µm) (mg/L)	TSS (mg/L)	TDS (mg/L)	Turbidity (NTU)
10/11/2004	0	149	141	102	62	65
10/11/2004	2	125	117	84	45	60
10/11/2004	3	113	111	63	45	48
10/11/2004	6	70	72	35	50	32
10/11/2004	25	76	74	30	54	23
10/11/2004	75	92	86	20	71	27
10/11/2004	116	75	92	10	76	13

Table C5

Sampling date	Swale length (ft)	Total solids (mg/L)	Total solids (< 106 µm) (mg/L)	TSS (mg/L)	TDS (mg/L)	Turbidity (NTU)
10/19/2004	25	119	113	51	73	23
10/19/2004	75	58	59	12	43	17
10/19/2004	116	41	41	6	37	9

Table C6

Sampling date	Swale length (ft)	Total solids (mg/L)	Total solids (< 106 µm) (mg/L)	TSS (mg/L)	TDS (mg/L)	Turbidity (NTU)
10/23/2004	0	144	125	55	74	34
10/23/2004	2	148	137	85	58	40
10/23/2004	3	183	167	105	71	52
10/23/2004	6	123	115	58	65	33
10/23/2004	25	121	120	34	81	26
10/23/2004	75	103	88	29	71	20
10/23/2004	116	120	111	19	97	12

Table C7

Sampling date	Swale length (ft)	Total solids (mg/L)	Total solids (< 106 µm) (mg/L)	TSS (mg/L)	TDS (mg/L)	Turbidity (NTU)
11/1/2004	0	246	247	153	101	137
11/1/2004	2	210	206	116	111	151
11/1/2004	3	218	217	127	104	143
11/1/2004	6	213	200	110	93	131
11/1/2004	25	160	147	42	110	91
11/1/2004	75	145	134	38	113	62
11/1/2004	116	129	126	25	110	12

Table C8

Sampling date	Swale length (ft)	Total solids (mg/L)	Total solids (< 106 µm) (mg/L)	TSS (mg/L)	TDS (mg/L)	Turbidity (NTU)
11/11/2004	0	103	70	31	63	21
11/11/2004	2	87	65	36	48	21
11/11/2004	3	83	53	39	35	20
11/11/2004	6	65	51	65	31	19
11/11/2004	25	71	74	30	42	22
11/11/2004	75	54	65	19	40	20
11/11/2004	116	85	74	13	64	8

Table C9

Sampling date	Swale length (ft)	Total solids (mg/L)	Total solids (< 106 µm) (mg/L)	TSS (mg/L)	TDS (mg/L)	Turbidity (NTU)
11/21/2004	0	29	36	18.8	24.8	38
11/21/2004	2	62	53	42.6	29.7	24
11/21/2004	3	139	114	108.0	27.0	18
11/21/2004	6	104	87	67.7	29.3	11
11/21/2004	25	53	44	20.6	32.4	26
11/21/2004	75	48	46	23.2	30.3	16
11/21/2004	116	34	27	0.0	35.0	10

Table C10

Sampling date	Swale length (ft)	Total solids (mg/L)	Total solids (< 106 µm) (mg/L)	TSS (mg/L)	TDS (mg/L)	Turbidity (NTU)
11/22/2004	0	14	11	6.0	13.0	7
11/22/2004	2	16	14	8.1	13.1	9
11/22/2004	3	24	25	3.1	15.3	9
11/22/2004	6	19	18	8.1	15.2	9
11/22/2004	25	23	27	9.0	21.0	12
11/22/2004	75	15	20	7.1	6.1	12
11/22/2004	116	15	14	-4.0	5.0	5

Table C11

Sampling date	Swale length (ft)	Total solids (mg/L)	Total solids (< 106 µm) (mg/L)	TSS (mg/L)	TDS (mg/L)	Turbidity (NTU)
12/6/2004	0	139	116	120.0	4.0	18
12/6/2004	2	68	71	54.5	10.1	22
12/6/2004	3	46	51	48.0	10.0	46
12/6/2004	6	17	14	12.7	-3.9	34
12/6/2004	25	50	50	27.7	29.7	10
12/6/2004	75	21	31	12.1	17.2	13
12/6/2004	116	11	29	5	16	7

Table C12

Sampling date	Swale length (ft)	Total solids (mg/L)	Total solids (< 106 µm) (mg/L)	TSS (mg/L)	TDS (mg/L)	Turbidity (NTU)
12/8/2004	0	235	222	157	69	88
12/8/2004	2	150	142	105	40	61
12/8/2004	3	122	119	83	32	39
12/8/2004	6	103	95	61	26	31
12/8/2004	25	85	86	39	28	34
12/8/2004	75	141	131	90	33	71
12/8/2004	116	110	99	69	34	63

Appendix D: Initial Experiments – Box-and-Whisker Plots of Total Solids and Turbidity by Experimental Variables

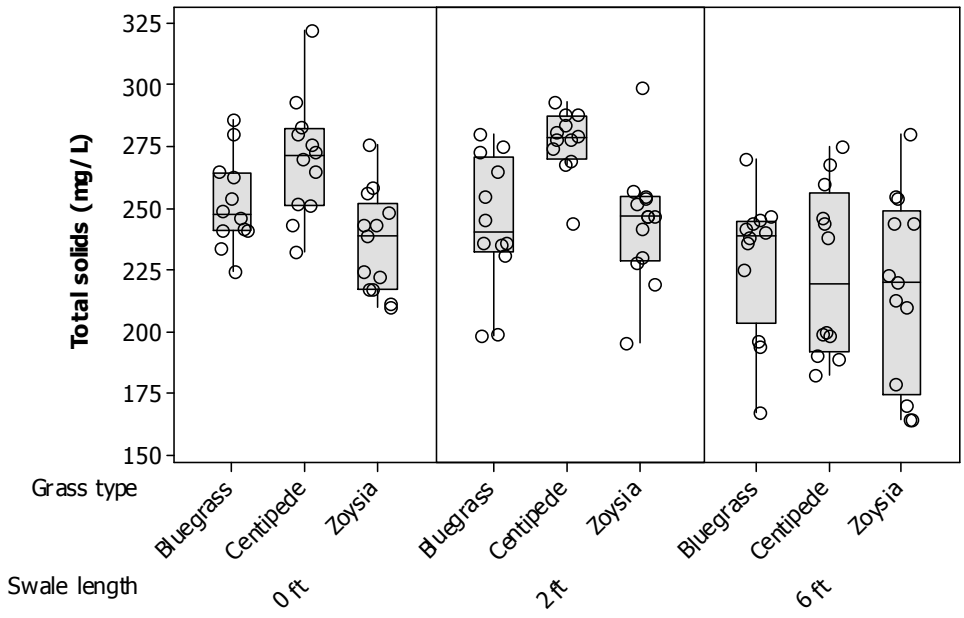

Figure D1

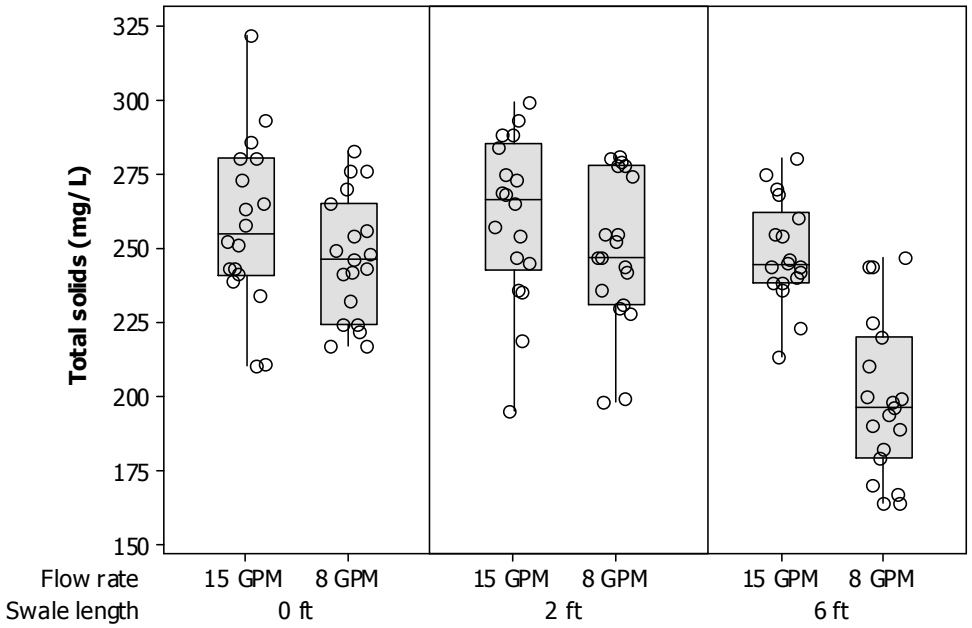

Figure D2

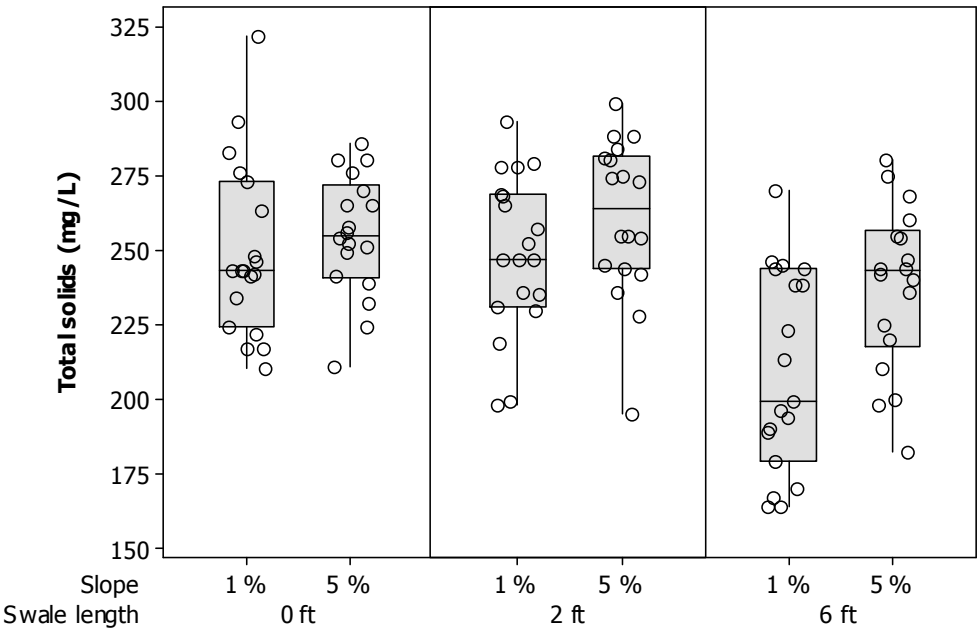

Figure D3

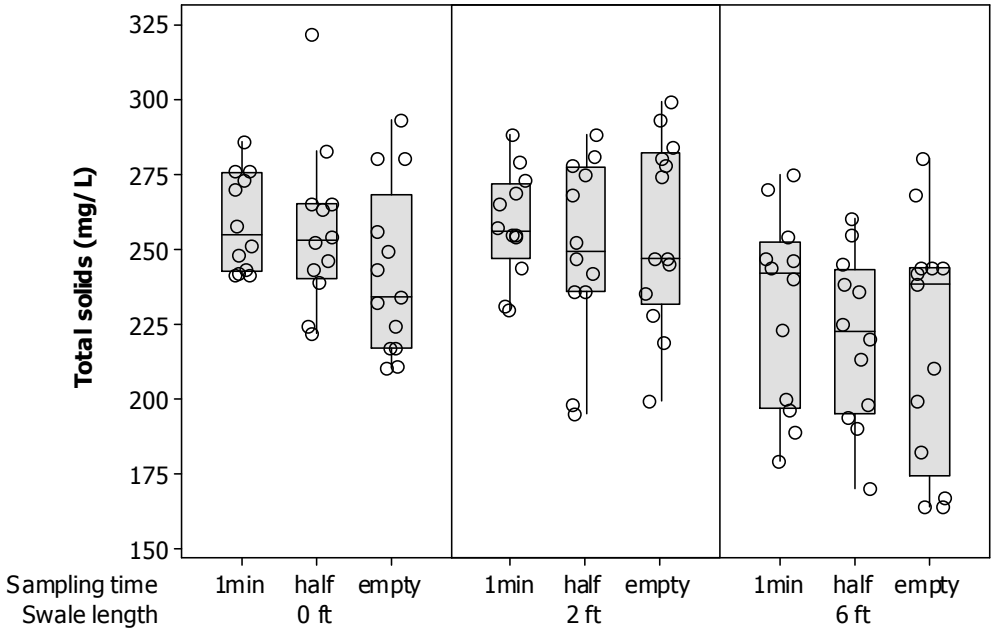

Figure D4

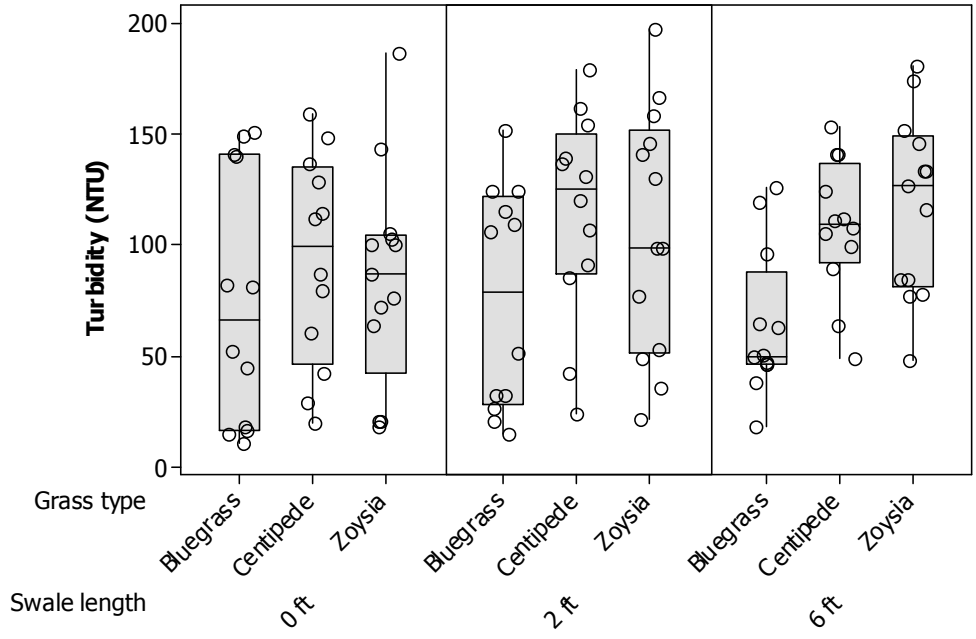

Figure D5

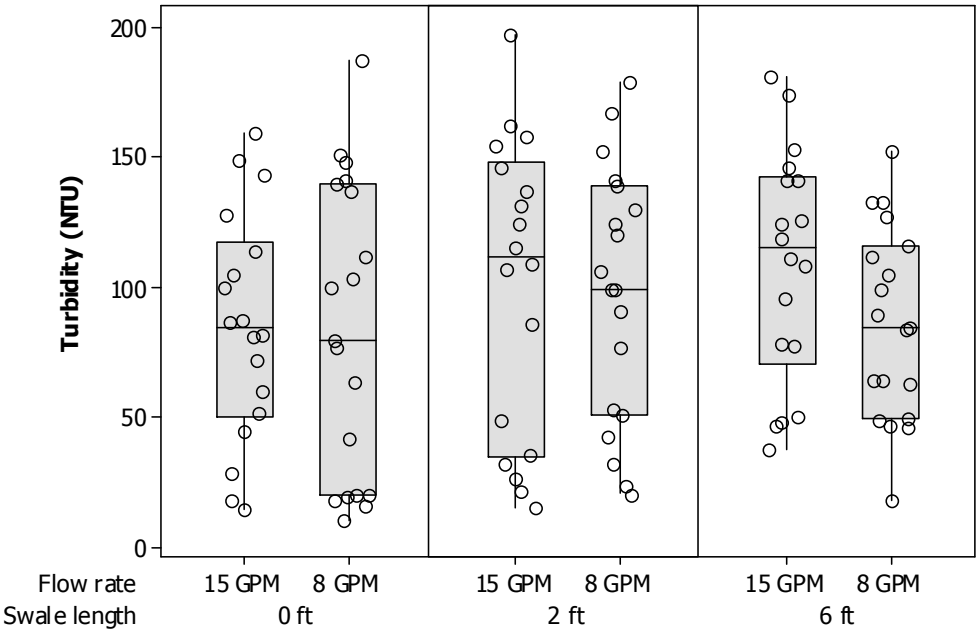

Figure D6

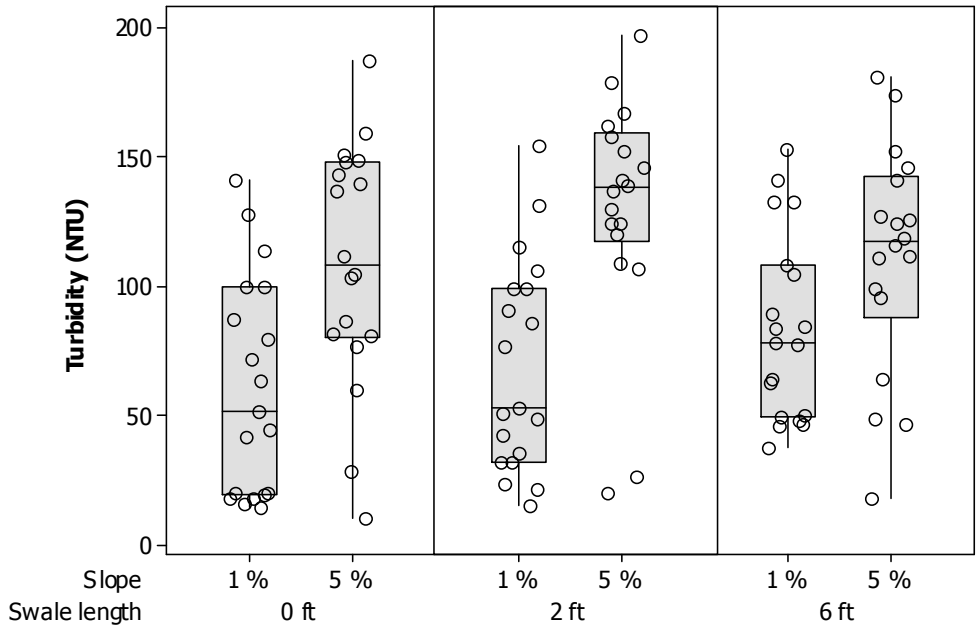

Figure D7

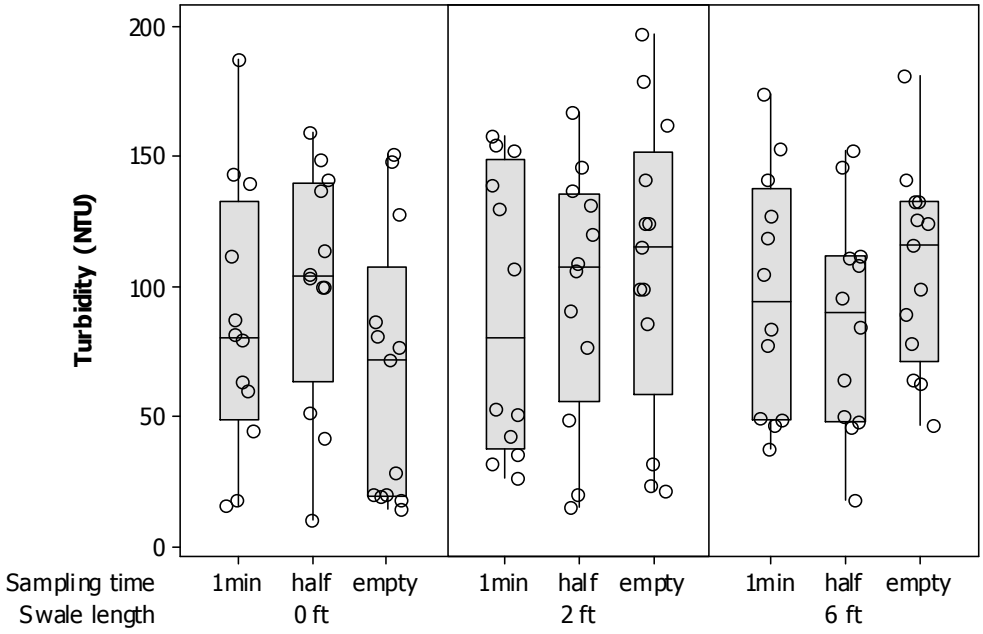
Turbidity (NTU)
200
150
100
50
0
Sampling time
Swale length
1min
half
empty
0 ft
2 ft
6 ft

Figure D8

Appendix E: Initial Experiments – Line Plots for Total Solids and Turbidity

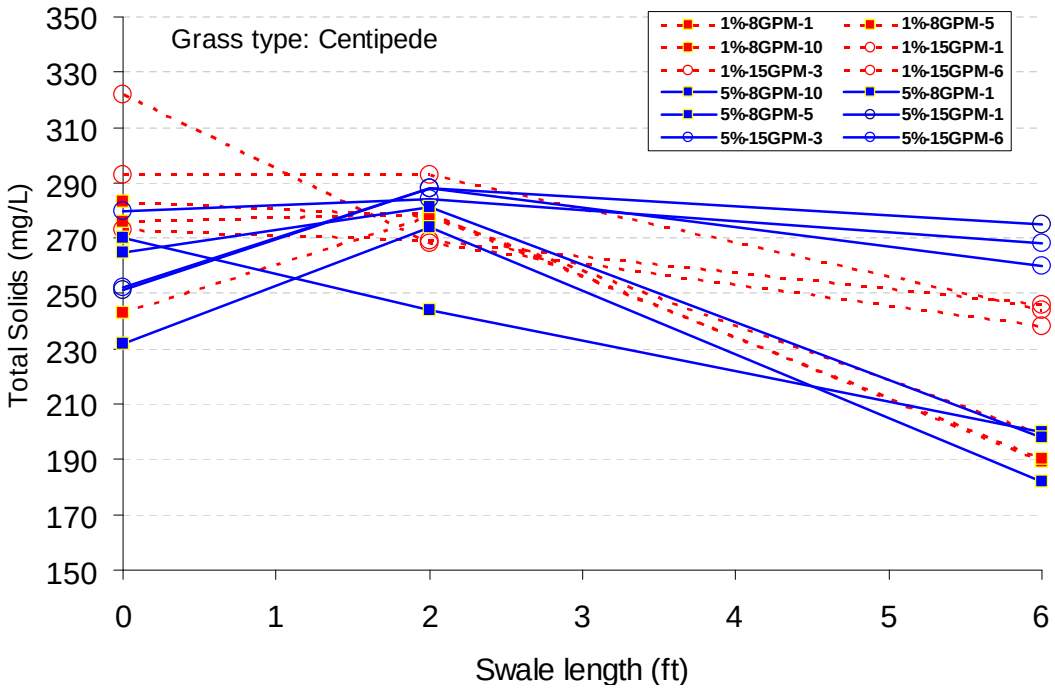

Figure E1

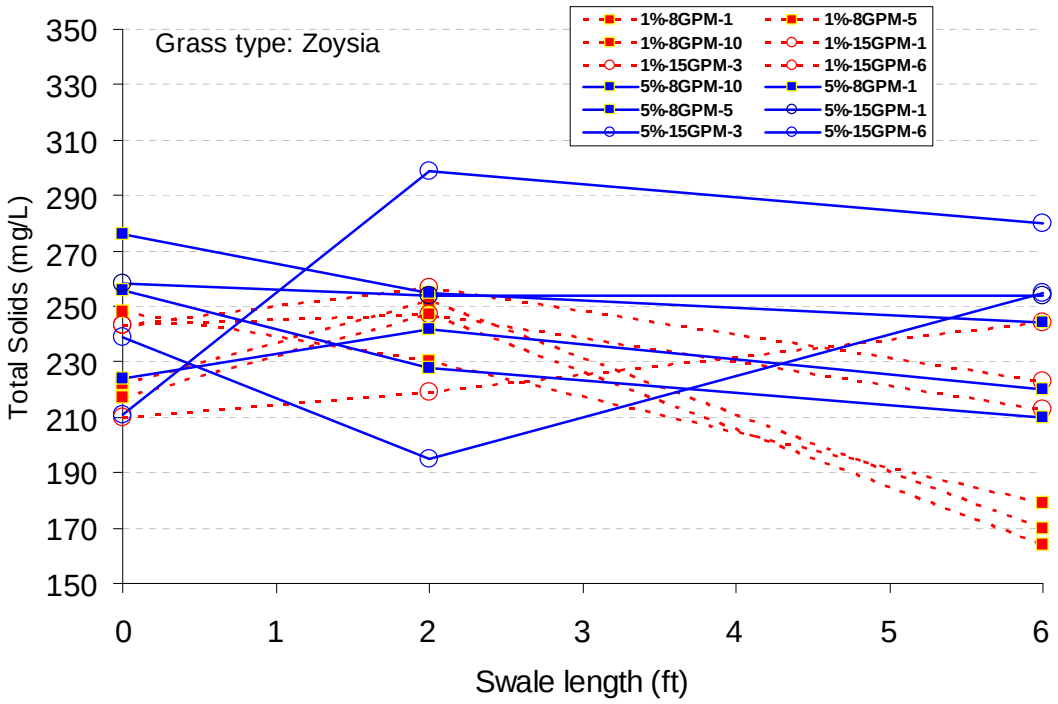

Figure E2

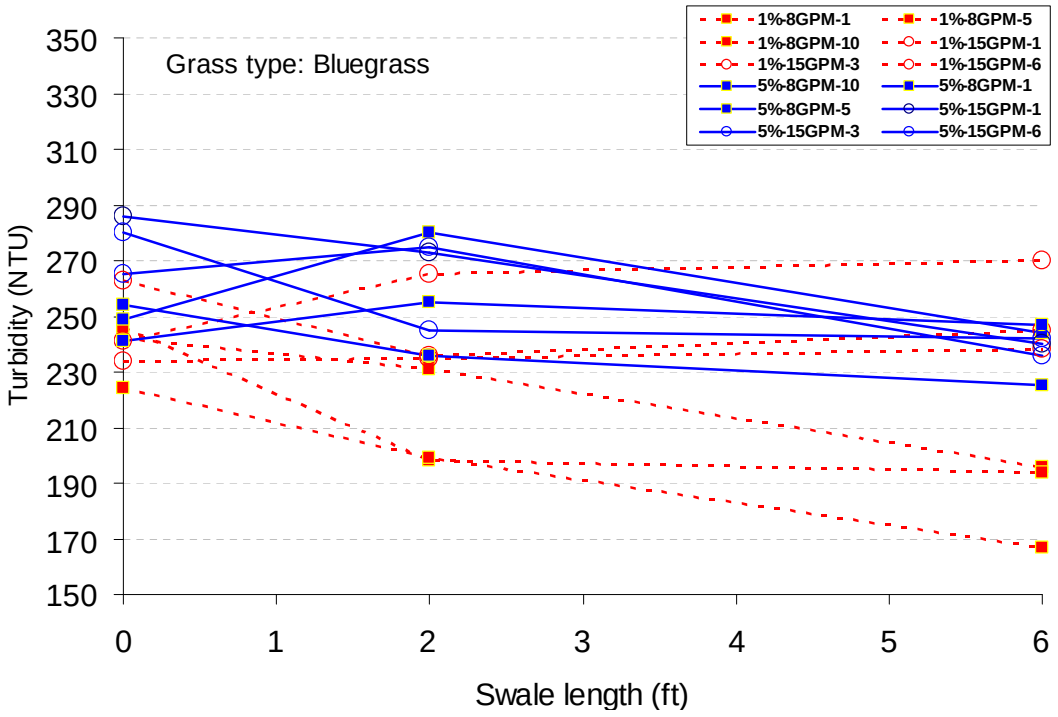

Figure E3

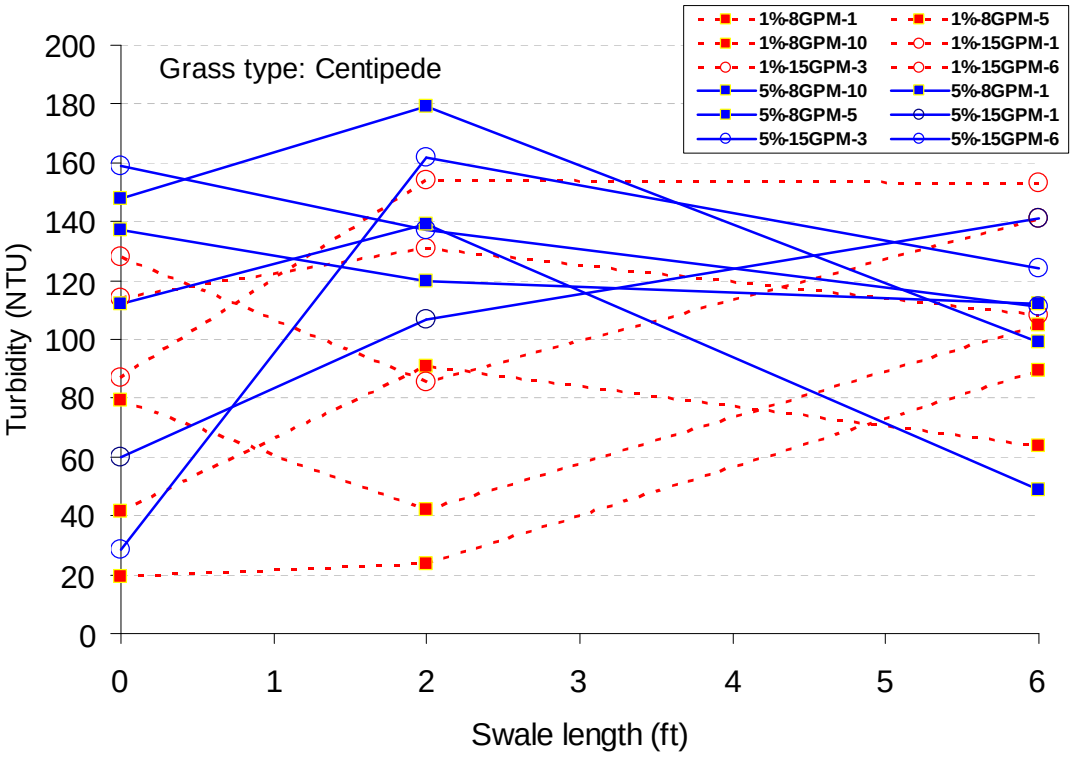

Figure E4

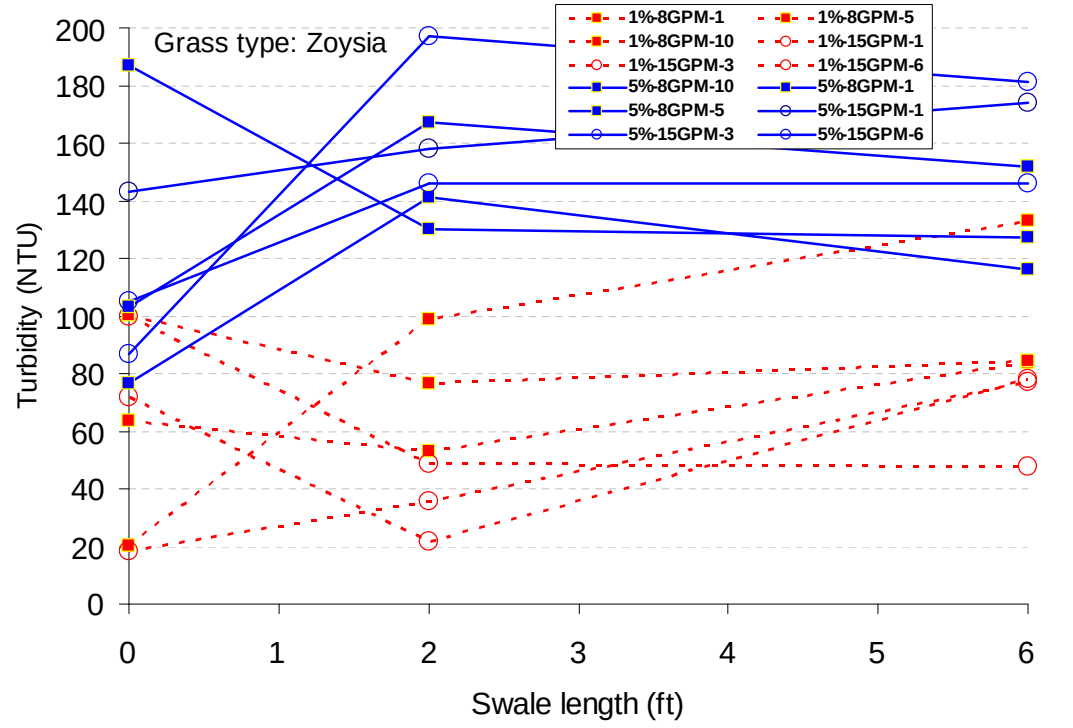

Figure E5

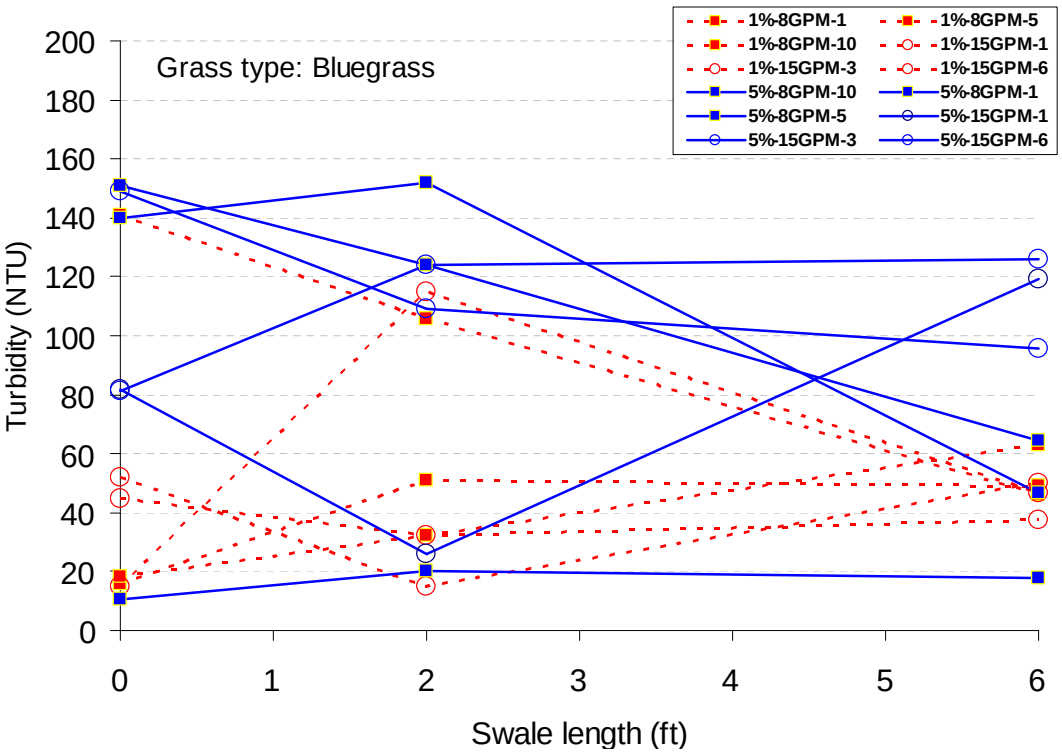
Grass type: Bluegrass
1%-8GPM-1
1%-8GPM-5
1%-8GPM-10
1%-15GPM-1
1%-15GPM-3
1%-15GPM-6
5%-8GPM-10
5%-8GPM-1
5%-8GPM-5
5%-15GPM-1
5%-15GPM-3
5%-15GPM-6
Turbidity (NTU)
200
180
160
140
120
100
80
60
40
20
0
0
1
2
3
4
5
6
Swale length (ft)

Figure E6

Appendix F: Initial Experiments – Particle Size Distributions (Coulter Counter Beckman® Multi-Sizer III) for each Experimental Condition

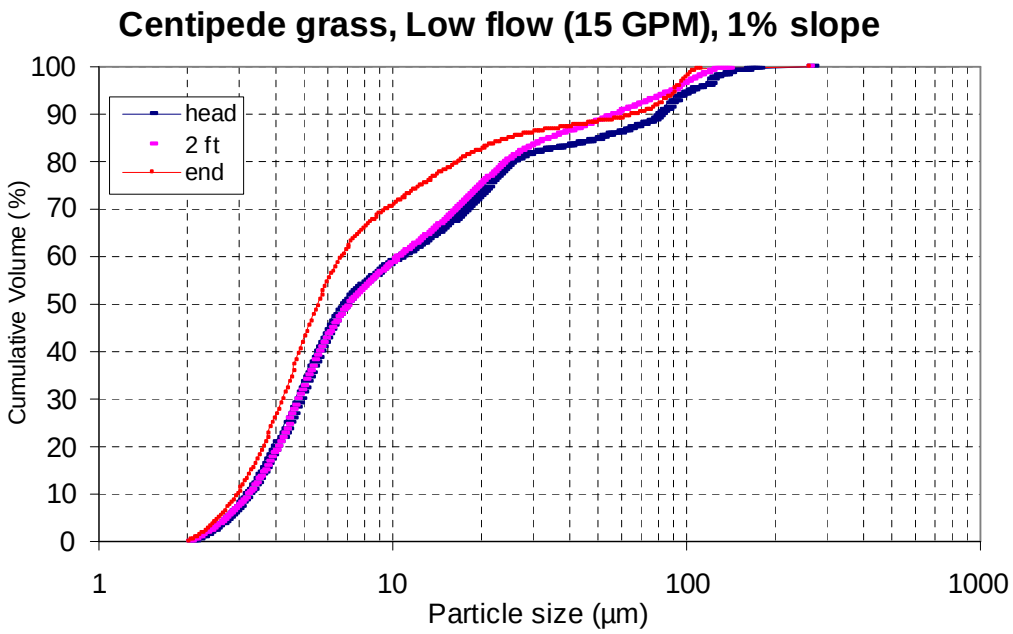

Figure F1

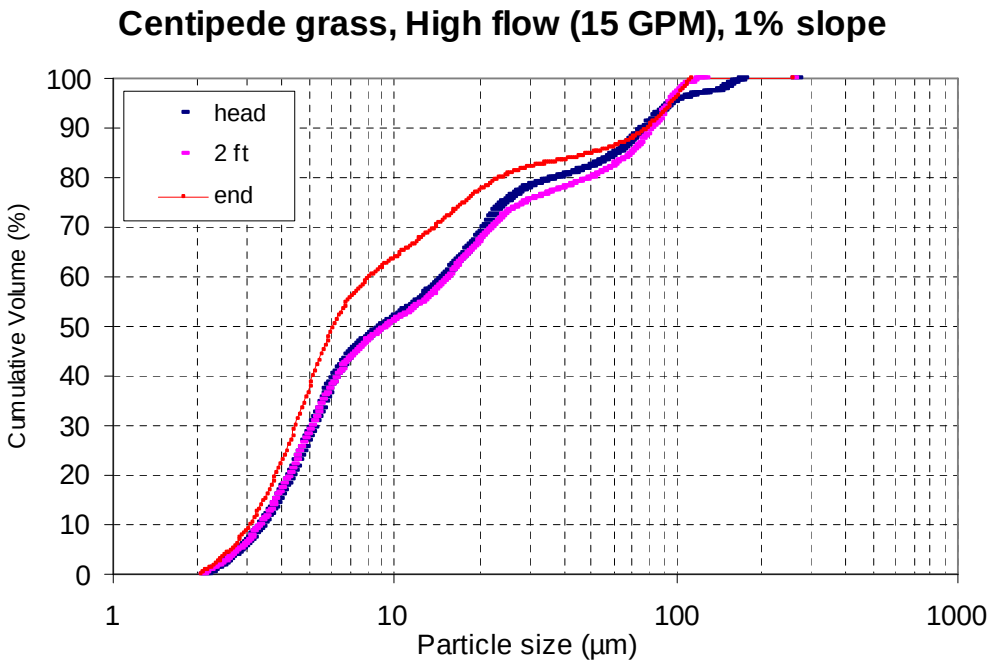

Figure F2

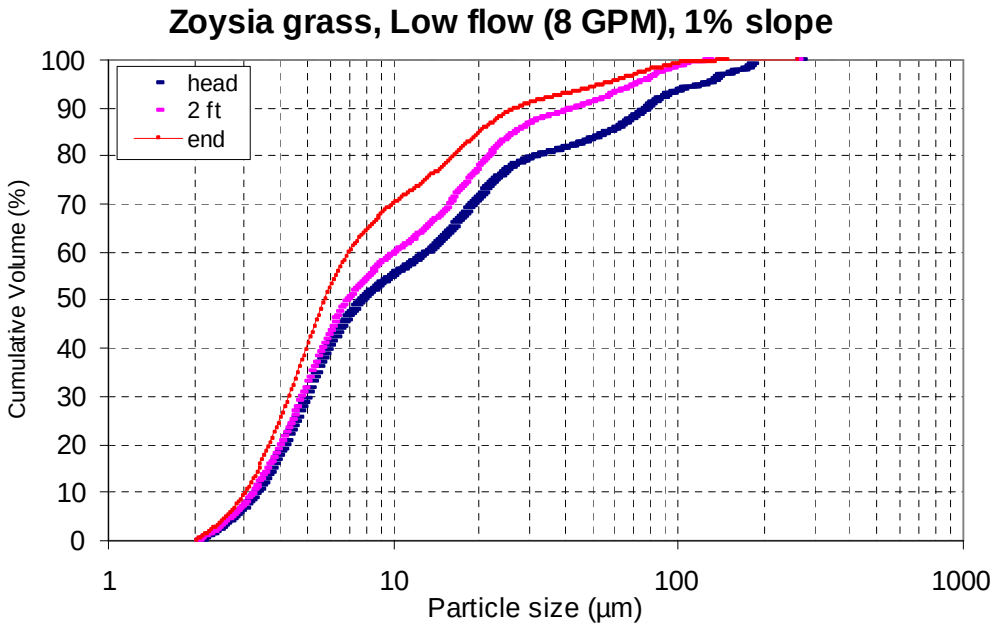

Figure F3

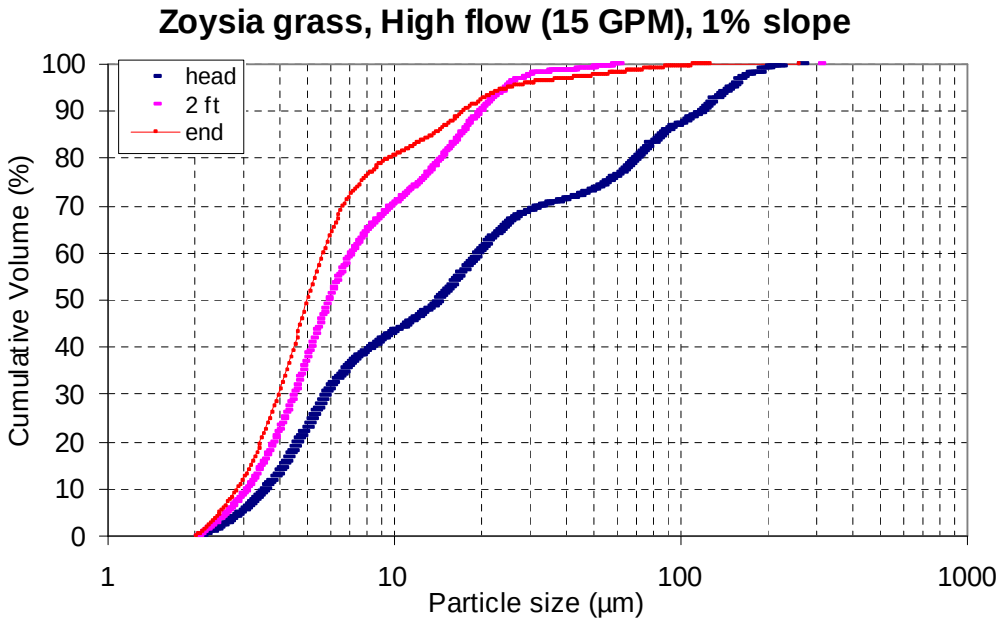

Figure F4

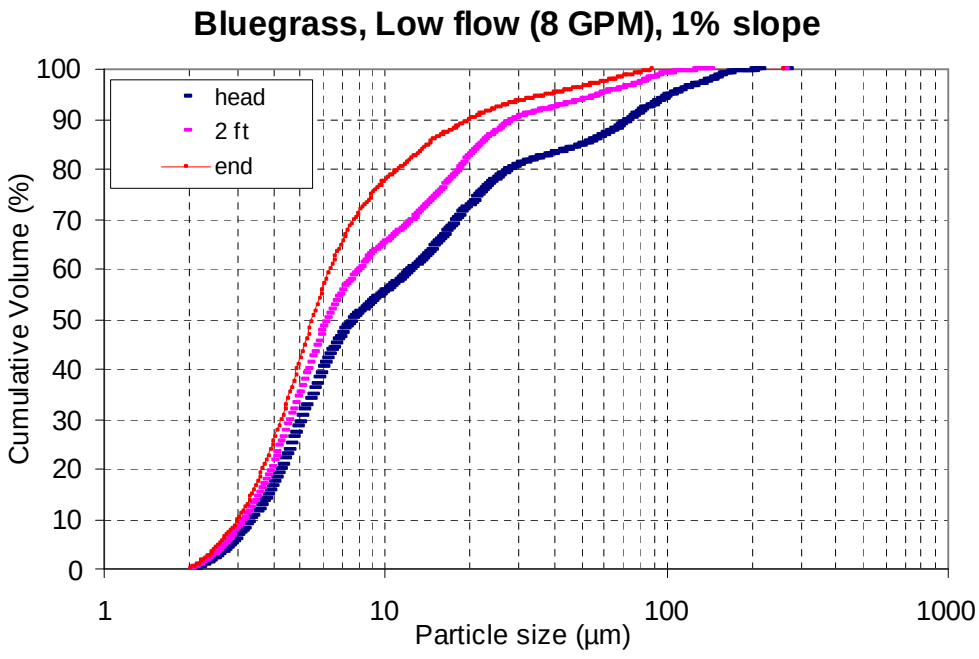

Figure F5

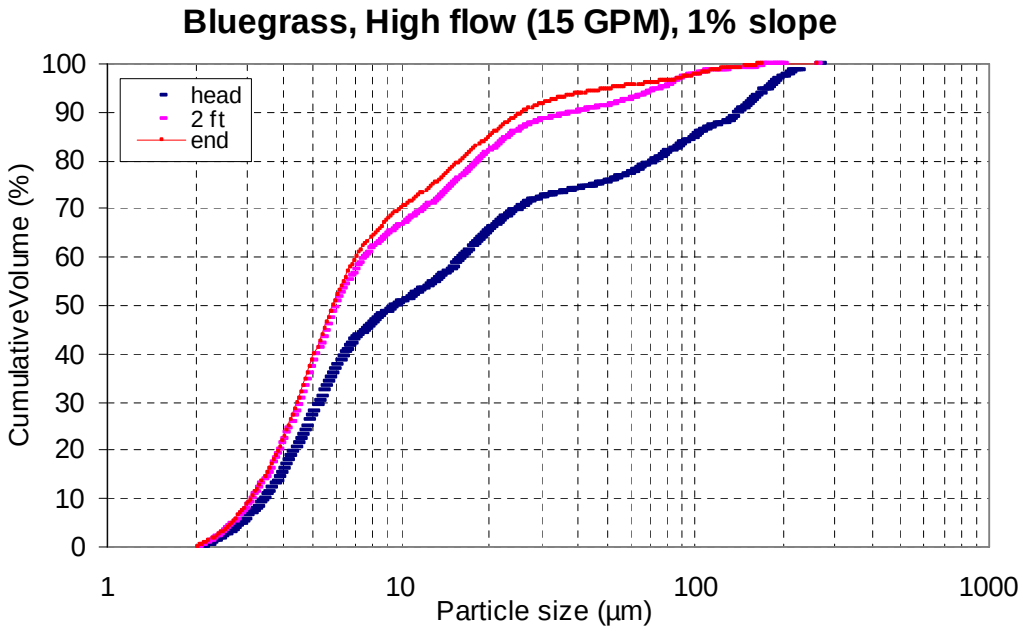

Figure F6

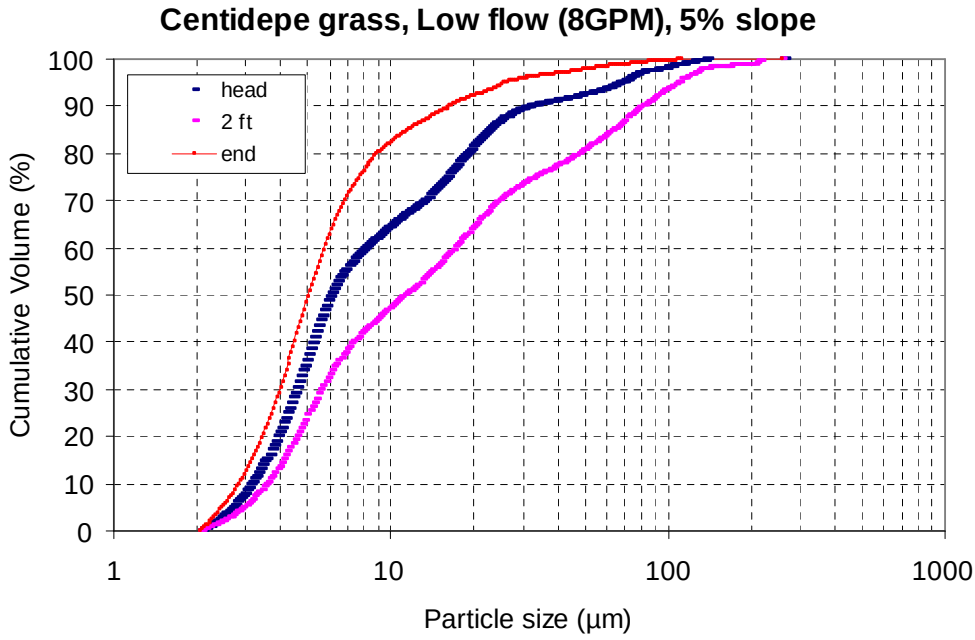

Figure F7

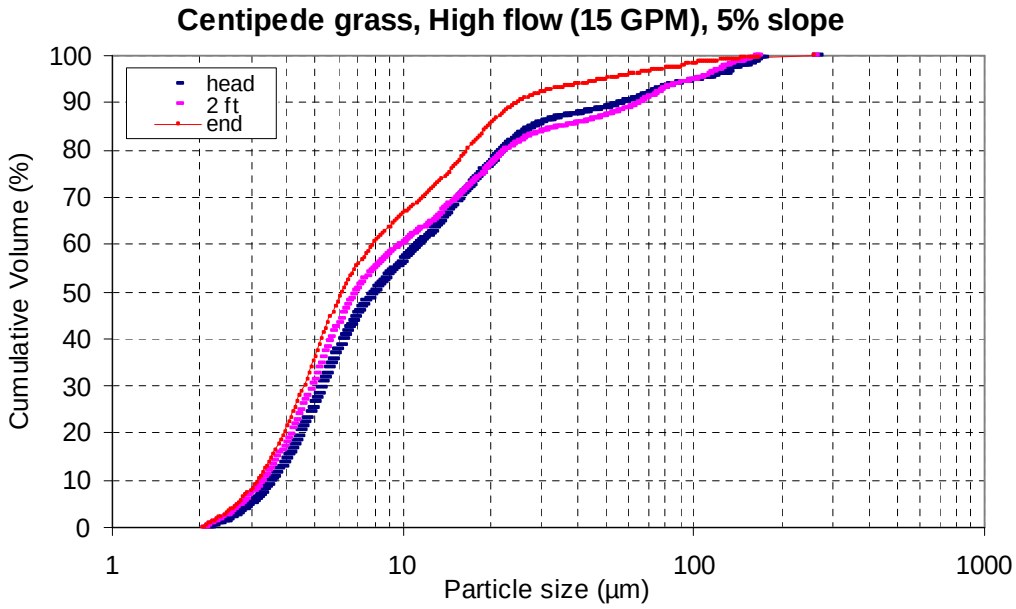

Figure F8

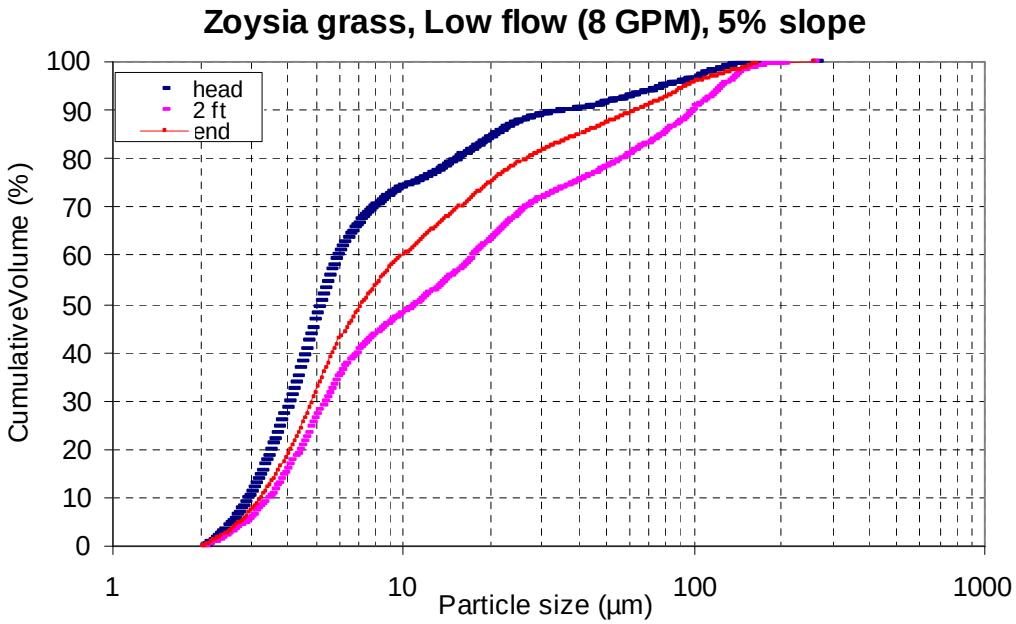

Figure F9

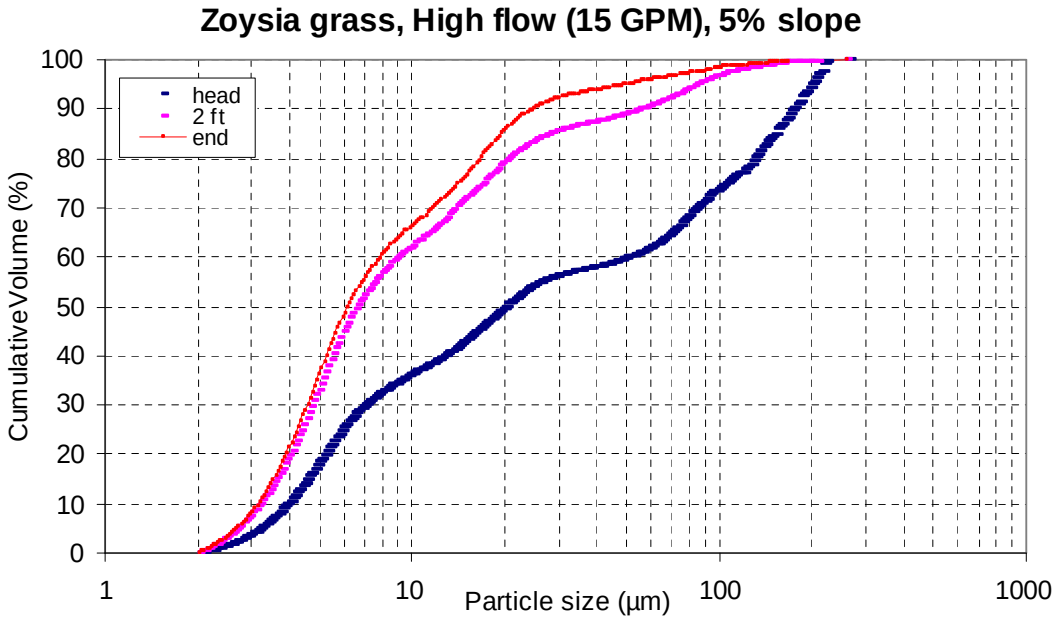

Figure F10

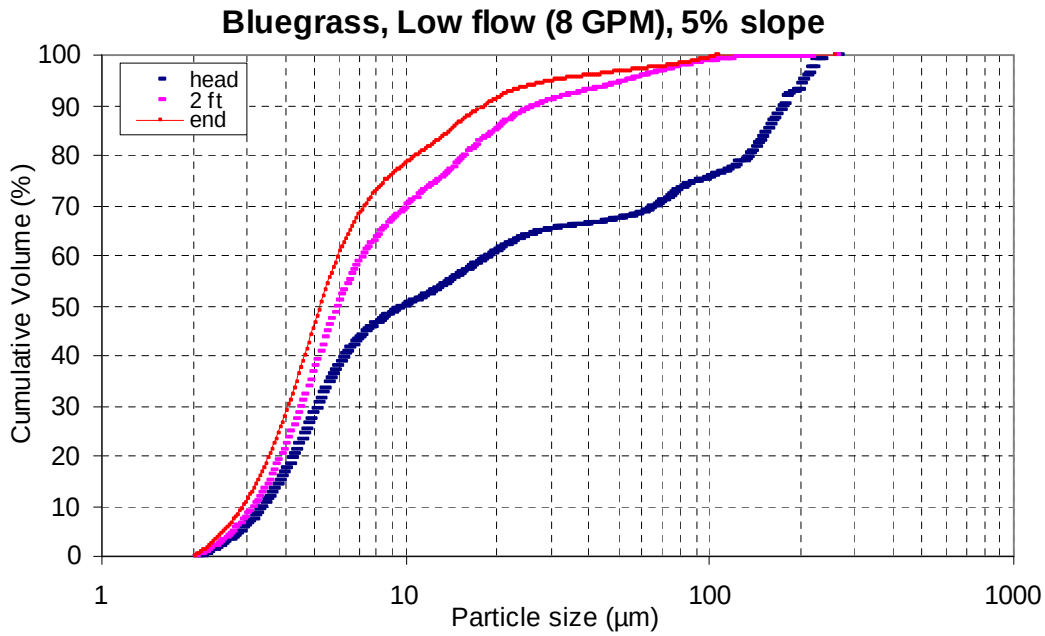

Figure F11

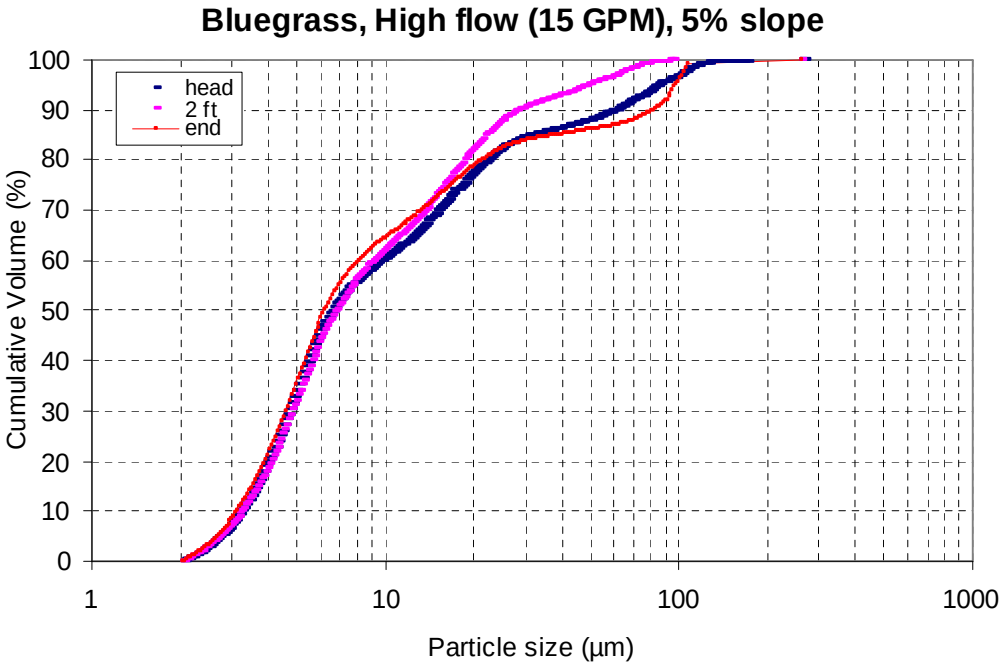
Bluegrass, High flow (15 GPM), 5% slope
head
2 ft
end
Cumulative Volume (%)
100
90
80
70
60
50
40
30
20
10
0
1
10
100
1000
Particle size (µm)

Figure F12

Appendix G: Second Experiments – Box-and-Whisker Plots of Constituents by Experimental Variables

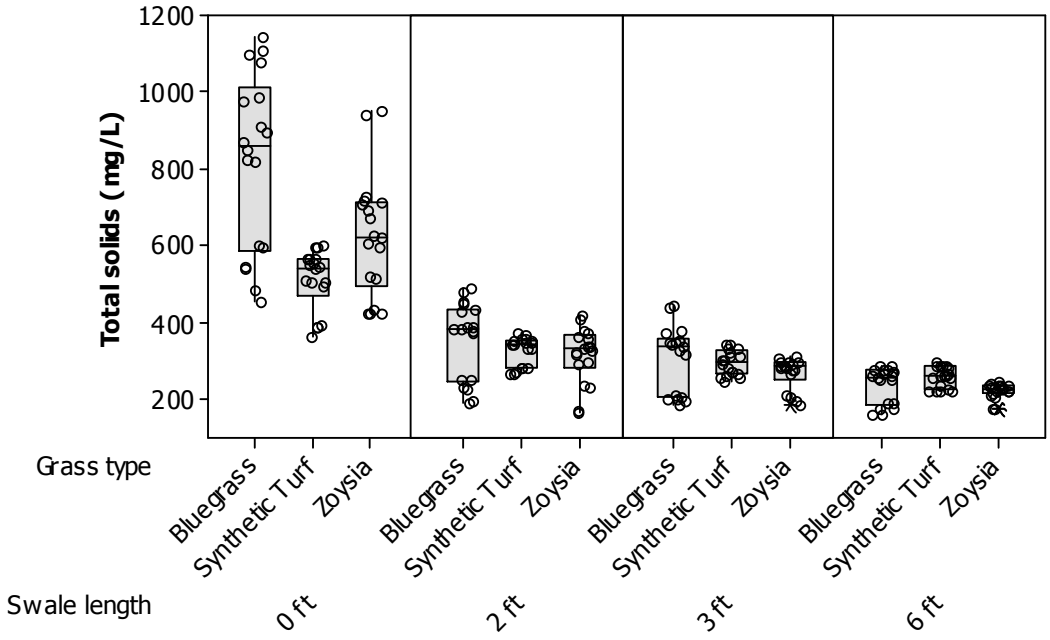

Figure G1

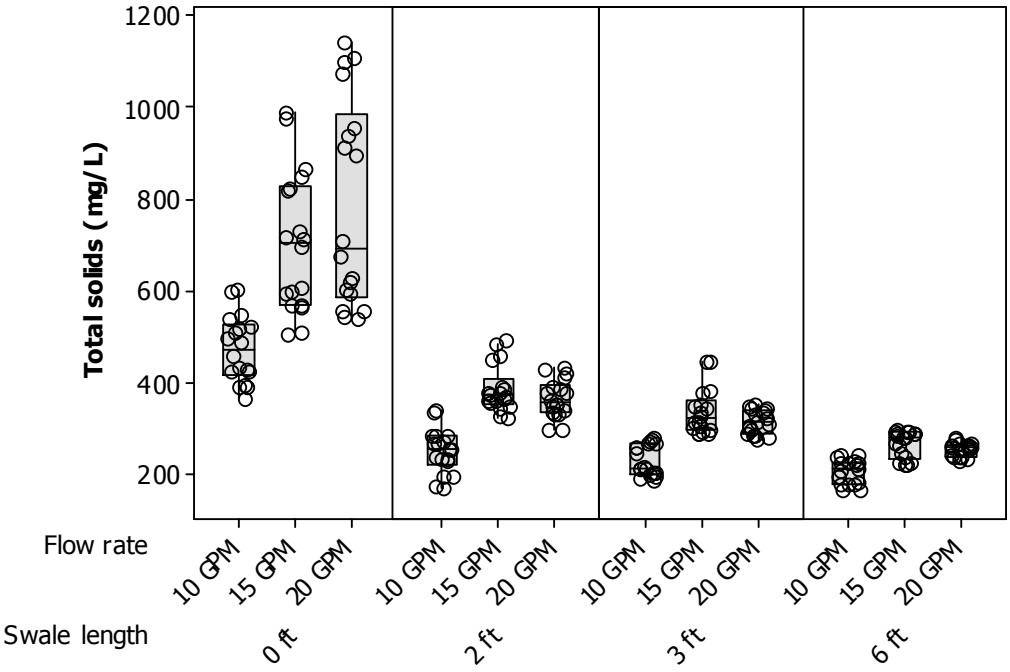

Figure G2

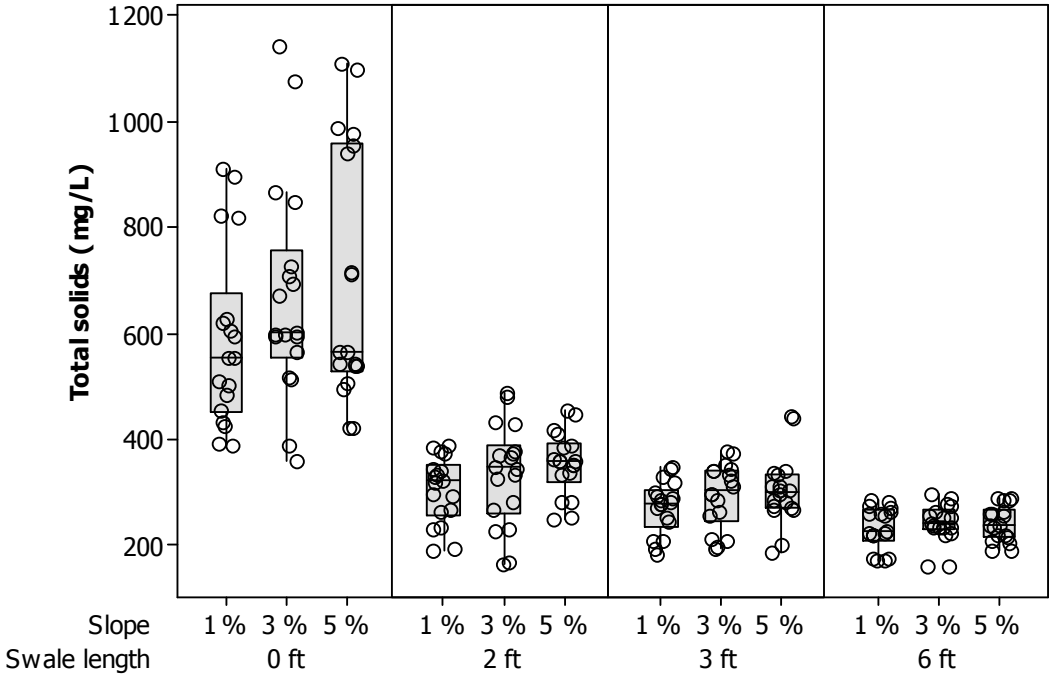

Figure G3

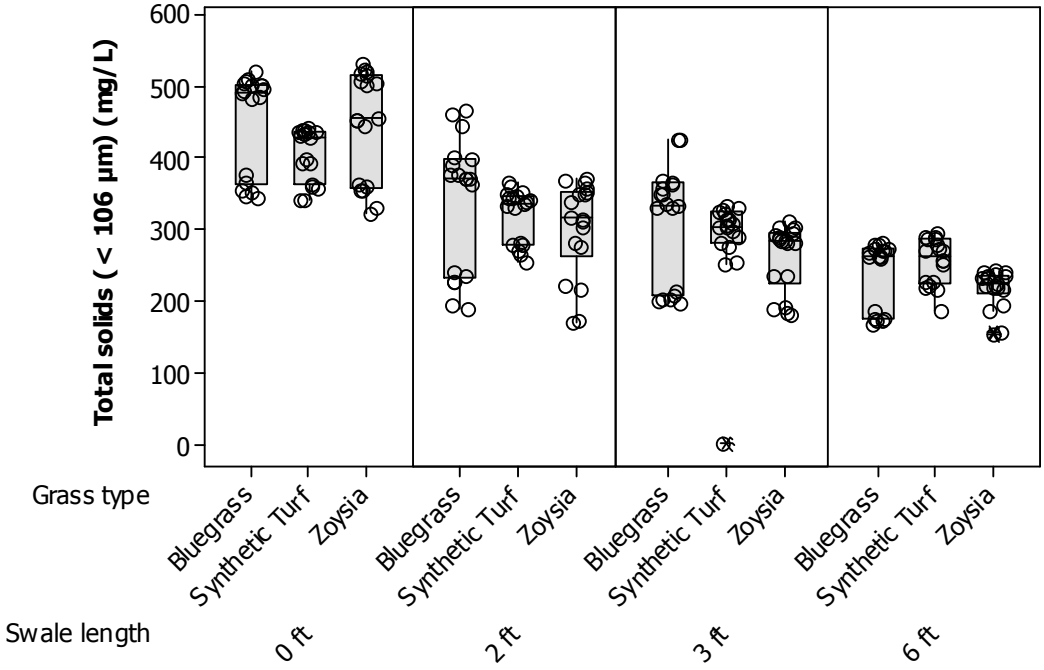

Figure G4

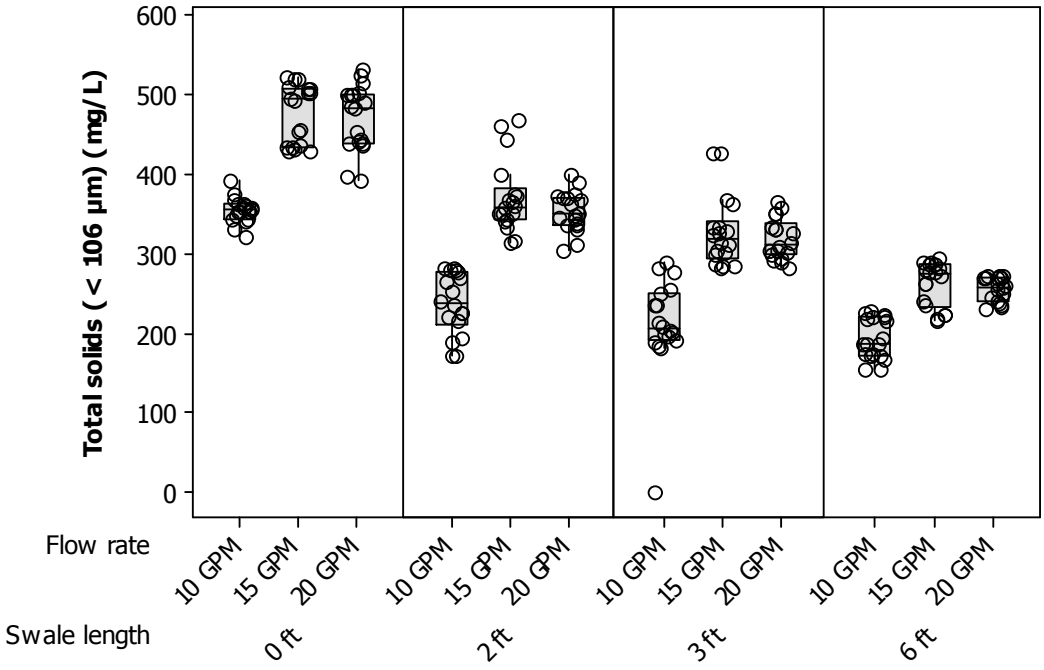

Figure G5

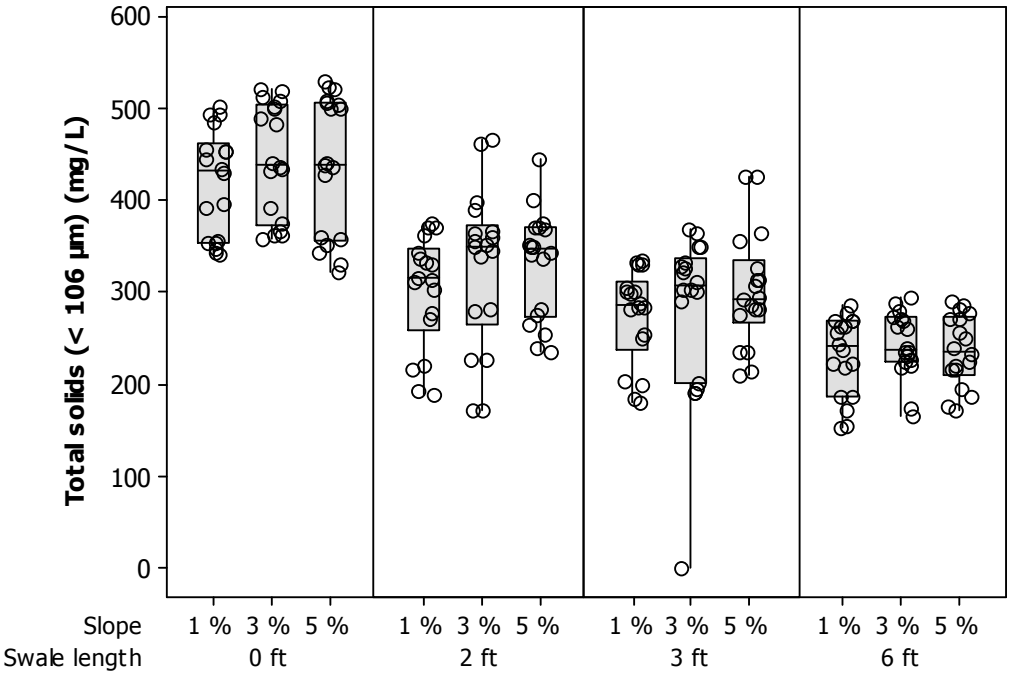

Figure G6

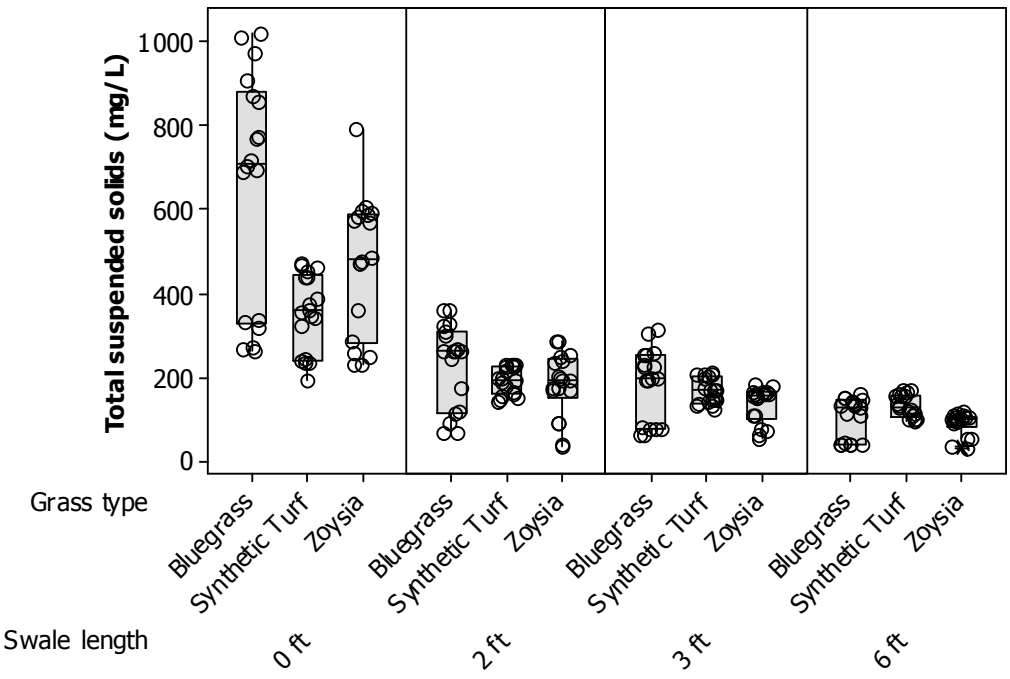

Figure G7

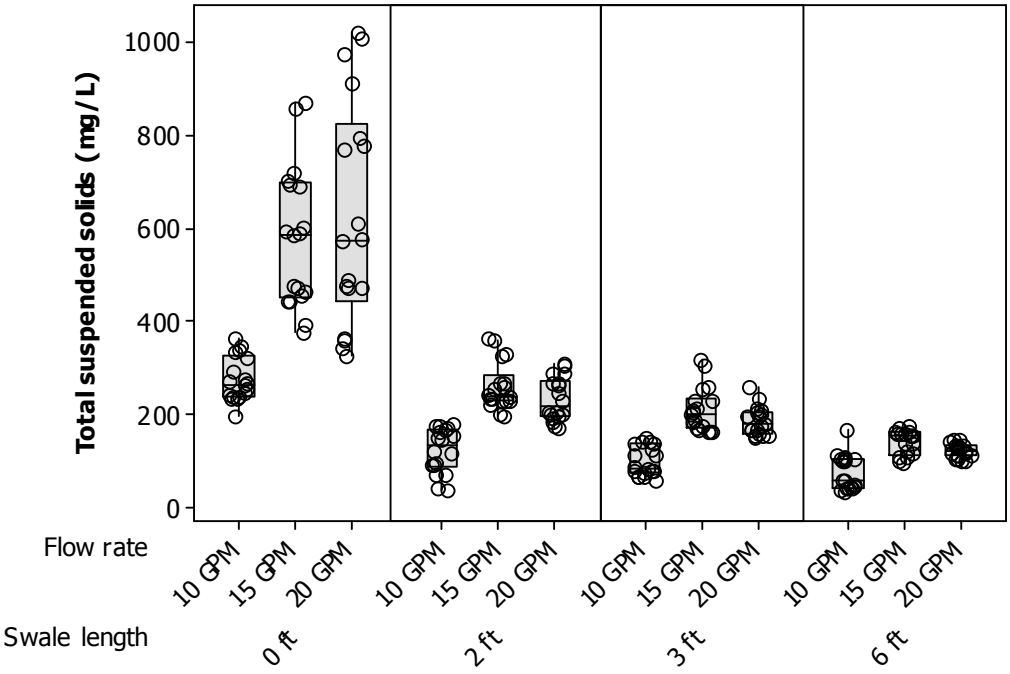

Figure G8

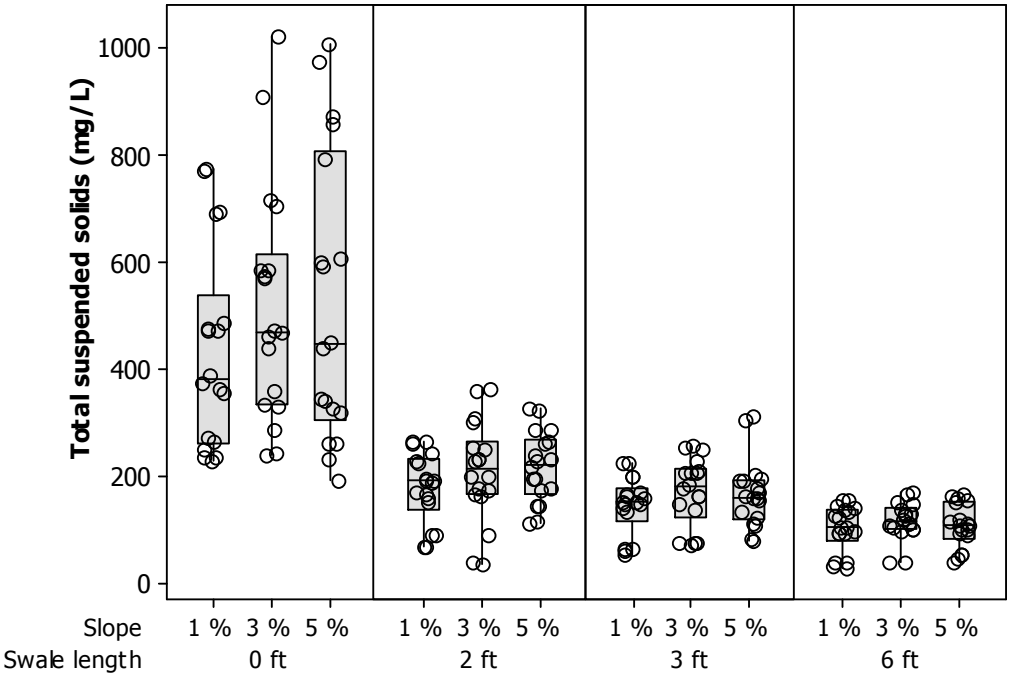

Figure G9

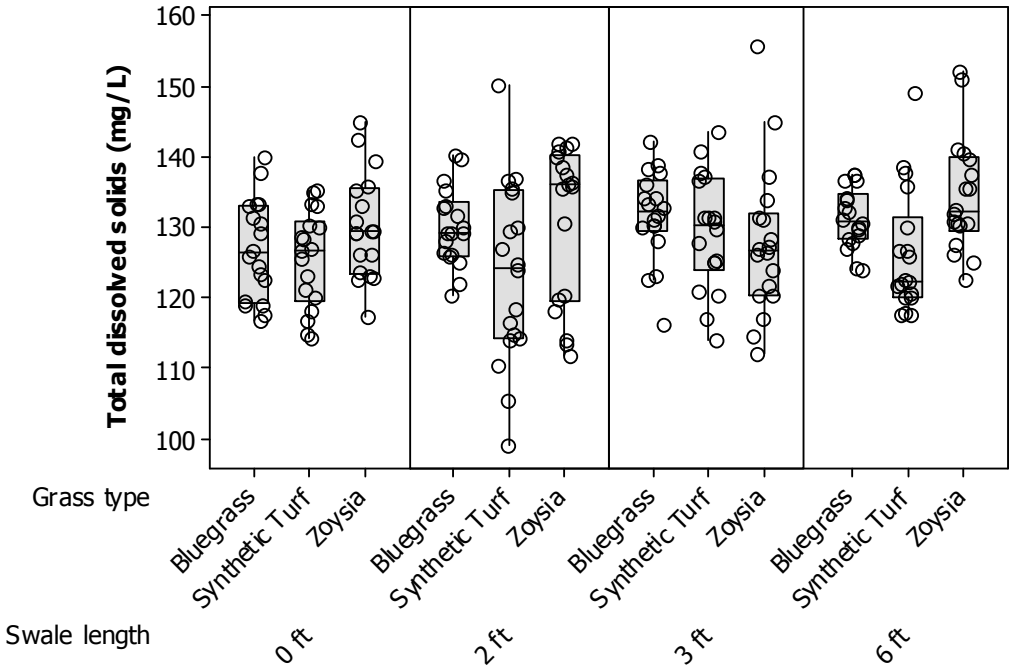

Figure G10

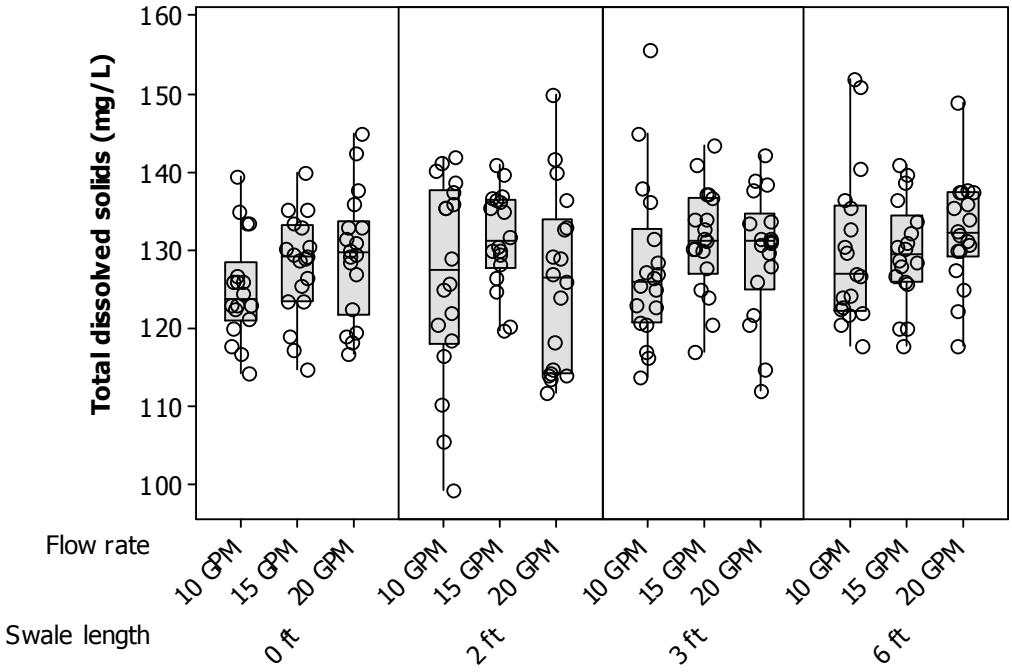

Figure G11

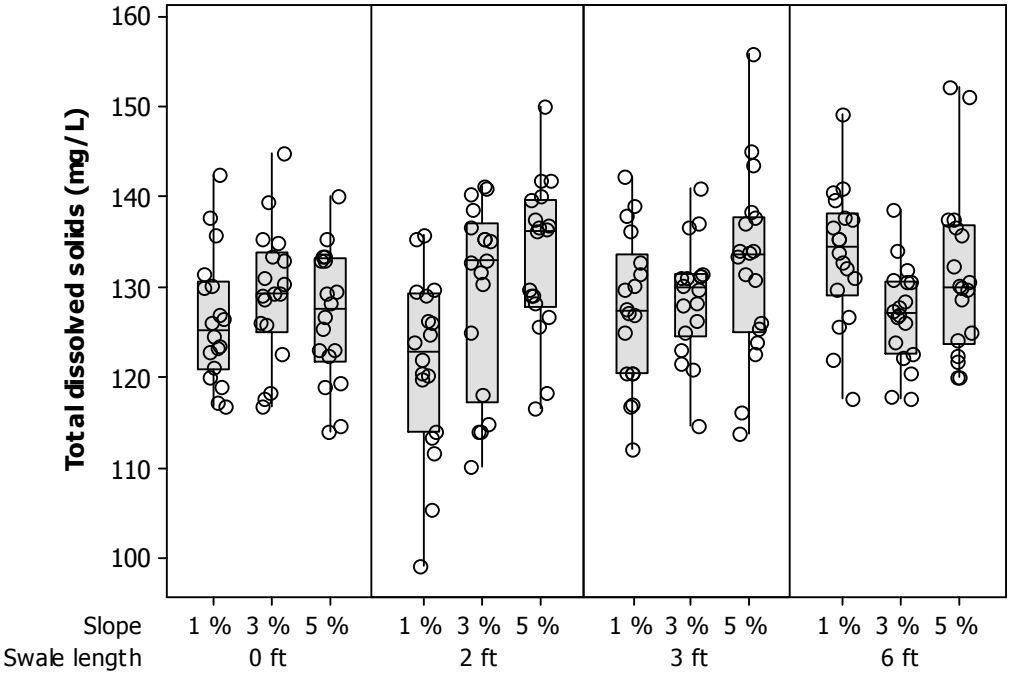

Figure G12

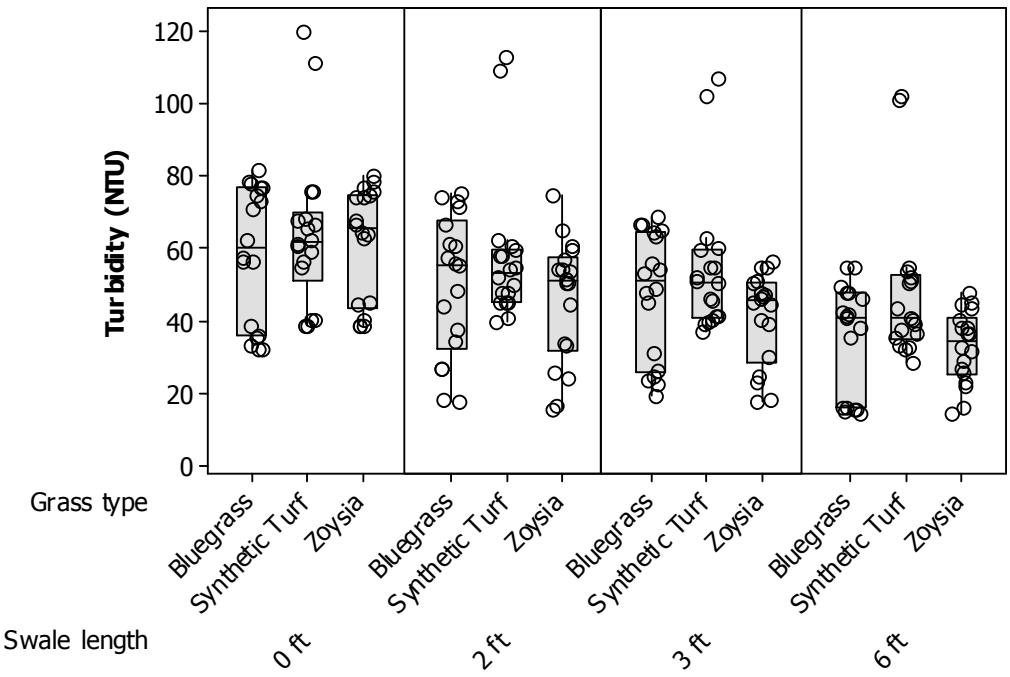

Figure G13

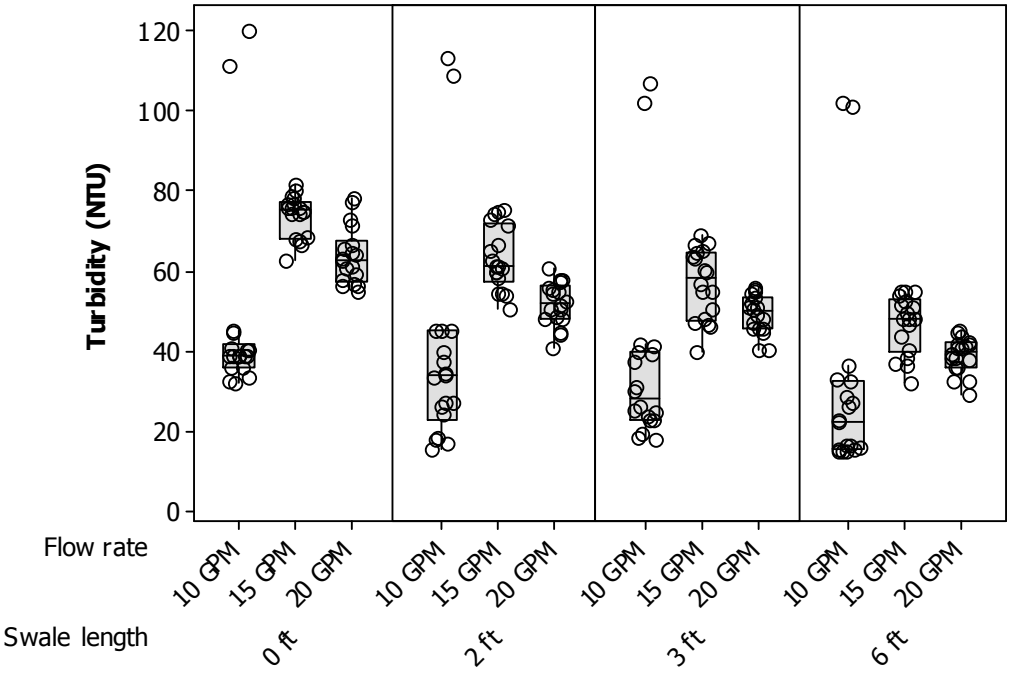

Figure G14

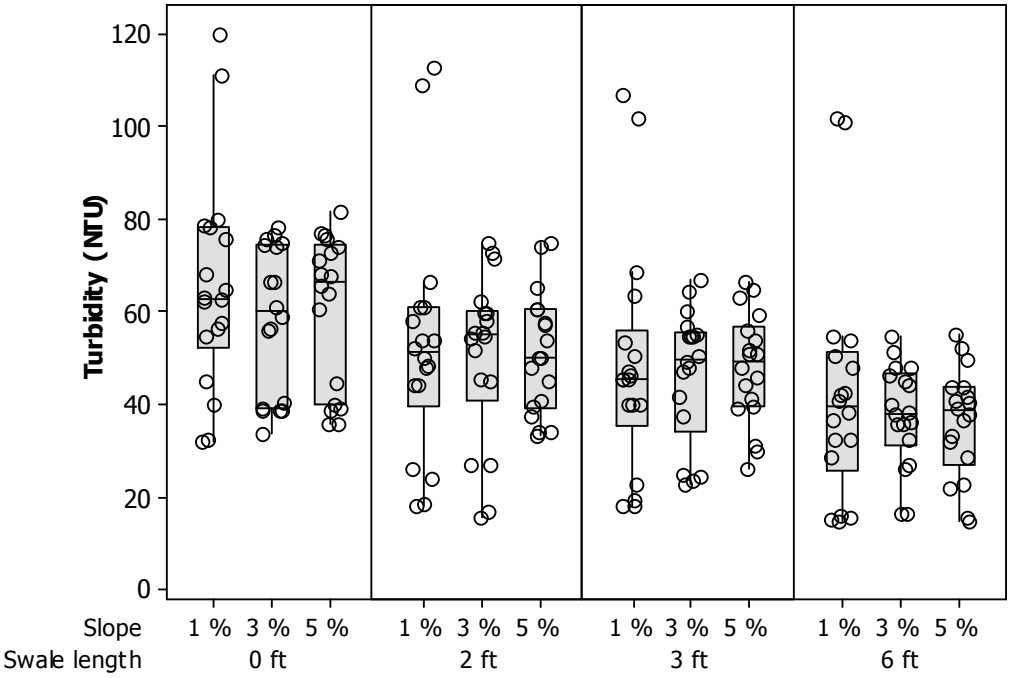

Figure G15

Appendix H: Second Experiments –Statistical Summaries of Particle Size Distributions for each Experiment

Table H1

Synthetic turf, 1% slope, 10 GPM

	10%	25%	50%	75%	90%
0 ft (0 m)	2.1	4.7	12.9	24.4	35.9
2 ft (0.6 m)	2.3	4.1	10.2	19.4	29.1
3 ft (0.9 m)	2	3.7	9.1	18.8	28
6 ft (1.8 m)	1.7	2.9	6.6	14.3	27.5

Table H2

Synthetic turf, 1% slope, 15 GPM

	10%	25%	50%	75%	90%
0 ft (0 m)	3.1	7.2	15.5	25.9	35.5
2 ft (0.6 m)	2.9	6.2	13.3	22.1	32.5
3 ft (0.9 m)	3.7	6.8	12.8	21.1	30.3
6 ft (1.8 m)	2.5	4.9	10.4	18.7	27.3

Table H3

Synthetic turf, 1% slope, 20 GPM

	10%	25%	50%	75%	90%
0 ft (0 m)	2.8	5.9	12.6	22.8	37.1
2 ft (0.6 m)	2.7	6.1	14.2	24.5	36.2
3 ft (0.9 m)	2.5	5.4	12.1	20.8	29.6
6 ft (1.8 m)	2.5	5.1	10.8	18.8	27.7

Table H4

Synthetic turf, 3% slope, 10 GPM

	10%	25%	50%	75%	90%
0 ft (0 m)	3.3	6.6	13.7	23.9	36.6
2 ft (0.6 m)	2.9	5.8	11.8	19.6	28.4
3 ft (0.9 m)	2.9	5.9	13.1	22.5	33.3
6 ft (1.8 m)	2.4	4.5	9.6	17.1	27

Table H5

Synthetic turf, 3% slope, 15 GPM

	10%	25%	50%	75%	90%
0 ft (0 m)	3.2	6.8	14.2	24.1	36.8
2 ft (0.6 m)	3	6.1	12.9	22.4	32.8
3 ft (0.9 m)	2.9	6.1	13.1	21.4	29.5
6 ft (1.8 m)	2.7	5.4	10.7	19	27

Table H6

Synthetic turf, 3% slope, 20 GPM

	10%	25%	50%	75%	90%
0 ft (0 m)	3.1	7.4	16.7	29.9	43.8
2 ft (0.6 m)	2.7	5.8	12.6	21.3	30.4
3 ft (0.9 m)	7	10.7	16.4	24.2	33.2
6 ft (1.8 m)	2.4	4.7	9.8	17.4	25.9

Table H7

Synthetic turf, 5% slope, 10 GPM

	10%	25%	50%	75%	90%
0 ft (0 m)	3.2	6.9	15.5	30.9	44.2
2 ft (0.6 m)	2.9	6.5	14.6	24.6	35.8
3 ft (0.9 m)	2.8	5.7	12.1	20.4	30.5
6 ft (1.8 m)	2.5	4.6	10.2	18.7	30.3

Table H8

Synthetic turf, 5% slope, 5 GPM

	10%	25%	50%	75%	90%
0 ft (0 m)	3.1	6.6	14	23.7	33.1
2 ft (0.6 m)	3.1	6.6	13.6	23	33.9
3 ft (0.9 m)	2.1	4.9	12.7	24.6	105.5
6 ft (1.8 m)	2.6	5.1	10.7	18.9	29.2

Table H9

Synthetic turf, 5% slope, 20 GPM

	10%	25%	50%	75%	90%
0 ft (0 m)	3.3	7.1	14.7	23.8	34
2 ft (0.6 m)	3.2	6.5	13.6	23	33.3
3 ft (0.9 m)	2.8	5.9	12.4	21.4	32.5
6 ft (1.8 m)	2.8	5.2	10.9	19.6	29.2

Table H10

Bluegrass, 1% slope, 10 GPM

	10%	25%	50%	75%	90%
0 ft (0 m)	3	5.8	11.3	19.8	29.9
2 ft (0.6 m)	4.2	7.3	12.2	19.7	30.8
3 ft (0.9 m)	4.2	7.1	11.6	18.7	27.6
6 ft (1.8 m)	4.8	8.2	12.9	19.1	26.9

Table H11

Bluegrass, 1% slope, 15 GPM

	10%	25%	50%	75%	90%
0 ft (0 m)	3.1	6.9	14.7	26	36.8
2 ft (0.6 m)	3	6.1	12.3	20.6	30.3
3 ft (0.9 m)	2.7	5.7	11.2	19	27.8
6 ft (1.8 m)	2.7	5.4	11.1	19	27.3

Table H12

Bluegrass, 1% slope, 20 GPM

	10%	25%	50%	75%	90%
0 ft (0 m)	3.1	6.4	12.8	21.1	30.4
2 ft (0.6 m)	3.2	6.6	13.3	23.2	35.6
3 ft (0.9 m)	3.3	6.6	14.1	24.2	37.3
6 ft (1.8 m)	2.7	5.3	10.4	18.4	26.7

Table H13

Bluegrass, 3% slope, 10 GPM

	10%	25%	50%	75%	90%
0 ft (0 m)	3.9	7.9	16.7	29.2	43.6
2 ft (0.6 m)	2.3	4.5	9.2	18.5	31.5
3 ft (0.9 m)	3.2	6.1	11.9	21.6	38.6
6 ft (1.8 m)	4.5	7.3	11.1	16.3	27.5

Table H14

Bluegrass, 3% slope, 15 GPM

	10%	25%	50%	75%	90%
0 ft (0 m)	2.7	5.7	13.3	22.4	31.8
2 ft (0.6 m)	3.5	8.1	18.4	32.6	50.2
3 ft (0.9 m)	2.8	5.6	11.8	19.8	28.8
6 ft (1.8 m)	2.3	4.3	9.4	18.5	29

Table H15

Bluegrass, 3% slope, 20 GPM

	10%	25%	50%	75%	90%
0 ft (0 m)	3.6	7.7	15.6	25	35
2 ft (0.6 m)	3.4	6.8	14.5	24.2	33.9
3 ft (0.9 m)	3.6	6.8	12.6	21.4	32.5
6 ft (1.8 m)	3.2	5.8	11.1	19.6	29.6

Table H16

Bluegrass, 5% slope, 10 GPM

	10%	25%	50%	75%	90%
0 ft (0 m)	3.2	7	15.6	27.8	38.3
2 ft (0.6 m)	3.7	7.4	14.3	24.4	37.7
3 ft (0.9 m)	4.2	7.2	12.5	21.4	34.5
6 ft (1.8 m)	4.7	8	13.2	21.8	38.2

Table H17

Bluegrass, 5% slope, 15 GPM

	10%	25%	50%	75%	90%
0 ft (0 m)	3.2	7	15	25	36.5
2 ft (0.6 m)	3.4	7.6	16.3	27.2	38.7
3 ft (0.9 m)	3.8	7.6	15.4	26.8	39.5
6 ft (1.8 m)	3.2	6.3	12.8	22.4	32.8

Table H18

Bluegrass, 5% slope, 20GPM

	10%	25%	50%	75%	90%
0 ft (0 m)	3	6.1	12.7	22.1	32.6
2 ft (0.6 m)	3.6	7	14.3	23.4	32.2
3 ft (0.9 m)	3.4	6.8	14.5	25.8	38.3
6 ft (1.8 m)	3.3	6	10.2	17.2	23.3

Table H19

Zoysia, 1% slope, 10 GPM

	10%	25%	50%	75%	90%
0 ft (0 m)	3.5	7.6	16.6	27.3	38.3
2 ft (0.6 m)	3.4	6.1	11.1	18.8	28.5
3 ft (0.9 m)	3.9	6.9	12.5	20.9	39
6 ft (1.8 m)	4.1	6.8	11.9	18.6	29.9

Table H20

Zoysia, 1% slope, 15 GPM

	10%	25%	50%	75%	90%
0 ft (0 m)	3.5	7.6	16.9	29.4	41.8
2 ft (0.6 m)	2.7	5.4	10.9	19	28.2
3 ft (0.9 m)	3.1	5.6	9.9	16.4	24.2
6 ft (1.8 m)	3.6	7.9	16.3	27.3	37.5

Table H21

Zoysia, 1% slope, 20 GPM

	10%	25%	50%	75%	90%
0 ft (0 m)	3.6	7.9	16.3	27.3	37.5
2 ft (0.6 m)	2.7	5.5	11.8	22.1	33.6
3 ft (0.9 m)	2.7	5.4	11.4	19.3	28.2
6 ft (1.8 m)	3.1	5.7	11.2	19.2	30.5

Table H22

Zoysia, 3% slope, 10 GPM

	10%	25%	50%	75%	90%
0 ft (0 m)	4.2	8.1	15.8	27.9	61.1
2 ft (0.6 m)	4.4	7.3	12.3	28.3	65.8
3 ft (0.9 m)	4	7.5	14.4	31.7	98.3
6 ft (1.8 m)	5.5	9	15.1	25.8	61.5

Table H23

Zoysia, 3% slope, 15 GPM

	10%	25%	50%	75%	90%
0 ft (0 m)	3.4	7.7	16.5	27.3	37.3
2 ft (0.6 m)	3.3	6.6	12.9	21.6	31.9
3 ft (0.9 m)	2.8	5.5	11.1	18.6	27
6 ft (1.8 m)	2.7	4.8	9.1	15.4	23.4

Table H24

Zoysia, 3% slope, 20 GPM

	10%	25%	50%	75%	90%
0 ft (0 m)	3.4	7.7	16.8	28.5	43.3
2 ft (0.6 m)	3.3	6.9	14	23.8	33.9
3 ft (0.9 m)	3.1	6.2	12.7	22	30.9
6 ft (1.8 m)	2.9	5.4	10.3	17.8	26.8

Table H25

Zoysia, 5% slope, 10 GPM

	10%	25%	50%	75%	90%
0 ft (0 m)	2.5	5.9	12.7	22.4	37.9
2 ft (0.6 m)	2.2	3.9	12.2	26.7	58.3
3 ft (0.9 m)	6.8	11.5	20.8	50.4	91.8
6 ft (1.8 m)	3.5	6.9	13.5	27.5	147.4

Table H26

Zoysia, 5% slope, 15 GPM

	10%	25%	50%	75%	90%
0 ft (0 m)	3.2	6.9	15.3	25.5	35.5
2 ft (0.6 m)	3.6	7.4	14.7	23.7	32.1
3 ft (0.9 m)	3.3	6.6	13.2	22.8	33
6 ft (1.8 m)	3.2	5.8	10.8	17.3	26.8

Table H27

Zoysia, 5% slope, 20 GPM

	10%	25%	50%	75%	90%
0 ft (0 m)	3.4	8.4	18.4	32.6	43.1
2 ft (0.6 m)	3.5	8	17.2	27.6	39.2
3 ft (0.9 m)	3.2	6.3	12.6	21.6	30.6
6 ft (1.8 m)	2.8	5.2	10.1	17.9	28.1

Appendix I: Second Experiments – Particle Size Distributions for each Experimental Condition

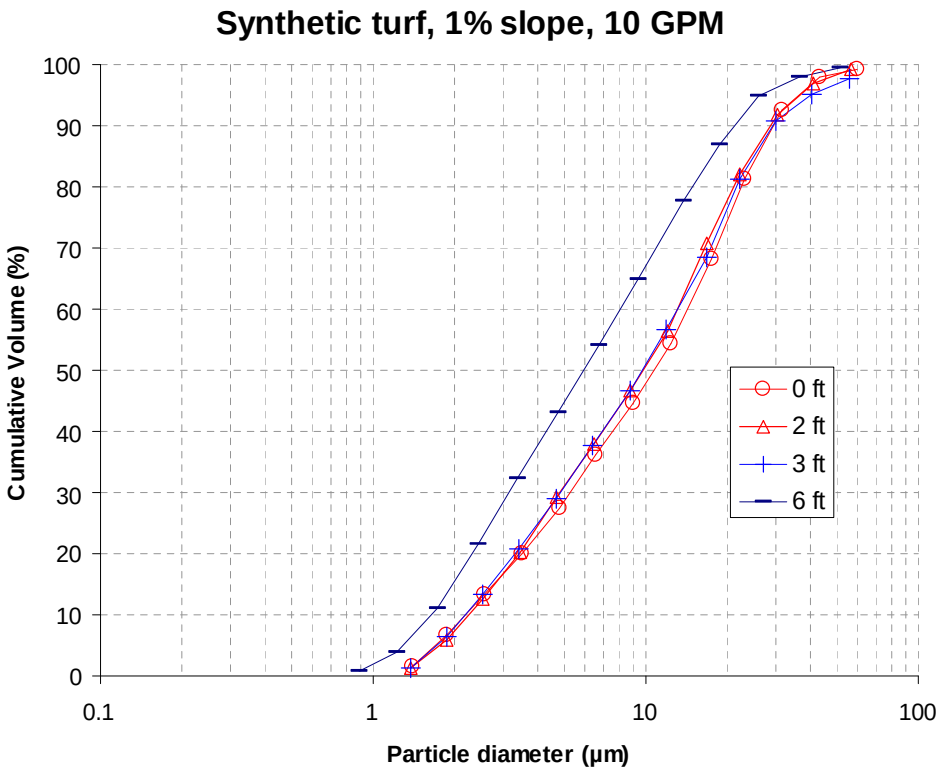

Figure I1

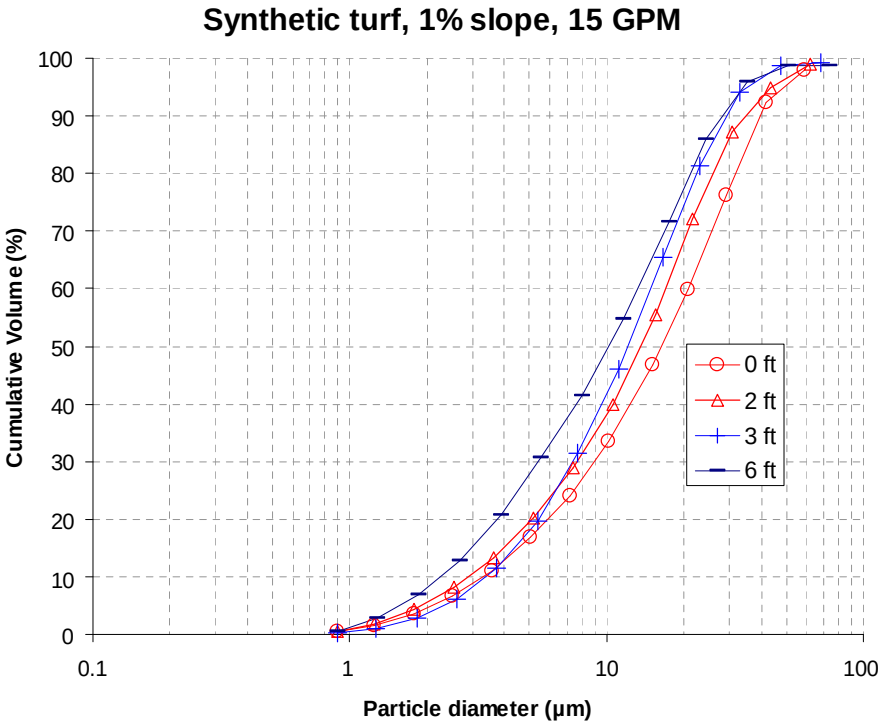

Figure I2

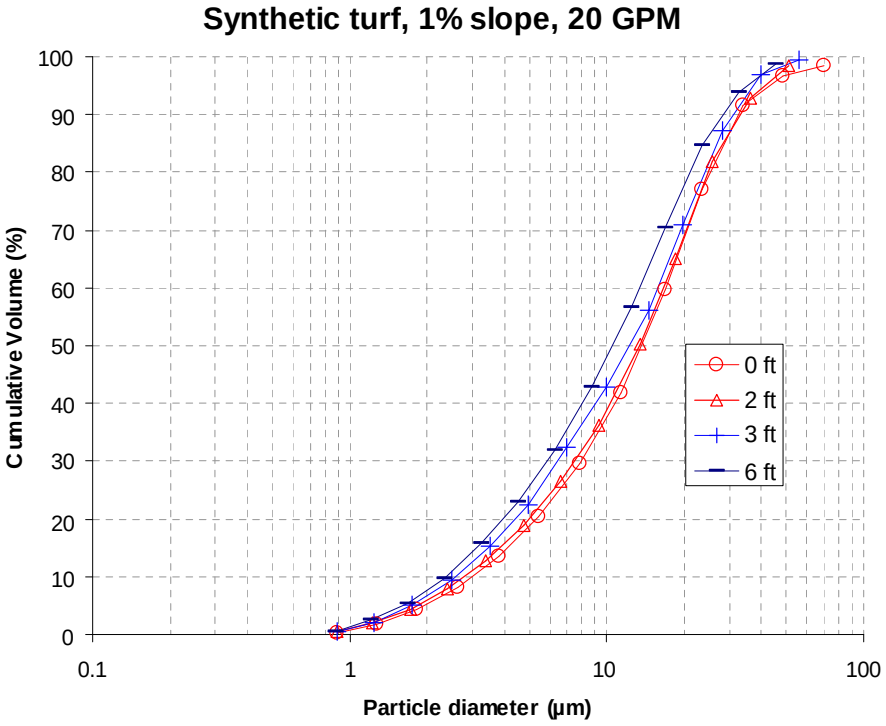

Fig.I3

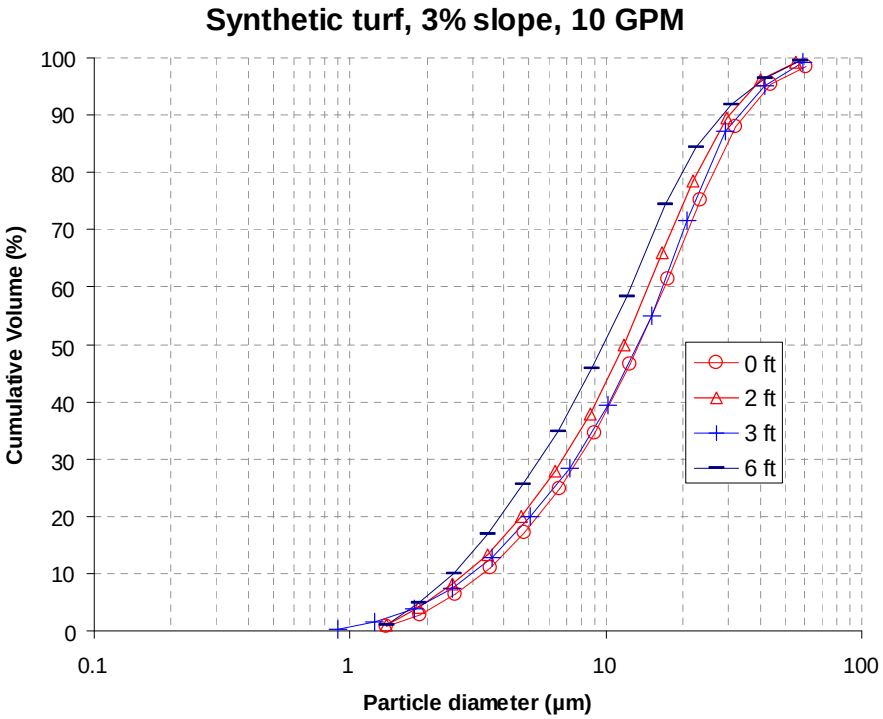

Figure I4

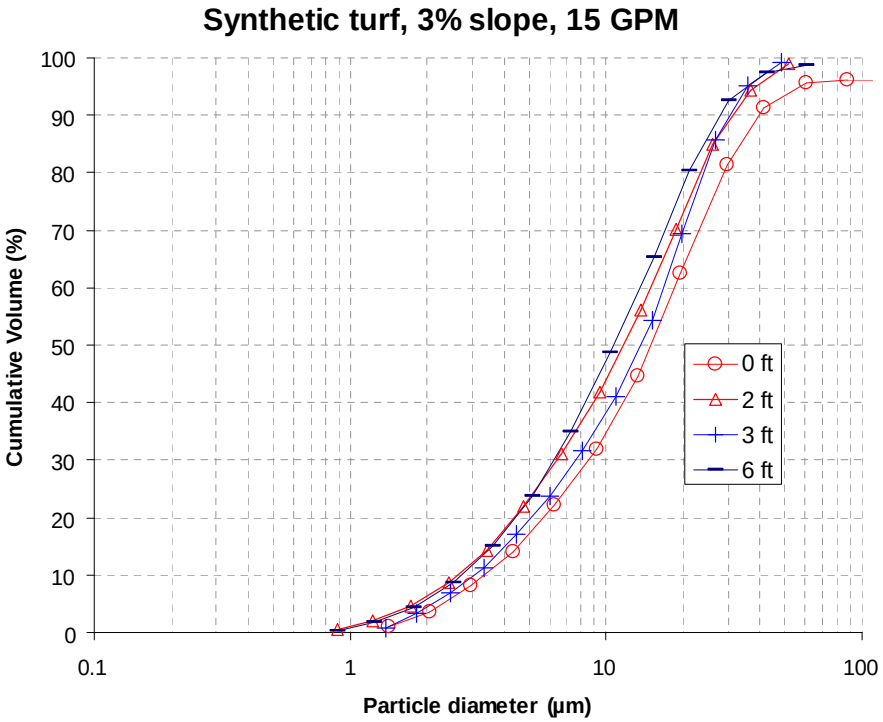

Figure I5

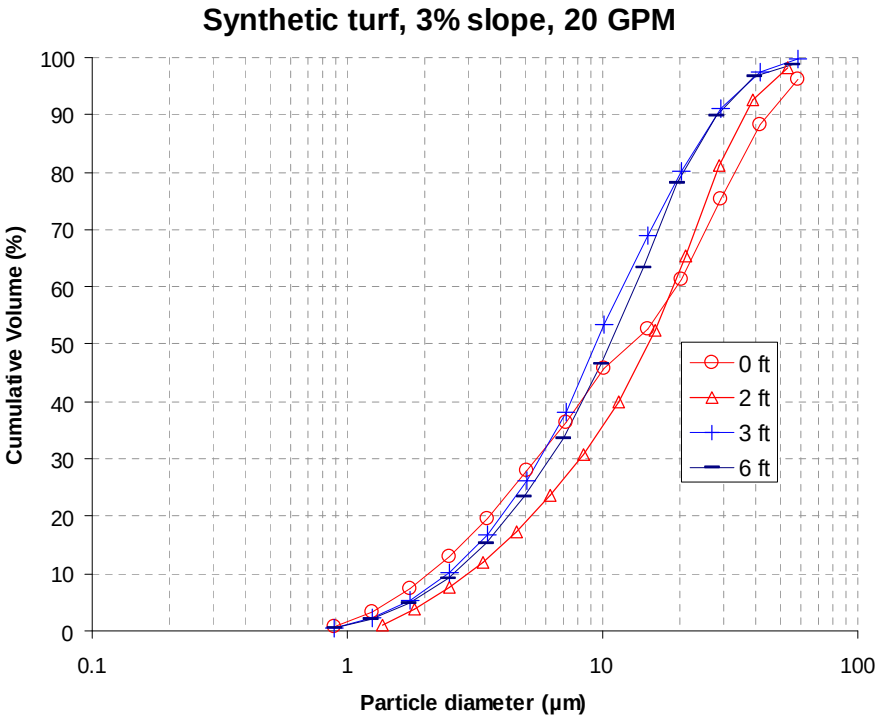

Figure I6

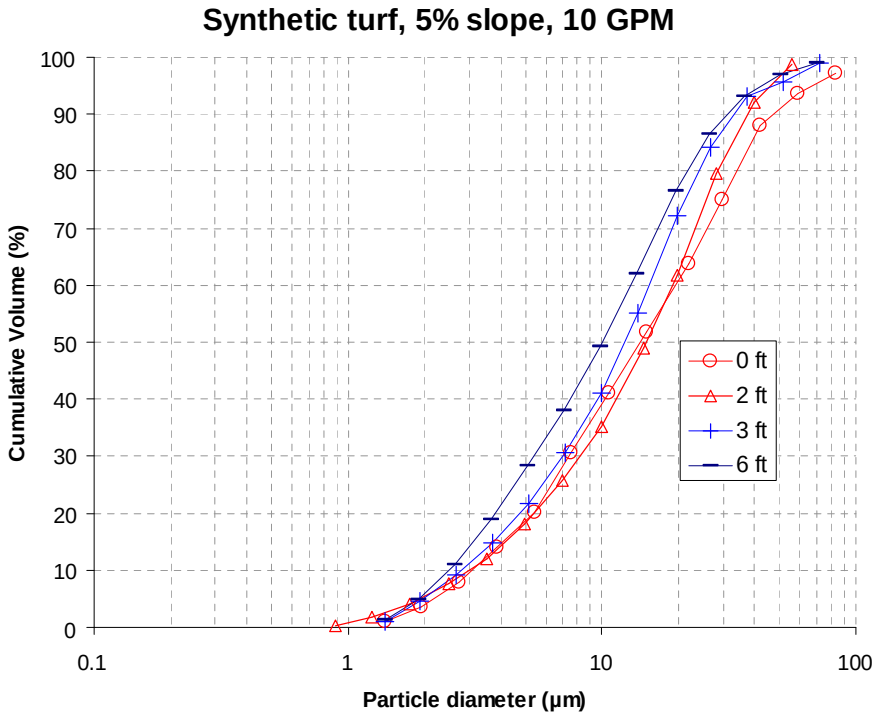

Figure I7

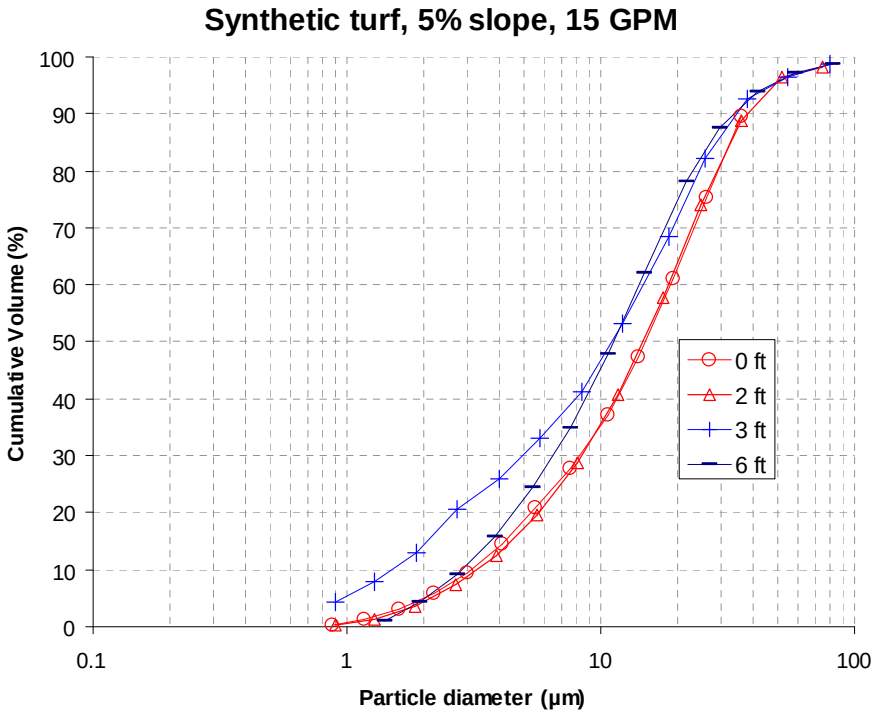

Figure I8

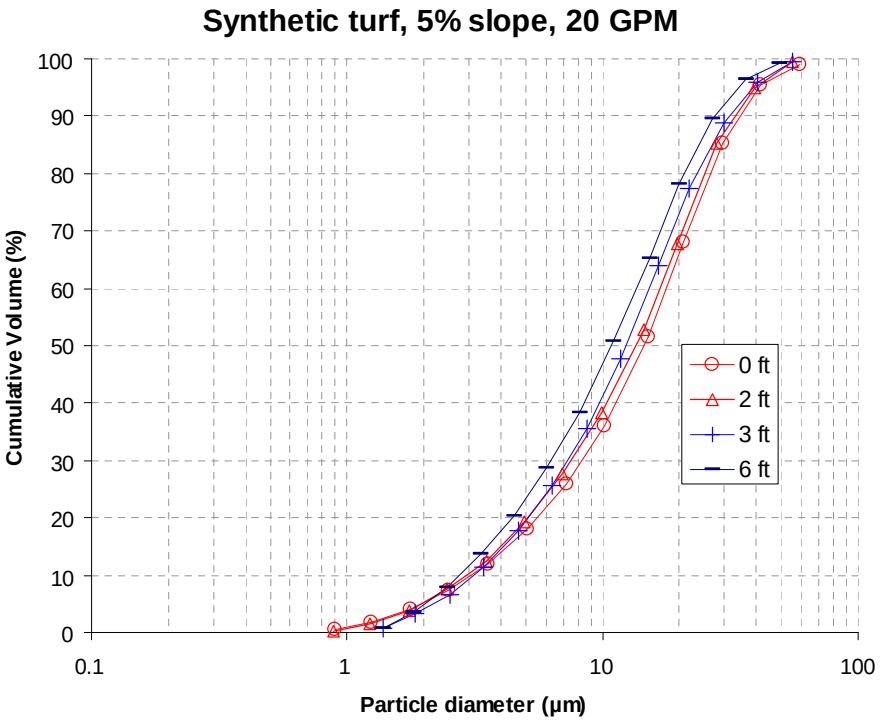

Figure I9

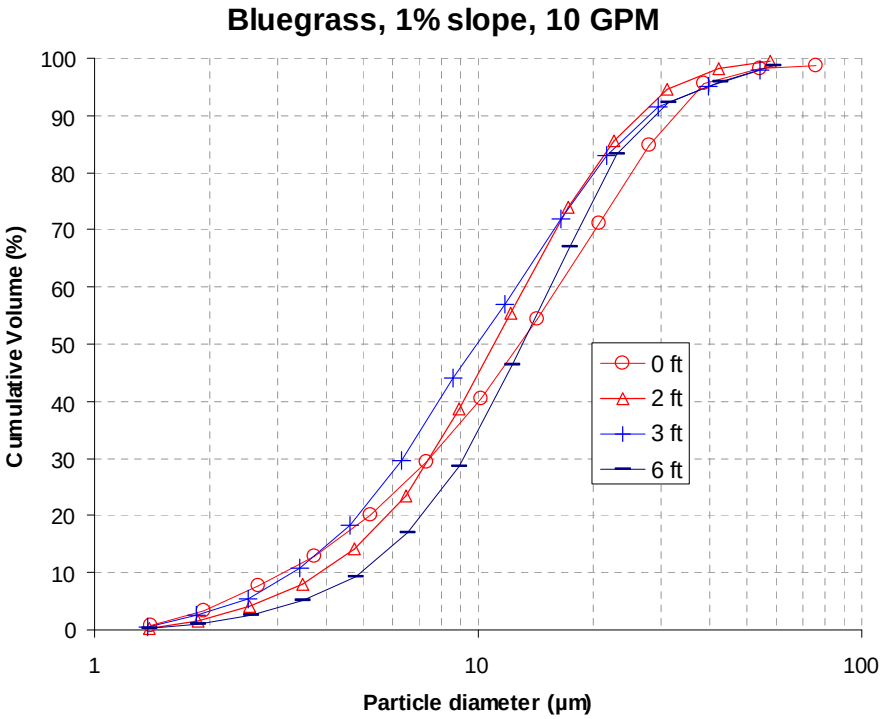

Figure I10

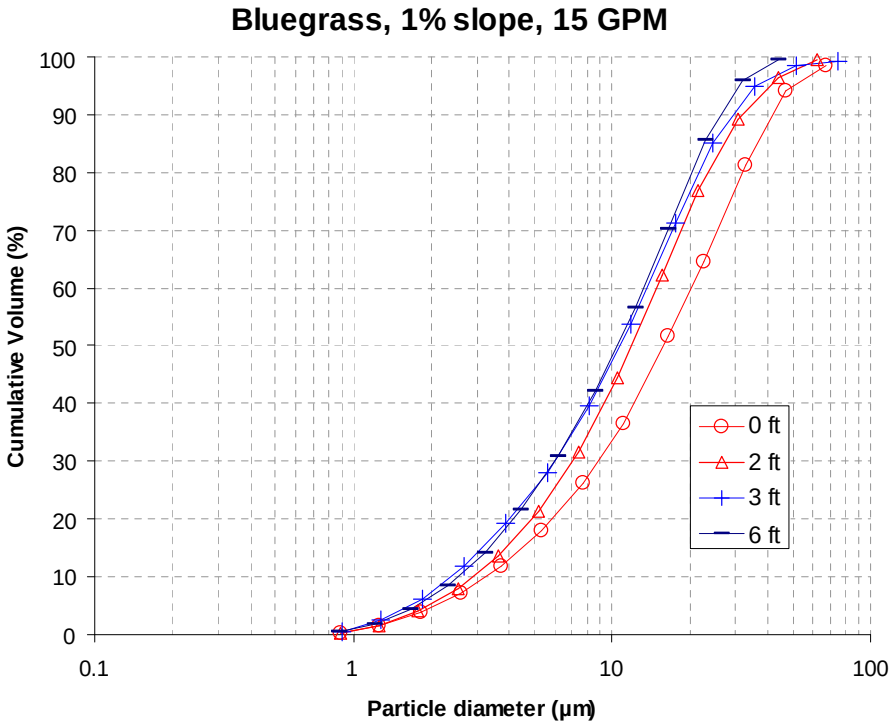

Figure I11

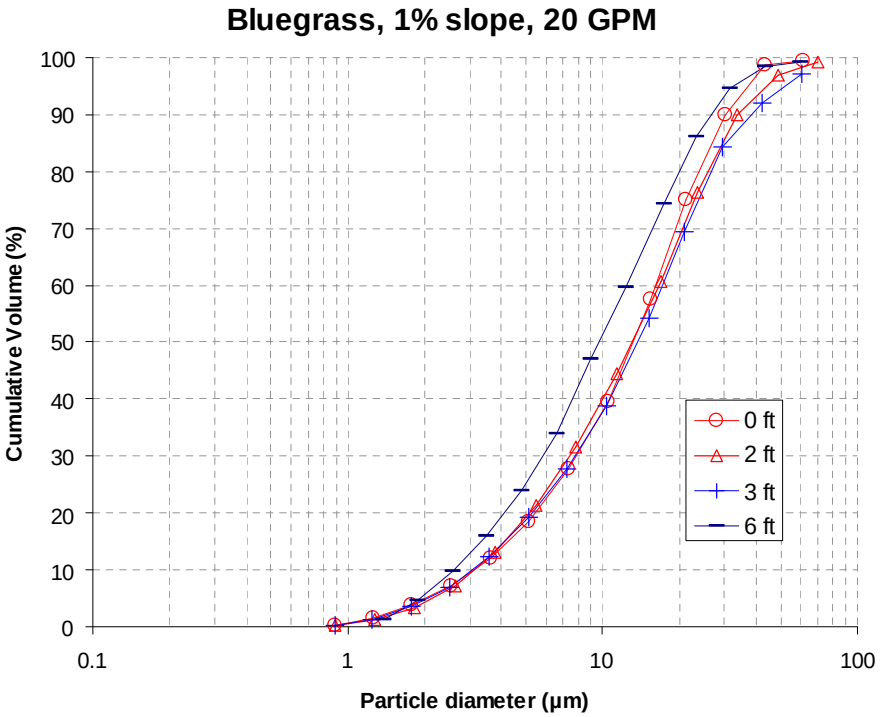

Figure I12

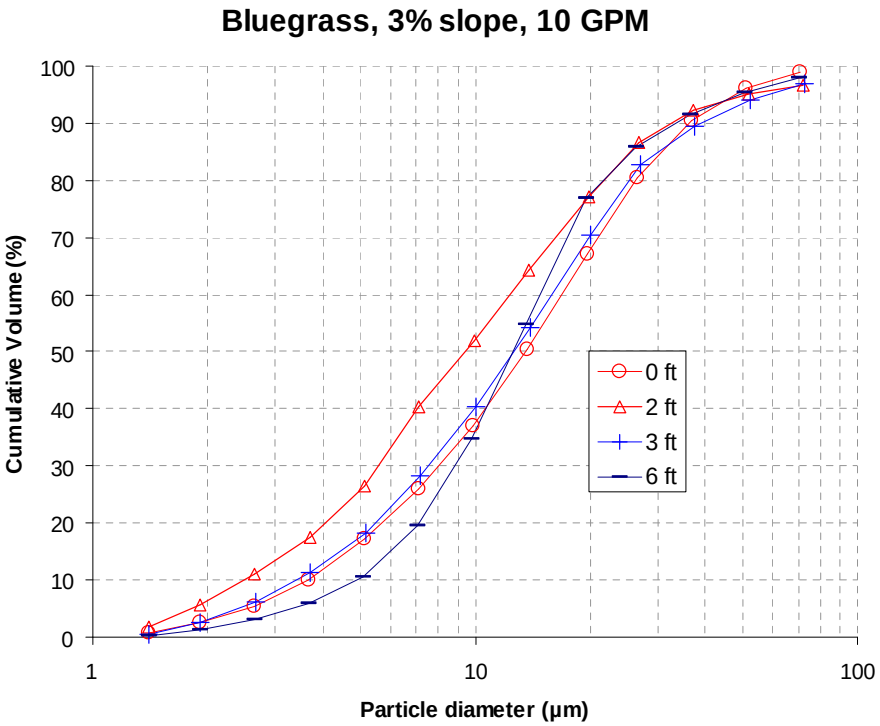

Figure I13

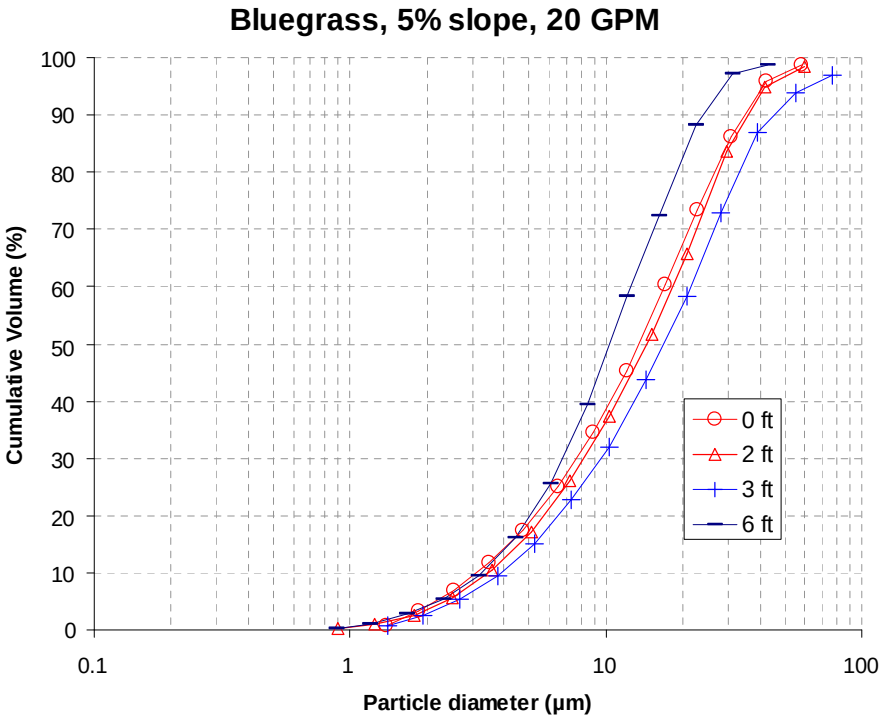

Figure I14

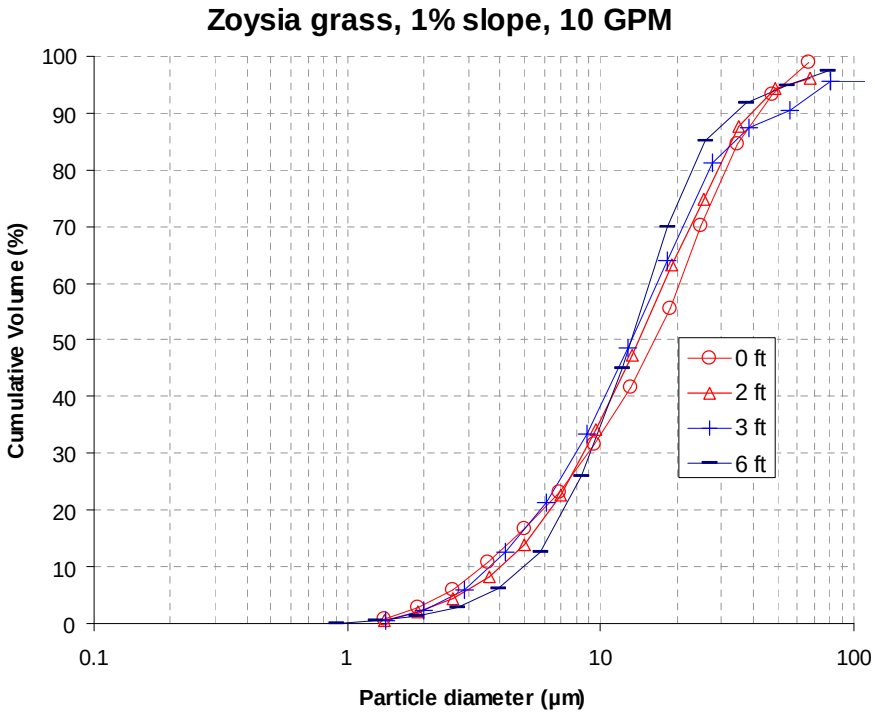

Figure I15

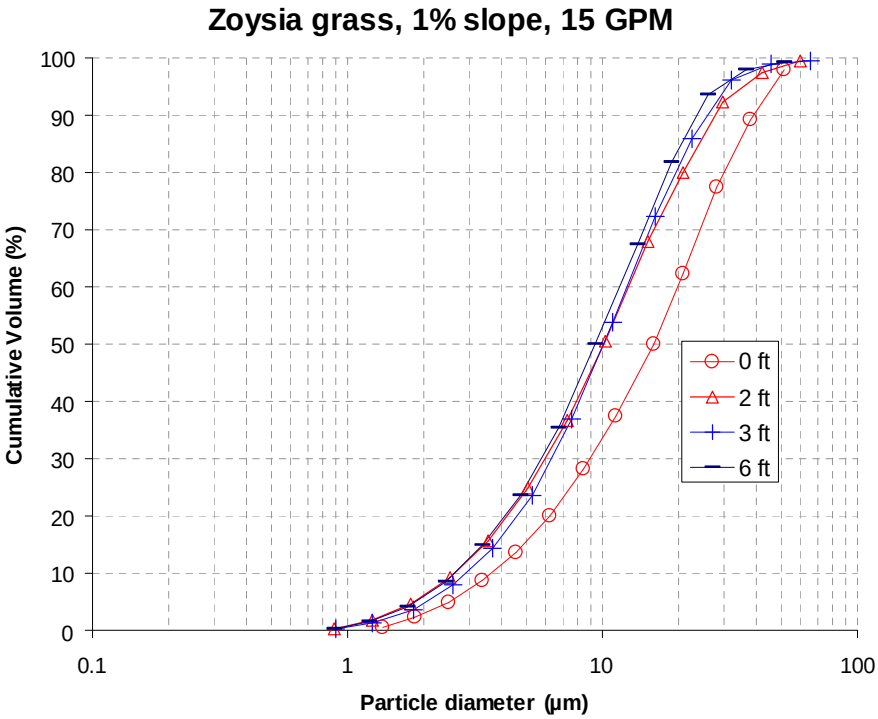

Figure I16

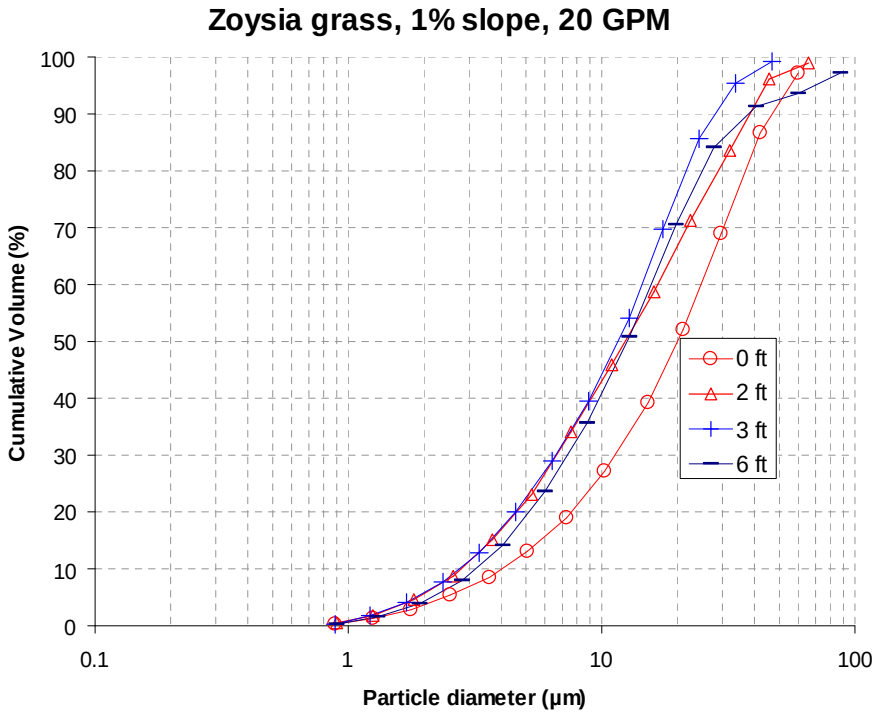

Figure I17

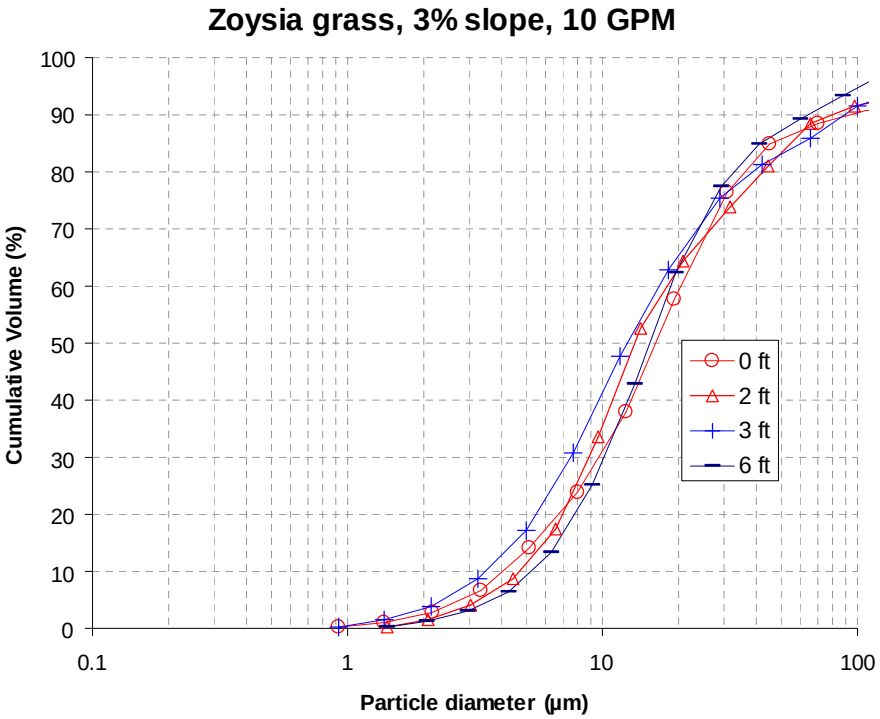

Figure I18

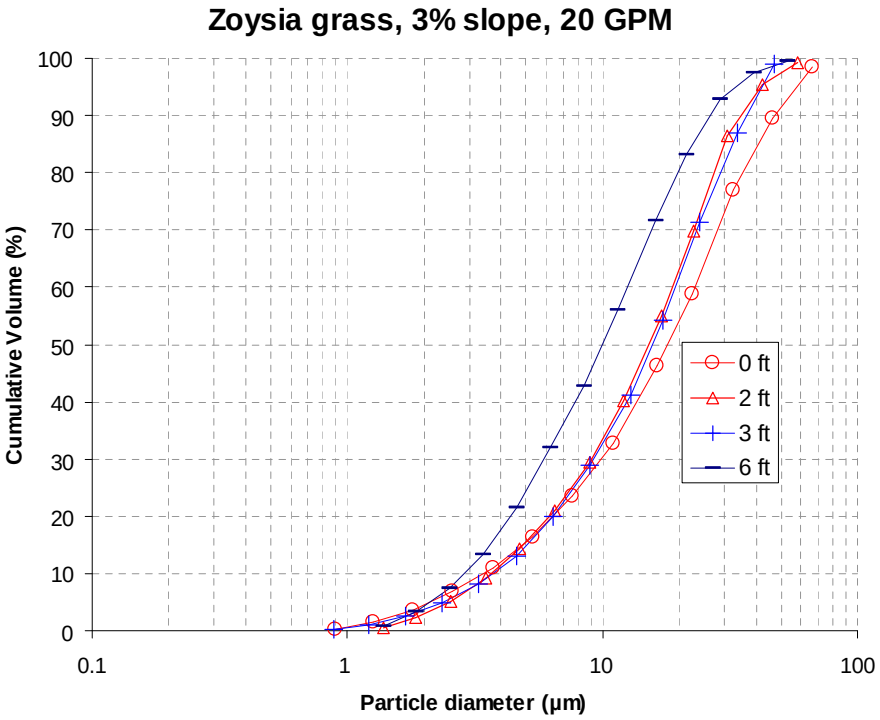

Figure I19

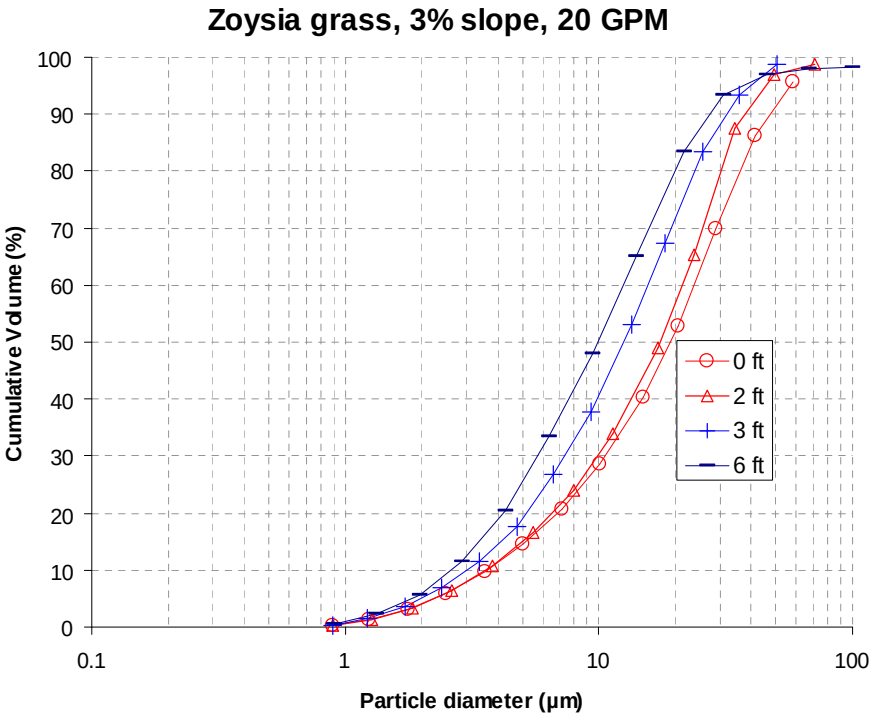
Zoysia grass, 3% slope, 20 GPM
Cumulative Volume (%)
100
90
80
70
60
50
40
30
20
10
0
0.1
1
10
100
Particle diameter (µm)
0 ft
2 ft
3 ft
6 ft

Figure I20

Appendix J: Second Experiments – Performance of USGS/Dekaport Cone Sample Splitter (Rickly Hydrological Company)

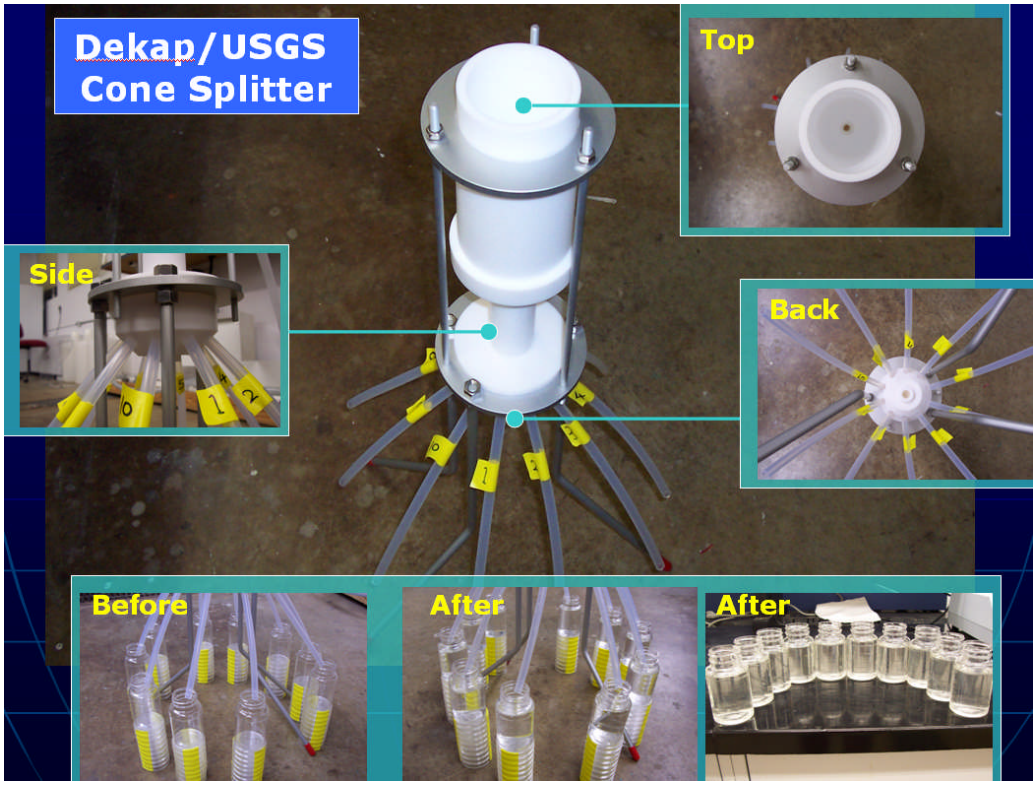

Figure J1

The USGS (US Geological Survey)/Dekaport Cone Sample Splitter is a device that divides a water sample into ten identical sub-samples. It was utilized in the second experiments and outdoor observations for analyzing the six different analytical parameters and for producing duplicates. To ensure identical sediment characteristics of the sub-samples, the performance of the sample splitter was tested by using the same mix of the test sediments that were used in the second experiments. In addition to the mix of the test sediments, SIL-CO-SIL®250 and Sieved Sand (90 to 250 µm) were also tested separately to compare the variability of the three different sediment constituents. Two separate runs were conducted for each sediment mixture.

Known amounts of the sediments were measured (approximately 0.5 g) and mixed with one litter of water so that sediment concentration would be approximately 500 mg/L. Then, the test solution was poured into the top of the USGS/Dekaport Cone Sample Splitter to produce ten identical sub-samples. Total solids analyses were conducted on all of the sub-samples for the three sediment constituents.

The following tables show the sediment constituents and amounts of the sediments used for testing the performance of the sample splitter.

Table J1. Sediment Constituent: Mixture of Sediments

		First run	Second run
Sediments	Contribution	(g)	(g)
SIL-CO-SIL®106	15%	0.0752	0.0752
SIL-CO-SIL®250	50%	0.2408	0.2408
Sieved Sand (90 to250 µm)	25%	0.1225	0.1225
Sieved Sand (300 to 425µm)	10%	0.0532	0.0532
Total	*100%*	*0.4917*	*0.4917*

Table J2. Sediment Constituent: SIL-CO-SIL®250

	First run	Second run
SIL-CO-SIL®250	0.5004 (g)	0.5002 (g)

Table J3. Sediment Constituent: Sieved Sand (90 to 250 µm)

	First run	Second run
Sieved Sand (90 to 250 µm)	0.5003 (g)	0.5006 (g)

The test results shown below shows that the averaged total solids concentration for each sediment constituent was approximately 560 mg/L due to the presence of dissolved solids in the tap water adding additional solids to the mixture.

As result, we found that the USGS/Dekaport Cone Sample Splitter was very efficient in splitting a sample equally into sub-samples. Very little variability was determined between the sub-samples for both sample volumes and sediments. The coefficient of variations (COV) of all the sub-sample sets for the three different sediment constituents were found to be below 0.10 which shows that the sediment concentrations between the different sub-samples were very similar. Although COVs for the three sediment constituents were found to be quite small, it was determined that larger particles had slightly greater variability than smaller particles when comparing the COVs of SIL-CO-SIL®250 and sieved Sand (90 to 250 µm). The following tables and graphs show the performance of the USGS/Dekaport Cone Sample Splitter for the different sediment constituents and for volume.

Table J4 Test Results: SIL-CO-SIL®250

Tube ID	First run Total solids (mg/L)	Second run Total solids (mg/L)	*Avg.*	*Std. Dev*	*COV*
1	573.1	563.2	*568.1*	*7.0*	*0.012*
2	556.0	559.8	*557.9*	*2.7*	*0.005*
3	563.7	547.6	*555.6*	*11.4*	*0.021*
4	553.5	558.8	*556.1*	*3.8*	*0.007*
5	558.2	560.6	*559.4*	*1.7*	*0.003*
6	564.3	565.3	*564.8*	*0.7*	*0.001*
7	577.4	523.1	*550.2*	*38.4*	*0.070*
8	565.3	571.9	*568.6*	*4.7*	*0.008*
9	563.6	559.0	*561.3*	*3.3*	*0.006*
10	574.5	570.4	*572.4*	*2.9*	*0.005*
Avg.	*564.95*	*557.96*			
Std. Dev	*7.98*	*14.01*			
COV	*0.014*	*0.025*			

Table J5 Test Results: Mix Sediments

Tube ID	First run Total solids (mg/L)	Second run Total solids (mg/L)	*Avg.*	*Std. Dev*	*COV*
1	547.4	561.9	*554.6*	*10.2*	*0.018*
2	549.5	572.6	*561.1*	*16.4*	*0.029*
3	560.6	556.0	*558.3*	*3.2*	*0.006*
4	550.0	561.5	*555.8*	*8.2*	*0.015*
5	565.0	552.0	*558.5*	*9.2*	*0.016*
6	576.2	563.4	*569.8*	*9.1*	*0.016*
7	573.8	572.9	*573.4*	*0.7*	*0.001*
8	556.8	587.5	*572.2*	*21.7*	*0.038*
9	560.0	561.0	*560.5*	*0.7*	*0.001*
10	563.3	572.4	*567.9*	*6.5*	*0.011*
Avg.	*560.26*	*566.12*			
Std. Dev	*9.83*	*10.33*			
COV	*0.018*	*0.018*			

Table J6 Test Results: Sieved Sand (90 to 250 µm)

Tube ID	First run Total solids (mg/L)	Second run Total solids (mg/L)	*Avg.*	*Std. Dev*	*COV*
1	573.7	554.7	*564.2*	*13.4*	*0.024*
2	578.4	536.9	*557.7*	*29.4*	*0.053*
3	558.8	575.7	*567.3*	*12.0*	*0.021*
4	565.0	565.0	*565.0*	*0.0*	*0*
5	586.7	576.5	*581.6*	*7.2*	*0.012*
6	598.0	627.6	*612.8*	*20.9*	*0.034*
7	587.9	602.8	*595.3*	*10.6*	*0.018*
8	576.3	592.7	*584.5*	*11.6*	*0.02*
9	581.0	563.0	*572.0*	*12.7*	*0.022*
10	569.7	537.4	*553.5*	*22.9*	*0.041*
Avg.	*577.55*	*573.24*			
Std. Dev	*11.58*	*28.57*			
COV	*0.02*	*0.05*			

Table J7 Volumetric Test

Tube ID	First run (mL)	Second run (mL)	Third run (mL)	Fourth run (mL)	Fifth run (mL)	Sixth run (mL)	*Avg.*	*Std.Dev*	*COV*
1	97	97	97	97	97	97	*97.0*	*0*	*0*
2	95	95	96	96	95	95	*95.3*	*0.52*	*0.005*
3	109	109	108	108	109	109	*108.7*	*0.52*	*0.005*
4	104	103	103	103	104	104	*103.5*	*0.55*	*0.005*
5	101	99	100	99	100	100	*99.8*	*0.75*	*0.008*
6	101	99	99	100	101	101	*100.2*	*0.98*	*0.010*
7	107	107	107	108	107	107	*107.2*	*0.41*	*0.004*
8	97	95	96	94	95	96	*95.5*	*1.05*	*0.011*
9	101	100	100	101	100	100	*100.3*	*0.52*	*0.005*
10	99	98	97	98	98	98	*98.0*	*0.63*	*0.006*
Avg.	*101.1*	*100.2*	*100.3*	*100.4*	*100.6*	*100.7*			
Std.Dev	*4.48*	*4.76*	*4.37*	*4.74*	*4.79*	*4.67*			
COV	*0.04*	*0.05*	*0.04*	*0.05*	*0.05*	*0.05*			

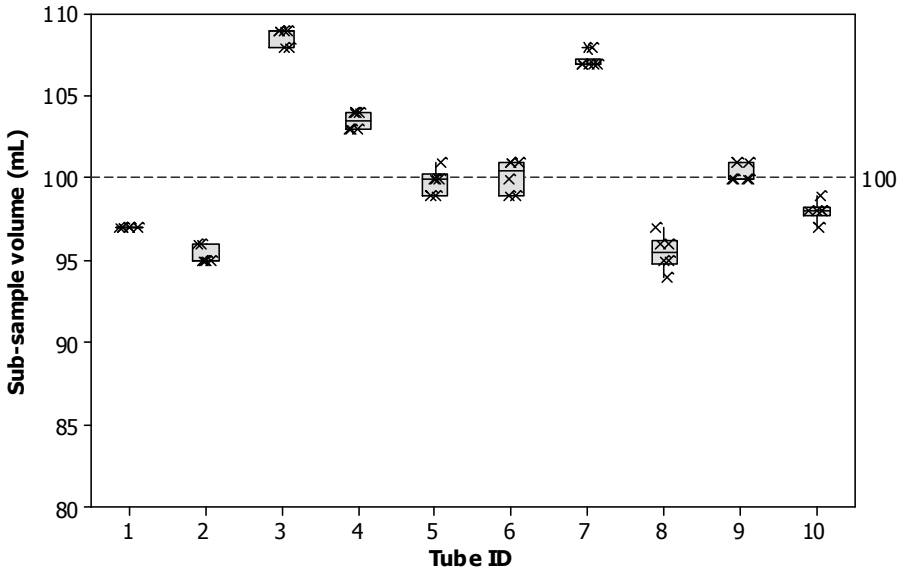

Figure J2 Box and whisker plot showing the volumes of the sub-samples

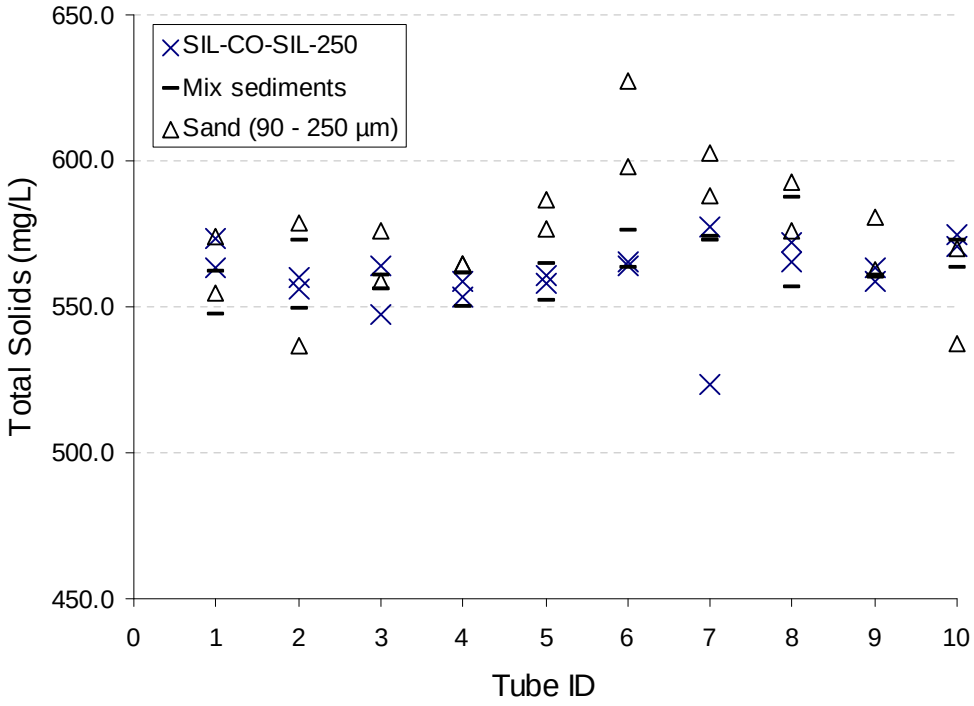

Figure J3 Scatter plot showing sediment concentrations of the sub-samples for each sediment constituent

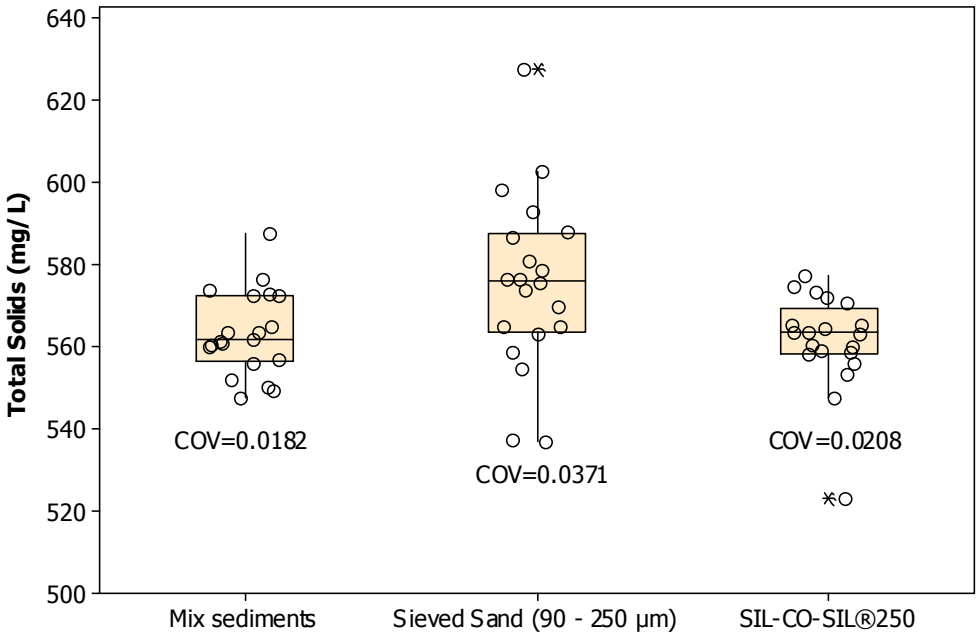

Figure J4. Box and whisker plots of total solids content of the subsamples of the different sediment test mixtures.

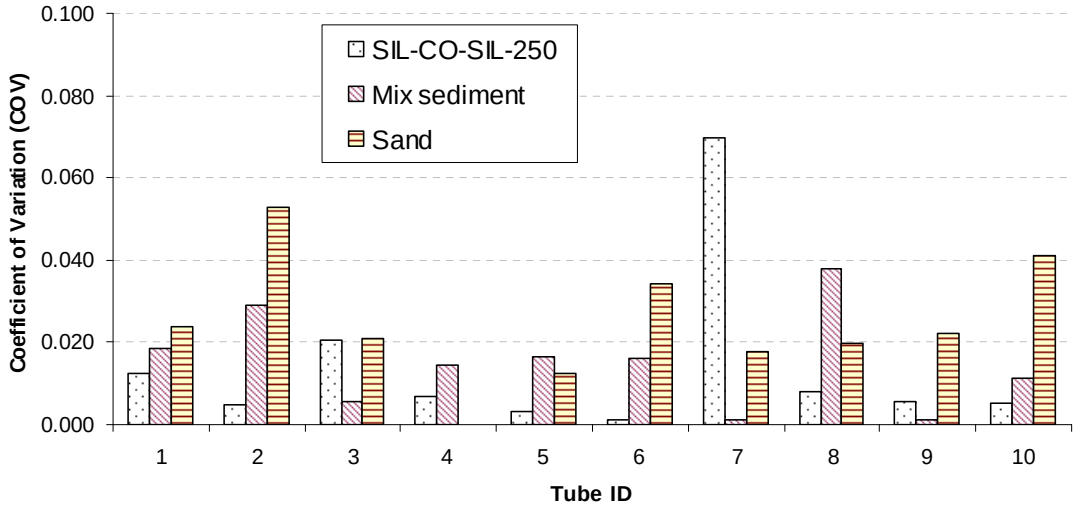

Figure J5. Bar chart of COVs obtained from the three different sediment test mixtures.

Appendix K: Outdoor Swale - Rain Information of Monitored Storm Events

The rainfall data shown in this appendix was obtained from a weather station located 1.5 mile (2.4 km) away from the outdoor swale test site, at the University of Alabama campus.

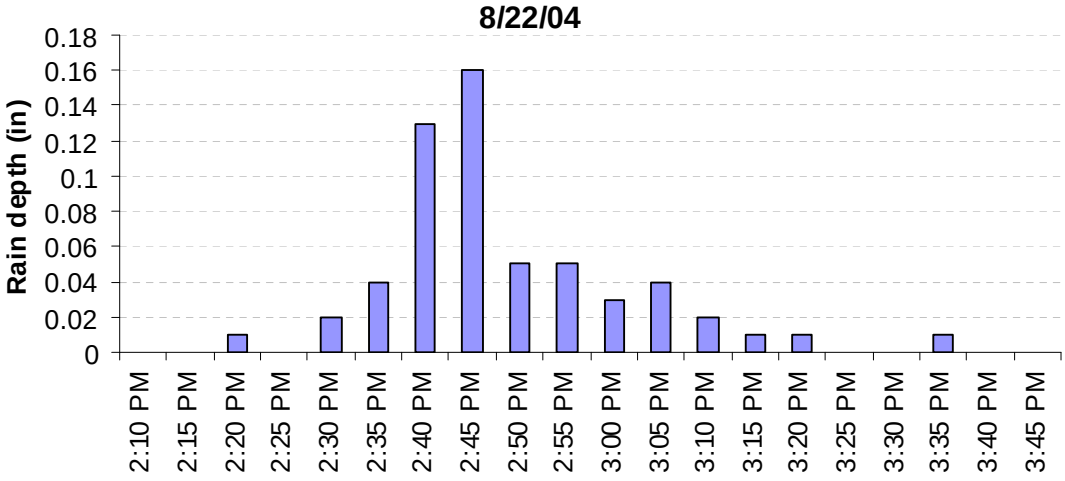

Figure K1

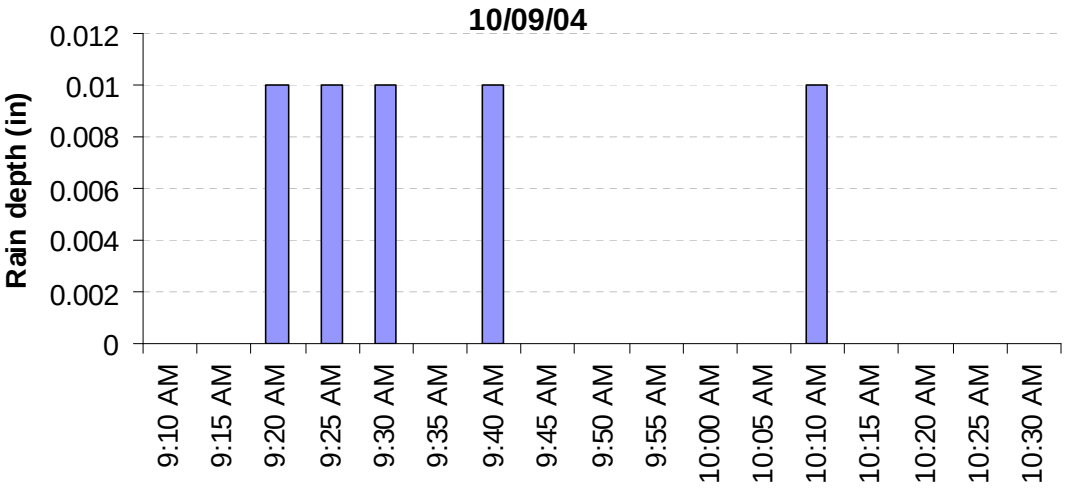

Figure K2

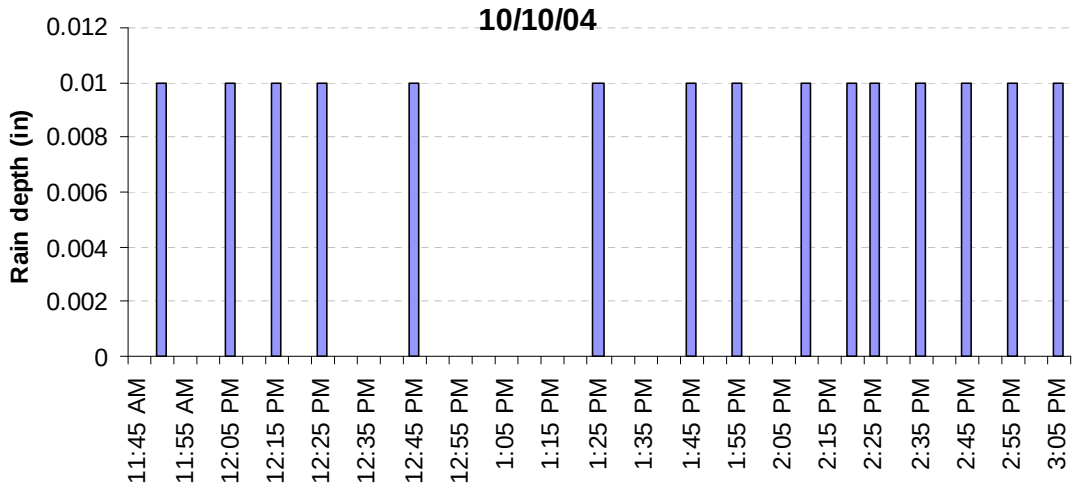

Figure K3

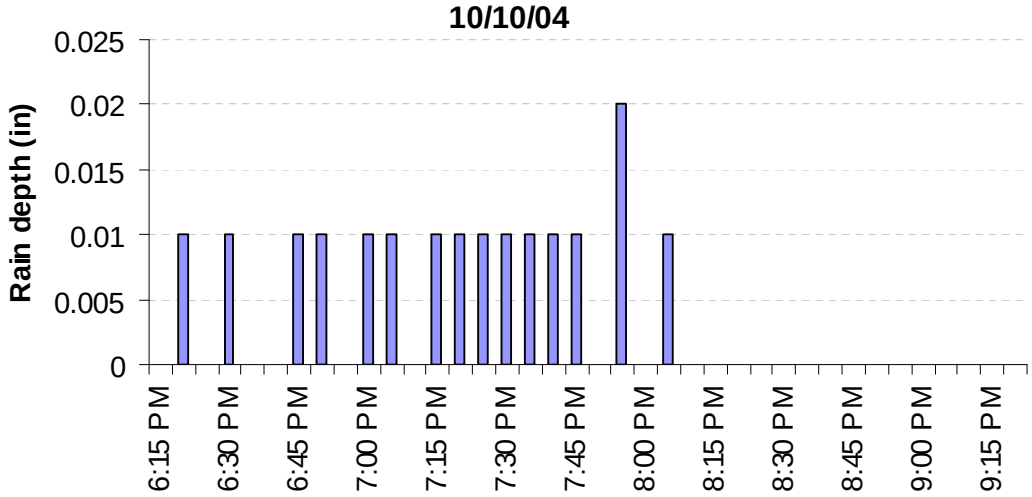

Figure K4

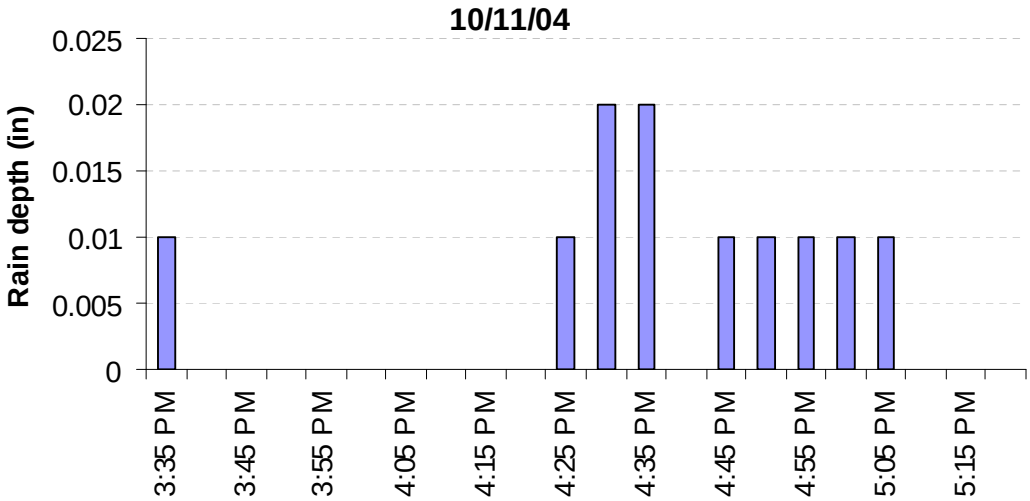

Figure K5

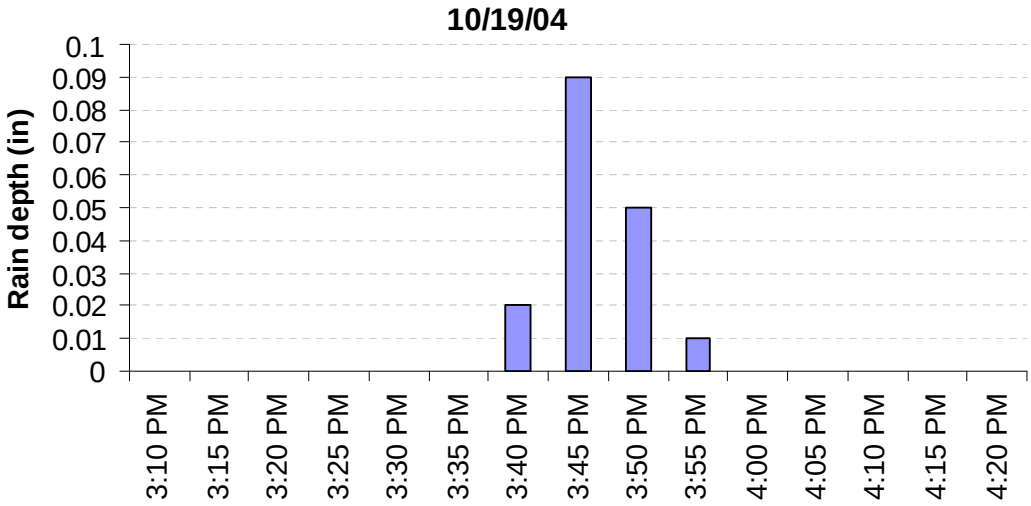

Figure K6

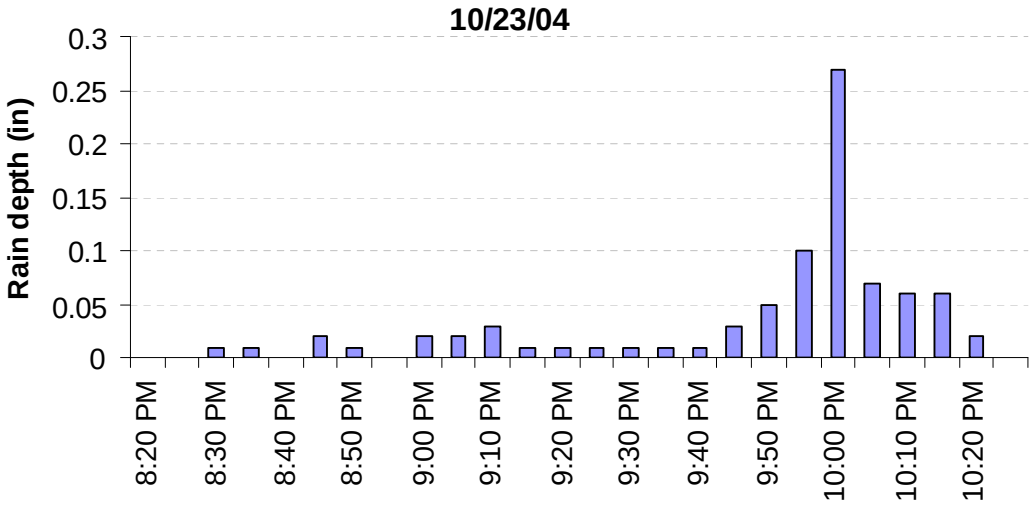

Fig.K7

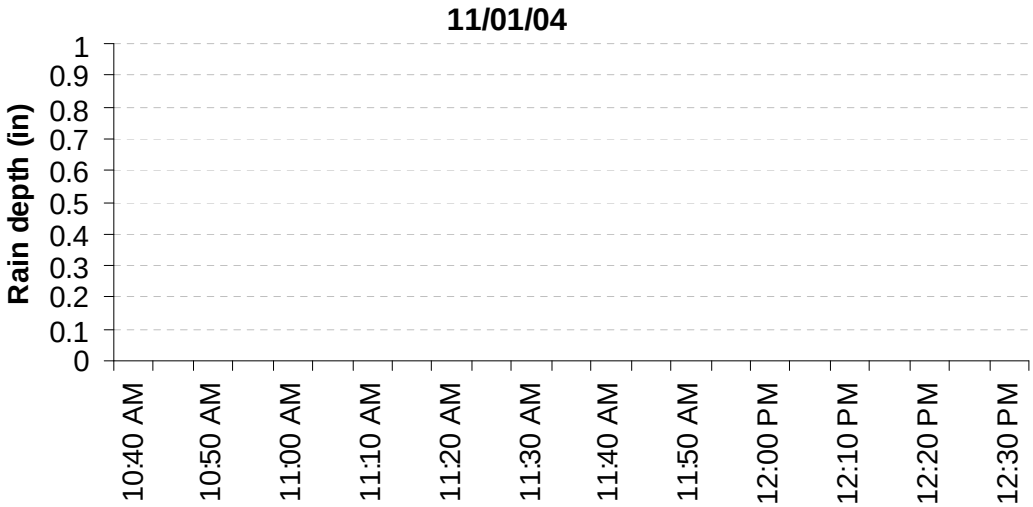

Figure K8

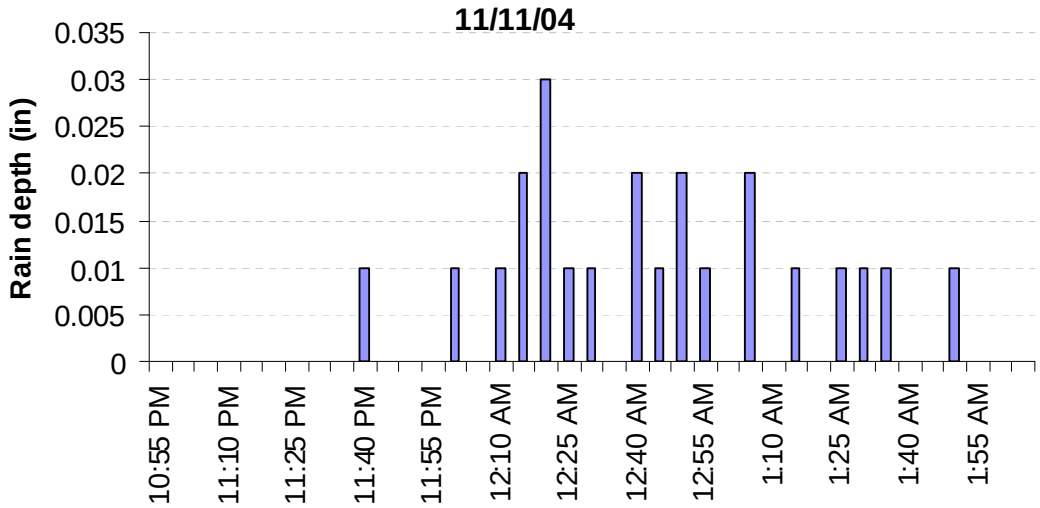

Figure K9

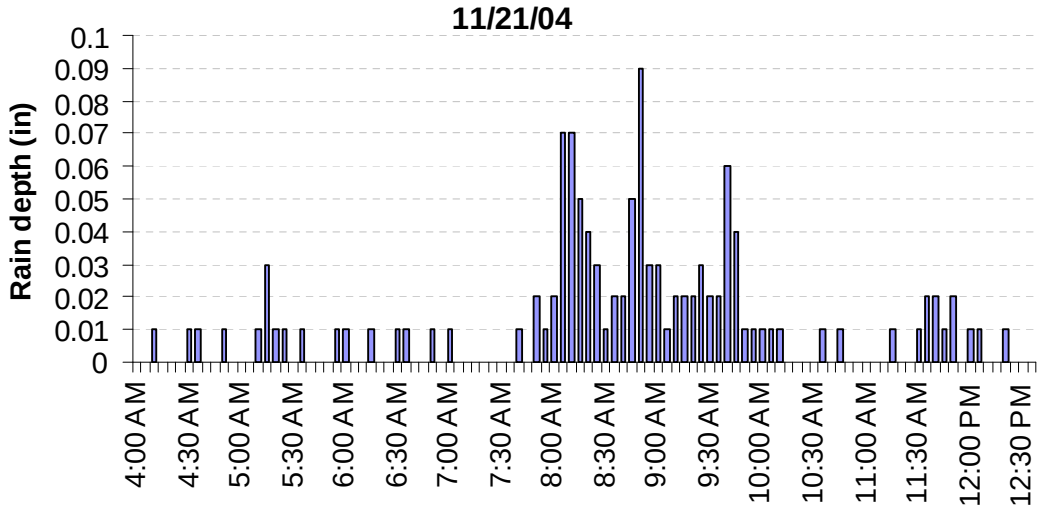

Figure K10

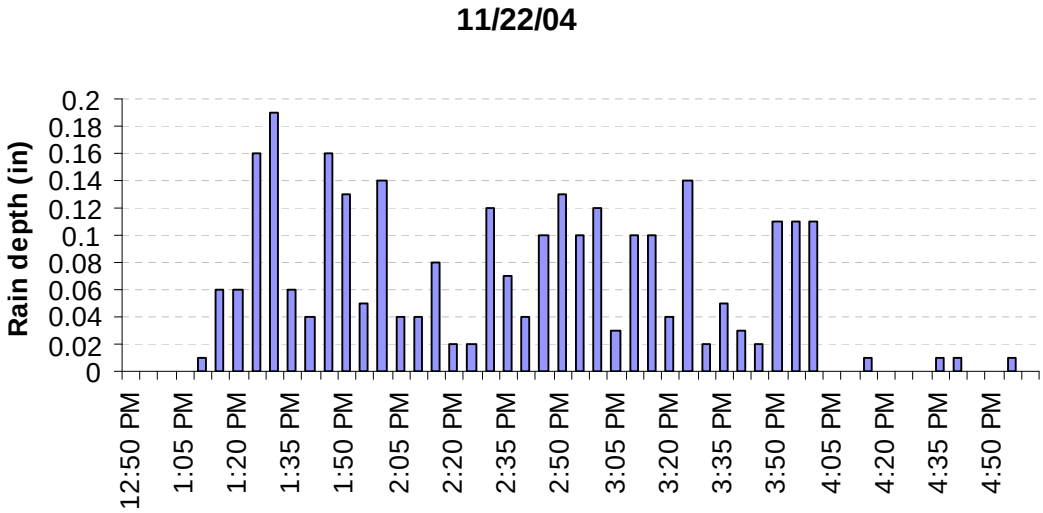

Figure K11

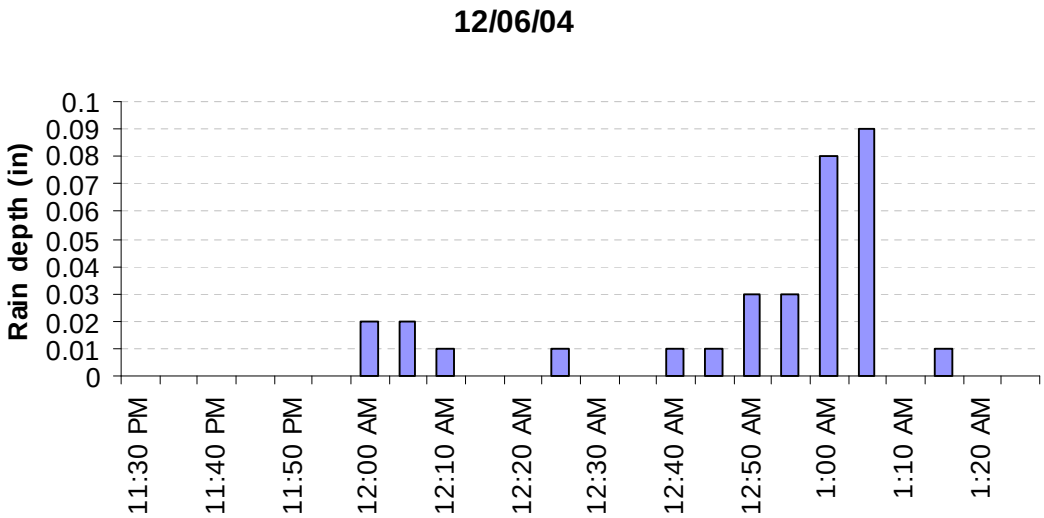

Figure K12

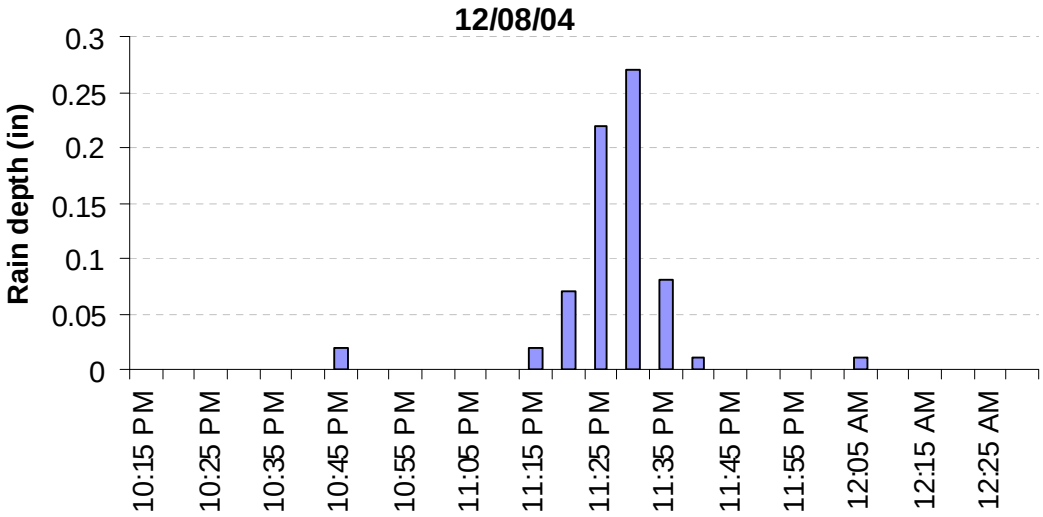
12/08/04
Rain depth (in)
0.3
0.25
0.2
0.15
0.1
0.05
0
10:15 PM
10:25 PM
10:35 PM
10:45 PM
10:55 PM
11:05 PM
11:15 PM
11:25 PM
11:35 PM
11:45 PM
11:55 PM
12:05 AM
12:15 AM
12:25 AM

Figure K13

Appendix L: Infiltration Rates of Soils at the Outdoor Grass Swale Site

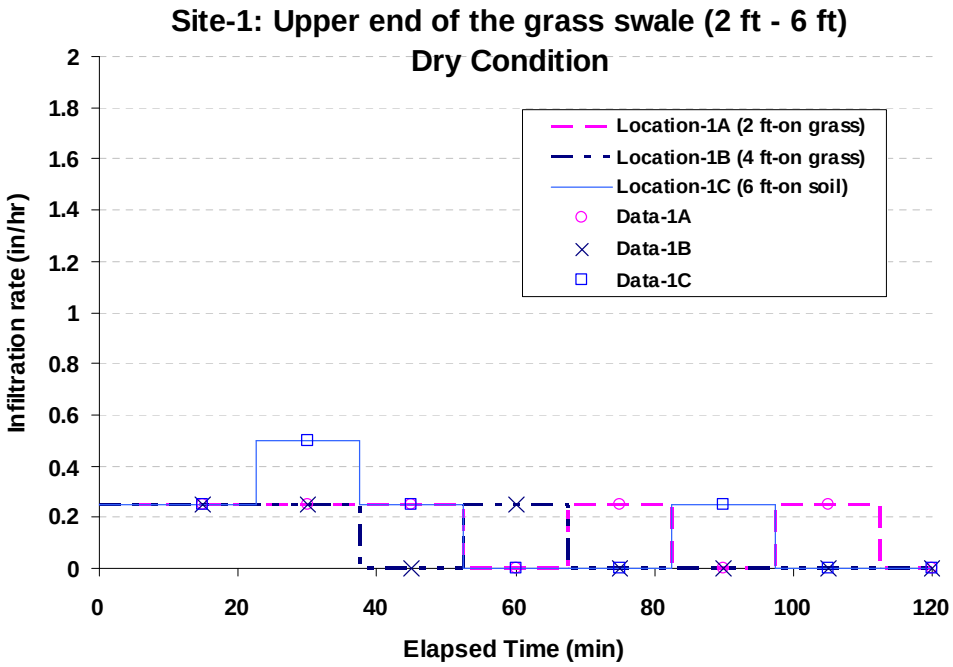

Figure L1

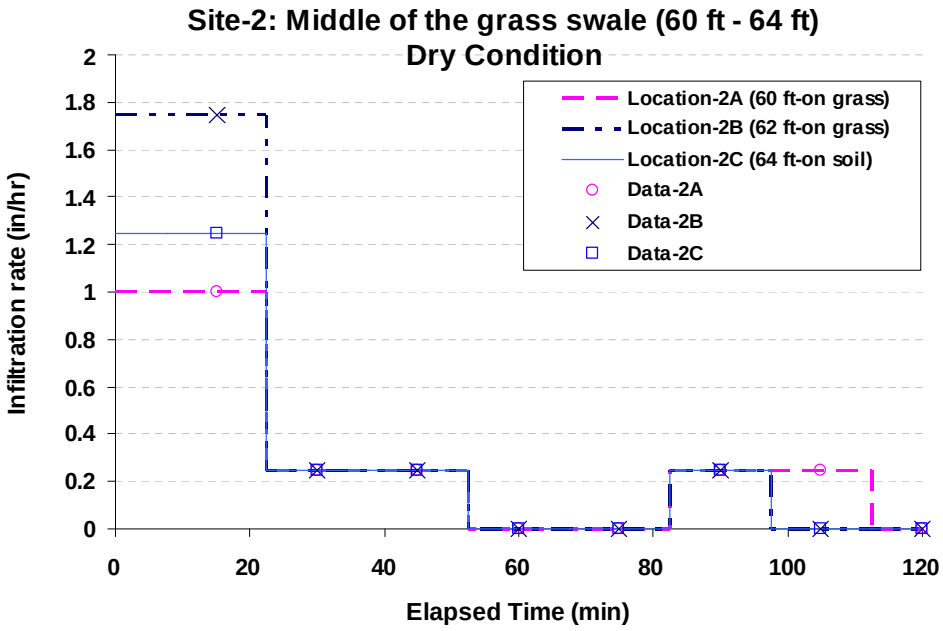

Figure L2

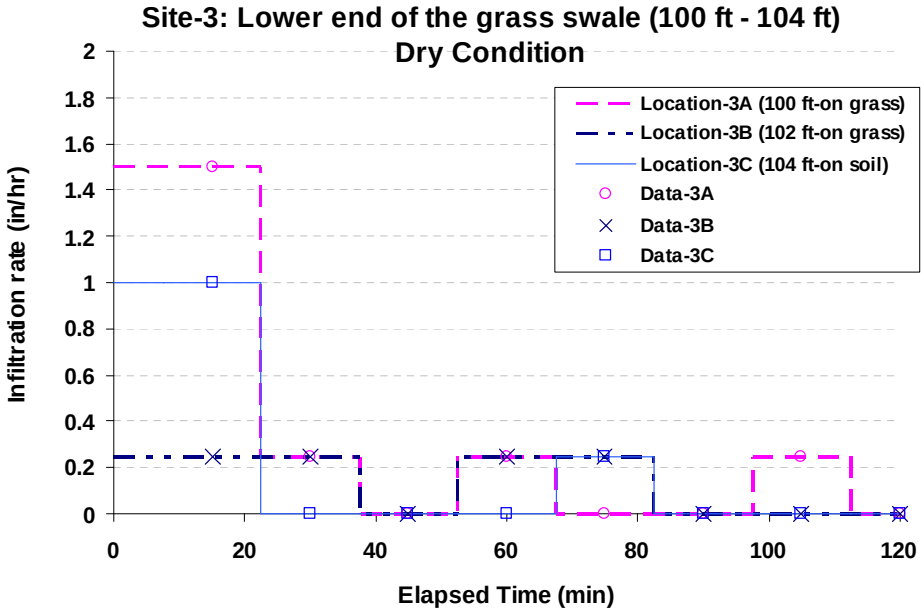

Figure L3

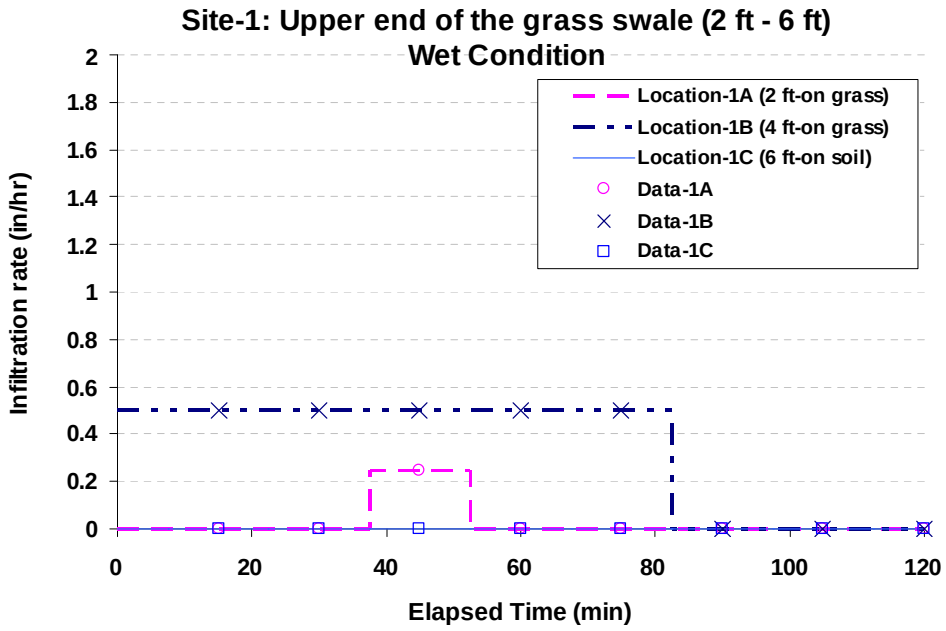

Figure L4

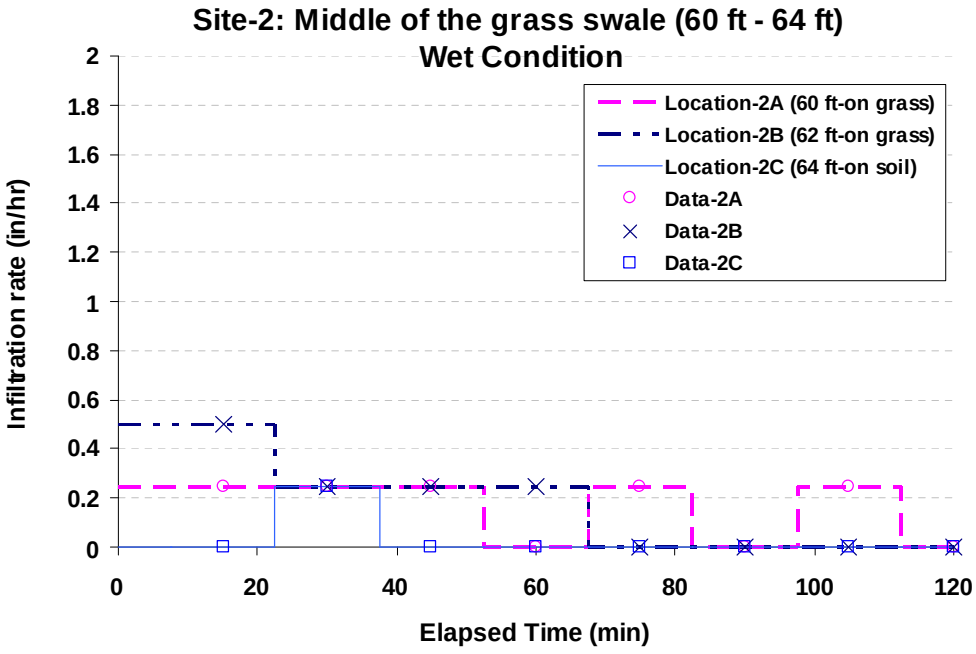

Figure L5

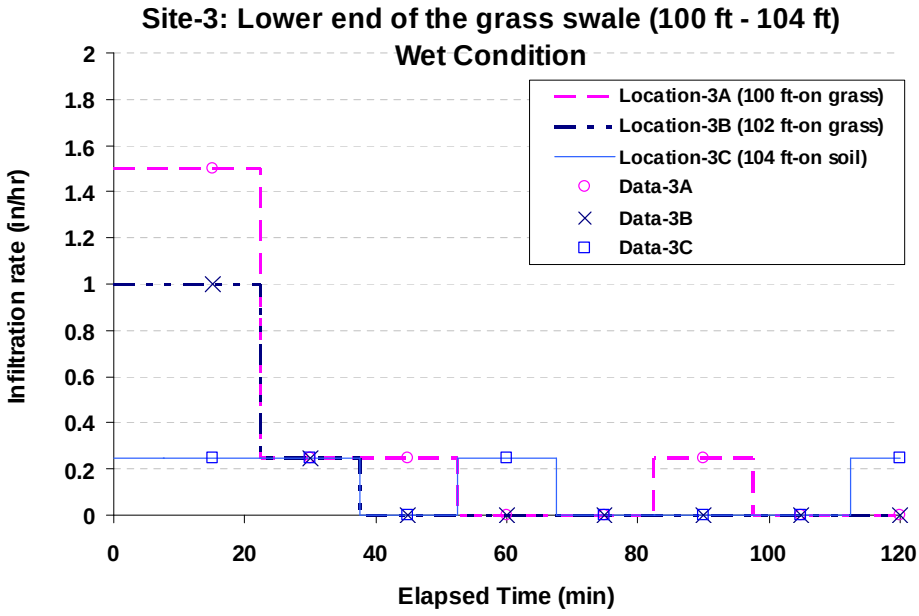
Site-3: Lower end of the grass swale (100 ft - 104 ft)
Wet Condition
Location-3A (100 ft-on grass)
Location-3B (102 ft-on grass)
Location-3C (104 ft-on soil)
Data-3A
Data-3B
Data-3C
Infiltration rate (in/hr)
Elapsed Time (min)
0
0.2
0.4
0.6
0.8
1
1.2
1.4
1.6
1.8
2
0
20
40
60
80
100
120

Figure L6

Appendix M: Cross-Sectional Elevation Profiles of the Outdoor Grass Swale

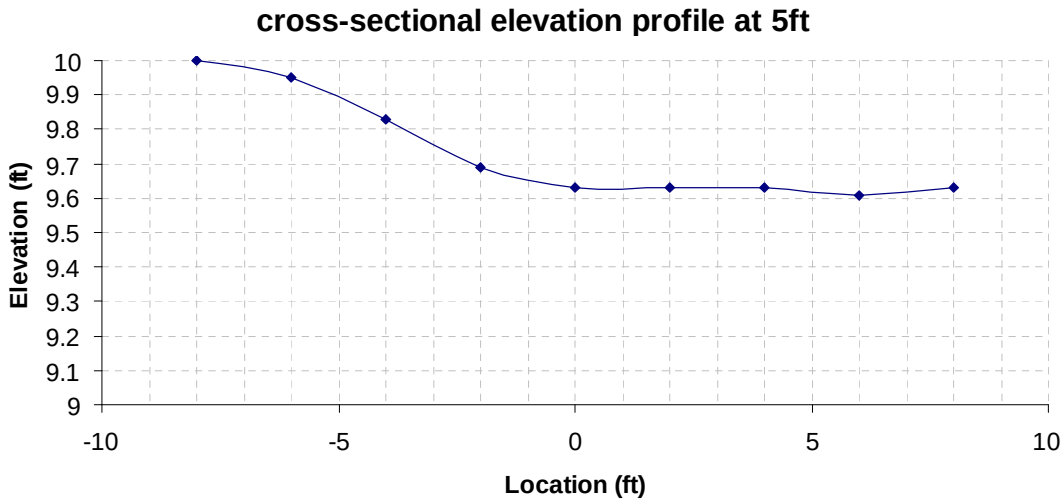

Figure M1

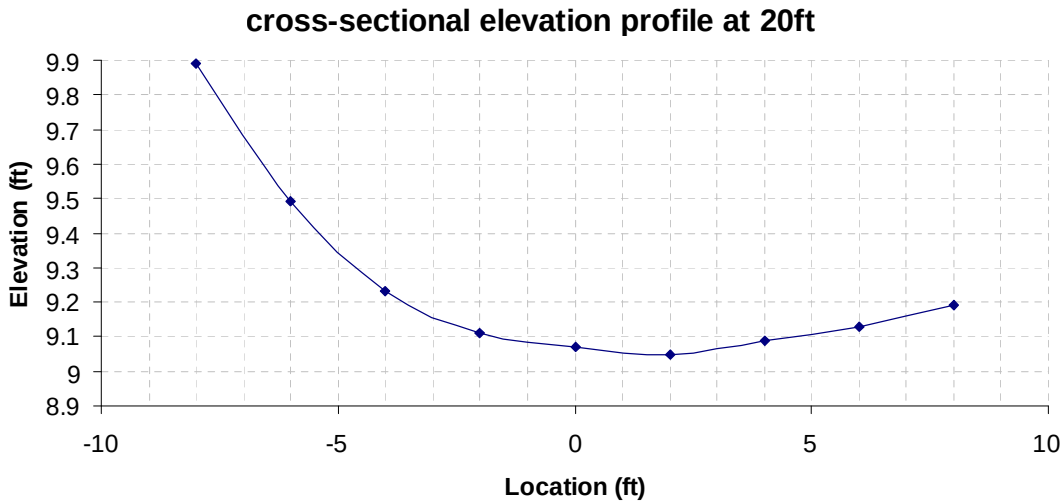

Figure M2

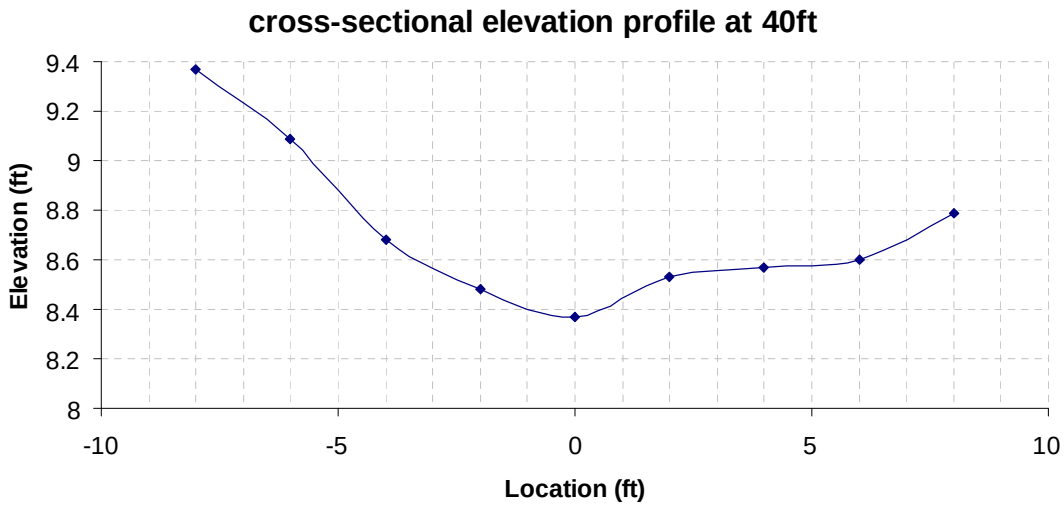

Figure M3

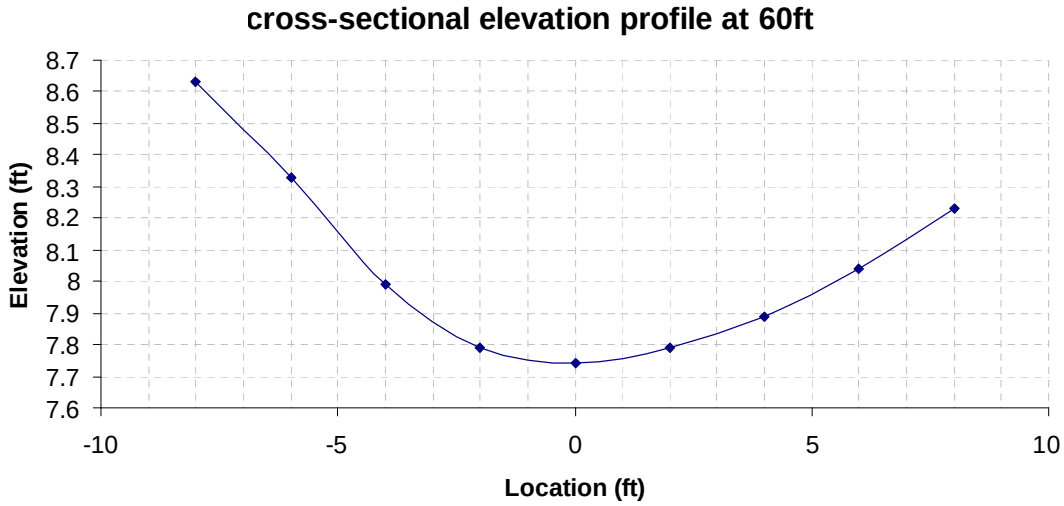

Figure M4

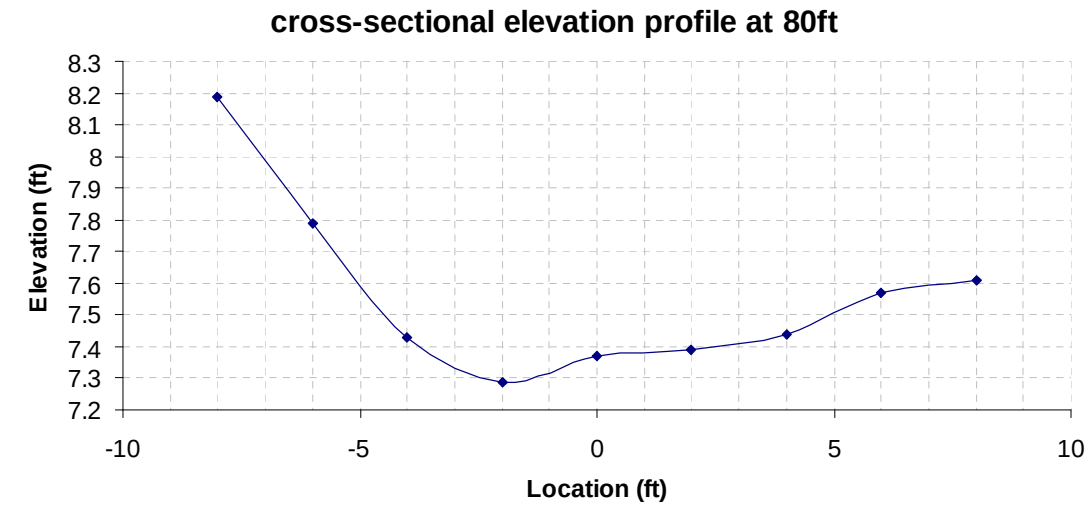

Figure M5

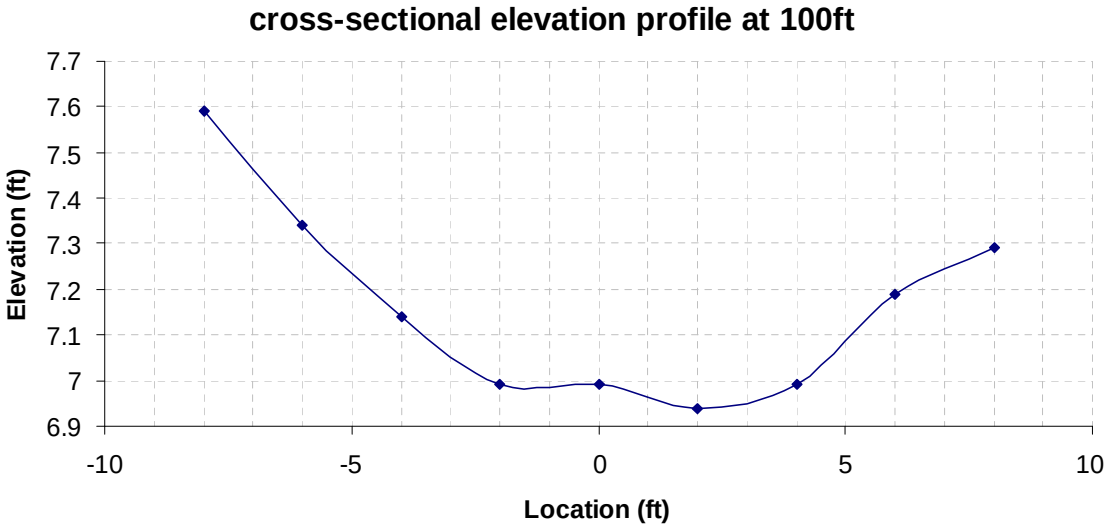

Figure M6

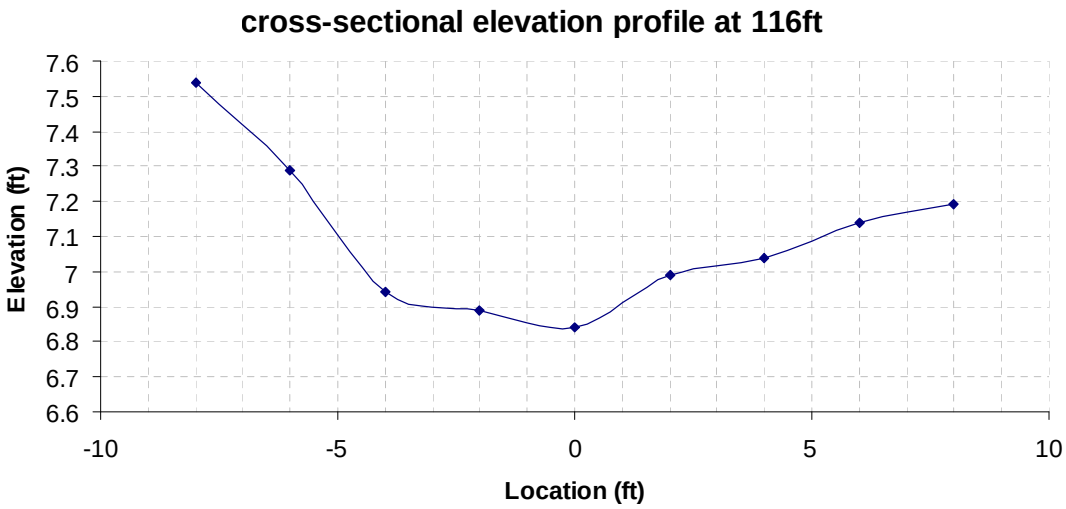
cross-sectional elevation profile at 116ft
Elevation (ft)
7.6
7.5
7.4
7.3
7.2
7.1
7
6.9
6.8
6.7
6.6
-10
-5
0
5
10
Location (ft)

Figure M7

Appendix N: Outdoor Swale – Removal Efficiencies Observed for the Different Constituents

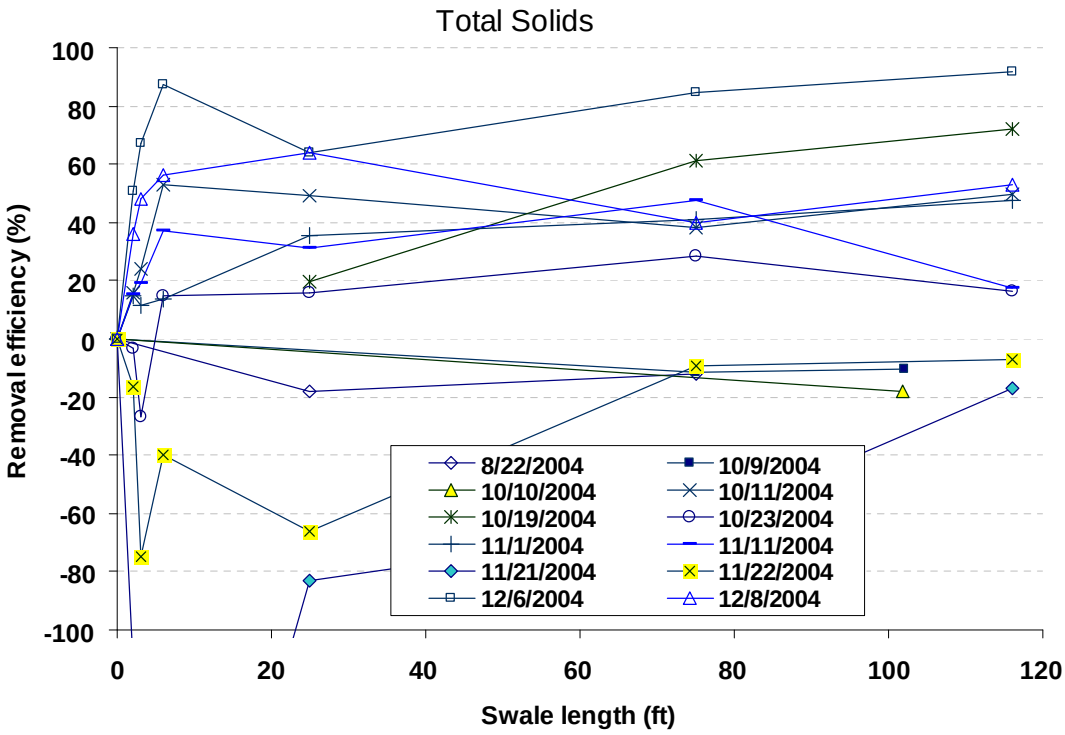

Figure N1

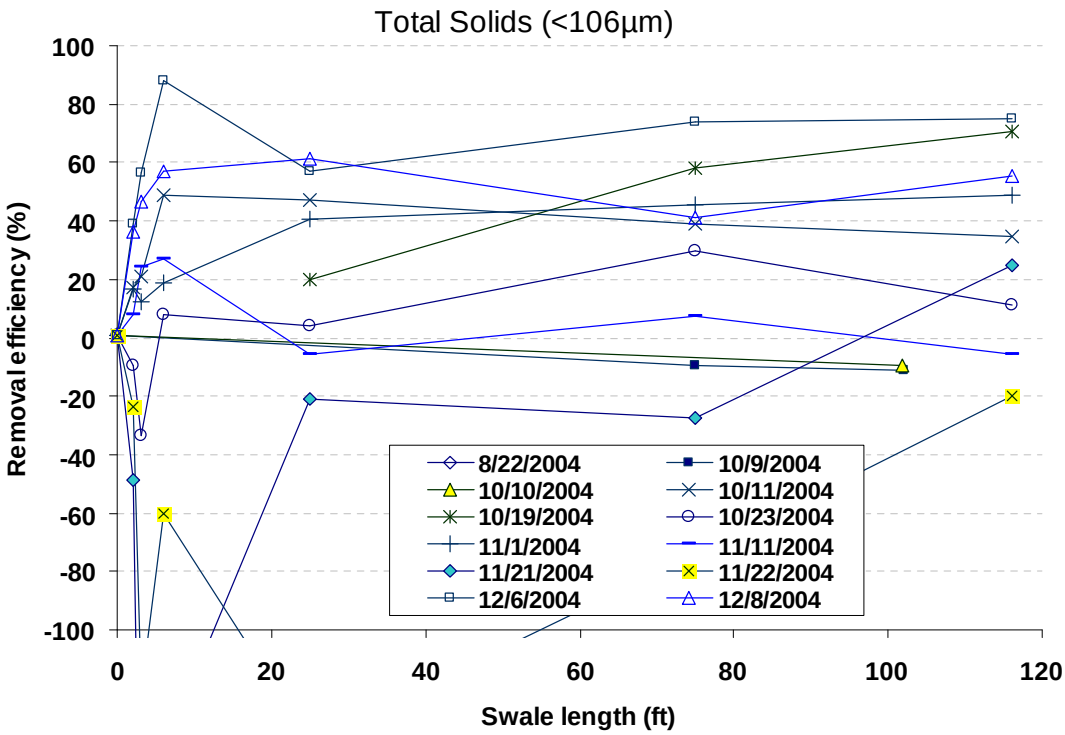

Figure N2

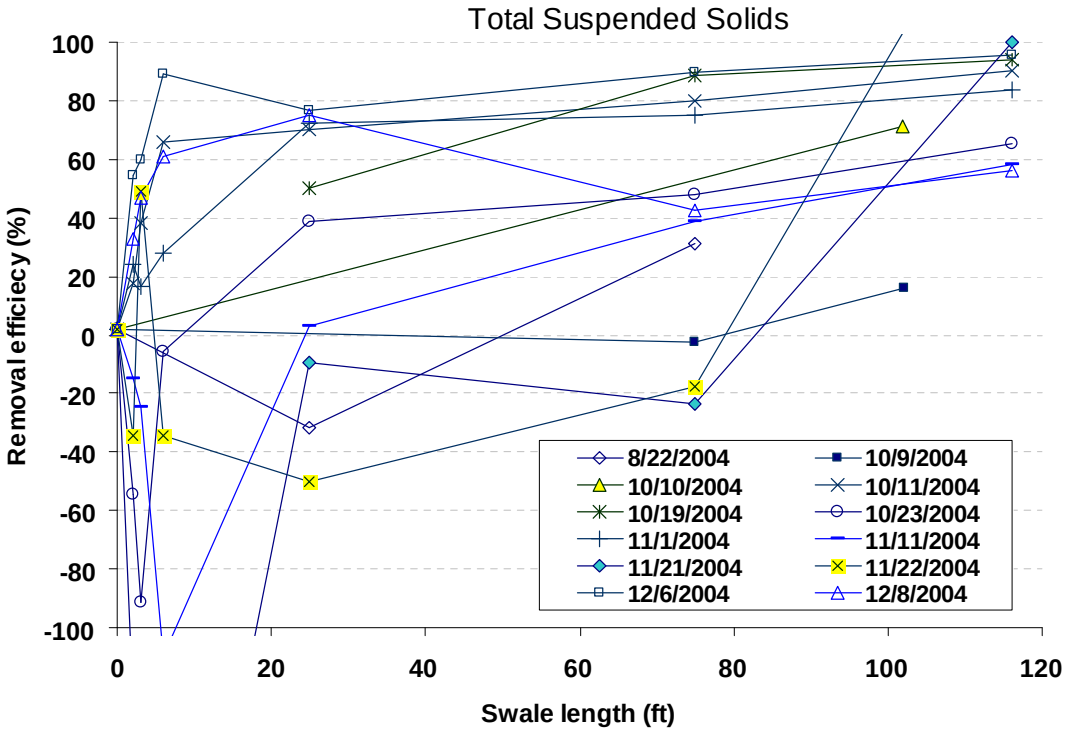

Figure N3

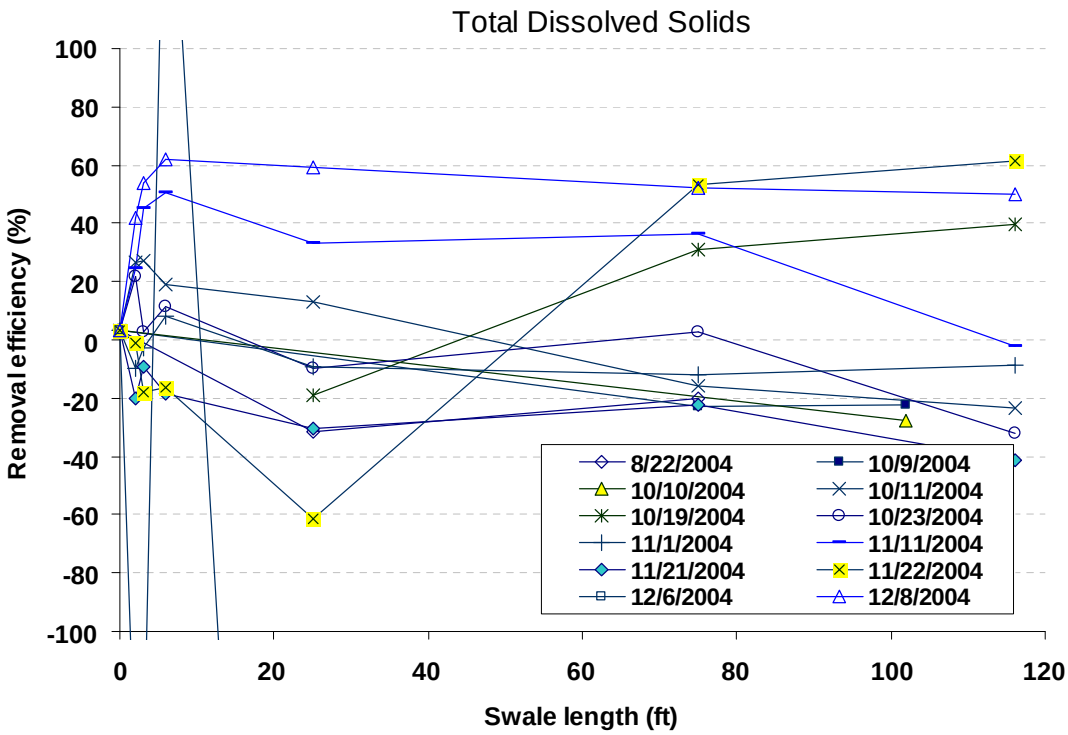

Figure N4

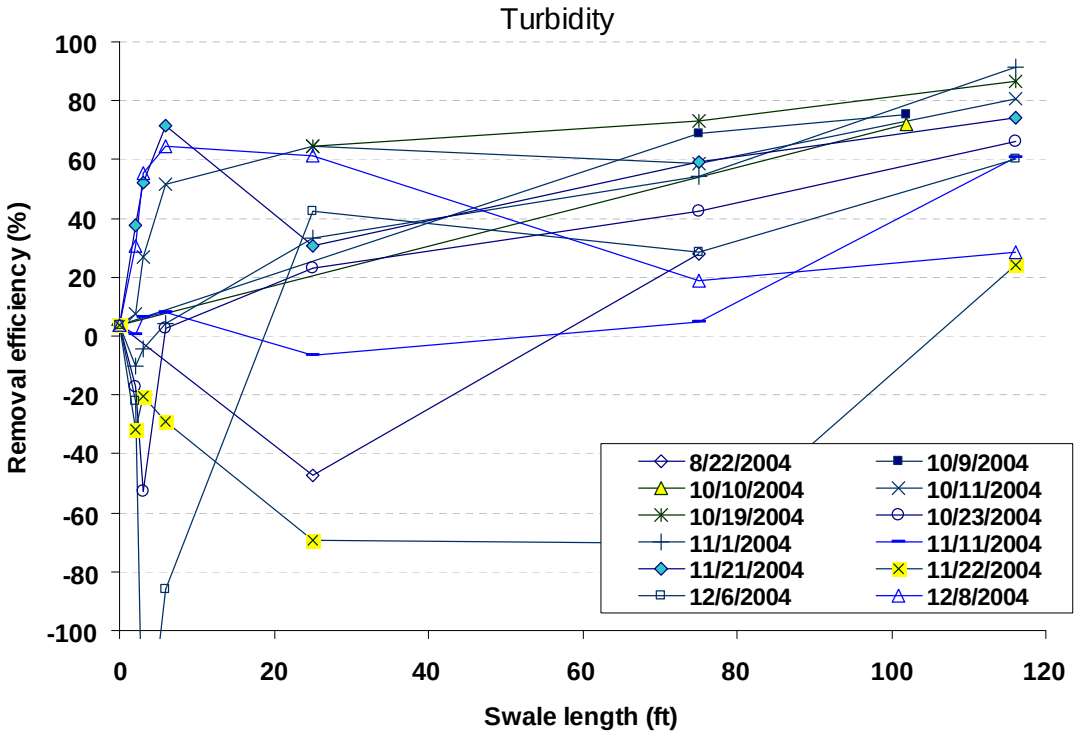

Figure N5

Appendix O: Outdoor Swale –Particle Size Distributions for each Sample

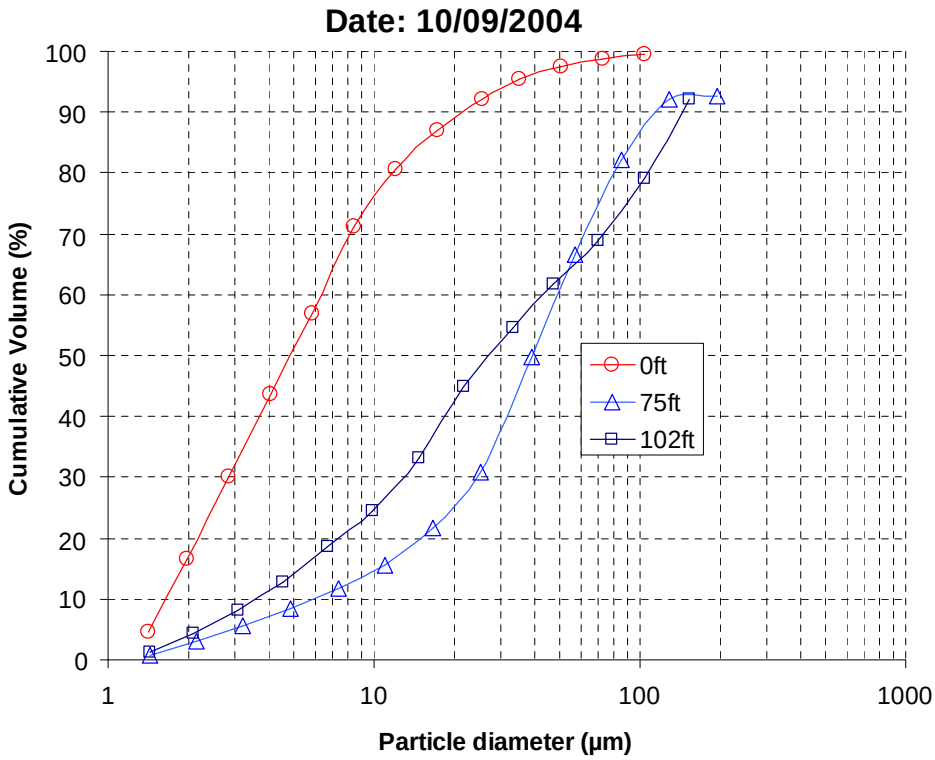

Figure O1

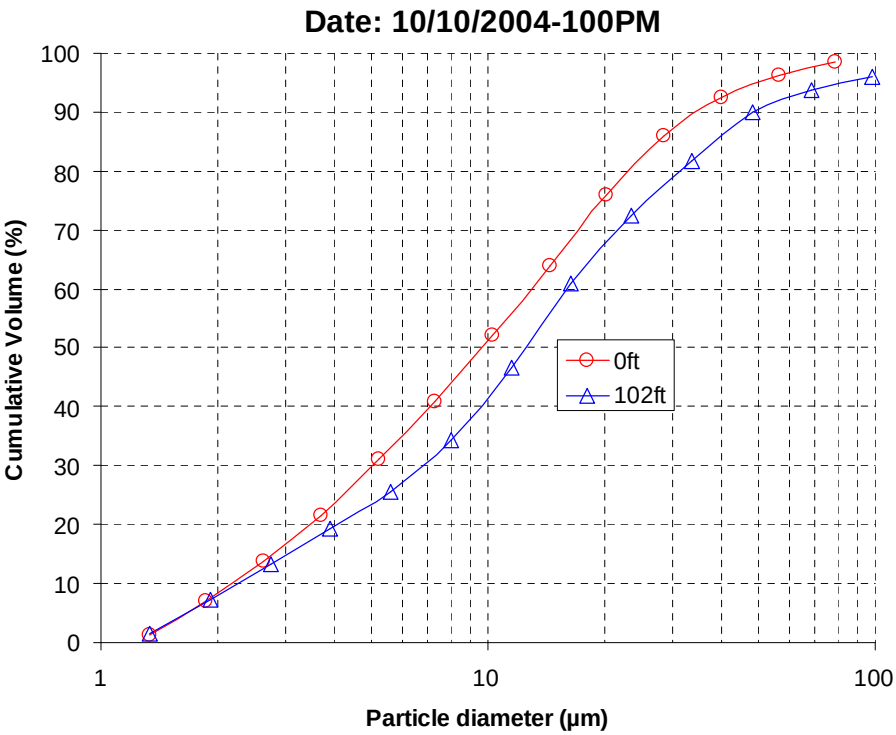

Figure O2

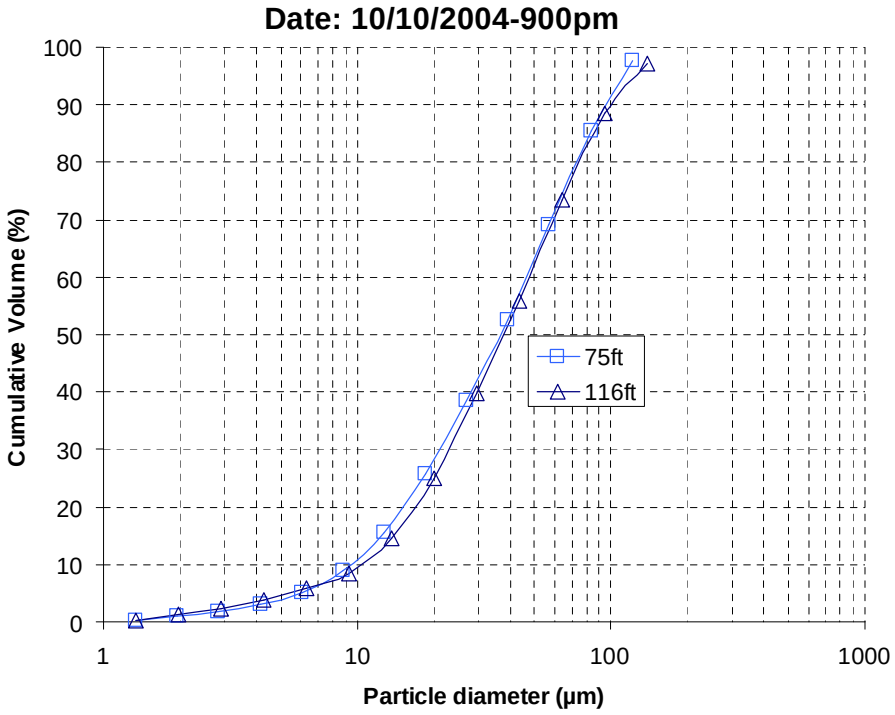

Figure O3

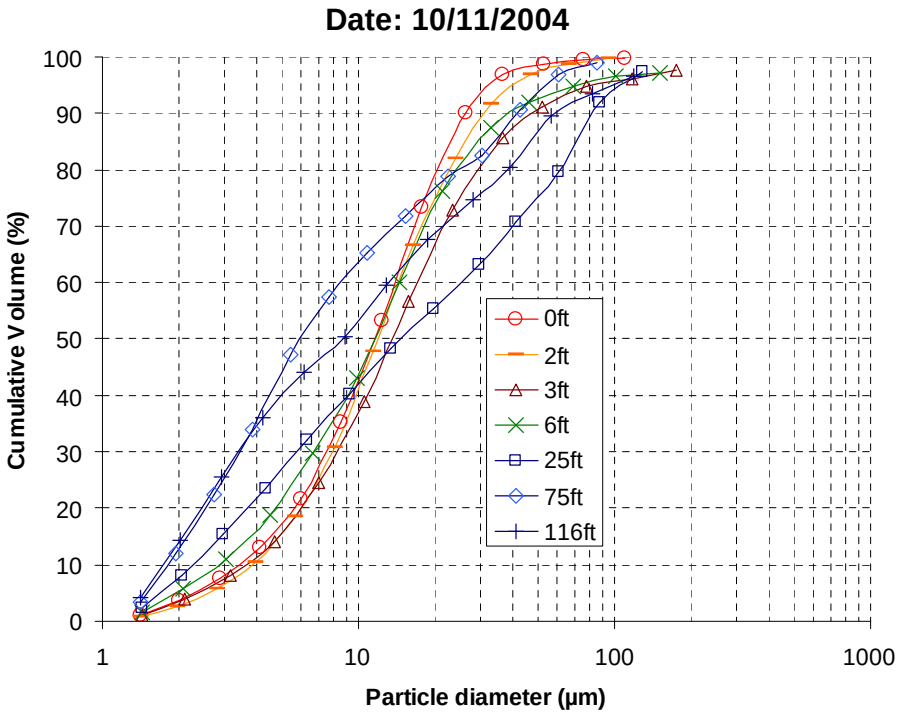

Figure O4

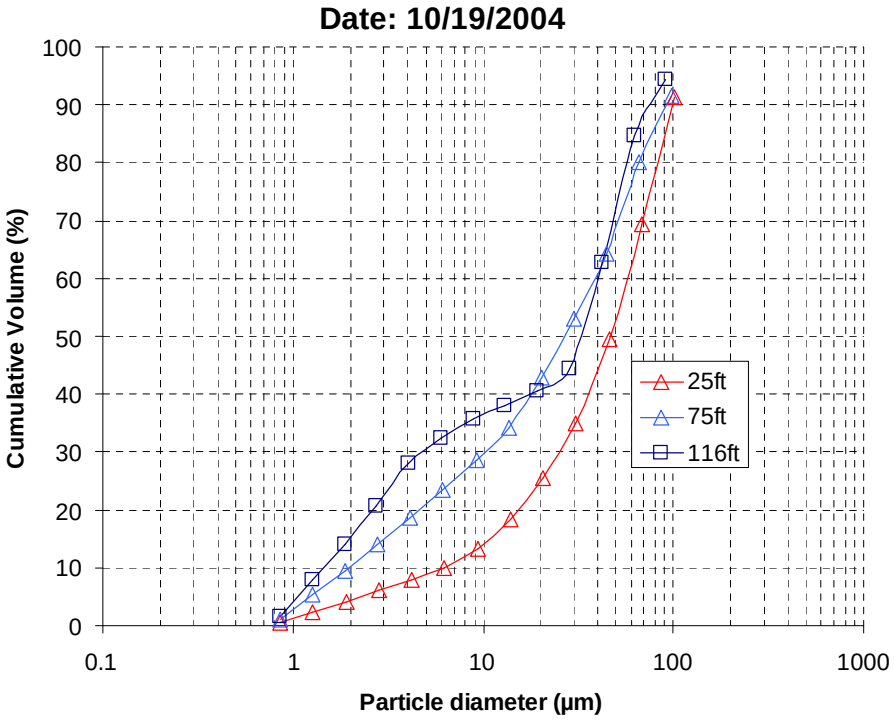

Figure O5

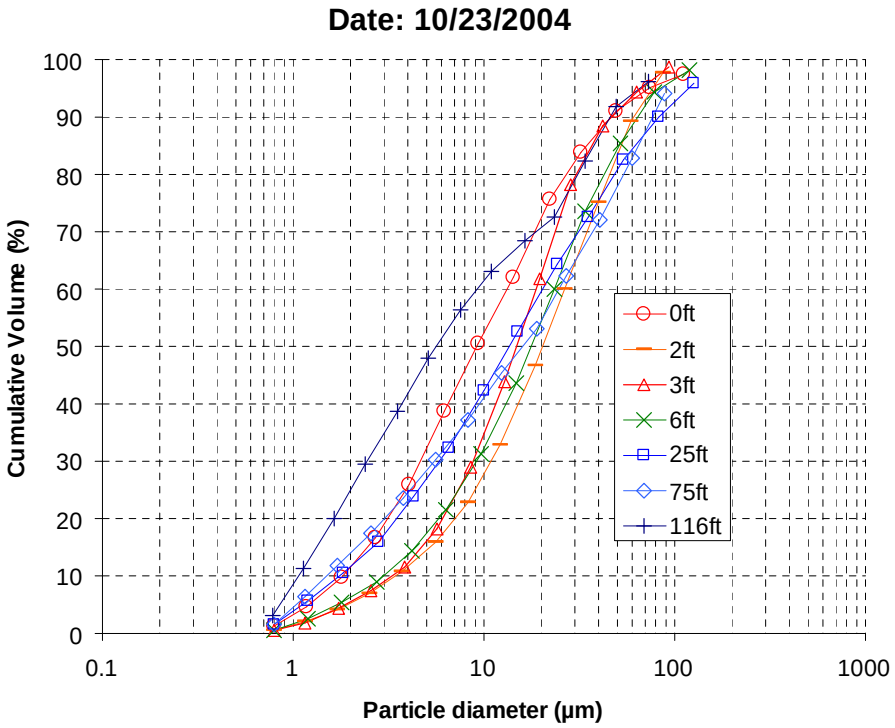

Figure O6

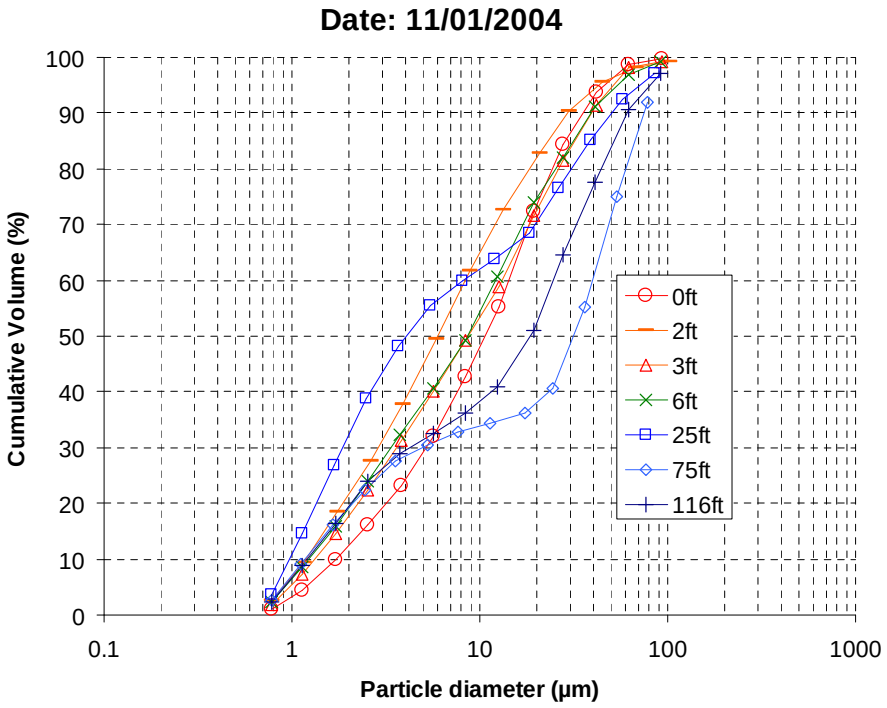

Figure O7

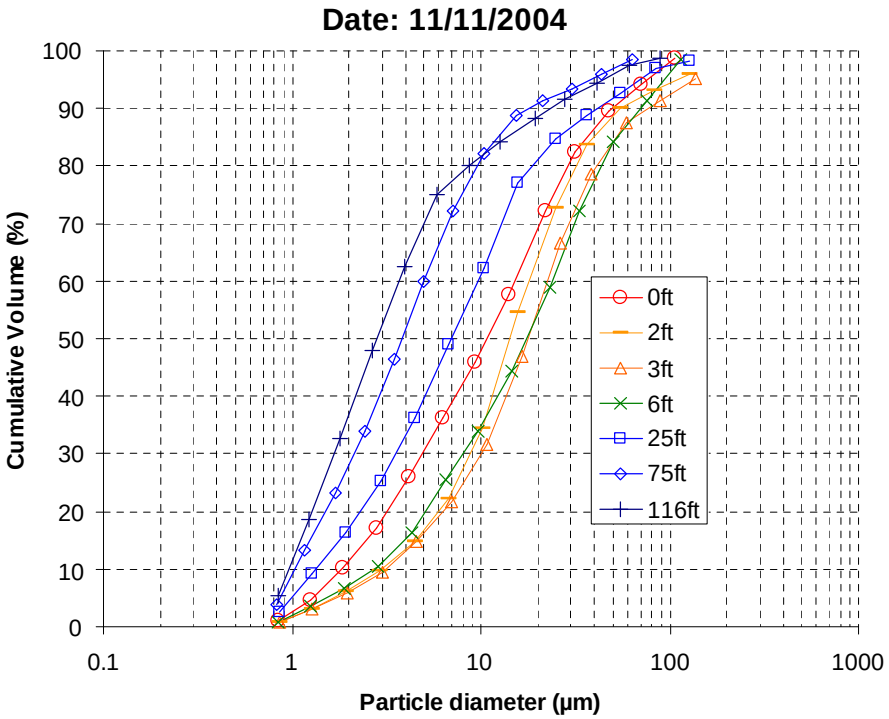

Figure O8

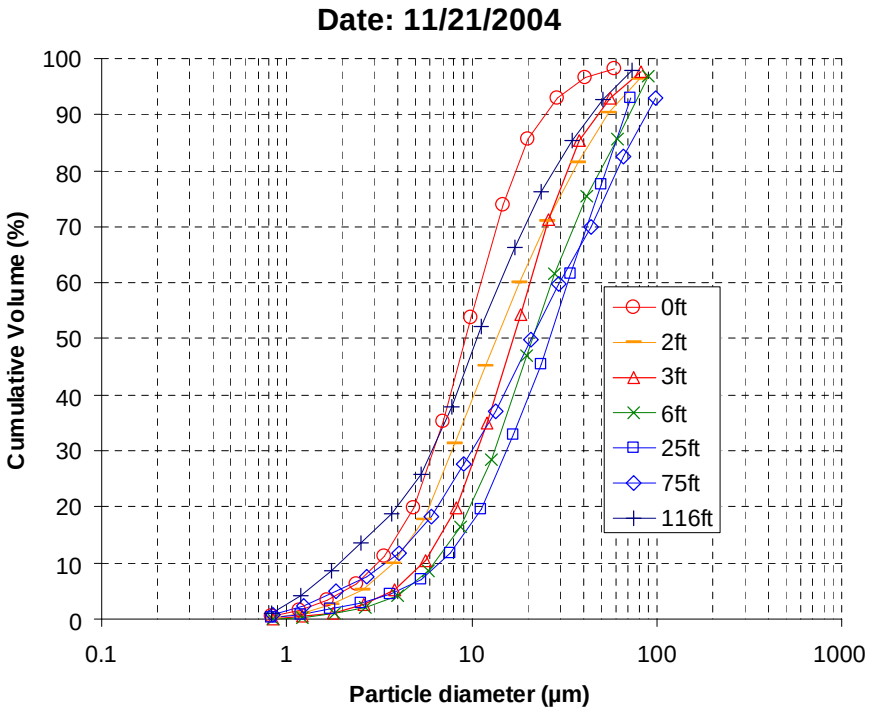

Figure O9

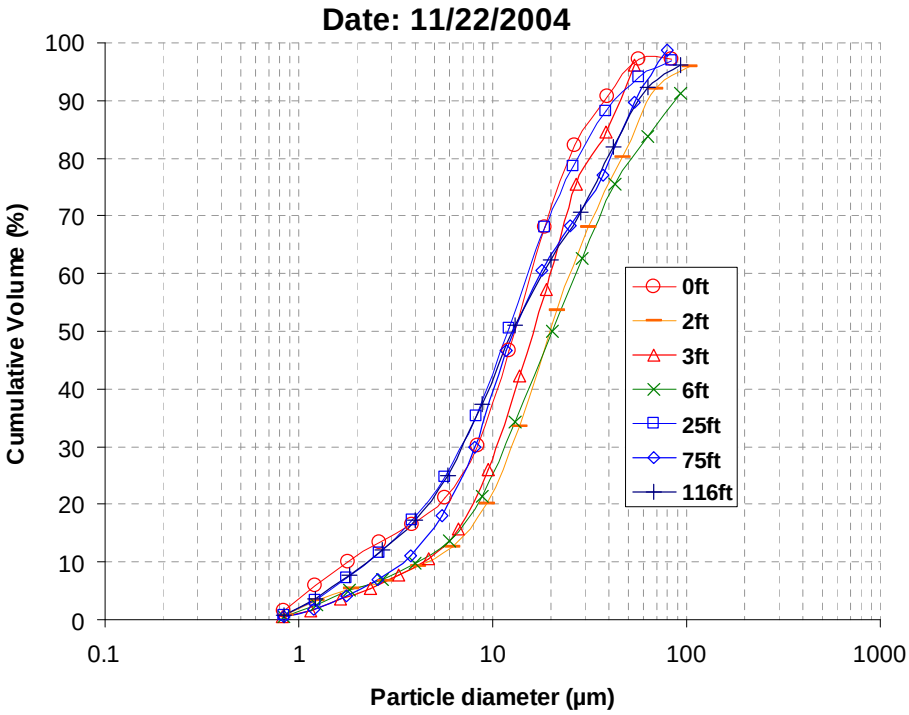

Figure O10

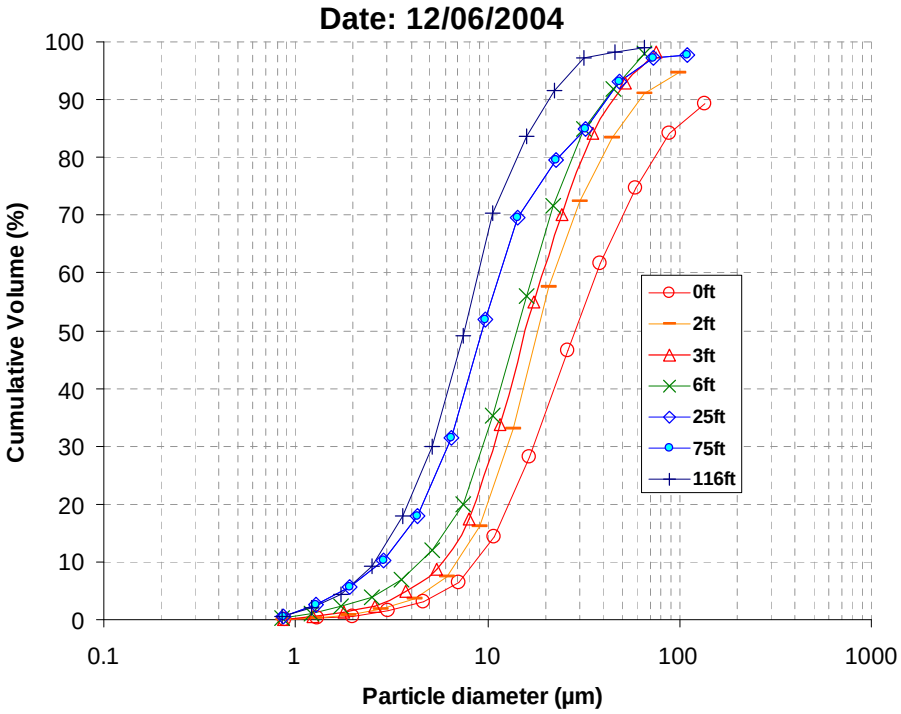

Figure O11

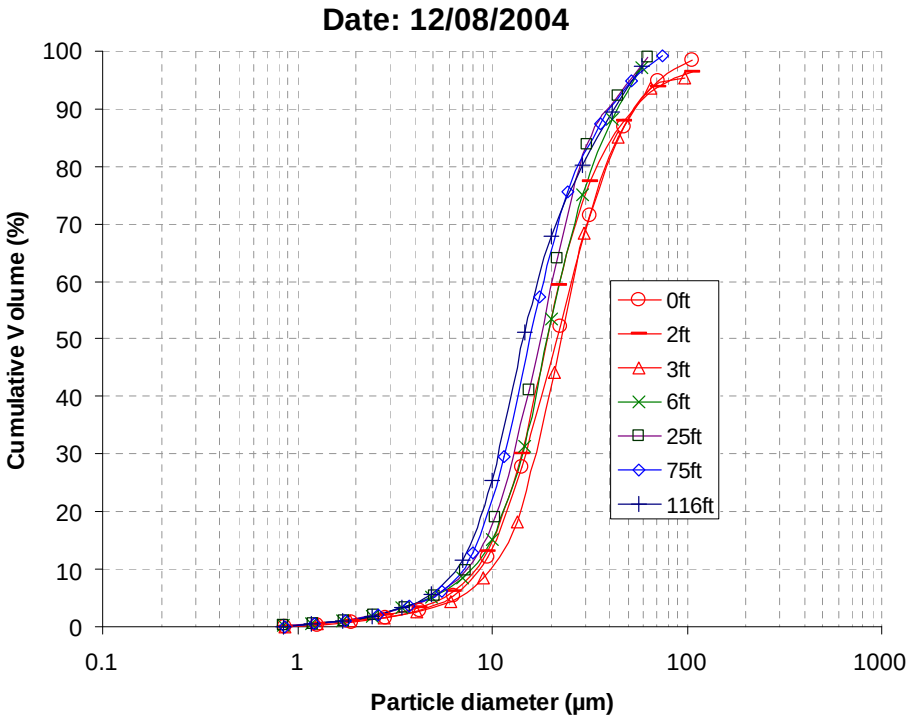
Date: 12/08/2004
Cumulative Volume (%)
Particle diameter (µm)
0
10
20
30
40
50
60
70
80
90
100
0.1
1
10
100
1000
0ft
2ft
3ft
6ft
25ft
75ft
116ft

Figure O12

Appendix P: Outdoor Swale – Graphs of Sediment Concentrations for Different Particle Ranges and Observed Irreducible Concentrations

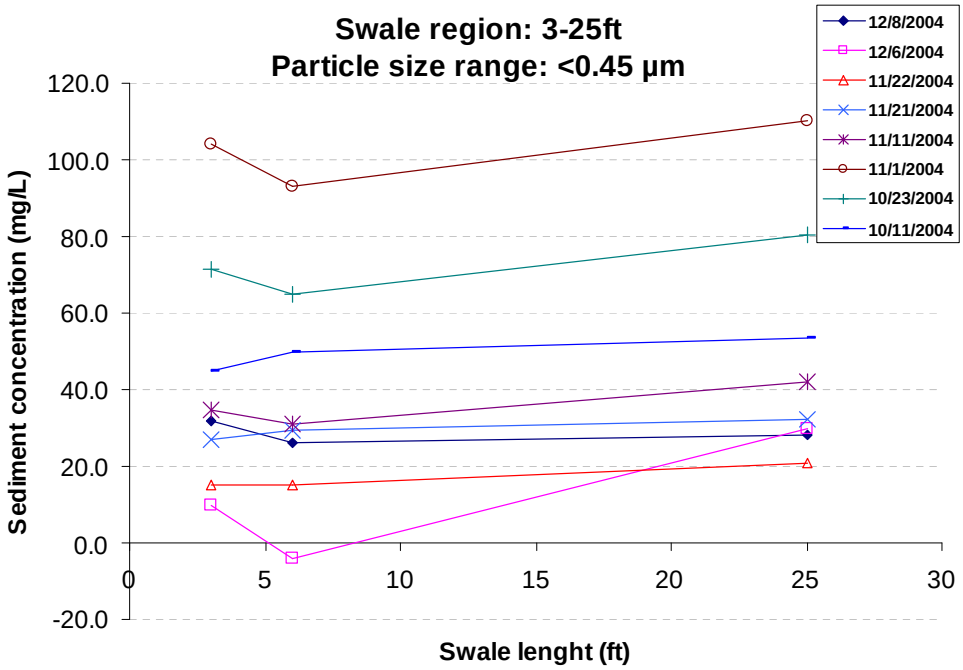

Figure P1

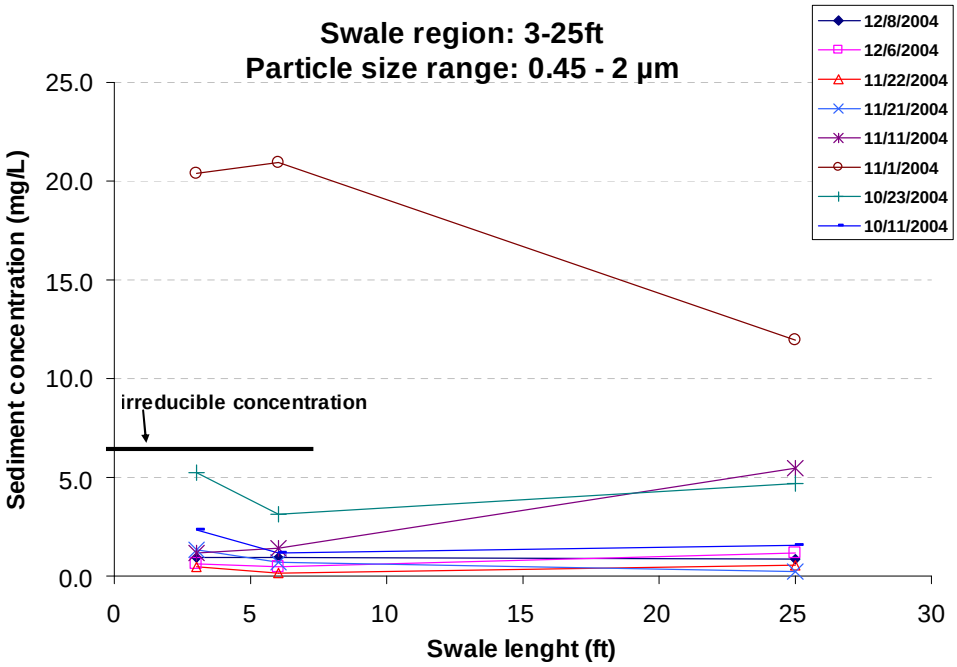

Figure P2

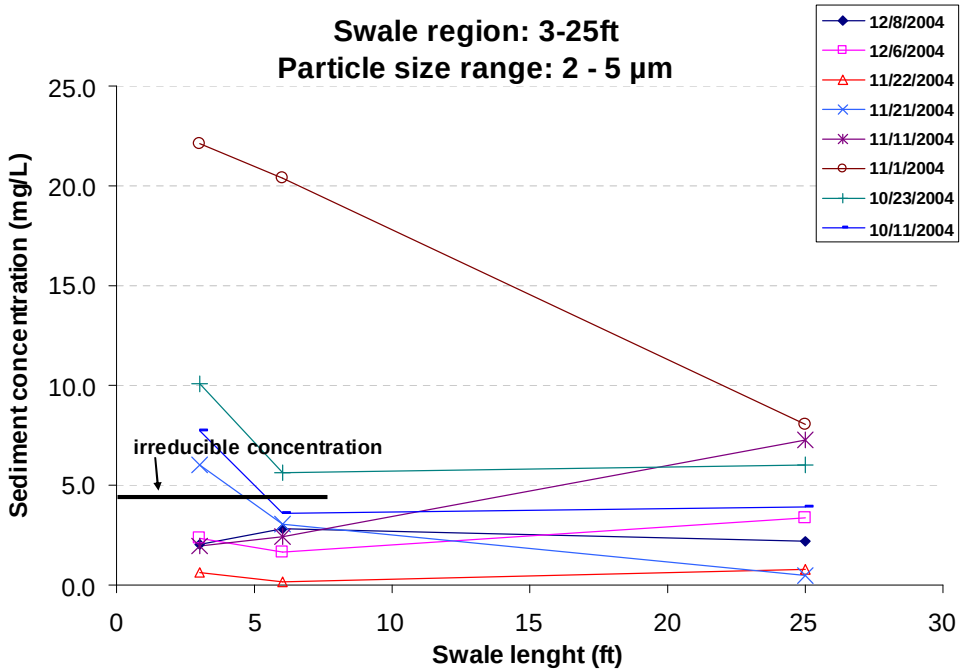

Figure P3

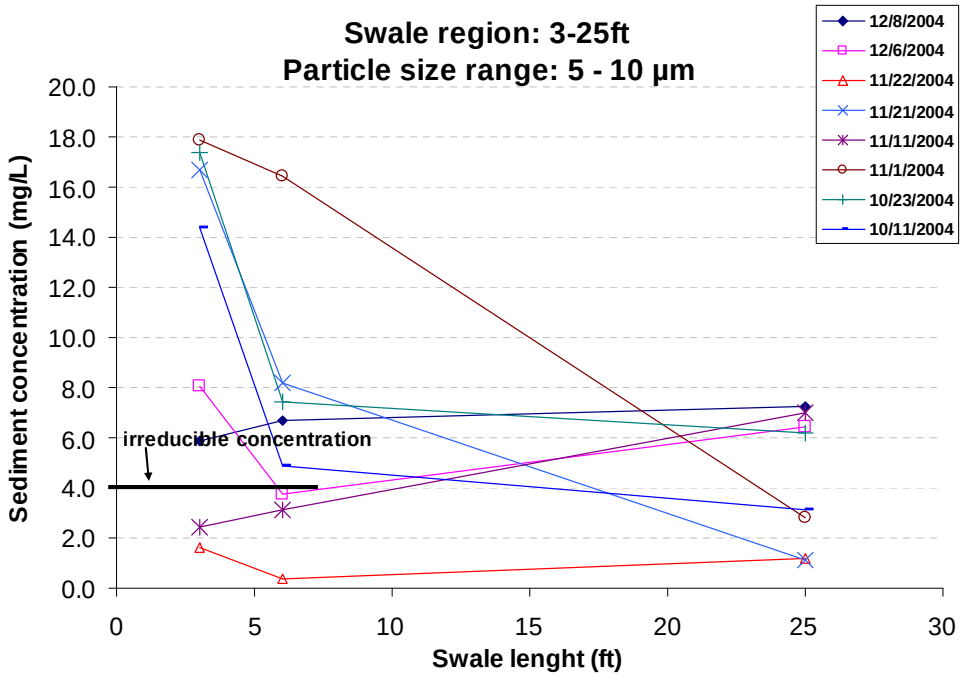

Figure P4

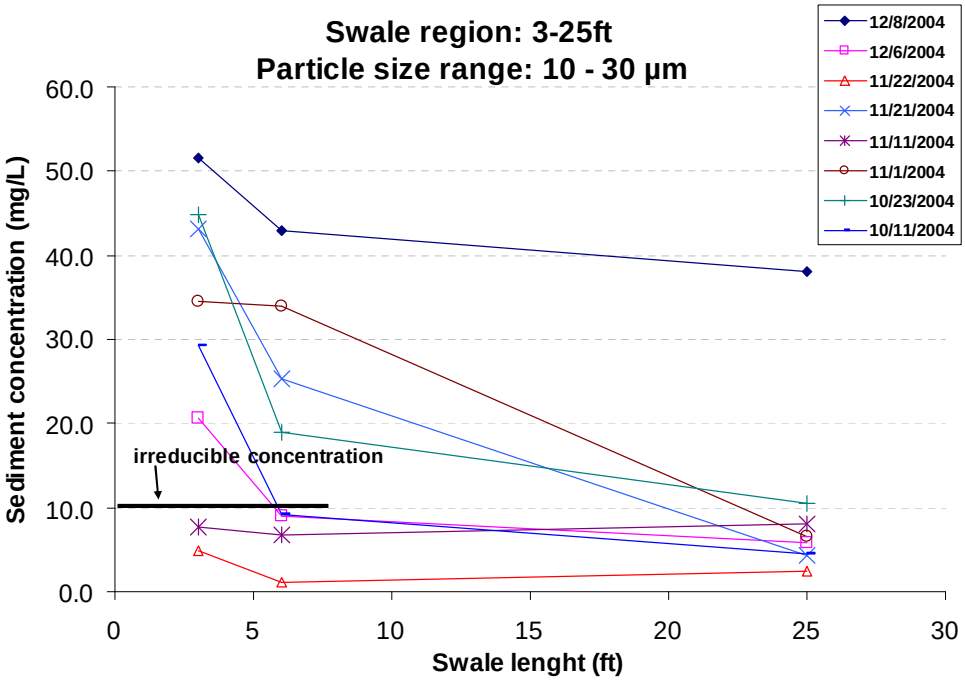

Figure P5

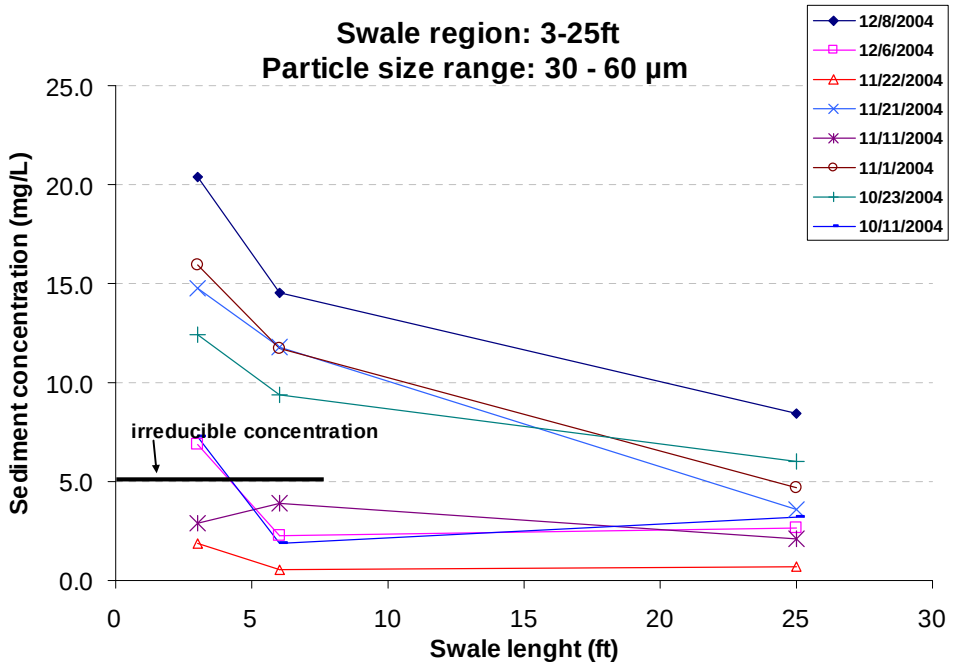

Figure P6

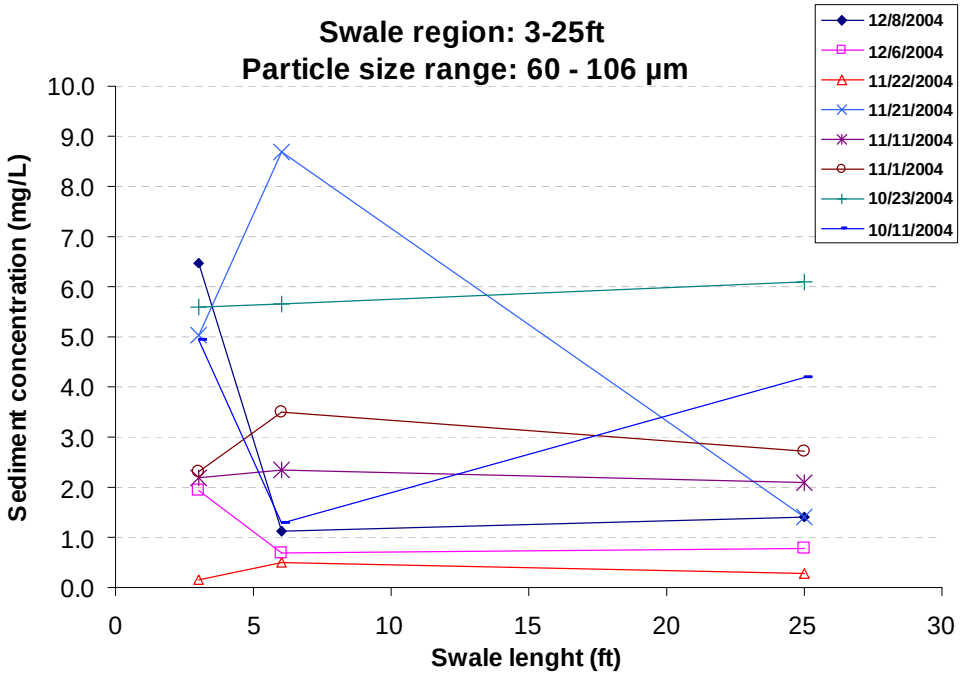

Figure P7

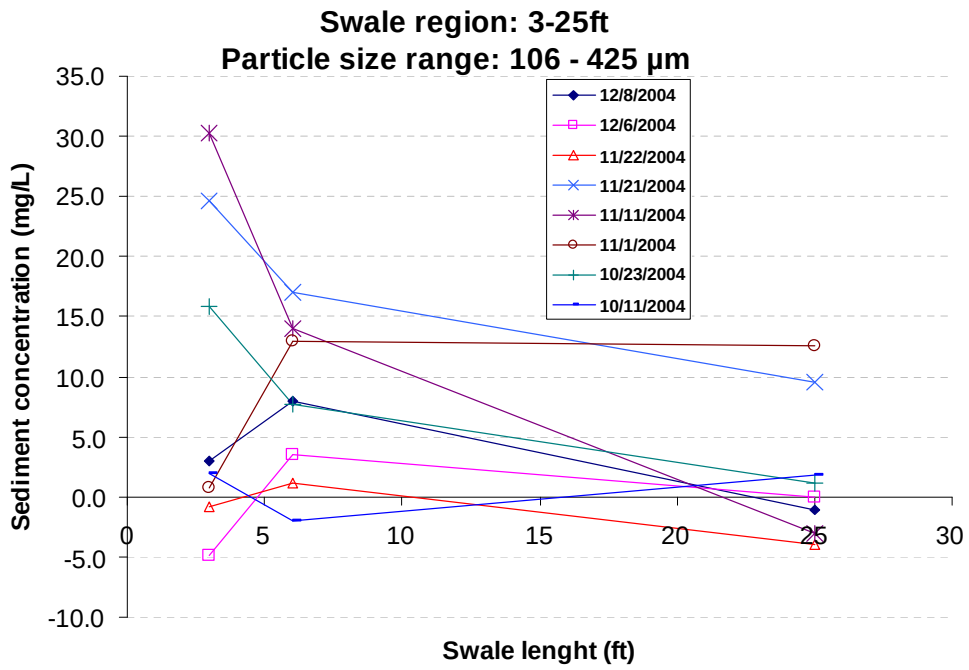

Figure P8

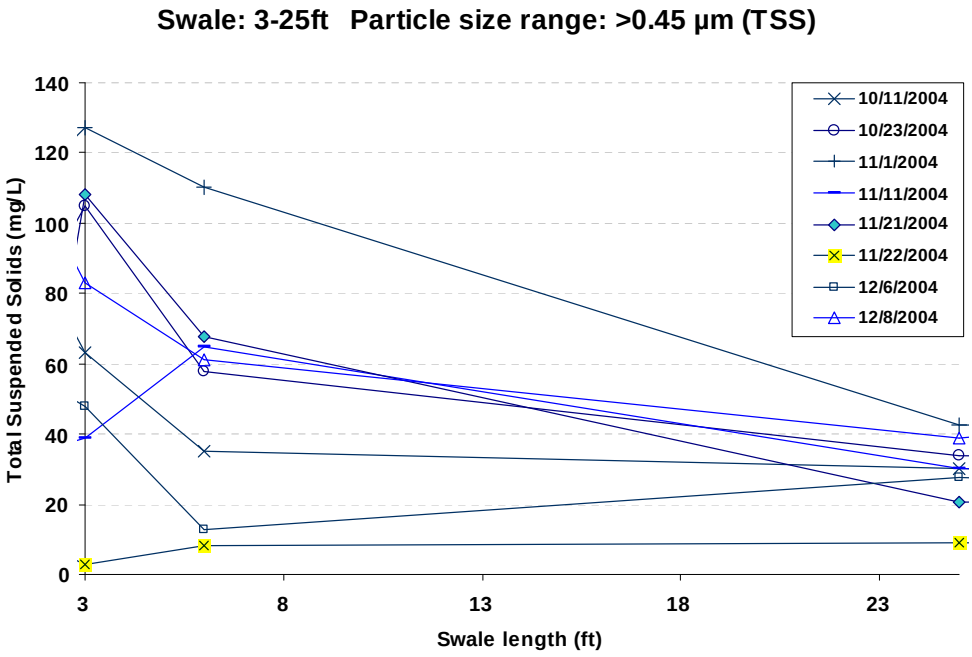

Figure P9

Appendix Q: K – Constants Plotted against Shear Stress for Different Particle Size Ranges

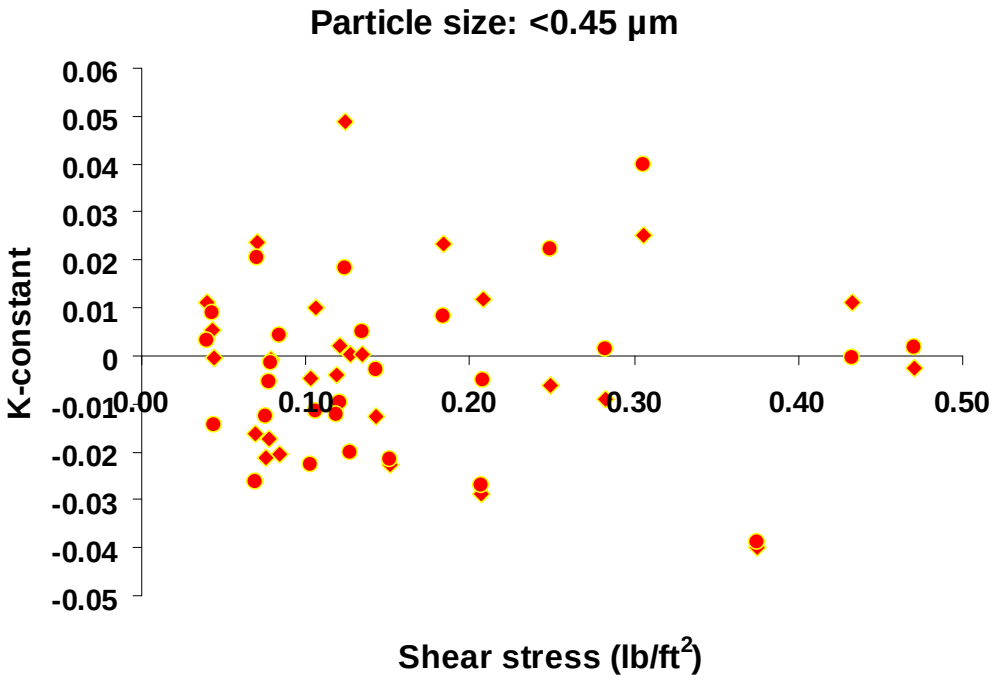

Figure Q1

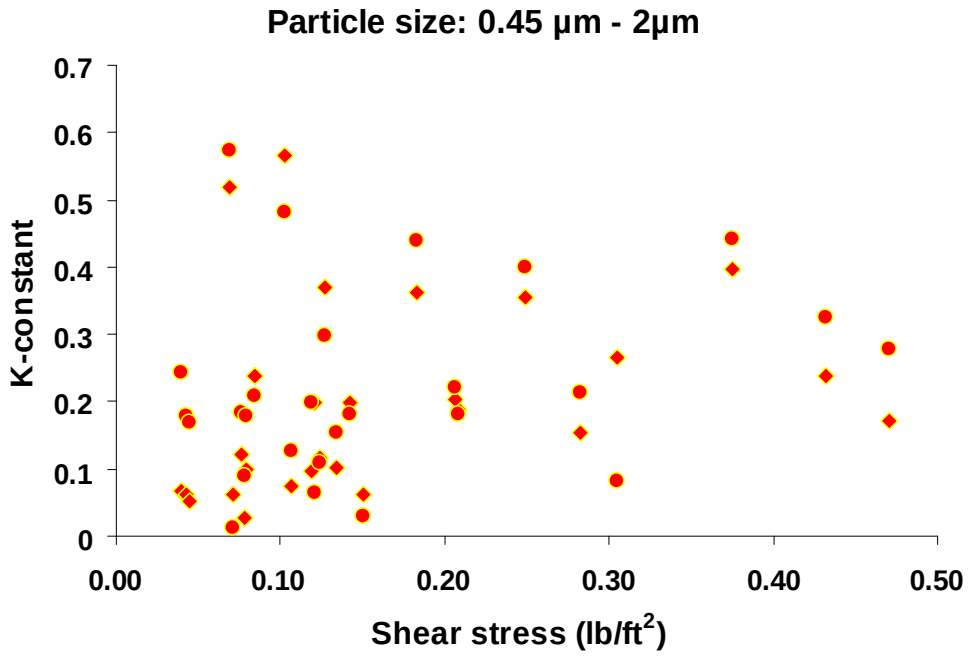

Figure Q2

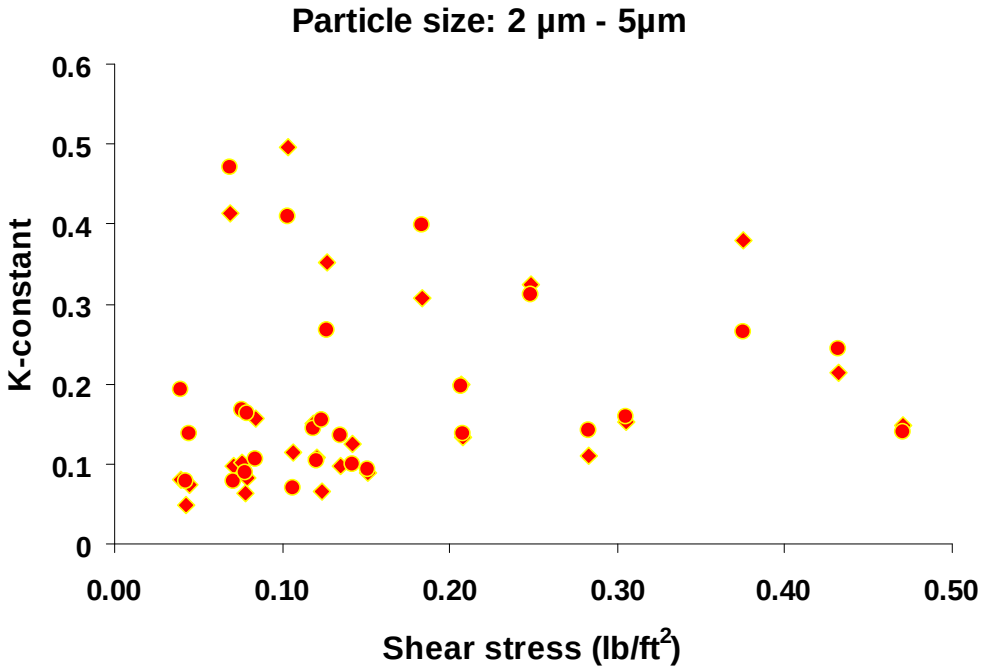

Figure Q3

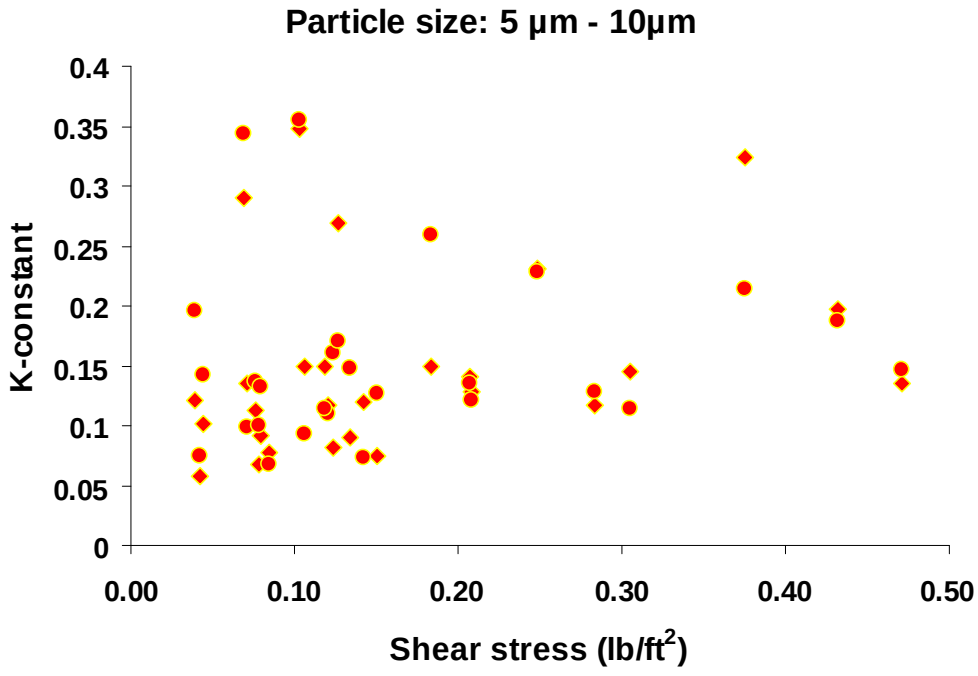

Figure Q4

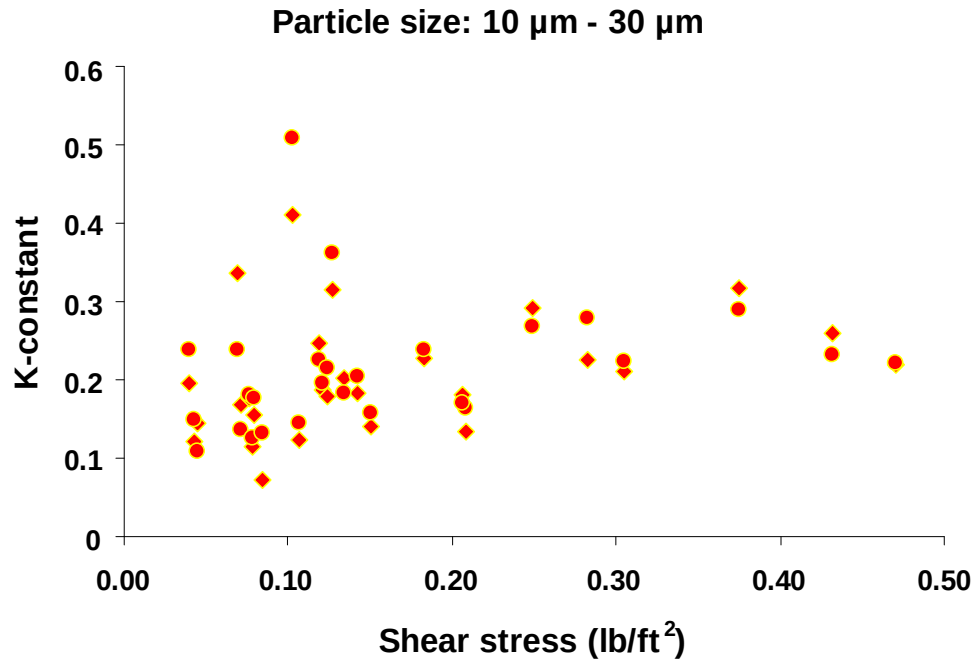

Figure Q5

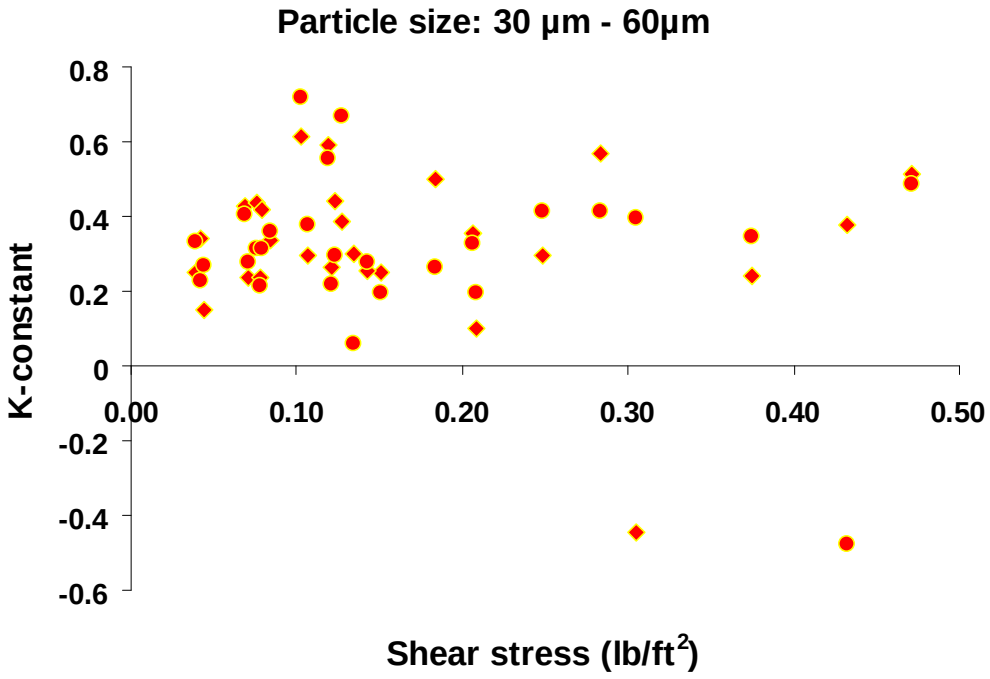

Figure Q6

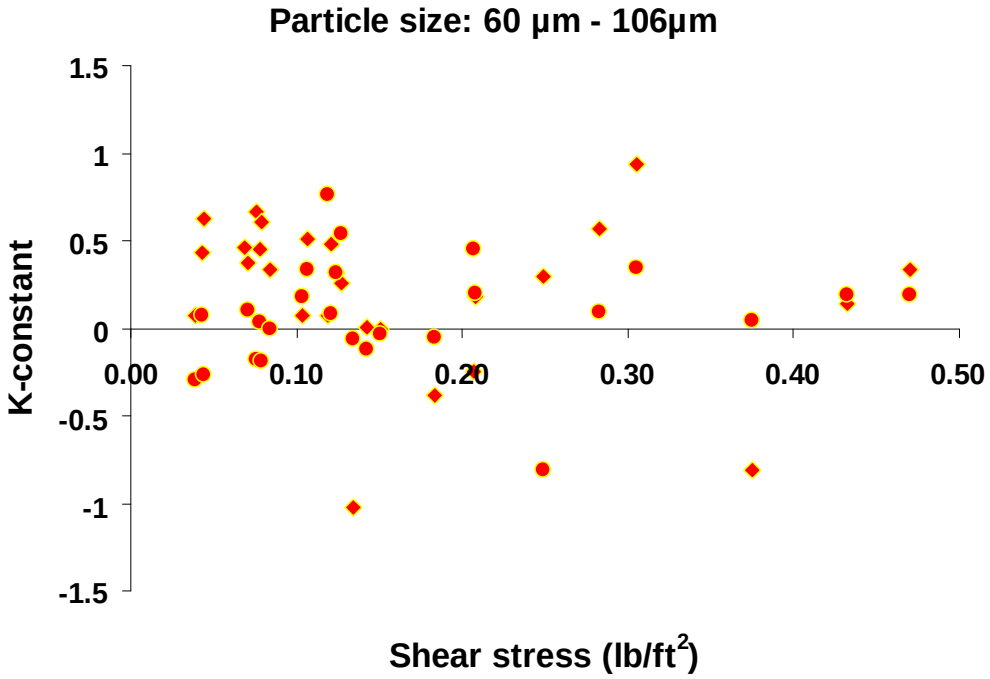

Figure Q7

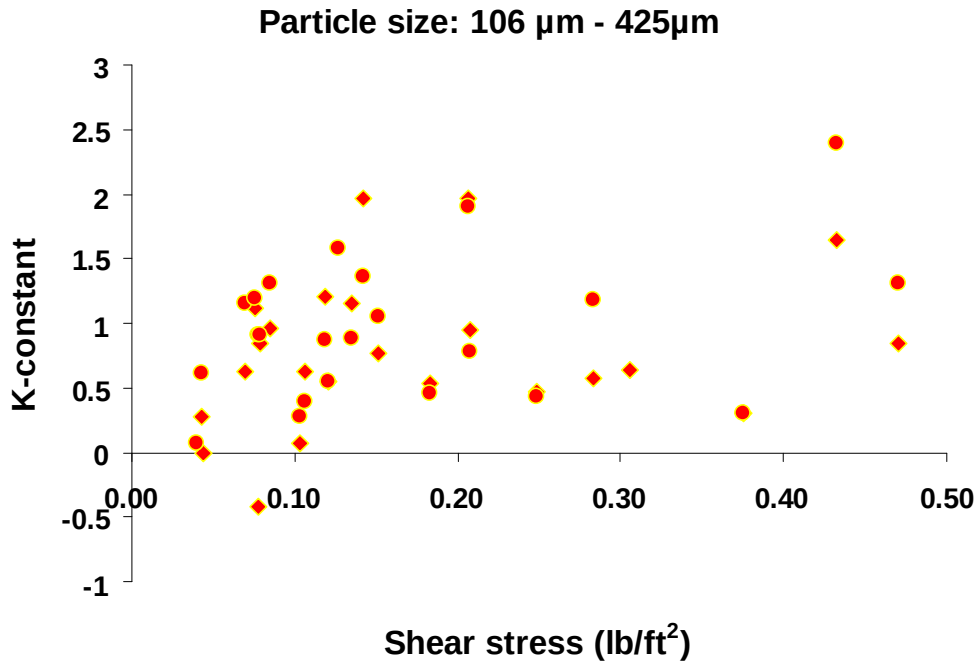

Figure Q8

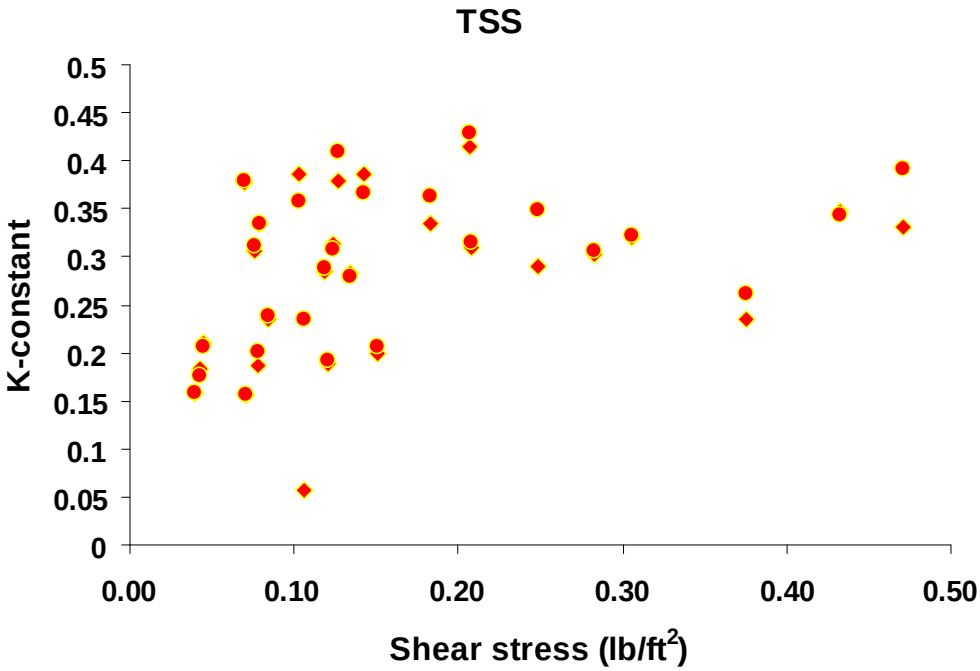

Figure Q9

Appendix R: Sediment Percent Reductions Plotted against Settling Frequency

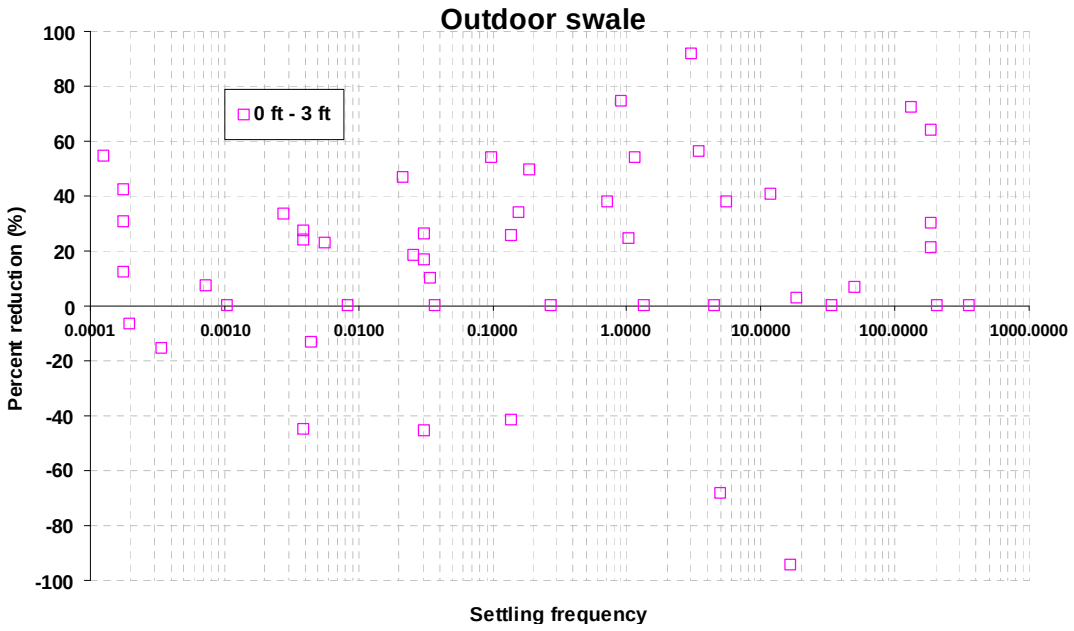

Figure R1

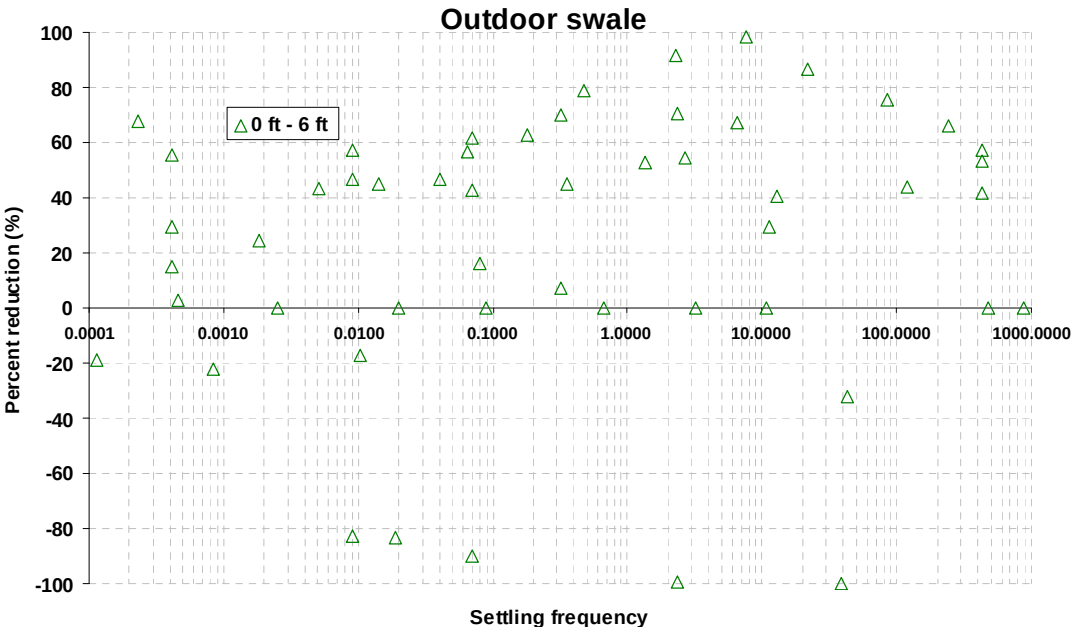

Figure R2

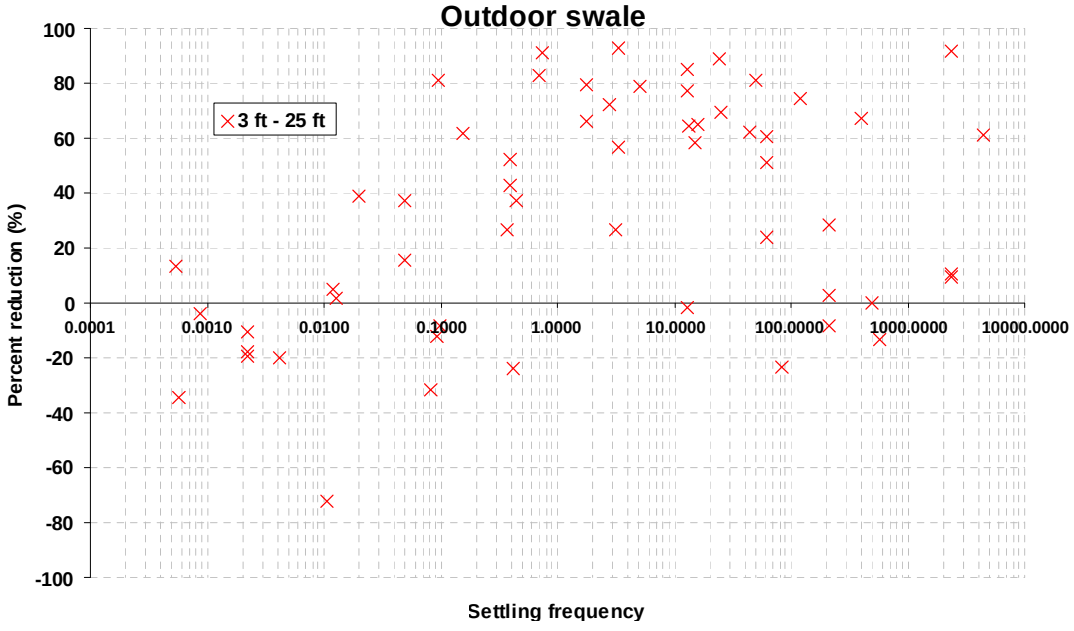

Figure R3

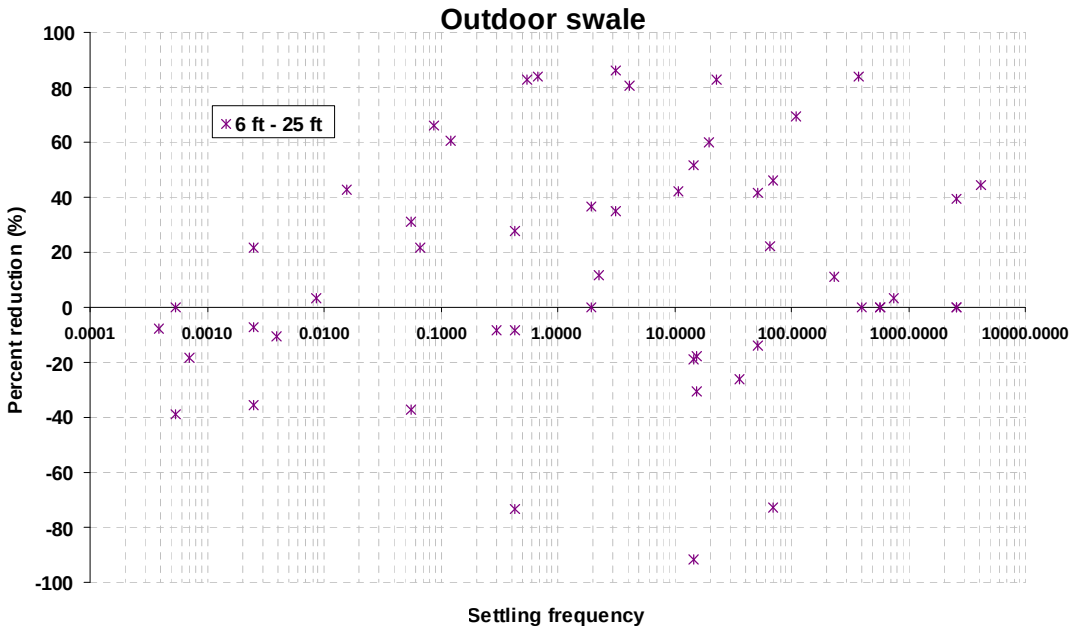

Figure R4

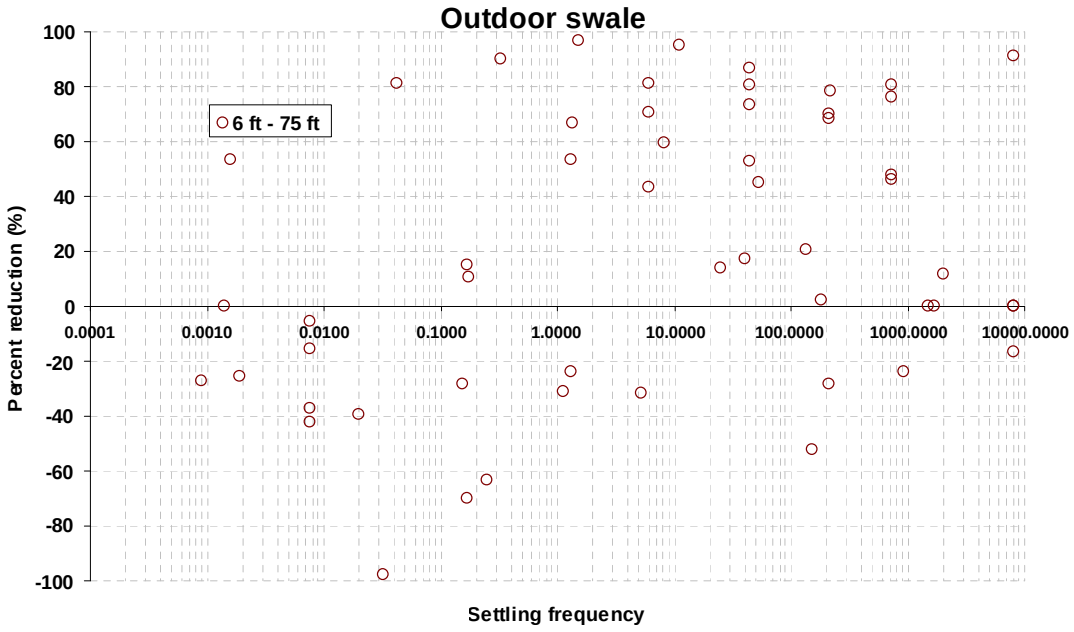

Figure R5

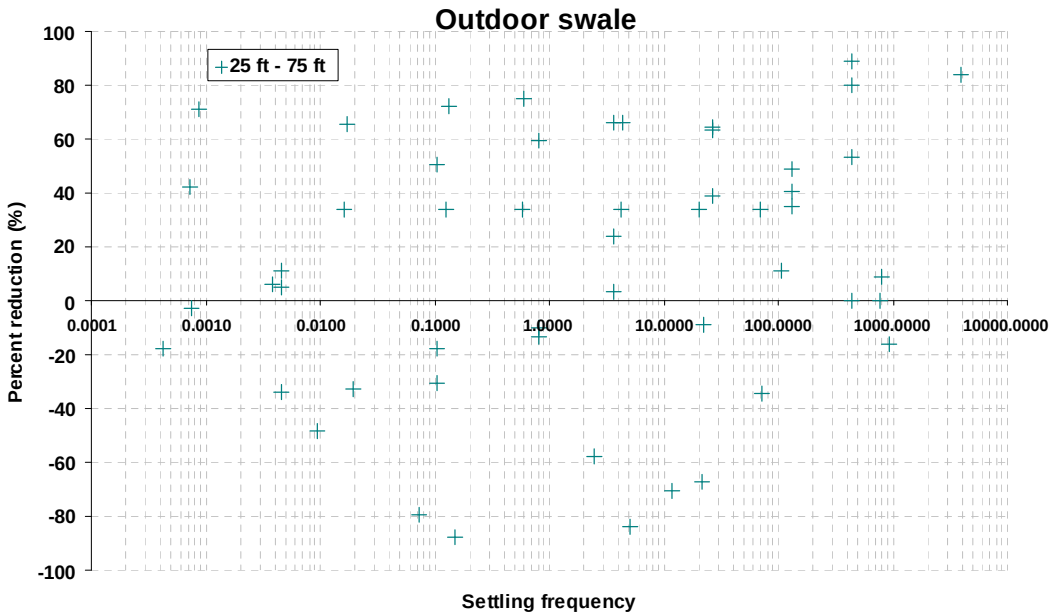

Figure R6

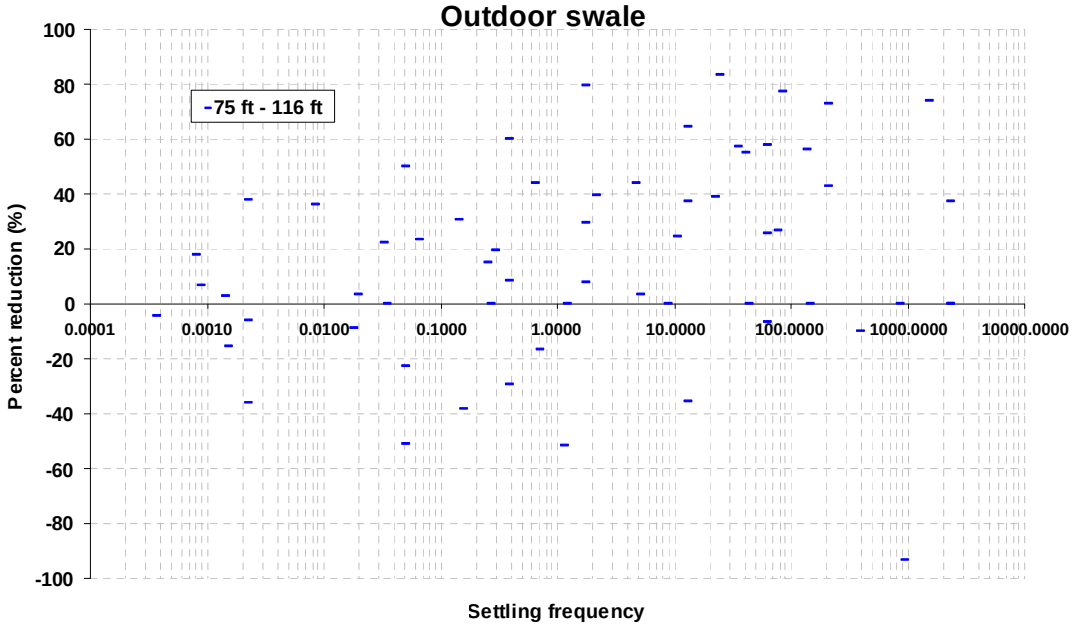

Figure R7